



# **Gold cyanidation – Gold associated with silver minerals embedded within base-metal sulphide matrices**

**Thèse**

**Muhammad Khalid**

**Doctorat en génie chimique  
Philosophiae Doctor (Ph.D.)**

Québec, Canada

© Muhammad Khalid, 2017

**Gold cyanidation – Gold associated with silver  
minerals embedded within base-metal sulphide  
matrices**

**Thèse**

**Muhammad Khalid**

Sous la direction de :

Faiçal Larachi, Directeur de recherche

## Résumé

Les problématiques dans le traitement des minerais aurifères deviennent de plus en plus significatives avec la déplétion des gisements à haute teneur autour du monde. L'or est trouvé principalement sous forme métallique dans la nature et est fréquemment associé avec des minéraux d'argent ou des sulfures métalliques. Dans la présente thèse, le rôle des minéraux d'argent sur la cyanuration de l'or au sein de sulfures métalliques est étudié en détail relativement aux interactions galvaniques et aux phénomènes de passivation de surface. Puisque les contacts galvaniques permanents naturellement présents à l'intérieur des grains des minéraux sont difficiles à répliquer en utilisant des montages standards d'électrodes à disques rotatifs ou de la pulpe de minerais riches en sulfures, une stratégie utilisant un réacteur à lit fixe (PBR) a été adoptée afin d'isoler et de quantifier les contributions des interactions galvaniques et des réactions de passivation sur les taux de lixiviation de l'or et de l'argent au sein de sulfures métalliques. Des mélanges d'or, de minéraux d'argent et d'autres sulfures métalliques ont été placés dans le réacteur à lit fixe afin de créer des contacts galvaniques inter-particules permanents parmi les constituants. La pyrite, la sphalérite et la stibnite ont été choisis comme sulfures métalliques modèles. De l'argent métallique (Ag), de l'acanthite  $\text{Ag}_2\text{S}$  et de la pyrargyrite ( $\text{Ag}_3\text{SbS}_3$ ) sont pour leur part les minéraux d'argent qui ont été étudiés.

Les interactions galvaniques entre l'or, l'argent et la pyrite ainsi que la sphalérite ont résulté en un comportement complexe de la lixiviation de l'or et de l'argent sous l'impact direct des contacts galvaniques ainsi que sous l'impact des effets de passivation. Les minéraux d'argent ont pour leur part démontré un effet amoindrissant pour la lixiviation de l'or dans de la chalcopryrite et de la stibnite. Des stratégies ont été investiguées pour améliorer la cinétique de lixiviation de l'or en présence de minéraux d'argent et de sulfures métalliques. Des solutions de cyanure contenant des sels de plomb ont augmenté la récupération de l'or et ont permis une neutralisation des effets négatifs issus de la présence des sulfures métalliques, particulièrement dans le cas de la chalcopryrite. De plus, l'addition de plomb a augmenté les cinétiques de lixiviation de l'or de manière significative pour l'or et l'argent associé à de la pyrite, de la chalcopryrite et de la sphalérite. Un prétraitement à l'aide d'une solution alcaline d'acétate de plomb a été étudié pour les mêmes couples de minéraux et il a été démontré que

cette stratégie augmente la récupération de l'or dans le cas de la pyrite, de la chalcopirite et de la sphalérite. D'autre part, la stibinite a démontré un effet net de réduction de la dissolution de l'or avec des minéraux d'argent. Des films recouvrant la surface des particules d'or dans le cas de la cyanuration de l'or en présence des sulfures métalliques ont aussi été observés dans le cas de la chalcopirite et de la stibnite.

## Abstract

Numerous non-idealities in gold processing are becoming increasingly significant with the depletion of free-milling oxide ores around the globe. Gold is mostly found in nature in metallic form and is associated with silver minerals and base-metal sulphides. In the present thesis work, the role of silver minerals on gold cyanidation with base-metal sulphides was elucidated in detail on the relative importance of galvanic interactions and passivation phenomena. As the permanent galvanic contacts, inherently present within the ore grains, are hard to achieve between gold rotating disk electrode and slurried base-metal sulphide-rich ores, a packed-bed reactor (PBR) strategy was thus adopted to single out and quantify the virtual contributions of galvanic interaction and passivation effect on the gold and silver leaching rates during gold cyanidation with silver minerals and base-metal sulphides. The mixtures of gold, silver-minerals and sulphides were filled in the PBR to ensure the permanent particle-particle micro-electrical contacts among all ore constituents. Pyrite, chalcopyrite, sphalerite and stibnite were the sulphidic minerals investigated in the present gold-silver cyanidation study. Metallic silver (Ag), acanthite ( $\text{Ag}_2\text{S}$ ) and pyrargyrite ( $\text{Ag}_3\text{SbS}_3$ ), were the silver-minerals taken into account.

Galvanic interactions were found to alleviate the leaching of gold and silver to various extents, for gold and silver minerals associated with pyrite and sphalerite, both under galvanic and passivation impact from the sulphide minerals. Silver minerals were found retarding to the gold leaching for chalcopyrite and stibnite minerals. Strategies were investigated to enhance the gold leaching kinetics in the presence of silver minerals and base-metal sulphides. Lead containing cyanide solution enhanced gold recovery and was found to neutralize significantly the negative effect of sulphidic minerals, particularly for chalcopyrite. Moreover, lead addition enhanced gold leaching kinetics significantly for gold and silver minerals associated with pyrite, chalcopyrite and sphalerite. Pre-treatment with alkaline lead acetate tested on sulphide associated mixtures of gold and silver minerals affirmed enhanced gold recovery in case of pyrite, chalcopyrite and sphalerite minerals. Stibnite found severely retarding towards gold dissolution with silver minerals. Surface obstructing films were observed on gold particles for gold cyanidation with silver minerals and base-metal sulphides in case of chalcopyrite and stibnite.

## Table of Contents

Résumé .....	iii
Abstract .....	v
Table of Contents .....	vi
List of Figures .....	x
List of Tables.....	xiv
Acknowledgements .....	xv
Foreword .....	xvi
Chapter 1: Introduction and Objectives .....	1
1.1. Background .....	1
1.2. Gold Cyanidation .....	2
1.2.1. Chemistry of Gold Dissolution .....	2
1.2.2. Chemistry of Cyanide Solution.....	4
1.2.3. Chemistry of Gold Cyanidation.....	5
1.3. Kinetics of Gold Dissolution .....	9
1.3.1 Effect of Cyanide and Dissolved Oxygen Concentration .....	10
1.3.2. Effect of pH .....	12
1.3.3. Effect of Particle Size .....	13
1.3.4. Effect of Temperature, Pressure and Agitation.....	13
1.4. Galvanic Interactions and Passivation Effect .....	14
1.5. Effect of Lead and Other Metal Ions .....	15
1.6. Effect of Silver Minerals .....	16
1.7. Effect of Sulphide Minerals .....	18
1.8. Effect of Copper Minerals.....	19
1.9. Effect of Antimony Minerals .....	21
1.10. Effect of Carbonaceous Minerals .....	21
1.11. Effect of Telluride Minerals .....	22
1.12. Research Objectives .....	23
1.13. Hypothesis.....	25
1.14. Research Strategy Adopted for Ph.D. Thesis .....	26
1.15. References .....	28
Chapter 2: Effect of Silver on Gold Cyanidation in Mixed and Segregated Sulphidic Minerals.....	34
Résumé .....	34

Abstract .....	35
2.1. Introduction .....	36
2.2. Experimental .....	38
2.2.1. Materials and Reagents.....	38
2.2.2. Packed-bed Reactor: Device Sophistication .....	39
2.2.3. Equipment and Procedures .....	40
2.3. Results and Discussion.....	44
2.3.1. Gold Leaching with Pyrite, Chalcopyrite, Sphalerite and Stibnite Minerals.....	44
2.3.2. Gold Leaching in Pyrite-Chalcopyrite-Silica System.....	46
2.3.3. Effect of Silver on Gold Leaching in Pyrite-Chalcopyrite-Silica System .....	48
2.3.4. Gold Leaching in Pyrite-Sphalerite-Silica System .....	50
2.3.5. Effect of Silver on Gold Leaching in Pyrite-Sphalerite-Silica System.....	52
2.3.6. Gold Leaching in Pyrite-Stibnite-Silica System.....	54
2.3.7. Effect of Silver on Gold Leaching in Pyrite-Stibnite-Silica System .....	55
2.4. Conclusion.....	56
2.5. References .....	58
Chapter 3: Impact of Silver Sulphide on Gold Cyanidation with Conductive Sulphide Minerals....	62
Résumé .....	62
Abstract .....	63
3.1. Introduction .....	64
3.2. Experimental .....	66
3.2.1. Materials and Reagents .....	66
3.2.2. Equipment and Procedures.....	66
3.2.3. X-Ray Photoelectron Spectroscopy .....	69
3.3. Results and Discussion.....	70
3.3.1. Benchmark Tests for Gold and Silver Sulphide Leaching.....	70
3.3.2. Gold Leaching with Pyrite-Silica System.....	71
3.3.3. Effect of Silver Sulphide on Gold Leaching with Pyrite-Silica System .....	73
3.3.4. Gold Leaching with Chalcopyrite-Silica System.....	74
3.3.5. Effect of Silver Sulphide on Gold Leaching with Chalcopyrite-Silica System .....	75
3.3.6. Gold Leaching with Sphalerite-Silica System .....	76
3.3.7. Effect of Silver Sulphide on Gold Leaching with Sphalerite-Silica System.....	77
3.3.8. Gold Leaching with Stibnite-Silica System .....	78

3.3.9. Effect of Silver Sulphide on Gold Leaching with Stibnite-Silica System .....	79
3.3.10. X-Ray Photoelectron Spectroscopy of Gold Particles Isolated Post-Cyanidation .....	80
3.4. Conclusion.....	85
3.5. References.....	86
Chapter 4: Assessment of the Impact of Silver Sulphides on Gold Cyanidation with Polymetal Sulphides.....	91
Résumé .....	91
Abstract .....	92
4.1. Introduction.....	93
4.2. Experimental .....	95
4.2.1. Materials and Reagents .....	95
4.2.2. Equipment and Procedures.....	95
4.3. Results and Discussion.....	99
4.3.1. Benchmark Tests for Gold and Pyrargyrite Leaching.....	99
4.3.2. Effect of Pyrargyrite on Au Leaching with Pyrite-Silica System .....	100
4.3.3. Effect of Pyrargyrite on Au Leaching with Chalcopyrite-Silica System.....	102
4.3.4. Effect of Pyrargyrite on Au Leaching with Sphalerite-Silica System.....	104
4.3.5. Effect of Pyrargyrite on Au Leaching with Stibnite-Silica System .....	105
4.3.6. Benchmark Tests for Gold and Silver Minerals ( $\alpha\beta\gamma$ ) Leaching .....	106
4.3.7. Effect of Ag, Ag <sub>2</sub> S and Ag <sub>3</sub> SbS <sub>3</sub> on Au Leaching with Pyrite-Silica System .....	108
4.3.8. Effect of Ag, Ag <sub>2</sub> S and Ag <sub>3</sub> SbS <sub>3</sub> on Au Leaching with Chalcopyrite-Silica System .....	109
4.3.9. Effect of Ag, Ag <sub>2</sub> S and Ag <sub>3</sub> SbS <sub>3</sub> on Au Leaching with Sphalerite-Silica System.....	110
4.3.10. Effect of Ag, Ag <sub>2</sub> S and Ag <sub>3</sub> SbS <sub>3</sub> on Au Leaching with Stibnite-Silica System .....	111
4.4. Conclusion.....	112
4.5. References .....	114
Chapter 5: The Role of Lead on the Cyanidation of Gold Associated with Silver Minerals Embedded within Base-metal Sulphide Mineral Matrices.....	118
Résumé .....	118
Abstract .....	119
5.1. Introduction .....	120
5.2. Experimental .....	122
5.2.1. Materials and Reagents.....	122
5.2.2. Equipment and Procedures .....	122
5.2.3. Lead Acetate Pre-treatment and Lead Acetate Addition Tests .....	123



5.2.4. X-Ray Photoelectron Spectroscopy .....	124
5.3. Results and Discussion.....	125
5.3.1. Lead Acetate Effect on Benchmark Leaching of Gold and Silver Minerals.....	125
5.3.2. Lead Acetate Effect on Leaching of Gold and Silver with Pyrite-Silica System .....	127
5.3.3. Lead Acetate Effect on Leaching of Gold and Silver with Chalcopyrite-Silica System .	129
5.3.4. Lead Acetate Effect on Leaching of Gold and Silver with Sphalerite-Silica System.....	131
5.3.5. Lead Acetate Effect on Leaching of Gold and Silver with Stibnite-Silica System .....	133
5.3.6. Alkaline Lead Acetate Pre-treatment of Sulphides and Gold Leaching .....	135
5.3.7. X-ray Photoelectron Spectroscopy of Gold Particles Isolated after Cyanidation.....	137
5.4. Conclusion.....	139
5.5. References .....	141
Chapter 6: General Discussion, Conclusions and Recommendations.....	145
6.1. General Discussion.....	145
6.2. Conclusions .....	148
6.3. Future Work Recommendations.....	150

## List of Figures

<b>Figure 1.1.</b> Eh-pH diagram for the Au-H <sub>2</sub> O-CN <sup>-</sup> system at 25 °C. Concentrations of all soluble gold species = 10 <sup>-4</sup> M. [CN <sup>-</sup> ] <sub>total</sub> = 10 <sup>-3</sup> M .....	7
<b>Figure 1.2.</b> Anodic cyanidation model for gold in the absence or presence of dissolved silver(I); boundary i: gold-film interface, boundary o: film-solution interface .....	8
<b>Figure 1.3.</b> Schematic representation of the local corrosion cell at a gold surface in contact with an oxygen-containing cyanide solution .....	10
<b>Figure 1.4.</b> Effect of cyanide concentration on gold leaching .....	11
<b>Figure 1.5.</b> Effect of oxygen concentration on gold leaching .....	12
<b>Figure 1.6.</b> Effect of lead addition on gold dissolution: 10 mmol/L cyanide, 50 mg/L pure gold powder and various sulfide minerals .....	16
<b>Figure 1.7.</b> Distribution of Cu complexes as a function of NaCN concentration and pH .....	20
<b>Figure 1.8.</b> A representative demonstration of the strategy adopted in this thesis.....	26
<b>Figure 2.1.</b> Sketch of two packed-bed reactors (PBRs). Follows as: 1- inlet section; 2- working section (Teflon); 3- outlet section; 4- stainless-steel cylinder; 5- peristaltic pump; 6- magnetic stirrer plate; 7- oxygen probe electrode; 8- pH-meter electrode; 9- air bubbling system; 10- magnetic stirrer bar.....	41
<b>Figure 2.2.</b> Galvanic and passivation effects of sulphidic minerals on gold dissolution: (a) gold dissolution with pyrite mineral, (b) gold dissolution with chalcopyrite mineral, (c) gold dissolution with sphalerite mineral, (d) gold dissolution with stibnite mineral. Reaction conditions: CN <sup>-</sup> = 30 mM, DO <sub>2</sub> = 0.45 mM, pH = 11. ....	45
<b>Figure 2.3.</b> Gold dissolution within a sulphidic mineral layer system: (a) Py+Au//Cp, bi-layer arrangement, (b) Py//Cp+Au, bi-layer arrangement, (c) Py+Cp+Au, mono-layer arrangement, (d) Py//Cp//Si+Au, tri-layer arrangement. Reaction conditions: CN <sup>-</sup> = 30 mM, DO <sub>2</sub> = 0.45 mM, pH = 11. ....	47
<b>Figure 2.4.</b> Effect of silver on the dissolution of gold within a sulphidic mineral layer system: (a) Py+Au+Ag//Cp, bi-layer arrangement, (b) Py//Cp+Au+Ag, bi-layer arrangement, (c) Py+Cp+Au+Ag, mono-layer arrangement, (d) Py+Ag//Cp+Au, bi-layer arrangement, (e) Py+Au//Cp+Ag, (f) Py//Cp//Si+Au+Ag, tri-layer arrangement. Reaction conditions: CN <sup>-</sup> = 30 mM, DO <sub>2</sub> = 0.45 mM, pH = 11. ....	49
<b>Figure 2.5.</b> Gold dissolution within a sulphidic mineral layer system: (a) Py+Au//Sp, bi-layer arrangement, (b) Py//Sp+Au, bi-layer arrangement, (c) Py+Sp+Au, mono-layer arrangement, (d) Py//Sp//Si+Au, tri-layer arrangement. Reaction conditions: CN <sup>-</sup> = 30 mM, DO <sub>2</sub> = 0.45 mM, pH = 11. ....	51
<b>Figure 2.6.</b> Effect of silver on the dissolution of gold within a sulphidic mineral layer system: (a) Py+Au+Ag//Sp, bi-layer arrangement, (b) Py//Sp+Au+Ag, bi-layer arrangement, (c) Py+Sp+Au+Ag, mono-layer arrangement, (d) Py+Ag//Sp+Au, bi-layer arrangement, (e) Py+Au//Sp+Ag, bi-layer arrangement, (f) Py//Sp//Si+Au+Ag, tri-layer arrangement. Reaction conditions: CN <sup>-</sup> = 30 mM, DO <sub>2</sub> = 0.45 mM, pH = 11.....	53
<b>Figure 2.7.</b> Gold dissolution within a sulphidic mineral layer system: (a) Py+Au//Sb, bi-layer arrangement, (b) Py//Sb+Au, bi-layer arrangement, (c) Py+Sb+Au, mono-layer arrangement, (d)	

Py//Sb//Si+Au, tri-layer arrangement. Reaction conditions:  $\text{CN}^- = 30 \text{ mM}$ ,  $\text{DO}_2 = 0.45 \text{ mM}$ ,  $\text{pH} = 11$ ..... 54

**Figure 2.8.** Effect of silver on the dissolution of gold within a sulphidic mineral layer system: **(a)** Py+Au+Ag//Sb, bi-layer arrangement, **(b)** Py//Sb+Au+Ag, bi-layer arrangement, **(c)** Py+Sb+Au+Ag, mono-layer arrangement, **(d)** Py+Ag//Sb+Au, bi-layer arrangement, **(e)** Py+Au//Sb+Ag, bi-layer arrangement, **(f)** Py//Sb//Si+Au+Ag, tri-layer arrangement. Reaction conditions:  $\text{CN}^- = 30 \text{ mM}$ ,  $\text{DO}_2 = 0.45 \text{ mM}$ ,  $\text{pH} = 11$ . ..... 55

**Figure 3.1.** Gold dissolution: **(a)** Au dispersion pattern within sulfide (X) and quartz powder layers, **(b)** Au &  $\text{Ag}_2\text{S}$  dispersion pattern within sulfide (X) and quartz powder layers: Reaction conditions:  $\text{CN}^- = 30 \text{ mM}$ ,  $\text{DO}_2 = 0.25 \text{ mM}$ ,  $\text{pH} = 11$ . ..... 68

**Figure 3.2.** Gold dissolution: **(a)** gold and silver sulfide dissolution within quartz layer, **(b)** effect of  $\text{Ag}_2\text{S}$  on gold dissolution within quartz layer. Reaction conditions:  $\text{CN}^- = 30 \text{ mM}$ ,  $\text{DO}_2 = 0.25 \text{ mM}$ ,  $\text{pH} = 11$ ..... 70

**Figure 3.3.** Gold dissolution: **(a)** gold dissolution with pyrite, Py+Au//Si, **(b)**  $\text{Ag}_2\text{S}$  on gold dissolution with pyrite, Py+Au+ $\text{Ag}_2\text{S}$ //Si, **(c)** gold dissolution with pyrite, Py//Si+Au, **(d)**  $\text{Ag}_2\text{S}$  on gold dissolution with pyrite, Py//Si+Au+ $\text{Ag}_2\text{S}$ . Reaction conditions:  $\text{CN}^- = 30 \text{ mM}$ ,  $\text{DO}_2 = 0.25 \text{ mM}$ ,  $\text{pH} = 11$ ..... 72

**Figure 3.4.** Gold dissolution: **(a)** gold dissolution with chalcopyrite, Cp+Au//Si, **(b)**  $\text{Ag}_2\text{S}$  on gold dissolution with chalcopyrite, Cp+Au+ $\text{Ag}_2\text{S}$ //Si, **(c)** gold dissolution with chalcopyrite, Cp//Si+Au, **(d)**  $\text{Ag}_2\text{S}$  on gold dissolution with chalcopyrite, Cp//Si+Au+ $\text{Ag}_2\text{S}$ . Reaction conditions:  $\text{CN}^- = 30 \text{ mM}$ ,  $\text{DO}_2 = 0.25 \text{ mM}$ ,  $\text{pH} = 11$ . ..... 75

**Figure 3.5.** Gold dissolution: **(a)** gold dissolution with sphalerite, Sp+Au//Si, **(b)**  $\text{Ag}_2\text{S}$  on gold dissolution with sphalerite, Sp+Au+ $\text{Ag}_2\text{S}$ //Si, **(c)** gold dissolution with sphalerite, Sp//Si+Au, **(d)**  $\text{Ag}_2\text{S}$  on gold dissolution with sphalerite, Sp//Si+Au+ $\text{Ag}_2\text{S}$ . Reaction conditions:  $\text{CN}^- = 30 \text{ mM}$ ,  $\text{DO}_2 = 0.25 \text{ mM}$ ,  $\text{pH} = 11$ ..... 77

**Figure 3.6.** Gold dissolution: **(a)** gold dissolution with stibnite, Sb+Au//Si, **(b)**  $\text{Ag}_2\text{S}$  on gold dissolution with stibnite, Sb+Au+ $\text{Ag}_2\text{S}$ //Si, **(c)** gold dissolution with stibnite, Sb//Si+Au, **(d)**  $\text{Ag}_2\text{S}$  on gold dissolution with stibnite, Sb//Si+Au+ $\text{Ag}_2\text{S}$ . Reaction conditions:  $\text{CN}^- = 30 \text{ mM}$ ,  $\text{DO}_2 = 0.25 \text{ mM}$ ,  $\text{pH} = 11$ ..... 79

**Figure 3.7.** X-ray spectra of gold surface: **(a)** Au  $4f_{7/2}$  for gold with  $\text{Ag}_2\text{S}$  and chalcopyrite, **(b)** Cu  $2p_{3/2}$  on gold surface with  $\text{Ag}_2\text{S}$  and chalcopyrite, **(c)** Ag  $3d_{5/2}$  on gold surface with  $\text{Ag}_2\text{S}$  and chalcopyrite. Reaction conditions:  $\text{CN}^- = 30 \text{ mM}$ ,  $\text{DO}_2 = 0.25 \text{ mM}$ ,  $\text{pH} = 11$ ..... 81

**Figure 3.8.** X-ray spectra of gold surface: **(a)** Au  $4f$  spectra for gold with stibnite, **(b)** Sb  $3d$  spectra for gold with stibnite, **(c)** Au  $4f$  spectra for gold with  $\text{Ag}_2\text{S}$  and stibnite, **(d)** Sb  $3d$  spectra for gold with  $\text{Ag}_2\text{S}$  and stibnite, **(e)** Ag  $3d_{5/2}$  spectra for gold with  $\text{Ag}_2\text{S}$  and stibnite, **(f)** S  $2p$  spectra for gold with  $\text{Ag}_2\text{S}$  and stibnite. Reaction conditions:  $\text{CN}^- = 30 \text{ mM}$ ,  $\text{DO}_2 = 0.25 \text{ mM}$ ,  $\text{pH} = 11$ . ..... 83

**Figure 4.1.** Gold dissolution: **(a)** Gold (Au) & silver minerals ( $\gamma/\alpha\beta\gamma$ ) dispersion pattern within sulphide (X) layer, **(b)** Gold (Au) & silver minerals ( $\gamma/\alpha\beta\gamma$ ) dispersion pattern within quartz layer. Reaction conditions:  $\text{CN}^- = 30 \text{ mM}$ ,  $\text{DO}_2 = 0.25 \text{ mM}$ ,  $\text{pH} = 11$ ..... 97

<b>Figure 4.2.</b> Gold dissolution: (a) gold and pyrrargyrite ( $\gamma$ ) dissolution within quartz layer, (b) effect of pyrrargyrite ( $\gamma$ ) on gold dissolution within quartz layer. Reaction conditions: $\text{CN}^- = 30 \text{ mM}$ , $\text{DO}_2 = 0.25 \text{ mM}$ , $\text{pH} = 11$ .	99
<b>Figure 4.3.</b> Gold dissolution: (a) gold dissolution with pyrite and pyrrargyrite, $\text{Py}+\text{Au}+\gamma//\text{Si}$ , (b) Gold dissolution with pyrite and pyrrargyrite, $\text{Py}//\text{Si}+\text{Au}+\gamma$ . Reaction conditions: $\text{CN}^- = 30 \text{ mM}$ , $\text{DO}_2 = 0.25 \text{ mM}$ , $\text{pH} = 11$ .	101
<b>Figure 4.4.</b> Gold dissolution: (a) gold dissolution with chalcopyrite and pyrrargyrite, $\text{Cp}+\text{Au}+\gamma//\text{Si}$ , (b) Gold dissolution with chalcopyrite and pyrrargyrite, $\text{Cp}//\text{Si}+\text{Au}+\gamma$ . Reaction conditions: $\text{CN}^- = 30 \text{ mM}$ , $\text{DO}_2 = 0.25 \text{ mM}$ , $\text{pH} = 11$ .	103
<b>Figure 4.5.</b> Gold dissolution: (a) gold dissolution with sphalerite and pyrrargyrite, $\text{Sp}+\text{Au}+\gamma//\text{Si}$ , (b) Gold dissolution with sphalerite and pyrrargyrite, $\text{Sp}//\text{Si}+\text{Au}+\gamma$ . Reaction conditions: $\text{CN}^- = 30 \text{ mM}$ , $\text{DO}_2 = 0.25 \text{ mM}$ , $\text{pH} = 11$ .	104
<b>Figure 4.6.</b> Gold dissolution: (a) gold dissolution with stibnite and pyrrargyrite, $\text{Sb}+\text{Au}+\gamma//\text{Si}$ , (b) Gold dissolution with stibnite and pyrrargyrite, $\text{Sb}//\text{Si}+\text{Au}+\gamma$ . Reaction conditions: $\text{CN}^- = 30 \text{ mM}$ , $\text{DO}_2 = 0.25 \text{ mM}$ , $\text{pH} = 11$ .	106
<b>Figure 4.7.</b> Gold dissolution: (a) gold (Au) and silver minerals ( $\alpha\beta\gamma$ ) dissolution within quartz layer, (b) effect of silver minerals on gold ( $\text{Au}+\alpha\beta\gamma$ ) dissolution within quartz layer. Reaction conditions: $\text{CN}^- = 30 \text{ mM}$ , $\text{DO}_2 = 0.25 \text{ mM}$ , $\text{pH} = 11$ .	107
<b>Figure 4.8.</b> Gold dissolution: (a) gold dissolution with pyrite and silver minerals $\alpha\beta\gamma$ , $\text{Py}+\text{Au}+\alpha\beta\gamma//\text{Si}$ , (b) Gold dissolution with pyrite and silver minerals $\alpha\beta\gamma$ , $\text{Py}//\text{Si}+\text{Au}+\alpha\beta\gamma$ . Reaction conditions: $\text{CN}^- = 30 \text{ mM}$ , $\text{DO}_2 = 0.25 \text{ mM}$ , $\text{pH} = 11$ .	108
<b>Figure 4.9.</b> Gold dissolution: (a) gold dissolution with chalcopyrite and silver minerals $\alpha\beta\gamma$ , $\text{Cp}+\text{Au}+\alpha\beta\gamma//\text{Si}$ , (b) Gold dissolution with chalcopyrite and silver minerals $\alpha\beta\gamma$ , $\text{Cp}//\text{Si}+\text{Au}+\alpha\beta\gamma$ . Reaction conditions: $\text{CN}^- = 30 \text{ mM}$ , $\text{DO}_2 = 0.25 \text{ mM}$ , $\text{pH} = 11$ .	109
<b>Figure 4.10.</b> Gold dissolution: (a) gold dissolution with sphalerite and silver minerals $\alpha\beta\gamma$ , $\text{Sp}+\text{Au}+\alpha\beta\gamma//\text{Si}$ , (b) Gold dissolution with sphalerite and silver minerals $\alpha\beta\gamma$ , $\text{Sp}//\text{Si}+\text{Au}+\alpha\beta\gamma$ . Reaction conditions: $\text{CN}^- = 30 \text{ mM}$ , $\text{DO}_2 = 0.25 \text{ mM}$ , $\text{pH} = 11$ .	111
<b>Figure 4.11.</b> Gold dissolution: (a) gold dissolution with stibnite and silver minerals $\alpha\beta\gamma$ , $\text{Sb}+\text{Au}+\alpha\beta\gamma//\text{Si}$ , (b) Gold dissolution with stibnite and silver minerals $\alpha\beta\gamma$ , $\text{Sb}//\text{Si}+\text{Au}+\alpha\beta\gamma$ . Reaction conditions: $\text{CN}^- = 30 \text{ mM}$ , $\text{DO}_2 = 0.25 \text{ mM}$ , $\text{pH} = 11$ .	112
<b>Figure 5.1.</b> Lead acetate effect: (a) Gold dissolution with silver-minerals ( $\alpha\beta\gamma$ ) within quartz layer, (b) Silver dissolution for Au & silver-minerals ( $\alpha\beta\gamma$ ) within quartz layer. Reaction conditions: Lead acetate = (10, 20, 100 mg/L), $\text{CN}^- = 30 \text{ mM}$ , $\text{DO}_2 = 0.25 \text{ mM}$ , $\text{pH} = 11$ .	126
<b>Figure 5.2.</b> Lead acetate effect: (a) Gold dissolution with pyrite and silver-minerals ( $\alpha\beta\gamma$ ), $\text{Py}+\text{Au}+\alpha\beta\gamma//\text{Si}$ , (b) Silver dissolution with pyrite and silver-minerals ( $\alpha\beta\gamma$ ), $\text{Py}+\text{Au}+\alpha\beta\gamma//\text{Si}$ , (c) Gold dissolution with pyrite and silver-minerals ( $\alpha\beta\gamma$ ), $\text{Py}//\text{Si}+\text{Au}+\alpha\beta\gamma$ , (d) Silver dissolution with pyrite and silver-minerals ( $\alpha\beta\gamma$ ), $\text{Py}//\text{Si}+\text{Au}+\alpha\beta\gamma$ . Reaction conditions: Lead acetate = (10, 20, 100 mg/L), $\text{CN}^- = 30 \text{ mM}$ , $\text{DO}_2 = 0.25 \text{ mM}$ , $\text{pH} = 11$ .	128
<b>Figure 5.3.</b> Lead acetate effect: (a) Gold dissolution with chalcopyrite and silver-minerals ( $\alpha\beta\gamma$ ), $\text{Cp}+\text{Au}+\alpha\beta\gamma//\text{Si}$ , (b) Silver dissolution with chalcopyrite and silver-minerals ( $\alpha\beta\gamma$ ), $\text{Cp}+\text{Au}+\alpha\beta\gamma//\text{Si}$ , (c) Gold dissolution with chalcopyrite and silver-minerals ( $\alpha\beta\gamma$ ), $\text{Cp}//\text{Si}+\text{Au}+\alpha\beta\gamma$ , (d) Silver dissolution with chalcopyrite and silver-minerals ( $\alpha\beta\gamma$ ), $\text{Cp}//\text{Si}+\text{Au}+\alpha\beta\gamma$ . Reaction conditions: Lead acetate = (10, 20, 100 mg/L), $\text{CN}^- = 30 \text{ mM}$ , $\text{DO}_2 = 0.25 \text{ mM}$ , $\text{pH} = 11$ .	130

**Figure 5.4.** Lead acetate effect: **(a)** Gold dissolution with sphalerite and silver-minerals ( $\alpha\beta\gamma$ ),  $\text{Sp}+\text{Au}+\alpha\beta\gamma//\text{Si}$ , **(b)** Silver dissolution with sphalerite and silver-minerals ( $\alpha\beta\gamma$ ),  $\text{Sp}+\text{Au}+\alpha\beta\gamma//\text{Si}$ , **(c)** Gold dissolution with sphalerite and silver-minerals ( $\alpha\beta\gamma$ ),  $\text{Sp}//\text{Si}+\text{Au}+\alpha\beta\gamma$ , **(d)** Silver dissolution with sphalerite and silver-minerals ( $\alpha\beta\gamma$ ),  $\text{Sp}//\text{Si}+\text{Au}+\alpha\beta\gamma$ , Reaction conditions: Lead acetate = (10, 20, 100 mg/L),  $\text{CN}^- = 30 \text{ mM}$ ,  $\text{DO}_2 = 0.25 \text{ mM}$ ,  $\text{pH} = 11$ . ..... 132

**Figure 5.5.** Lead acetate effect: **(a)** Gold dissolution with stibnite and silver-minerals ( $\alpha\beta\gamma$ ),  $\text{Sb}+\text{Au}+\alpha\beta\gamma//\text{Si}$ , **(b)** Silver dissolution with stibnite and silver-minerals ( $\alpha\beta\gamma$ ),  $\text{Sb}+\text{Au}+\alpha\beta\gamma//\text{Si}$ , **(c)** Gold dissolution with stibnite and silver-minerals ( $\alpha\beta\gamma$ ),  $\text{Sb}//\text{Si}+\text{Au}+\alpha\beta\gamma$ , **(d)** Silver dissolution with stibnite and silver-minerals ( $\alpha\beta\gamma$ ),  $\text{Sb}//\text{Si}+\text{Au}+\alpha\beta\gamma$ , Reaction conditions: Lead acetate = (10, 20, 100 mg/L),  $\text{CN}^- = 30 \text{ mM}$ ,  $\text{DO}_2 = 0.25 \text{ mM}$ ,  $\text{pH} = 11$ . ..... 134

**Figure 5.6.** Lead acetate pre-treatment: **(a)** Gold dissolution with (X= pyrite, chalcopyrite, sphalerite, stibnite) and silver-minerals ( $\alpha\beta\gamma$ ),  $\text{X}+\text{Au}+\alpha\beta\gamma//\text{Si}$ , **(b)** Silver dissolution with (X= pyrite, chalcopyrite, sphalerite, stibnite) and silver-minerals ( $\alpha\beta\gamma$ ),  $\text{X}+\text{Au}+\alpha\beta\gamma//\text{Si}$ , Reaction conditions: Lead acetate = 100 mg/L,  $\text{CN}^- = 30 \text{ mM}$ ,  $\text{DO}_2 = 0.25 \text{ mM}$ ,  $\text{pH} = 11$ . ..... 136

**Figure 5.7.** X-ray spectra of gold surface: **(a)** Au 4f spectra for gold with stibnite and silver-minerals ( $\alpha\beta\gamma$ ), **(b)** Sb 3d spectra for gold with stibnite and silver-minerals ( $\alpha\beta\gamma$ ), **(c)** Ag 3d<sub>5/2</sub> spectra for gold with stibnite and silver-minerals ( $\alpha\beta\gamma$ ), **(d)** Pb 4f spectra of gold with stibnite and silver-minerals ( $\alpha\beta\gamma$ ), **(e)** S 2p spectra for gold with stibnite and silver-minerals ( $\alpha\beta\gamma$ ). Reaction conditions: Lead acetate = 100 mg/L,  $\text{CN}^- = 30 \text{ mM}$ ,  $\text{DO}_2 = 0.25 \text{ mM}$ ,  $\text{pH} = 11$ . ..... 138

## List of Tables

<b>Table 2.1.</b> Elemental composition of sulfide ore samples investigated in present study. ....	39
<b>Table 4.1.</b> Effect of silver sulphide on gold dissolution with conductive sulphides. ....	100
<b>Table 5.1.</b> Effect of silver-minerals ( $\alpha\beta\gamma$ ) on Au recovery (%) with polymetal sulphides after 6 h cyanidation. ....	125

## **Acknowledgements**

Firstly, I offer my sincere appreciation to my affectionate parents for their amiable support and encouragement during my whole life. Also, I would like to express my gratitude for the consistent support of my loving wife during the challenging times of my Ph.D. studies. Thank you so much.

This thesis would not be in good shape without the inspirational attitude of my siblings who wisely advised me in the final stretch of my education.

I would like to express my heartfelt gratitude and appreciation to my supervisor, Prof. Faïçal Larachi, for his ample guidance and support. He made my Ph.D. study productive through his unique, supportive, and composed approach. I am also deeply indebted for his contributions to my professional development.

Thank you my friends and colleagues. My sincere gratefulness to all my friends, an inspiring group of people especially Amir Motamed, Olivier Gravel, Ali Entezari, Dariush Azizi, Shahab Boroun, Diana Aksenova and Jian Zhang. You were the sources of laughter, joy and encouragement, bearing the brunt of frustrations and sharing the joy of successes. My cordial thanks to Amir Motamed; you are a special friend and a very caring fellow. Special thanks to Dr. Masud Riaz and Dr. Muhammad Hasib-ur-Rahman for helping me in starting the project. I would like to thank Olivier Gravel, for his kindness in translating parts of this thesis into French. The help of the chemical engineering department technical staff, Jérôme Noël, Marc Lavoie, Yann Giroux, and Jean-Nicolas Ouellet during this research project is also appreciated.

Finally, I acknowledge the financial support from the Natural Sciences and Engineering Research Council through its Cooperative Research & Development Grants Program as well as from the supporting partners Agnico Eagle, Barrick, Camiro, Corem, Glencore, IamGold, Niobec and Teck is thankfully acknowledged.

**Thank you all**

## Foreword

This Ph.D. thesis is composed of six chapters. First chapter comprises the introduction which is devoted to the review of the literature on the prominent factors influencing the kinetics of gold leaching in a typical sulphide-rich cyanidation medium, research objectives and the scientific research methodology adopted in this project. Chapters 2-5, present the results of this project in the form of scientific articles. Out of these four chapters, two research articles have already been published; the third one has been accepted for publication while the last one is under review for publication in hydrometallurgy journal. Chapter 6 consists of general discussions, conclusion and future recommendations. This project was supervised by Prof. Faïçal Larachi.

1. M. Khalid, F. Larachi. Effect of silver on gold cyanidation in mixed and segregated sulphidic minerals. *Can. J. Chem. Eng.* 2017, 95, 698-707.
2. M. Khalid, F. Larachi, A. Adnot. Impact of silver sulphide on gold cyanidation with conductive sulphide minerals. *Can. J. Chem. Eng.* 2017, (online 04 May, 2017).
3. M. Khalid, F. Larachi. Accumulative Impact of Silver Sulphides on Gold Cyanidation in Polymetal Sulphides. *Trans. Nonferrous Met. Soc. China.* 2017, (accepted 09 June, 2017).
4. M. Khalid, F. Larachi, A. Adnot. The role of lead on the cyanidation of gold associated with silver minerals embedded within base-metal sulphide mineral matrices. *Hydrometallurgy*, submitted May 8, 2017.

Each publication is a separate chapter comprising the body of the thesis. The research articles were prepared by me and revised by my director, Prof. Faïçal Larachi. Prof. Larachi guided me and provided expertise in designing experiments and interpretation of data during the entire research work.

Some of the research results were presented in the following conference:

- M. Khalid, F. Larachi, A. Adnot. Disentangling the Effects of Silver and Sulphide Minerals on Gold Cyanidation. 66th CSChE, 2016, Québec QC, Canada.

Some of the research results were presented in poster form in the following events:



- 6e conférence annuelle du CCVC, May 2015, Université Laval, Québec QC, Canada.
- Colloque annuel de centre E4m, November 2016, Université Laval, Québec QC, Canada.

# Chapter 1: Introduction and Objectives

## 1.1. Background

Gold is noblest of all metals known. It is a highly sought precious metal because of its rarity and physical and chemical properties. Prominent gold consuming sectors comprise jewellery, coinage, international financial systems and high-tech industrial and medicine sectors. The technological developments in gold ore processing have been resulted in periodic step changes for the gold industry over the decades. The total gold mined from 19<sup>th</sup> century to the present is estimated to be about 141,000 tons. Keeping in view the course of history, it has been estimated that humans have mined a total of 165,000 tons of gold. It demonstrates that only about 24,000 tons of gold has been mined before the 20<sup>th</sup> century, and roughly 85% of the world's gold has been mined during the 20<sup>th</sup> century. The development of cyanidation process was the step change that catalyzed the economical production of mineral-bound gold at lower grades [1-4].

Gold is soft metal and is usually alloyed with other metals to give it more strength. Gold in metallic form and/or alloyed with other metals, have been progressively used in electronics and in the space and aeronautics industries in more recent decades because of their high electrical conductivity and high infrared reflectivity. Gold as well as its alloys have been used as a catalyst in the chemical industry, also as a medicine for the treatment of arthritis and the radiotherapy of certain cancers [5-7].

Gold is usually found in nature as native gold, while the only gold compounds that exist in nature are gold tellurides ( $\text{AuTe}_2$ ) and gold stibnides ( $\text{AuSb}_2$ ). Gold is usually associated with quartz and pyrite, both in and alluvial or placer deposits. It is commonly found to be associated with copper and silver in rocks, as it belongs to the same group of the periodic table. The average concentration of gold in earth's crust is 0.005 g/t [3]. Gold is classified as a noble metal due to its inertness to chemical reactions in non-complex media, however it reacts with numerous reagents. Gold can be recovered from the ores by various methods, such as gravity concentration, flotation and leaching. Cyanidation evolved as a commercial process after a patent filed by MacArthur et al. in 1887. Gold cyanidation has been the main

metallurgical process for gold extraction for more than a century, because of the high solubility of gold in an aerated cyanide solution. Cyanidation is the most frequent process for gold extraction in the gold mining industry, regardless of toxicity, safety related costs and adverse environmental effects [3,8].

Gold is not oxidized in air or water by either oxygen or sulfur even at high temperature and also not attacked in corrosive environments. Chemistry of gold complexes in aqueous solutions is of prime interest in gold hydrometallurgy. Gold can occur in one of the oxidation states from -1 to +5, the most pervasive oxidation states of hydrometallurgical interests are the aurous ( $\text{Au}^{+1}$ ) and auric ( $\text{Au}^{+3}$ ) forms. Gold in the form ( $\text{Au}^{+1}$ ) and ( $\text{Au}^{+3}$ ) ions are thermodynamically unstable in aqueous solution. Nevertheless, the ( $\text{Au}^{+1}$ ) and ( $\text{Au}^{+3}$ ) ions can be stabilized by a number of complexing ligands thus allowing the formation of complexes [3,4,8]. Since the evolution of the gold cyanidation process, the chemistry and leaching kinetics have been the subjects of intensive investigation. Plenty of theories have been proposed to explain the reaction mechanism. The prominent variables affecting gold cyanidation are the free cyanide/dissolved oxygen concentration, temperature, pH and particle size.

Due to rapid depletion of free-type of gold-bearing oxide deposits around the globe, which divert marginal quantities of cyanide and dissolved oxygen concentration, the gold extraction from low grade and refractory sulphide deposits is stretching the limits of cyanidation process. Gold cyanidation is a complex system due to the fact that gold particles occur as alloys or compounds which are embedded in a sulphide matrix and galvanic interactions play a significant role between the phases [3,9,10].

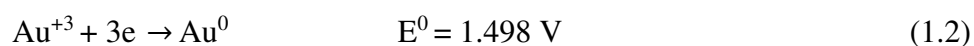
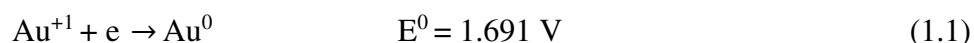
## **1.2. Gold Cyanidation**

### **1.2.1. Chemistry of Gold Dissolution**

Leaching is the process of dissolution of a metal or a mineral in a liquid. Gold is present in nature as a native metal (Au), but it can be oxidized to aurous ( $\text{Au}^{+1}$ ) and auric ( $\text{Au}^{+3}$ ), in the presence of a suitable oxidant. The dissolution of gold in aqueous solutions is a simultaneous process of oxidation and complexation with suitable oxidizing and complexing agents. Gold

cations both aurous ( $\text{Au}^{+1}$ ) and auric ( $\text{Au}^{+3}$ ) are  $\beta$ -type metal ions, which means that the stability of their complexes tends to decrease as the electronegativity of the donor ligand increases, leading to the stability orders such as  $\text{I} > \text{Br} > \text{Cl} > \text{F}$ , in case of halides. Dissolution of gold is an electrochemical process with the involvement of anodic and cathodic half reactions [3,4,8].

Anodic half reaction involves the oxidation of gold during the dissolution of gold in aqueous solutions and is expressed as the following equations:



$E^0$  represents the standard reduction potential. Simultaneous cathodic process involves the reduction of an appropriate oxidant.



Both the aurous ( $\text{Au}^{+1}$ ) and auric ( $\text{Au}^{+3}$ ) ions spontaneously get reduced to gold ( $\text{Au}^0$ ) with the oxidation of water to oxygen at a potential value of,  $E^0 = 1.229 \text{ V}$  [3,4]. These potential values demonstrates that gold cannot be oxidized without the presence of a suitable complexing agent. The complexation reaction of the gold cations, aurous ( $\text{Au}^{+1}$ ) and auric ( $\text{Au}^{+3}$ ) ions with the appropriate ligands, can be represented by the following reactions and their stability constant calculations are given as under:



Where L represents the complexing ligand, such as cyanide, chloride, thiourea and/or thiosulfate ions, etc. Similarly, the stability constants for the gold cations ( $\text{Au}^{+\delta}$ ,  $\delta = +1, +3$ ) can be represented as under:

$$\beta_x = [\text{AuL}_x^{+\delta}] / [\text{Au}^{+\delta}][\text{L}]^x \quad (1.5)$$

The Nernst equation can be written by summarizing the equations (1.4) and (1.5), respectively.

$$E^0_{complex} = E^0_{Au^{+δ}/Au} - (0.0592/n)\log \beta_x \quad (1.6)$$

*n = no. of electrons involved.*

In case of gold dissolution, the strength of the oxidizing agent is held responsible for the formation of either aurous ( $Au^{+1}$ ) and auric ( $Au^{+3}$ ) complexes. *Soft donors* or the atoms with low electronegativity prefer to make complexes with low valence metal ions, while atoms with high electronegativity or *hard donors* prefer complexation with high valence metal ions. In short, aurous ( $Au^{+1}$ ) ion preferably makes more stable complexes with the ligands like cyanide, thiourea and thiocyanate. On the other hand auric ( $Au^{+3}$ ) ion makes more stable complexes with the ligands such as nitrogen, oxygen, fluoride and chloride ions [3,4,8].

Cyanide is the universal ligand in gold leaching because of its low cost and adaptability for gold ores and most common oxidant in this case is the oxygen from air. The stability of gold complexes decreases with the increase of the electronegativity of the ligands. The environmental pressures, slow leaching kinetics and poor recovery for refractory gold ores are the causes for non-cyanide lixivants in gold leaching. Chloride-chlorine, thiosulfate, thiourea, thiocyanate, ammonia, alkaline sulfide and halides (bromide, iodide) solutions have been extensively studied for the leaching of gold [3,4].

### 1.2.2. Chemistry of Cyanide Solution

The cyanide salts of sodium (NaCN), potassium (KCN) and calcium ( $CaCN_2$ ), dissociates to the respective metal cations and free cyanide ions. The cyanide ion on hydrolysis in water forms hydrogen cyanide (HCN) and hydroxyl ( $OH^-$ ) ions, as follows:



HCN, being a weak acid, dissociates in water as follows:



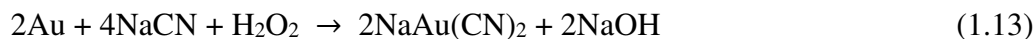
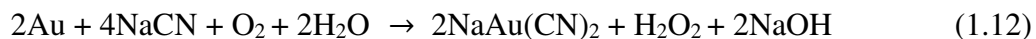
As elaborated in the equation (9.1), at pH 9.3 the total cyanide exists as 50% HCN and 50% free cyanide, while at higher pH free cyanide form dominates and at low pH HCN form

predominates. The oxidation of both the HCN and free cyanide in the presence of oxygen leads to the formation of cyanate ( $\text{CNO}^-$ ) which is unable to dissolve gold [3,4].

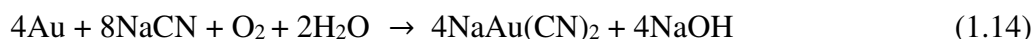


### 1.2.3. Chemistry of Gold Cyanidation

Although gold is inert to oxidation, the oxidation of gold is a prerequisite for its dissolution in alkaline cyanide solution. In the presence of a suitable complexing agent such as cyanide, gold is oxidized and dissolved to form a stable complex like  $[\text{Au}(\text{CN})_2]^-$ . Oxygen is reduced to hydroxide ( $\text{OH}^-$ ) species through a hydrogen peroxide ( $\text{H}_2\text{O}_2$ ) intermediate product in the first step which is also involved as an oxidizing agent in the second step. In 1896, Bodlander suggested that gold cyanidation reaction involves two steps according to following reactions [3,13,14].



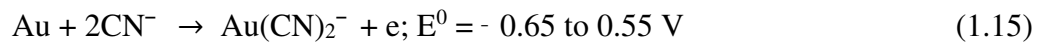
These equations have been summarized by Elsner, known as well-known Elsner's equation.



Formation of hydrogen peroxide as an intermediate product has been confirmed by many researchers during dissolution of gold. Increase in pH value could have a retarding effect on the decomposition reaction of hydrogen peroxide (reaction 1.13), means that the high hydroxide ion concentration could have a negative effect on the gold dissolution. It has also been reported that studies performed about the oxygen reduction phenomena on gold electrode revealed that almost 85% of hydrogen peroxide was diffused away from the gold surface, therefore it can be concluded that most of the gold dissolution follows the 1.12 reaction pathway. It means that the reduction of hydrogen peroxide to water as represented by the reaction 1.13 might have a small but significant role on the dissolution of gold. It is

worthy to mention the presence some metal ions act as catalyst to facilitate the decomposition reaction of hydrogen peroxide [12-16].

Keeping in view the electrochemical behavior of gold dissolution, the Eh-pH diagram for the Au-H<sub>2</sub>O-CN<sup>-</sup> system has been shown in the Figure 1.1. The oxidation-reduction potentials for the anodic gold dissolution and cathodic oxygen reduction have been described as follows:



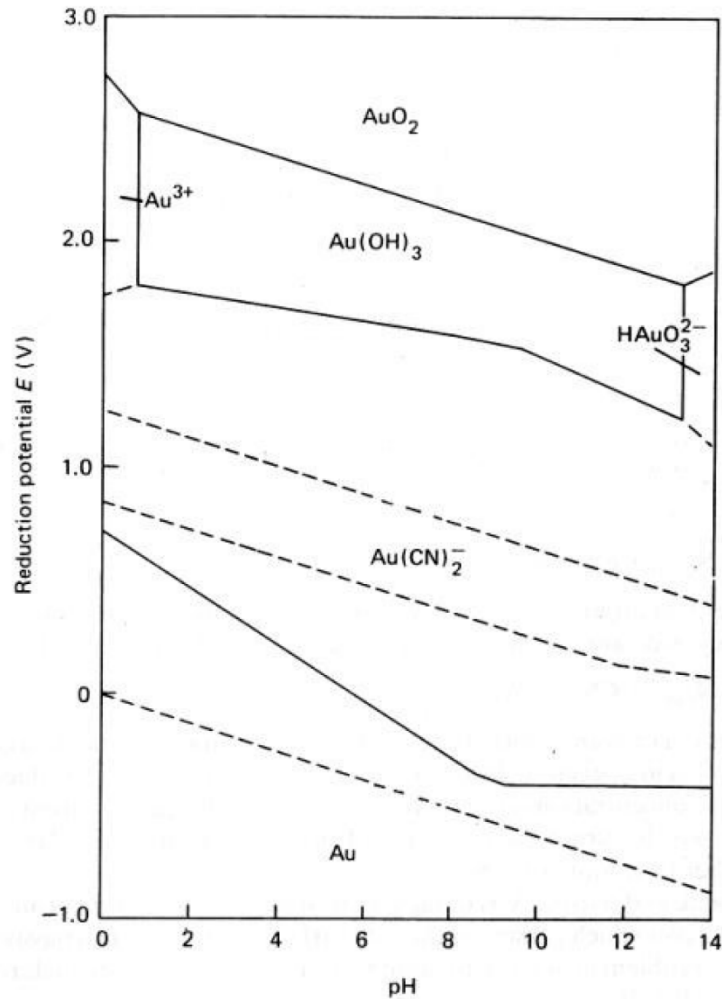


**Figure 1.1.** Eh-pH diagram for the Au-H<sub>2</sub>O-CN<sup>-</sup> system at 25 °C. Concentrations of all soluble gold species = 10<sup>-4</sup> M. [CN<sup>-</sup>]<sub>total</sub> = 10<sup>-3</sup> M [3].

The mechanism of gold dissolution has been debated under both acidic and alkaline conditions. Dissolution of gold is an electrochemical process that proceeds via anodic oxidation of gold and the cathodic reduction of oxygen. The anodic dissolution of gold with cyanide has been elaborated in Figure 1.2, both in the presence and absence of silver [10].



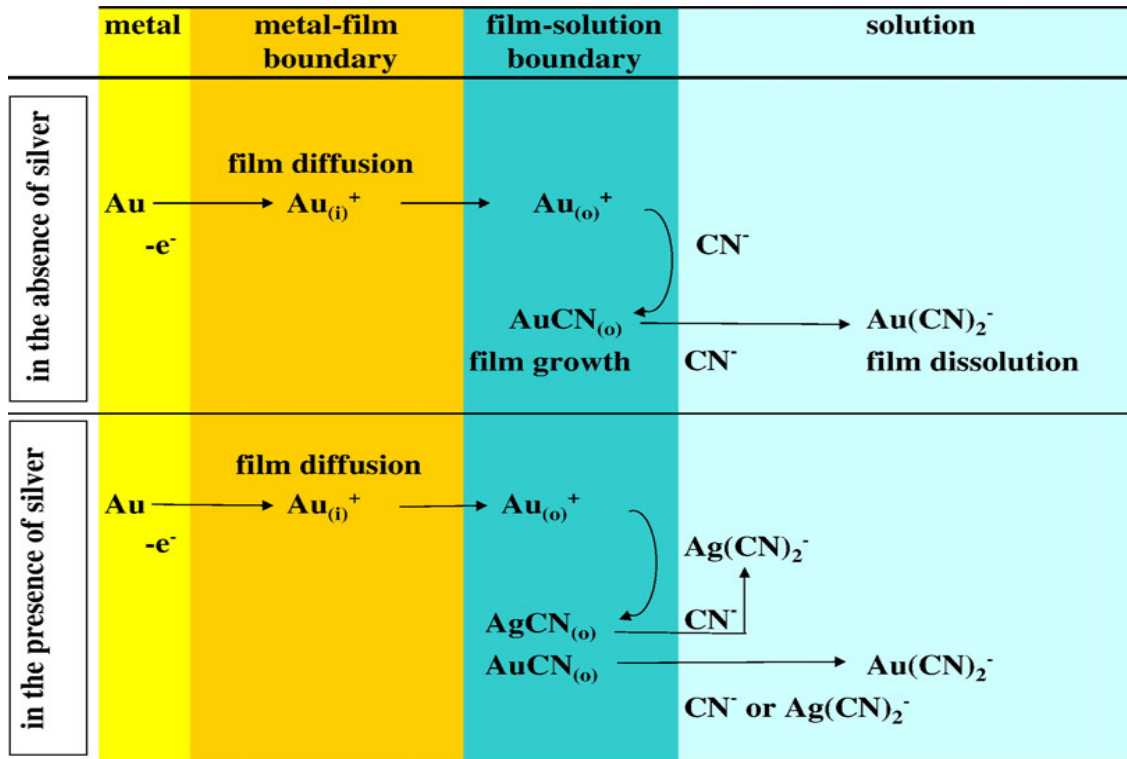


**Figure 1.2.** Anodic cyanidation model for gold in the absence or presence of dissolved silver(I); boundary i: gold-film interface, boundary o: film-solution interface [10].

The important steps during the anodic dissolution reaction of gold in the solution phase are presented below [11,17].

(a) Adsorption of cyanide on gold surface



(b) Electrochemical extraction of an electron



(c) Combination of the adsorbed intermediate with another cyanide ion



### 1.3. Kinetics of Gold Dissolution

In hydrometallurgical gold extraction processes, the most important reactions are heterogeneous. These processes involve the transfer of metals and minerals between solid and liquid phases. These heterogeneous reactions are either controlled by the inherent chemical reaction kinetics or by the rate of mass transfer of the individual reacting species across a phase boundary. The significant factors affecting the gold dissolution rate comprise cyanide and oxygen concentrations, temperature, pH, degree of agitation and mass transport, gold purity, surface area of the exposed gold and the presence of impurities with the gold. The rate of pure gold dissolution relies on the rate of film diffusion of cyanide ions or dissolved oxygen towards the gold surface as shown below [3,4,11].

The experimental behavior of the gold leaching process can be explained on the basis of this rate equation. At low cyanide concentration, gold dissolution is dependent on the cyanide concentration and independent of oxygen concentration.

$$-\frac{dN_{Au}}{A dt} = \frac{1}{2} \frac{D_{CN^-} [CN^-]}{\delta} = k_1 [CN^-] \quad (1.22)$$

But when cyanide concentration is high, the gold dissolution rate is dependent on the oxygen concentration while independent of the cyanide concentration.

$$-\frac{dN_{Au}}{A dt} = 2 \frac{D_{O_2} [O_2]}{\delta} = k_2 [O_2] \quad (1.23)$$

Where  $A$  is the surface area ( $\text{cm}^2$ ) of gold disc in contact with aqueous phase,  $[CN^-]$  is cyanide concentration ( $\text{mol}/\text{cm}^3$ ),  $[O_2]$  is oxygen concentration ( $\text{mol}/\text{cm}^3$ ),  $D_{CN^-}$  is diffusion coefficient of cyanide ( $\text{cm}^2/\text{s}$ ),  $D_{O_2}$  is diffusion coefficient of oxygen ( $\text{cm}^2/\text{s}$ ),  $N_{Au}$  is the amount of gold in particles (mole),  $t$  is time (s) and  $\delta$  is the boundary layer thickness (cm). The rate equations for the dissolution of gold have been proposed by various researchers based on different experimental settings. Gold ores are complex in nature, therefore, it is immensely difficult to establish a general kinetic model for leaching gold from different ores [11].

### 1.3.1 Effect of Cyanide and Dissolved Oxygen Concentration

Taking into consideration the equation for gold dissolution reaction (1.12), it is apparent that one mole of gold requires two moles of cyanide and half a mole of oxygen for the gold dissolution in a two electron process as shown in Figure 1.3, below:

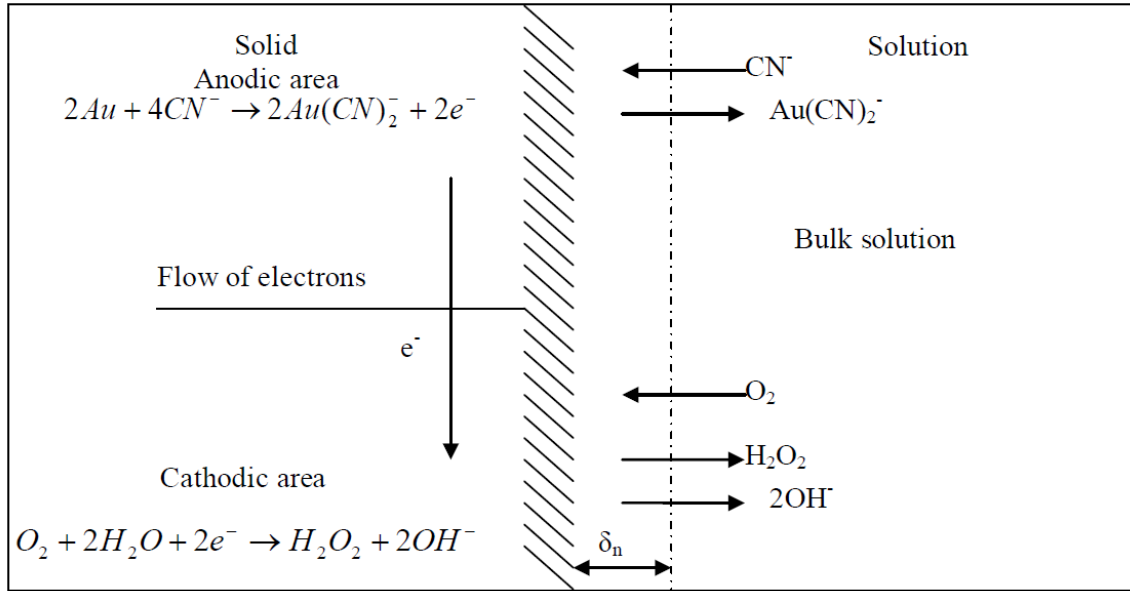


**Figure 1.3.** Schematic representation of the local corrosion cell at a gold surface in contact with an oxygen-containing cyanide solution [3].

The Elsner's equation(1.13) represents that the ideal cyanide:oxygen molar ratios to be 8:1 or 12.25 mg/L NaCN to 1 mg/L dissolved oxygen (DO<sub>2</sub>). As gold leaching is limited by the diffusion of either cyanide or oxygen to the gold surface, the relative diffusion rates of cyanide and oxygen should be considered seriously. The molar ratios for cyanide:oxygen concentrations, have been proposed in open literature, such as of 6:1 and 6.9:1, for gold dissolution . This ratio may vary from site to site, depending upon the interfering species associated with gold, while measuring cyanide and oxygen consumption [18,19].

The oxygen reduction and gold oxidation both occur at the gold surface for pure gold and oxide ores, while in case of sulphide ores the oxygen reduction does not necessarily occur at the gold surface. Oxygen reduction is equally facilitated by the gold and sulphide mineral surface acting as cathode [20,21]. A significantly less amount of dissolved oxygen is required to leach gold when gold is under galvanic contact with a semiconducting sulphide mineral.

Higher dissolved oxygen concentration may prove to be detrimental for gold leaching from sulphide rich gold ores. The gold dissolution rate is cyanide diffusion controlled at low cyanide concentrations, but at high cyanide levels gold dissolution is insensitive to the cyanide concentration [11,17,22], as shown below:

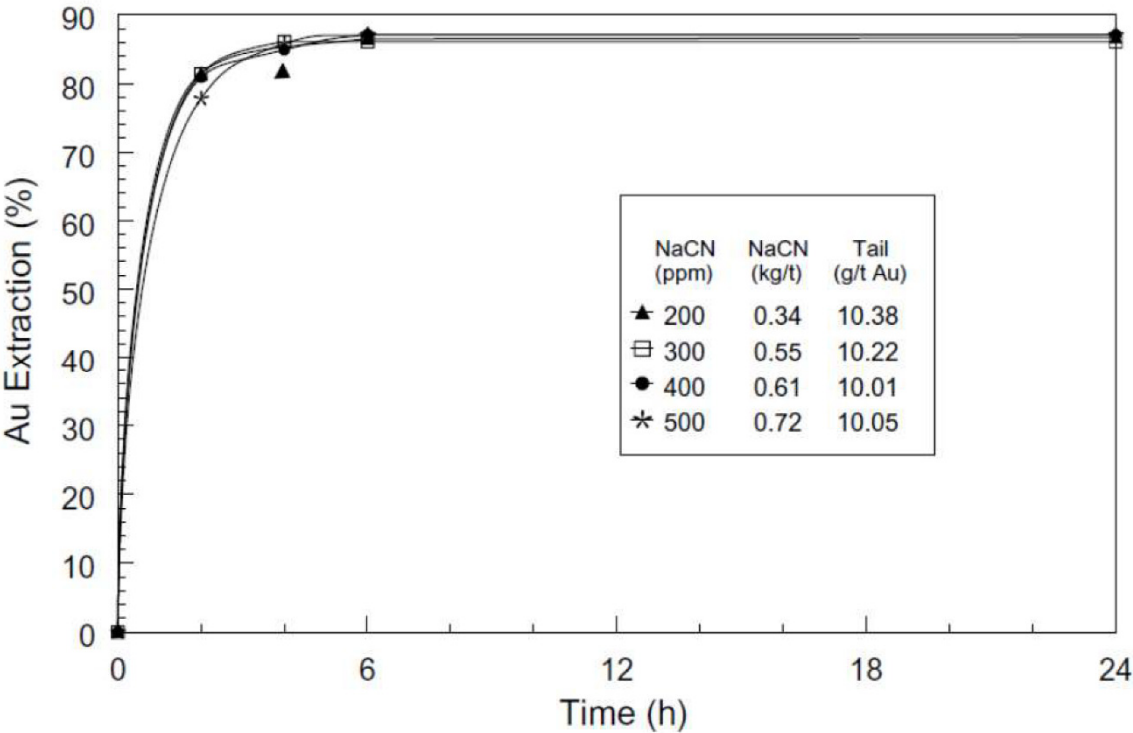


**Figure 1.4.** Effect of cyanide concentration on gold leaching [22].

The gold recovery from sulphidic ore was studied by varying the cyanide concentration in the range of 200 to 500 ppm. The reaction was cyanide diffusion controlled below 300 ppm, while the recovery with 400 and 500 ppm cyanide concentration was almost same, as clearly demonstrated by the Figure 1.4. The effect of dissolved oxygen concentration on the dissolution behaviour of gold has been investigated and shown in Figure 1.5, below.

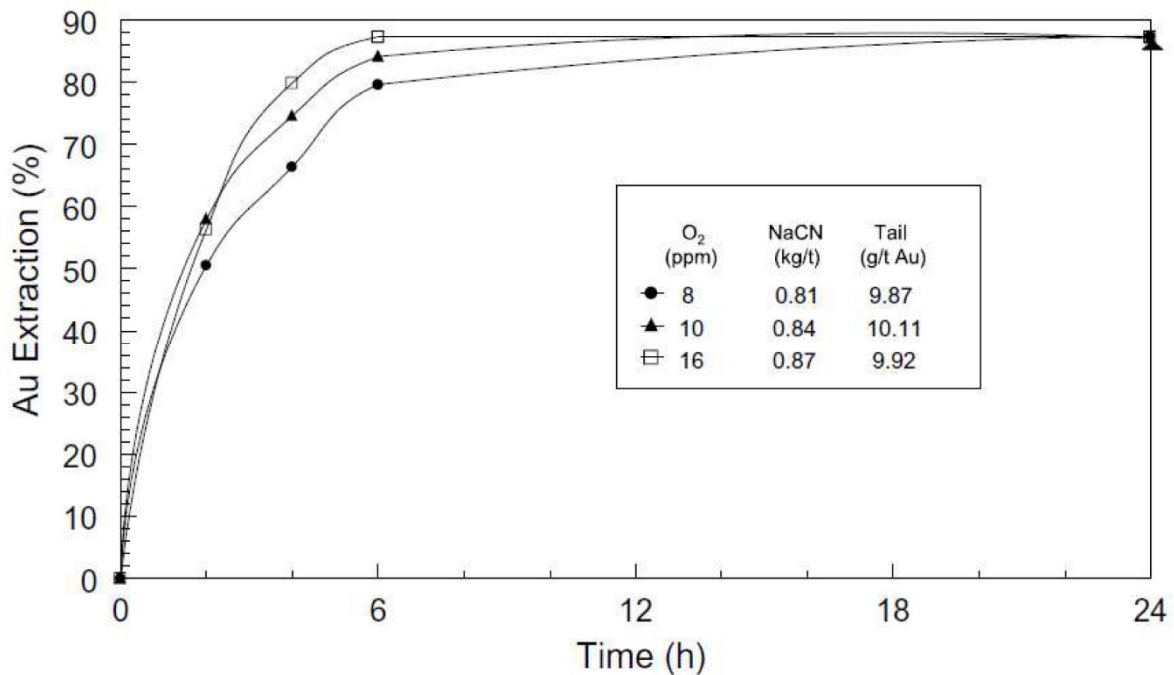


**Figure 1.5.** Effect of oxygen concentration on gold leaching [22].

Gold dissolution kinetics was significantly enhanced at elevated dissolved oxygen concentrations. The dissolved oxygen could be enhanced by the use of pure oxygen as compared to common practice of air in gold mining industries and also by using closed pressurized systems. All this contributes much towards the processing cost of gold ores. Therefore the optimum concentrations of dissolved oxygen and cyanide should be used and it is solely ore dependent and can vary from site to site. The concentrations higher and/or lower than the optimum value may have negative effect on the gold leaching process [18,19].

### 1.3.2. Effect of pH

In gold leaching circuits, lime (CaO) is generally used to maintain pH of the leach solution. The gold dissolution rate is expected to decrease with increasing pH since the adsorption of hydroxyl ions (OH<sup>-</sup>) passivates the gold surface [11].

The gold leaching with cyanide is typically performed at pH values greater than 9.4, in order to prevent the loss of cyanide ions by hydrolysis. The free cyanide ion concentration is reduced from 95 to 5.8% as pH is reduced from 10.5 to 8. This results in a 16-fold increase

in cyanide consumption to get acceptable leaching rates. The cyanide leaching at low pH values was investigated by the researchers to minimize the lime cost. The cyanide consumption can be reduced by using the closed leach tanks, as HCN gas loss is minimized. Ultimately the cyanide consumption is increased at low pH values, as HCN does not appear to leach gold at sufficient rates [23].

The effect of pH on the gold and silver extraction was studied in the pH range of 10.5–13, for a Bacís concentrate comprising silver iron sulphide, silver sulphide or argentite, pyrite, pyrrhotite, arsenopyrite, chalcopyrite, covellite, hematite, and magnetite. Gold and silver extraction tends to decrease above a pH value of 11.5, because of enhanced oxidation of pyrite and pyrrhotite in highly alkaline medium [24].

### **1.3.3. Effect of Particle Size**

The dissolution rate of gold in cyanide solution is directly proportional to the exposed surface area which is related to the particle size distribution and liberation characteristics of the feed material. The gold dissolution rate generally increases with decreasing particle size due to increase of the gold liberation and the surface area [9].

However this is not always the case, as the decrease in the particle size increases cyanide consumption. In the presence of cyanicides in gold ore, there is a competition between cyanicides and gold dissolution and consequently the dissolution rate of gold may decrease as well [3,4,11,22].

### **1.3.4. Effect of Temperature, Pressure and Agitation**

Temperature, pressure and agitation have a significant effect on gold dissolution rate and oxygen solubility. In practice. The rate of gold dissolution depends on temperature of the leach solution, aeration, agitation speed and pressure. The concentration of oxygen in water is one of the most important variables and it is a function of temperature, altitude and oxygen partial pressure. By rising the temperature, the dissolved oxygen concentration in the leach solution decreases and the diffusivity of reactants through the Nernst boundary layer becomes much faster with the decrease in viscosity of liquid. The effect of temperature on gold

dissolution should be optimized between these two cut-off marks. However, generally the increase of the temperature creates problems in plant related operations [3,4,25,26].

Gas solubility is enhanced by increasing pressure that can improve gold dissolution. High pressure, along with high temperature, is claimed to improve gold extraction. The gold dissolution with cyanide under normally applied conditions is considered to be mass transport control. The dissolution rate depends on the thickness of the diffusion layer and mixing characteristics. The thickness of the diffusion layer is reduced by increasing the solution flow rates. The gold dissolution is significantly enhanced by increasing the degree of agitation in poorly mixed systems. On the other hand in well-mixed systems, the mechanical mixing and air agitation is preferred [3,4,11,27].

#### **1.4. Galvanic Interactions and Passivation Effect**

The usual association of gold with the conducting sulphide minerals give rise to the concept of galvanic interactions in gold leaching. The conducting sulphide minerals allow the electron transfer reactions at their surfaces. The galvanic interaction between the gold particles and associated sulphide minerals significantly affect the gold leaching rate in cyanide solution. When two conducting minerals are brought in contact with each other, the galvanic corrosion occurs, depending upon the difference between the electrode potentials [3,4,28].

The sulphide minerals mostly associated with gold have lower potential than gold and act as cathode when in galvanic contacts with gold. The permanent galvanic contacts are not easy to achieve between the rotating disk gold electrodes and slurry of sulphide-rich ores. A packed bed reactor (PBR) was developed and tested to study the galvanic and passivation effects for the sulphide minerals, such as, pyrite ( $\text{FeS}_2$ ), chalcopyrite ( $\text{CuFeS}_2$ ), sphalerite ( $\text{ZnS}$ ), chalcocite ( $\text{Cu}_2\text{S}$ ), galena ( $\text{PbS}$ ), stibnite ( $\text{Sb}_2\text{S}_3$ ) and an industrial ore, with the mineral and gold particles having direct surface-to-surface contact. The gold powder was dispersed in the respective sulphide mineral for studying the galvanic effect and gold was dispersed in the silica to study the passivation effect of the sulphide mineral on the gold leaching.

The gold containing sulphide and silica layers were segregated from one another by means of a sintered glass disk. The leaching conditions used comprise: 30 mM NaCN, pH 11,

dissolved oxygen ( $\text{DO}_2$ ) 8.5 mg/L and at 25 °C temperature. The sulphide minerals, such as, pyrite, chalcopyrite and galena, enhanced gold dissolution rate significantly while under galvanic interaction from the respective sulphide minerals. On the other hand, sphalerite, chalcocite and stibnite were found to have severe retarding effect on gold dissolution, even under galvanic interaction from these minerals. Galena gives the highest gold recovery (90%) when galvanic contacts were enabled and 73% gold recovery for the gold particles associated with pyrite mineral. All sulphidic minerals mentioned above, except galena, were found to impose severe retarding effect on gold recovery, while gold particles were present within silica and contiguous to these sulphide mineral layers. Gold recovery under passivation effect from galena was found to be 70%, while for all other sulphides the gold recovery was less than 5% [21,29,30].

### **1.5. Effect of Lead and Other Metal Ions**

The dissolution of pure gold proceeds much more slowly as compared to gold alloyed with silver or the gold associated with other metals. It has been well established in the literature that this slow dissolution is due to the formation of a cyano-aurate, AuCN passivation film, on the surface of gold. Pure gold is more vulnerable to surface passivation and the presence of certain additives or cations can accelerate the gold dissolution kinetics. The presence of lead ions even at low concentration and ferro cyanide ions  $[\text{Fe}(\text{CN})_6]^{4-}$  at high concentration have a pronounced positive effect on the gold leaching while copper cyanide at moderate concentration has a tendency to slightly retard the gold dissolution. The effect of lead ions on gold dissolution have been investigated at a concentration of 10 mg/L lead acetate at pH value of 10.4 and 11.7. The presence of lime and lead acetate, have a marked decrease in gold dissolution at a high concentration of lead acetate. Addition of galena was observed to have an increasing effect on gold dissolution rate due to the released lead ions [8,10,30,31].

The REQCM was used to study the effect of lead on gold dissolution in presence of air-saturated cyanide solution system. The addition of lead, even in trace amounts, significantly enhances the dissolution rate, by cementing on the gold surface and disrupting the well-known AuCN passive film. The cementation of lead on gold surface enhances both the gold oxidation and oxygen reduction via a bimetallic corrosion process [32]. The presence of low



concentrations of lead, mercury, thallium or bismuth significantly improves the rate of leaching of gold by avoiding the gold surface passivation effect occurring at a potential value of -0.4 V. Lead present in the concentration range from  $10^{-6}$  to  $10^{-5}$  M, found to be beneficial, whereas the Pb (II) concentrations above  $10^{-4}$  M, were found to have rather a negative effect on the gold dissolution rate [33,34].

The silver ions in cyanide solution can also have positive effect on the gold dissolution rate but it is less pronounced as compared to the gold-silver alloy [34,35]. The effect of lead addition in leaching of the Goldcorp Red Lake Mine ore has been indicated below:

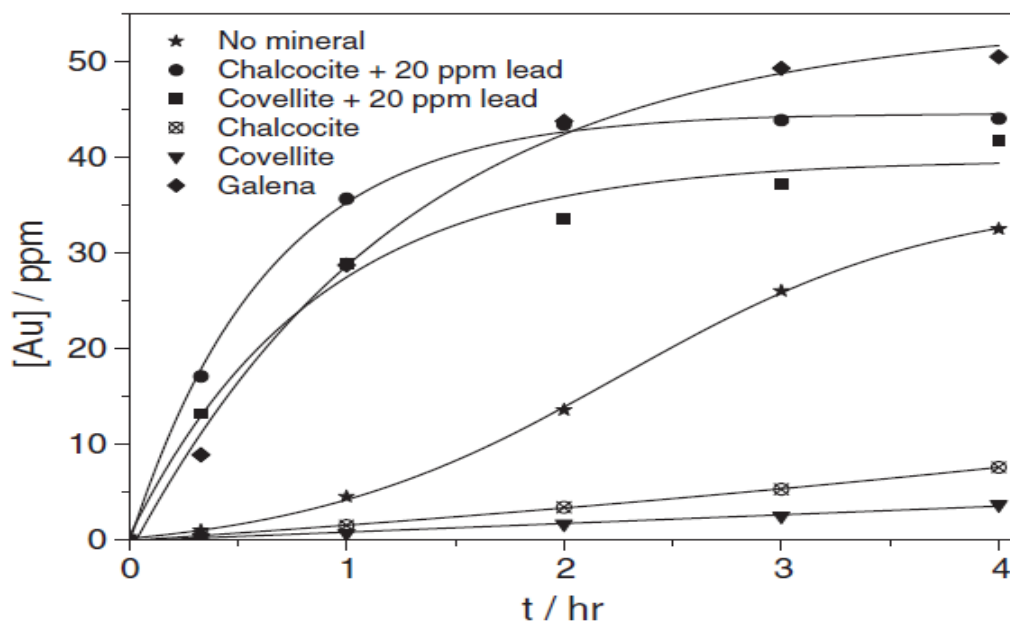


**Figure 1.6.** Effect of lead addition on gold dissolution: 10 mmol/L cyanide, 50 mg/L pure gold powder and various sulfide minerals [36].

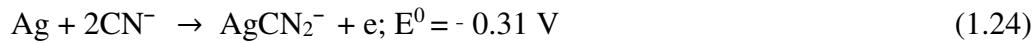
Chalcocite and covellite minerals were found to be severely retarding towards gold dissolution as shown in Figure 1.6. Lead addition have promoted the gold dissolution rate significantly in case of both chalcocite and covellite minerals.

## 1.6. Effect of Silver Minerals

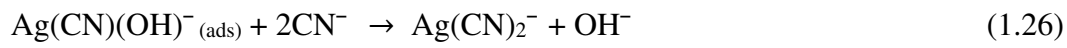
Gold is almost always associated with silver. When the silver grade is high (>10 g/t) and/or the gold is present as electrum, the gold recovery process may need some modifications in

the operation [3,4]. In case of high-silver gold ores, silver is frequently associated with polymetal sulphides and sulfosalts. There are over 200 argentiferous minerals reported in literature, the economically significant sulphide phases include acanthite ( $\text{Ag}_2\text{S}$ ), pyrrargyrite ( $\text{Ag}_3\text{SbS}_3$ ), aguilarite ( $\text{Ag}_4\text{SeS}$ ), andorite ( $\text{Sb}_3\text{PbAgS}_6$ ), tennantite  $\text{Cu}_6[\text{Cu}_4(\text{Fe,Ag,Zn})_2\text{As}_4\text{S}_{13}]$  and tetrahedrite  $[(\text{Cu,Fe,Ag,Zn})_{12}\text{Sb}_4\text{S}_{13}]$ , [4,37-39].

In a similar manner to gold, the anodic dissolution of metallic silver in aqueous cyanide solution, proceeds according to the following reaction [3,4].



At high cyanide concentrations, silver forms higher order complexes such as  $\text{Ag}[\text{CN}]_3^{2-}$  and  $\text{Ag}[\text{CN}]_4^{3-}$ , but these complexes have least practical importance. The mechanism of activation of gold dissolution by silver can be elaborated as follows [3,4,10].



The greater reactivity of silver particularly influences the behavior of gold in flotation, leaching and/or recovery processes. The dissolution of silver is slow as compared to gold under typical cyanidation conditions prevailing in gold leaching. This is because the more common silver minerals found in nature are the less soluble in aerated cyanide solution [3,4]. The refractory nature of the silver sulphide and sulfosalt minerals of silver is the prime cause of poor silver recovery. The sulphide ion must be oxidized to release the ionic silver, in case of silver sulphides and sulfosalts and this characteristic differentiates the mechanism of silver sulfides and sulfosalts leaching, from the mechanism involved in metallic and oxidized phase leaching [40-43].

The effect of sulphide minerals, on the leaching of silver metal in a packed-bed electrochemical reactor (PBER), has been studied. The galvanic effect of sulphide minerals plays a significant role in silver dissolution with aerated cyanide solution. The presence of silver also enhanced the leaching of gold associated with pyrite mineral [20,21].

Some attention has been given to effect of silver on gold dissolution rate. The effect of dissolved silver on the kinetic enhancement of gold dissolution and also the effect of gold-silver alloy (1-5%, silver alloyed with gold), has been investigated on the gold leaching behaviour. The addition of silver enhances the dissolution of gold whether alloyed or in solution form. While studying galvanic interactions, the presence of silver with gold is of utmost importance to get an insight of galvanic interactions and their effect on gold dissolution [34,35].

### **1.7. Effect of Sulphide Minerals**

The sulphide minerals associated with gold contain sulphide ( $S^{2-}$ ) as the main anion. Most metal sulphides decompose readily in aerated alkaline cyanide solutions. Sulphide minerals are also oxidized to form thiocyanate or to react with oxygen, forming sulphide and sulfate [3,4].

Sulphide ions ( $S^{2-}$ ), formed by the decomposition of sulphide minerals, have detrimental effect on the kinetics of gold and silver cyanidation. However, the effect of sulphide minerals on gold dissolution decreases in the order: stibnite ( $Sb_2S_3$ ) >>> orpiment ( $As_2S_3$ ) > arsenopyrite ( $FeAsS$ ) > realgar ( $As_4S_4$ ) > pyrrhotite ( $FeS$ ) > chalcopyrite ( $CuFeS_2$ ). The species formed during gold cyanidation with sulphide minerals, such as  $Au_2S$ ,  $Ag_2S$  and the formation of oxo and thioxo salts ( $SbO_3^{3-}$ ,  $SbS_3^{3-}$ ), passivate the gold surface and consequently retard the gold dissolution. Oxidation of sulphide minerals results in an enhancement of cyanide and dissolved oxygen consumption and affect the processing cost [10].

The dissolution of gold with sulphide minerals such as, pyrite ( $FeS_2$ ), chalcopyrite ( $CuFeS_2$ ), sphalerite ( $ZnS$ ), chalcocite ( $Cu_2S$ ), galena ( $PbS$ ), stibnite ( $Sb_2S_3$ ) was studied in detail. The operating conditions for gold dissolution were: 30 mM NaCN, pH 11, dissolved oxygen ( $DO_2$ ) 8.5 mg/L and at 25 °C temperature. The association of galena and pyrite enhanced the gold recovery significantly, while the gold recovery with chalcopyrite remained on the lower end. Sphalerite and stibnite severely hindered the gold dissolution. In case of chalcocite, because of high dissolution of copper, all of the available cyanide was consumed without giving any gold dissolution. The sulphide minerals have the ability to transfer electrons at

their surfaces, thus higher contents of sulphide minerals give rise higher surface area, resulting in an enhanced oxygen reduction process. This enhanced oxygen reduction ultimately increases the kinetics of gold dissolution [21,29,30].

### **1.8. Effect of Copper Minerals**

The association of gold and copper minerals in a commercially viable gold-copper ore is a common occurrence. The predominant spectrum is the copper ore, which contains levels of gold minerals. Most of the copper minerals react readily with aerated cyanide solutions [3,4,44]. Gold and copper dissolution in aerated cyanide solutions has been found to be dependent on both the cyanide and oxygen concentrations. It has further been reported that in aerated solutions, the dissolution of gold is cyanide diffusion controlled at cyanide concentrations, i.e., *less than 2 mM/L* and oxygen diffusion controlled at cyanide concentrations, i.e., *more than 2 mM/L*. Silmilarly, copper dissolution is cyanide diffusion controlled at cyanide concentrations i.e., *less than 1 mM/L* and oxygen diffusion controlled at cyanide concentrations, i.e., *more than 6 mM/L* [13,45].

Copper on reaction with aerated cyanide solution, results in the form of four complexes with the uptake of cyanide ligands up to four. The formation of the cyano-copper complexes depend on cyanide concentration and pH of the cyanide leach solution, as shown in Figure 1.7.

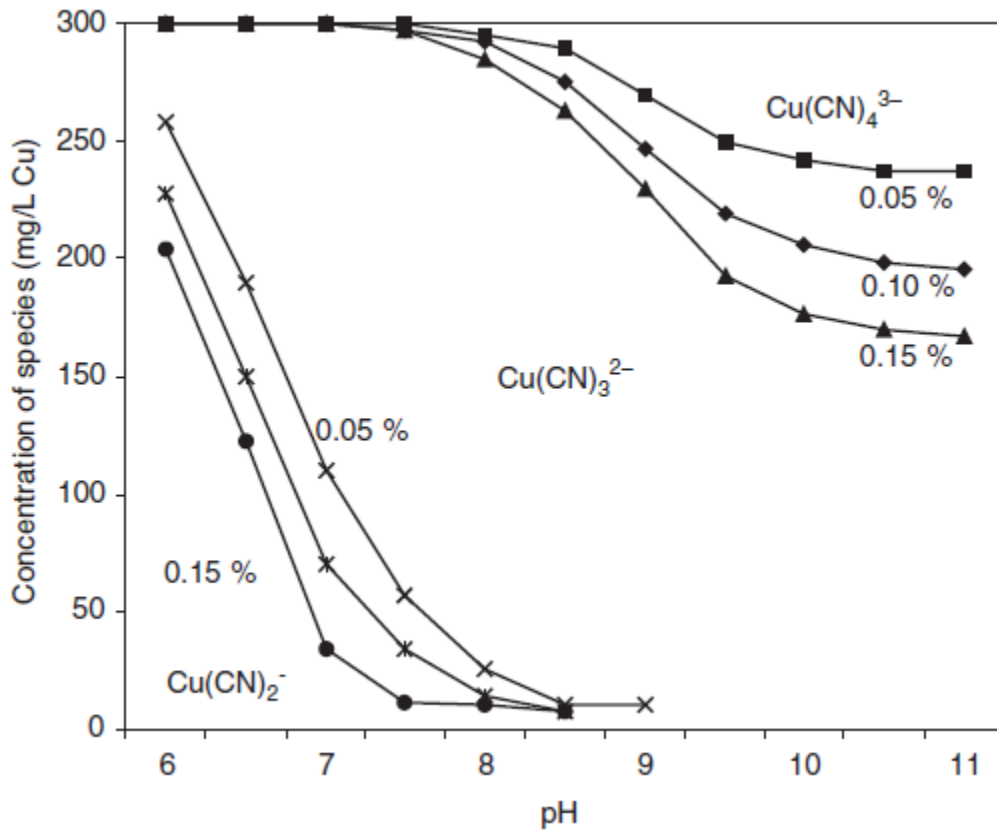


**Figure 1.7.** Distribution of Cu complexes as a function of NaCN concentration and pH [46].

Sodium cyanide concentration and pH dependent distribution of the various copper complexes indicates that higher-order copper (I) cyanide complexes are favourable at high pH and free-cyanide conditions. This figure also illustrates that for any given conditions usually only two of the species are present in any significant quantities [46]. The prime complication, while leaching gold in presence of copper minerals, is the possibility of low free cyanide concentration. This is eventually because of the formation of copper(I) cyanide complexes, such as  $\text{Cu(CN)}_2^-$ ,  $\text{Cu(CN)}_3^{2-}$  and  $\text{Cu(CN)}_4^{3-}$ , depending upon the pH and potential of the leaching process. Copper present as  $\text{Cu(CN)}_3^{2-}$ , can leach gold at reasonable rates but the gold leaching kinetics with  $\text{Cu(CN)}_2^-$  is very slow [3,4,36].

## 1.9. Effect of Antimony Minerals

Stibnite ( $\text{Sb}_2\text{S}_3$ ) is known to be the principal antimony sulphide mineral associated with gold, while the antimony sulphides such as, berthierite ( $\text{FeSb}_2\text{S}_4$ ) and gudmundite ( $\text{FeSbS}$ ) have also been reported in literature. The chemistry of stibnite in aerated alkaline cyanide solutions concerns the consumption of both cyanide and lime as well as the production of species like sulphides ( $\text{S}^{2-}$ ), thiosulfate ( $\text{S}_2\text{O}_3^{2-}$ ), and thiocyanate ( $\text{SCN}^-$ ) in the leach solution. The products formed by the oxidation of stibnite under these conditions include antimonites ( $\text{HSbO}_3^{2-}$ ), antimonates ( $\text{HSbO}_4^{2-}$ ), thioantimonites ( $\text{SbS}_3^{3-}$ ) and thioantimonates ( $\text{SbS}_4^{3-}$ ). Cyanide consumption following an increase in case of stibnite present within ore, is related to reactions of sulfur species with aqueous cyanide solution and resulting in the formation of thiocyanate. Antimony does not form complexes with aerated alkaline cyanide solution [8].

Hedley and Tabachnick (1958) performed the cyanidation of a synthetic ore containing 0.25% stibnite at pH values of 10, 11, and 12. The rate of gold dissolution with stibnite is strongly dependent on pH. The rate of gold dissolution decreases with the dissolution of stibnite mineral. Highest gold dissolution was observed at a pH value of 10, while lowest at pH value of 12. It is reported that the rate of stibnite dissolution is appreciable at pH 12, reducing to low levels at pH 10. At higher pH values, antimony pentoxide ( $\text{Sb}_2\text{O}_5$ ), has been observed on gold surfaces, which ultimately inhibit the gold dissolution [47].

The sulphur-containing anions such as sulphides ( $\text{S}^{2-}$ ), and thioantimonites ( $\text{SbS}_3^{3-}$ ), are known to be strong “*poisons*” in gold cyanidation. Dissolved sulphides even at very low levels as 0.5 mg/L, can have a significant retarding effect on the rates of gold dissolution. In case of minor quantities of stibnite present in gold bearing ores, the strategies like pre-aeration, lead addition, and pH control could negate the adverse effects due to the stibnite [8,48].

## 1.10. Effect of Carbonaceous Minerals

Naturally occurring carbon containing materials which are capable of adsorbing gold cyanide from cyanide leaching solutions are known as carbonaceous or preg-robbing minerals. The graphitic form of the carbon is generally preg-robbing and the extent of preg-robbing depends

upon the concentration of the carbonaceous material and the degree of disorder in the graphite structure. The carbonaceous ores may have a preg-robbing capacity of *less than* 1 g Au/t ore for the mild preg-robbing ores, while a preg-robbing capacity of *more than* 500 g Au/t ore, for the extreme preg-robbing gold ores. Carbon-in-leach circuits are used as an attractive option for the mild preg-robbing ores, while more extreme treatment options, such as roasting (Goldstrike) and chlorination, are required for the processing of very high preg-robbing ores [3,4,49].

Pure gold foils were coated with activated carbon, graphite, carbon black and the carbonaceous matter extracted from the Stawell gold ore, having a coating of thickness ( $< 1 \mu\text{m}$  for all). The leaching tests were conducted and the gold leaching rate was monitored for a total retention time of up to 48 h. The carbonaceous matter extracted from the Stawell gold ore, predominantly crystalline graphite, showed a very little gold adsorption at moderate cyanide concentration, i.e., *more than* 250 mg/L KCN. A significant detrimental effect of the carbonaceous coating was observed on gold dissolution, when gold was pre-ground with the carbonaceous ore. The detrimental effect of the sulphide coating on the gold surfaces was found to be less pronounced as compared to the carbonaceous coating.

The presence of the carbonaceous materials in many sulphide ores are widely considered to be the significant preg-robbing components. In cyanide leaching system, the behaviour of sulphide ions and lead was studied in the presence of carbon coatings. The retardation of gold dissolution with sulphides was almost the same in presence of carbon coatings and this effect became more pronounced at a higher sulphide concentration. The gold dissolution was slightly higher in a medium range of sulphides, 0.2–5 mg  $\text{S}^{2-}$ /L, with a carbon coating than without carbon coatings. Due to the reduction of lead hydroxide formed at the surface of gold foils, the dissolution rate was slightly higher for gold with a carbon coated foil at a concentration of 5 mg/L  $\text{Pb}^{2+}$ , even though carbon coating hindered the diffusion of lead and hence reduced the effect of lead on gold dissolution [50,51].

### **1.11. Effect of Telluride Minerals**

A small number of gold tellurides have been treated commercially in limited regions round the globe. The processing of the gold telluride ores has been proved to be problematic in gold

leaching without some oxidative pre-treatment steps. Roasting is the most frequently used oxidative method in case of tellurides. Calaverite [AuTe<sub>2</sub>] is known to be the most common associated mineral of tellurium with gold, whereas the association of silver comprise the minerals, such as: petzite [Ag<sub>3</sub>AuTe<sub>2</sub>], sylvanite [(Au,Ag)Te<sub>2</sub>] and krennerite [(Au,Ag)Te<sub>2</sub>], [3,4].

Flotation is considered to concentrate the tellurides from the telluride bearing gold ores, to be processed separately. The tellurides float readily at neutral pH values with frother only, but the addition of xanthates can improve the flotation. The telluride minerals were selectively floated by the integrated telluride-flotation circuits in the Emperor Mine in Fiji.

A two-stage leaching was performed on a high grade KCGM (Kalgoorlie Consolidated Gold Mines), flotation concentrate. The first stage leaching was performed by employing 0.1% NaCN at a pH value of 9.2 for 24 h, to dissolve the native gold. Stringent conditions, such as, 2% NaCN, pH 12.5 were employed for 96 h. The proportion of the gold dissolved was reported to be 6 and 11% for the first and second stages, respectively [52].

Direct leaching process with the tellurides cannot be carried out with ease. The leaching process is considered to be affected by the presence of sulphides which precipitates the free tellurium from the solution and is known to be detrimental for the gold dissolution by cyanide. The sulphide minerals have to be removed by pre-treatment before cyanidation. The gold recovery from tellurides can be increased by fine grinding, enhanced leaching times and excessive addition of lime. The high lime concentration along with the addition of lead nitrate significantly reduces the cyanide consumption. Thiourea, ammoniacal thiosulfate, carbon-in-pulp (CIP) and resin-in-pulp (RIP) processes have also been used for gold leaching from the telluride ores [3,4,53].

## **1.12. Research Objectives**

Till now, gold cyanidation is the most accomplished approach for gold leaching in the industry. Although several studies have dealt with the effect of silver on gold cyanidation, they nevertheless address some questions. First, few studies have assessed the effect of silver (alloyed with gold & in dissolved form) on the kinetic studies of gold dissolution with pure



aerated cyanide solution. Second, most studies have examined the effect silver on the kinetics of gold dissolution, without taking into account the presence of interactions from sulphide minerals, such as gold-sulphide, sulphide-sulphide, silver-sulphide and consequently their influence on the leaching of gold. Thirdly, no gold leaching studies have been carried out on the influence of prominent silver minerals (metallic silver, acanthite and pyrargyrite), in case of high-silver gold ores.

In this regard, the effect of silver minerals was investigated on the kinetics of gold leaching. These silver minerals are rightly considered as prominent constituents that possess some unique influences on the leaching behavior of gold, while gold and silver minerals embedded within sulphide mineral matrices. The present thesis aims at the following objectives:

1. The influence of various silver phases and soluble silver on the kinetics of gold leaching in free state as well as gold associated with sulphide minerals under galvanic and passivation effects.
2. The ease with which the silver metal itself is leached from its bearing mineral species while present within silica and sulphide mineral matrices under galvanic and passivation from the base-metal sulphides.

In view of the above stated goals, four sections (Chapters 2-5) presenting the theoretical background and experimental results related to this study are provided in this thesis:

In Chapter two a study was performed to investigate the effect of silver (Ag) on the kinetics of gold leaching in the presence of sulphidic minerals in an arrangement of mixed as well as segregated multi-layers system. The combination of mineral systems established were: pyrite-chalcopyrite-silica, pyrite-sphalerite-silica, and pyrite-stibnite-silica systems, to study the effect of silver (Ag), in relevance to the galvanic and passivation effects from mixed and segregated mineral layers.

Chapter three was intended to investigate the effect of silver sulphide (acanthite), on the kinetics of gold dissolution in the presence of sulphidic minerals, both under galvanic interaction and passivation effect. Pyrite-silica, chalcopyrite-silica, sphalerite-silica, and stibnite-silica, were the mineral systems established in this case. Gold leaching kinetics was

investigated by the simultaneous dispersion of both gold & acanthite within the sulphide as well as silica layers. Surface analysis was performed for elucidating the species present at the surface of gold particles isolated after gold cyanidation with chalcopyrite and stibnite minerals.

Chapter four was allocated to investigate the effect of pyrargyrite and also accumulative silver minerals on the kinetics of gold leaching. Pyrite-silica, chalcopyrite-silica, sphalerite-silica, and stibnite-silica were the system of sulphide mineral arrangements. In first part of this chapter the effect of pyrargyrite was investigated on the leaching kinetics of gold embedded within sulphide matrices. Second part of this chapter comprise the accumulative influence of silver mineral (metallic silver, acanthite and pyrargyrite), on the kinetics of gold leaching with reference to the galvanic and passivation effects from the base-metal sulphides.

Finally in fifth chapter kinetic aspects of gold dissolution were investigated with reference to the pre-treatment and additive effect, for the gold associated with silver minerals and embedded within base-metal sulphides. Strategies such as, lead acetate addition and pre-treatment with aerated alkaline lead acetate solution were adopted the remove the harmful effect of the species resulted by the dissolution of sulphides, especially in case of chalcopyrite and stibnite minerals. Lead addition and pre-treatment study was carried on gold dissolution behaviour already under the influence of accumulative silver minerals (metallic silver, acanthite and pyrargyrite) and base-metal sulphides. Pyrite-silica, chalcopyrite-silica, sphalerite-silica, and stibnite-silica were the sulphide mineral systems.

### **1.13. Hypothesis**

Taking into account the effects of the base-metal sulphides as well as those of the silver minerals on the dissolution behaviour of gold in aerated cyanide solution, it would be possible to identify the most significant criteria in the reaction kinetics of the gold particles in order to improve the dissolution of gold. This approach is vital for a precise knowledge and improvement of the gold cyanidation process because it would make it possible to produce an optimal gold cyanidation strategy keeping in view the simultaneous effects of sulphides and silver minerals on the gold cyanidation process. This assessment could influence the gold leaching processes because of the increasing trend of dealing with the processing of sulphide

ores in gold mining industry. The premises of this project cover the study starting from the role of base-metal sulphides to the effect of silver minerals on gold cyanidation. In this project, silver, being the key element in context of silver bearing ores, drove to the final synopsis of the project.

#### 1.14. Research Strategy Adopted for Ph.D. Thesis

Based on the research objectives elaborated above, the scientific strategy adopted in this Ph.D. thesis is shown in the Fig. 1.8., below:

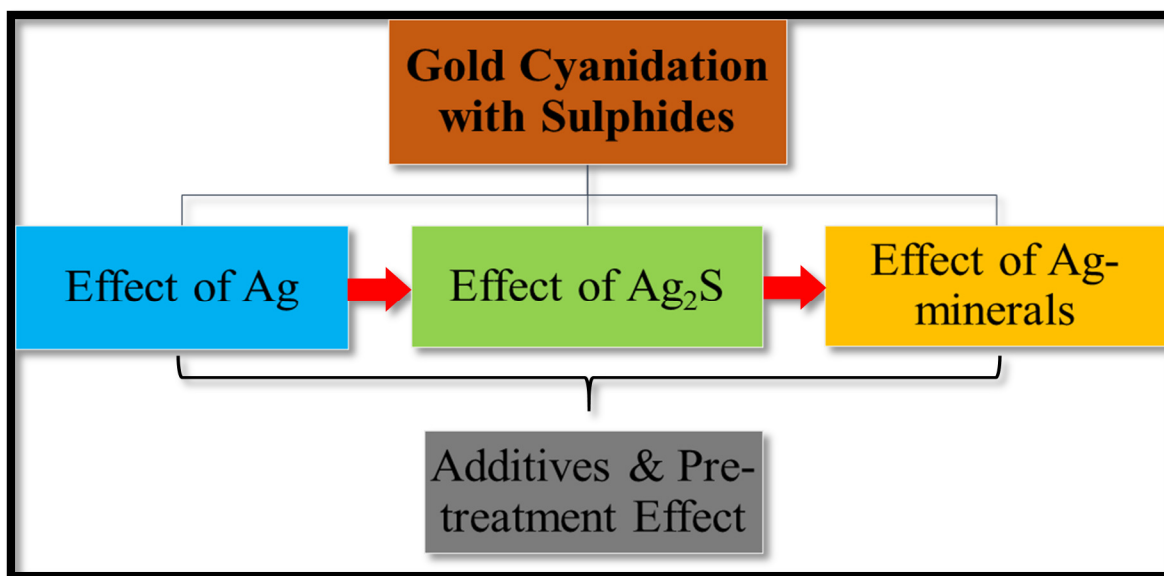






**Figure 1.8.** A representative demonstration of the strategy adopted in this thesis.

A brief description of the experimental methodology generally adopted in this thesis work has been explained as well.

- a) Gold dissolution behavior was monitored under galvanic as well as passivation effects from the base-metal sulphides. Pyrite, chalcopyrite, sphalerite and stibnite were the sulphidic minerals investigated in the present study. This would enable us to single out the galvanic interactions and passivation effect regarding the dissolution kinetics of gold. This study was performed by using a packed bed reactor approach.

- b) Effect of metallic silver on the dissolution behaviour of gold in mixed as well as segregated multi-layer sulphide mineral systems was investigated. Association of silver along with gold was study in comparison to base-metal sulphides, such as the pyrite-sphalerite-silica system, the pyrite-chalcopyrite-silica and the pyrite-stibnite-silica systems. Gold dissolution behaviour was monitored for a mixed as well as segregated multi-layer, multi-sulphidic mineral system.
- c) The impact of silver sulphide (acanthite) was investigated on the dissolution behaviour of gold both under the galvanic interaction and passivation phenomenon from the base-metal sulphides. Pyrite-silica, chalcopyrite-silica, sphalerite-silica systems and stibnite-silica systems, were the base-metal sulphide systems taken into account in the present thesis work. X-ray photoelectron spectroscopy was used to analyze the surface of the gold particles after the cyanidation process.
- d) Influence of pyrargyrite on the dissolution behaviour of gold was addressed for the Py-Si, Cp-Si, Sp-Si and Sb-Si systems, once again in context with galvanic interactions and passivation phenomenon. Also the effect of accumulative silver minerals ( $\text{Ag}+\text{Ag}_2\text{S}+\text{Ag}_3\text{SbS}_3$ ), was investigated towards their influence on the dissolution behaviour of gold, for the above stated sulphide mineral systems.
- e) Additives and pre-treatment effect were investigated on the dissolution kinetics of gold, while gold associated with the silver minerals and embedded within the base-metal sulphides. Lead acetate salt was used as an additive in various concentrations of 10, 20 and 100 mg/L, added to the aerated alkaline cyanide solution. Pre-treatment tests were performed with a 100 mg/L aerated alkaline lead acetate solution for 16 hrs prior to the cyanidation process.

The key points the various chapters presenting the results of this project, shaped into scientific articles, have been tabulated as under:

	<b>Chapter 2</b> Effect of silver on gold cyanidation in mixed and segregated sulphidic minerals
	Gold dissolution with base-metal sulphides Effect of silver on dissolution behaviour of gold Mixed and segregated multi-layer sulphide systems
	<b>Chapter 3</b> Impact of silver sulphide on gold cyanidation with conductive sulphide minerals
	Impact of acanthite on gold dissolution with sulphides XPS study of the gold particles isolated after cyanidation
	<b>Chapter 4</b> Accumulative Impact of Silver Sulphides on Gold Cyanidation in Polymetal Sulphides
	Effect of pyrargyrite on the dissolution of gold Accumulative effect of silver minerals on gold dissolution
	<b>Chapter 5</b> The role of lead on the cyanidation of gold associated with silver minerals embedded within base-metal sulphide mineral matrices
	Lead acetate addition towards gold dissolution with sulphides Effect of alkaline lead acetate pre-treatment XPS study of the gold particles for Sb-Si system

## 1.15. References

1. Marsden, J. O., and House, C. I., 2006. Chemistry of gold extraction. 2<sup>nd</sup> ed. Littleton, Colorado: Society for Mining, Metallurgy, and Exploration (SME), 2006.
2. U.S. Geological Survey, 2014. Gold statistics. In: Kelly, T.D., Matos, G.R. (Eds.), Historical Statistics for Mineral and Material Commodities in the United States, U.S. Geological Survey Data Series, vol. 140. <http://minerals.usgs.gov/minerals/pubs/historical-statistics/>.
3. Feldtmann, W. R., 1894. Notes on Gold Extraction by Means of Cyanide of Potassium (MacArthur-Forrest Patents), as Carried Out on the Witwatersrand Gold Fields, Transvaal, South Africa. Argus Printing & Publishing Co, Johannesburg, pp. 42.
4. Adams, M. D., 2016. Gold Ore Processing: Project Development and Operations, 2nd ed. Elsevier (ISBN 978-0-444-63658-4).
5. Jeffrey, M., 1997. PhD thesis: A kinetic and electrochemical study of the dissolution of gold in aerated cyanide solutions: the role of solid and solution phase purity. Curtin University of Technology, Western Australia.

6. Maxey, A., Gonnella, P., Ball, Y., Herkenhoff, P., 1997. Gold. In Register of Australian Mining 1996/1997, Ed. Louthean, R., Resource Information Unit Ltd. Bassendean, WA.
7. Chandler, B. D., Alexander, B., Schabel, A. B., and Pignolet, L. H., 2000. Preparation and Characterization of Supported Bimetallic Pt–Au and Pt–Cu Catalysts from Bimetallic Molecular Precursors. *Journal of Catalysis*, 193, 186-198.
8. Nicol, M., Fleming, C. and Paul, R., 1987. The chemistry of the extraction of gold, in *The Extractive metallurgy of gold*, vol. 2, Ed. Stanley, G.G., South African Institute of Mining and Metallurgy, Johannesburg, S. Africa, pp. 831-905.
9. d Andrade Lima, L. R. P., and Hodouin, D., 2005. A lumped kinetic model for gold ore cyanidation. *Hydrometallurgy* 79, 121-137.
10. Senanayake, G., 2008. A review of effects of silver, lead, sulfide and carbonaceous matter on gold cyanidation and mechanistic interpretation. *Hydrometallurgy*, 90, 46–73.
11. Ling, P., Papangelakis, V. G, Argyropoulos, S. A., and Kondos, P. D., 1996. An Improved Rate Equation for Cyanidation of a Gold Ore. *Can. Metal. Quaterly*. pp. 225-234.
12. Senanayake, G., 2005. Kinetics and reaction mechanism of gold cyanidation: surface reaction model via Au(I)–OH–CN complexes. *Hydrometallurgy* 80, 1–12.
13. Habashi, F., 1967. *Montana Bureau of Mines and Geology Bulletin* 59, Montana, USA.
14. Finkelstein, N. P., 1972. The chemistry of the extraction of gold from its ores, *Gold Metallurgy in South Africa*, Ed. Adamson, R. J., pp. 284–351.
15. Fisher, W. W., 1994. Comparison of chalcocite dissolution in the sulfate, perchlorate, nitrate, chloride, ammonia, and cyanide system, *Minerals Engineering*, 7, 99–103.
16. Abbot, J. and Brown, D. G., 1990. Kinetics of iron-catalyzed decomposition of hydrogen peroxide in alkaline solution, *International Journal of Chemical Kinetics*, 22, 963–974.
17. Wadsworth, M. E., Zhu, X., Thompson, J. S., and Pereira, C. J., 2000. Gold dissolution and activation in cyanide solution. *Hydrometallurgy*, 57, 1–11.
18. Heath, A. R., and Rumball, J. A., 1998. Optimising cyanide:oxygen ratios in gold CIP/CIL circuits. *Minerals Engineering* 11, 999–1010.
19. Rumball, J. A., Houchin, and M. R., 2003. Cyanide: oxygen ratios for leaching gold in sulfide ores. In: Lorenzen, L., Bradshaw, D.J. (Eds.), 22nd International Mineral Processing Congress, Cape Town, South Africa, September 2003. South African Institute of Mining and Metallurgy, Johannesburg, pp. 1590–1593.
20. Aghamirian, M. M., and Yen, W. T., 2005. A study of gold anodic behavior in the presence of various ions and sulfide minerals in cyanide solution. *Minerals Engineering*, 18, 89–102.

21. Azizi, A., Petre, C. F., Olsen, C., and Larachi, F., 2011. Untangling galvanic and passivation phenomena induced by sulfide minerals on precious metal leaching using a new packed-bed electrochemical cyanidation reactor. *Hydrometallurgy*, 107, 101–111.
22. Deschenes, G., Lacasse, S., and Fulton, M., 2003. Improvement of cyanidation practice at Goldcorp Red Lake Mine. *Minerals Engineering*, 16, 503–509.
23. Perry, R., 1999. Low pH cyanidation of gold. *Minerals Engineering* 12, 1431–1440.
24. Parga, J. R., Valenzuela, J. L., and Cepeda, T. F., 2007. Pressure cyanide leaching for precious metals recovery. *The Journal of The Minerals, Metals & Materials Society*, 59, 43–47.
25. Deschenes, G. and Wallingford, G., 1995, Effect of oxygen and lead nitrate on the cyanidation of a sulfide bearing gold ore, *Minerals Engineering*, 8, 923–931.
26. Deschenes, G. and Homme, P., 1997, Cyanidation of a copper-gold ore. *International Journal of Mineral Processing*, 50, 127–141.
27. Ellis, S., and Senanayake, G., 2004. The effects of dissolved oxygen and cyanide dosage on gold extraction from pyrrhotite-rich ore. *Hydrometallurgy* 72, 39–50.
28. Aghamirian, M. M., and Yen, W. T., 2005. Mechanisms of galvanic interactions between gold and sulfide minerals in cyanide solution. *Minerals Engineering*, 18, 393–407.
29. Azizi, A., Petre, C. F., and Larachi, F., 2012. Leveraging strategies to increase gold cyanidation in the presence of sulfide minerals—Packed bed electrochemical reactor approach. *Hydrometallurgy*, 111–112, 73–81.
30. Azizi, A., Petre, C. F., Assima, G. P., and Larachi, F., 2012. The role of multi-sulfidic mineral binary and ternary galvanic interactions in gold cyanidation in a multi-layer packed-bed electrochemical reactor. *Hydrometallurgy*, 113-114, 51–59.
31. Lorenzen, L., and van Deventer, J. S. J., 1992. The mechanism of leaching of gold from refractory ores. *Minerals Engineering*, 5, 1377–1387.
32. Jeffrey, M.I., and Ritchie, I.M., 2000. The leaching of gold in cyanide solutions in the presence of impurities: I. The effect of lead. *Journal of The Electrochemical Society*, 147, 3257–3262.
33. Deschênes, G., Lastra, R., Brown, J. R., Jin, S., May, O., and Ghali, E., 2000. Effect of lead nitrate on cyanidation of gold ores: progress on the study of the mechanism. *Minerals Engineering*, 13, 1263–1279.
34. Jeffrey, M. I., and Ritchie, I. M., 2000. The leaching of gold in cyanide solutions in the presence of impurities II. The effect of silver. *Journal of The Electrochemical Society*, 147, 3272–3276.

35. Wadsworth, M. E., and Zhu, X., 2003. Kinetics of enhanced gold dissolution: activation by dissolved silver. *International Journal of Mineral Processing*, 72, 301–310.
36. Dai, X., and Jeffrey, M. I., 2008. The effect of sulfide minerals on the leaching of gold in aerated cyanide solutions. *Hydrometallurgy* 82, 118–125.
37. Lin, H. K., Oleson, J. L., and Walsh, D. E., 2010. Behavior of gold and silver in various processing circuits at the Fort Knox Mine. *Minerals and Metallurgical Processing*, 27, 219–223.
38. Celep, O., Alp, I., Paktunc, D., and Thibault, Y., 2011. Implementation of sodium hydroxide pretreatment for refractory antimonial gold and silver ores. *Hydrometallurgy*, 2011, 108: 109–114.
39. Celep, O., Bas, A. D., Yazici, E. Y., Alp, I., and Deveci, H., 2015. Improvement of silver extraction by ultrafine grinding prior to cyanide leaching of the plant tailings of a refractory silver ore. *Mineral Processing and Extractive Metallurgy Review*, 36, 227–236.
40. Luna-Sanchez, R. M., and Lapidus, G. T., 2000. Cyanidation kinetics of silver sulfide. *Hydrometallurgy*, 56, 171–188.
41. Luna-Sánchez, R. M., and Lapidus, G. T., 2005. Mathematical model of the aguilarite ( $\text{Ag}_4\text{SeS}$ ) leaching process in the presence of other refractory silver phases. In: Dixon, D.G., Dry, M.J. (Eds.), *Proceedings of the International Symposium on Computational Analysis in Hydrometallurgy*. Canadian Institute of Mining, Metallurgy and Petroleum, Montreal, ISBN 1-894475-55-0, pp. 417–427.
42. Meléndez, A. M., Arroyo, R., and González, I., 2010. On the reactivity of sulfosalts in cyanide aqueous media: structural, bonding and electronic aspects. *ChemPhysChem* 11, 2879.
43. Meléndez, A. M., González, I., and Arroyo, R., 2010. An approach to the reactivity of isomorphous proustite ( $\text{Ag}_3\text{AsS}_3$ ) and pyrargyrite ( $\text{Ag}_3\text{SbS}_3$ ) in cyanide solutions. *ECS Transactions*, 28, 191–199.
44. Hedley, N., and Tabachnick, H., 1958. *Chemistry of cyanidation*. Mineral Dressing Note 23. New York: American Cyanamid Company.
45. Drok, K., and Ritchie, I., 1997. An investigation of the selective leaching of gold over copper using ammoniacal cyanide. *World Gold '97*, Singapore. The Australasian Institute of Mining and Metallurgy, Melbourne, 87–93.
46. Wang, X., Forsberg, K.S.E., 1990. The chemistry of cyanide-metal complexes in relation to hydrometallurgical processing of precious metals. *Mineral Processing and Extractive Metallurgy Review* 6, 81–125.



47. Young, A., and Luttrell, G. H., 2012. Separation Technologies for Minerals, Coal, and Earth Resources, Society for Mining, Metallurgy and exploration, USA.
48. Fink, C. G. and Putnam, G. L., 1950. The Action of Sulphide Ion and for Metal Salts on the Dissolution of Gold in Cyanide Solutions. Transactions AIME, 187, 952–955.
49. Dunne, R., Buda, K., Hill, M., Staunton, W., Wardell-Johnson, G., and Tjandrawan, V., Assessment of options for economic processing of preg-robbing gold ores. Mineral Processing and Extraxtive Metallurgy Review, 121, 217–223.
50. Tan, H., Feng, D., Lukey, G. C., and van Deventer, J. S. J., 2005. The behaviour of carbonaceous matter in cyanide leaching of gold. Hydrometallurgy, 78, 226–235.
51. Tan, H., Feng, D., Lukey, G. C., and van Deventer, J. S. J., 2005. Effect of carbon coatings on gold dissolution in the presence of sulphide and lead. Minerals Engineering, 18, 1361–1372.
52. Ellis, S., 2005. Treatment of gold-telluride ores. Developments in Mineral Processing 15, 973–984.
53. Zhang, J., Zhang, Y., Richmond, W., and Wang, H. P., 2010. Processing technologies for gold-telluride ores. International Journal of Minerals, Metallurgy and Materials, 17, 1–10.



## Chapter 2: Effect of Silver on Gold Cyanidation in Mixed and Segregated Sulphidic Minerals\*

### Résumé

L'or à l'état naturel est principalement retrouvé sous forme métallique et est fréquemment associé avec d'autres métaux précieux tels que l'argent. Pour la présente étude de cyanuration de l'or, la pyrite, la chalcoppyrite, la sphalérite, et la stibnite ont été retenus comme sulfures métalliques modèles dans l'adoption d'un concept de réacteur à lit fixe multicouches. À l'aide de cette approche, les cinétiques de lixiviation de l'or ont été investiguées. Ces cinétiques ont été accrues de manière notable en présence de pyrite et de chalcoppyrite, avec des récupérations d'or à 94,5% et 85%, respectivement. L'influence de systèmes bicouches de sulfures métalliques sur la dissolution de l'or a aussi été étudiée avec un maximum de dissolution obtenu à 87% dans le cas de la bicouche pyrite-chalcoppyrite. L'effet de la présence d'argent sur la dissolution de l'or a également été investiguée avec de l'or associé aux sulfures métalliques dans des arrangements de couches mélangées et isolées à l'intérieur du réacteur. Trois systèmes de minéraux ont été mis à l'essai, soient : pyrite-chalcoppyrite-silice, pyrite-sphalérite-silice et pyrite-stibnite-silice. L'addition d'argent a augmenté la dissolution de l'or dans le système pyrite-sphalérite-silice, a diminué légèrement la dissolution de l'or dans le système pyrite-stibnite-silice et a considérablement amoindri la dissolution de l'or dans le système pyrite-chalcoppyrite-silice, indépendamment de la présence d'or et d'argent dans des couches isolées ou mélangées dans le réacteur.

---

\* M. Khalid, F. Larachi, Can. J. Chem. Eng. 95 (2017) 698–707.

## **Abstract**

Gold is mostly found in nature in the metallic form and is associated with sulphide minerals and other precious metals most likely silver. Pyrite, chalcopyrite, sphalerite and stibnite were the sulphidic minerals investigated in the present gold-silver cyanidation study by adopting the metal-sulphide multi-layer packed-bed reactor approach. Gold leaching kinetics was enhanced remarkably for the pyrite and chalcopyrite sulphide minerals, with 94.5% and 85% recovery respectively. The influence of a bi-layer sulphidic mineral system on the dissolution of gold was also investigated with a maximum gold dissolution of 87% for the pyrite-chalcopyrite, bi-layer system. The effect of silver on the dissolution of gold was investigated with the gold associated with sulphidic minerals in an arrangement of mixed as well as segregated mineral layers. Three sets of mineral systems were established such as, pyrite-chalcopyrite-silica, pyrite-sphalerite-silica and pyrite-stibnite-silica systems. The addition of silver enhanced the gold dissolution for the pyrite-sphalerite-silica system, slightly lessened the gold dissolution with the pyrite-stibnite-silica system and retarded gold dissolution severely in case of the pyrite-chalcopyrite-silica system, irrespective of the dispersion of gold and silver in the same as well as in the segregated mineral layers.

## 2.1. Introduction

Depletion of the free-milling gold deposits around the globe drew attention of the mining industry towards the processing of refractory sulphidic gold ores. Cyanide is known to be the universal ligand for gold leaching, but not the selective one because most metal sulphides display a wide range of reactivity in alkaline gold cyanidation. In practice, the poor selectivity of cyanide ions towards gold over the enclosing sulphide minerals, leads to low gold extraction and the dissolution of transition (Cu, Fe, Zn, etc.) metals, and the formation of thiocyanate by the dissolution of sulphidic minerals inflict extra costs and profit losses resulting from high levels of cyanide consumption [1,2].

The readily soluble sulphide minerals in cyanide solution render the gold cyanidation process difficult to optimize. The species resulting from the dissolution of sulphide minerals were found to influence the gold cyanidation in various ways. It is generally accepted that these result in enhancement of reagent consumption, also the surface passivation by  $\text{Fe}(\text{OH})_3$  or sulfur are detrimental to gold leaching [3-7]. The surface of the gold particles could be passivated by the solid reaction products from the reacting sulphide minerals [8,9,10].

In presence of sulphide minerals, the leaching behavior of gold depends strongly on both the solubility of the sulphides as well as the dissolved oxygen concentration in the solution. The sulphide ions formed by the decomposition of sulphide minerals showed detrimental effect on the cyanidation kinetics of gold and silver. The effect of dissolved sulphides on gold cyanidation diminishes at higher cyanide concentrations, which favor the preferential formation of  $\text{Au}(\text{CN})_2^-$  on the gold surface instead of  $\text{AuS}_x$  [5,11]. Also one hypothesis suggest that the soluble sulphide ( $\text{S}_2^-$  or  $\text{HS}^-$ ) generated from mineral dissolution reacts with gold and forms a passive film on the gold surface, which decreases the rate of gold leaching [12,13]. The galvanic interaction between the sulphide phase and gold surface and also between two sulphidic mineral phases play a vital role in gold dissolution [8,14,15]. The activation energy for the dissolution of gold was determined to be  $93 \pm 8 \text{ kJ mol}^{-1}$  for a voltage range  $-0.82 - 0.50 \text{ V}$  (vs. SCE) and an activation energy of this range suggests that the rate controlling step includes surface chemical reaction or diffusion through a passivating layer [16].

The classical study of gold dissolution kinetics was performed by Kudryk and Kellogg [17]. The dissolution of pure gold in aerated cyanide solution was found to be less as compared to the leaching rate expected either by diffusion of cyanide or oxygen. This phenomenon was because of the formation of a tight passive layer of AuCN film on the surface of gold [16,18,19]. Several investigators have reported that the Kudryk and Kellogg results differ considerably from those obtained for pure gold and these differences in gold leaching kinetics were due to the presence of small amounts of impurity, most likely silver [20]. Heavy metals such as lead, mercury, bismuth, and thallium have also been shown to enhance the rate of dissolution of gold. Some organic activators were also investigated for the enhancement of gold dissolution, but their effect was not pronounced as in the case of lead and silver [19,20,21].

Electrochemical investigations revealed that the behavior of gold in cyanide solutions is different from a 50-50% gold-silver alloy and consequently gold-silver alloys exhibit remarkably enhanced gold dissolution and oxygen reduction resulting from the presence of silver [22]. A detailed study on the influence of small amounts of silver (1– 5%) present as a gold-silver alloy was performed. These investigations revealed that silver significantly enhanced the leaching of gold in aerated cyanide solutions. It has been experimentally proven that the surface of pure gold is blocked by a film of AuCN and the role of silver is to modify the surface of gold. While alloyed with gold, silver enhances both the gold oxidation and oxygen reduction half reactions. This results in a phenomenon like bimetallic corrosion, with oxygen reduction preferentially occurring at the active silver sites [19,22,23]. The effect of dissolved silver on the dissolution of gold was investigated as well and the enhancement in the leaching rate was found to be less pronounced as compared to the silver alloyed with gold [20].

Silver frequently occurs with gold in significant quantities. In gold bearing ores, silver occurs as a gold-silver alloy, while the other forms include native silver, chlorargyrite [AgCl], acanthite [Ag<sub>2</sub>S], and tetrahedrite [(Cu,Fe,Ag,Zn)<sub>12</sub>Sb<sub>4</sub>S<sub>13</sub>]. The greater reactivity of silver influences the gold leaching and its behaviour in cyanide solutions is most important [2]. Despite plenty of information available on the kinetics of gold dissolution at an anode, or by dissolved oxygen, comparative studies on the effect of silver are lacking and this has

hampered the progress of rationalisation of the beneficial or detrimental effect of silver, which mostly co-exists in natural gold ores. A systematic study would lead to a better understanding of the effect of essential reagents as well as impurities in solution or solid state and host minerals on reaction rates. Currently, there exists very little knowledge on the effect of silver on the leaching of gold in cyanide solutions when gold is associated with silver and sulphidic minerals, despite the fact that most naturally occurring gold do contain silver associated to it. The following study is therefore designed to investigate:

1. The enhanced effect of dissolved oxygen concentration on the dissolution of free gold as well as gold associated with sulphidic minerals in mono-layer, mixed and bi-layer arrangements.
2. The effect of silver on the dissolution of gold, in the solid as well as in dissolved form, while the sulphide minerals are arranged together, in mixed and bi-layer mineral assays.

## **2.2. Experimental**

### **2.2.1. Materials and Reagents**

Four sulphide-rich ore samples referred to as pyrite (Py), chalcopyrite (Cp), sphalerite (Sp) and stibnite (Sb), used in this study, were purchased from Ward's Natural Science. The samples were crush grinded and sieved to remove the particles coarser than 106  $\mu\text{m}$  and finer than 53  $\mu\text{m}$ . Subsequently, the same fraction was used for the different ores, to acquire nearly same granulometry for all the cyanidation experiments. Pure gold ( $P_{80} = 39 \mu\text{m}$ , 99.998%, Alfa Aesar USA) and pure silver ( $P_{80} = 26 \mu\text{m}$ , 99.9%, Alfa Aesar USA) powders were also used in the present study. The sulphidic ore samples were characterized and the elemental composition of sulphide ore samples investigated in the present study is exposed in the Table 2.1.

**Table 2.1.** Elemental composition of sulphide ore samples investigated in present study.

Ore/Element	Cu Wt%	Zn Wt%	Fe Wt%	S Wt%	Sb Wt%	Pb Wt%
Pyrite	0.1	0.02	45.4	53.5	0.01	0.02
Chalcopyrite	23.8	6.4	23.9	30.3	0.01	0.25
Sphalerite	0.1	27.8	5.3	16.6	0.01	12.2
Stibnite	0.03	0.01	0.18	15.2	35.6	0.02

The solutions used for all the cyanidation experiments were prepared from distilled water. The reagents used, such as sodium cyanide, NaCN (98%, Sigma-Aldrich Canada), sodium hydroxide, NaOH (Fisher Scientific Canada) and boric acid, H<sub>3</sub>BO<sub>3</sub> (99.5%, Sigma-Aldrich Canada), were all certified analytical grade. Unless otherwise specified, the solutions contained 30 mM sodium cyanide, 0.45 mM dissolved oxygen and a pH of 11 ± 0.01. The solutions were buffered using sodium hydroxide and boric acid.

### 2.2.2. Packed-bed Reactor: Device Sophistication

Several studies have been performed on the role of galvanic interactions on gold dissolution. This involved the galvanic cells of either naturally occurring or fabricated electrodes in which mineral and gold monolithic electrodes were connected through a conducting wire. The contact between gold and mineral particles was made via an external circuit and/or through an electrolyte solution in such cells. This arrangement might not reflect the environments present at micro-level within the industrial sulphide containing gold ores. The actual surface topochemistry of industrial ores in terms of permanent galvanic contacts at a particle-particle scale have not been reflected in the stated experimental strategies [5,8,14,15]. Also the presence of additives used in preparation of mineral electrodes does not represent true electrochemical behavior of the mineral particles [7]. The permanent galvanic contacts among gold and mineral particles, as is the case for actual gold ores, were nearly impossible to achieve while gold is leaching in slurries containing sulphide mineral particles and gold as well as silver powders or an Au/Ag disc electrode immersed in a slurry [5,9,14].



In order to achieve a direct surface-surface or particle-particle contact between the sulphide mineral and precious metal particles, the packed-bed reactor device was selected for gold cyanidation. In gold bearing ores, the precious metal particles could be associated with various ore constituents and will possibly affect gold dissolution in a direct as well as an indirect manner. Various strategies of dispersion of precious metals in the sulphide as well as silica phases have been adopted and have been elaborated in detail in the following equipment and procedure section.

### **2.2.3. Equipment and Procedures**

The influence of gold distribution within different mineral phases of synthetic ore samples on gold recovery as well as the effect of silver on gold dissolution in different mineral phases of the representative ore samples was studied using the packed-bed reactor (PBR) approach. The schematic diagram for the experimental setup is shown in Figure 2.1. In order to avoid the transfer of mineral as well as precious metal particles from one layer to another within the same packed-bed reactor, a set of two packed-bed reactors connected in a series was used for the segregation of the mineral layers. Both reactors were built from stainless-steel with a Teflon interior lining. Each of the reactors consisted of three sections: the inlet, working and outlet sections, as represented in Figure 2.1.

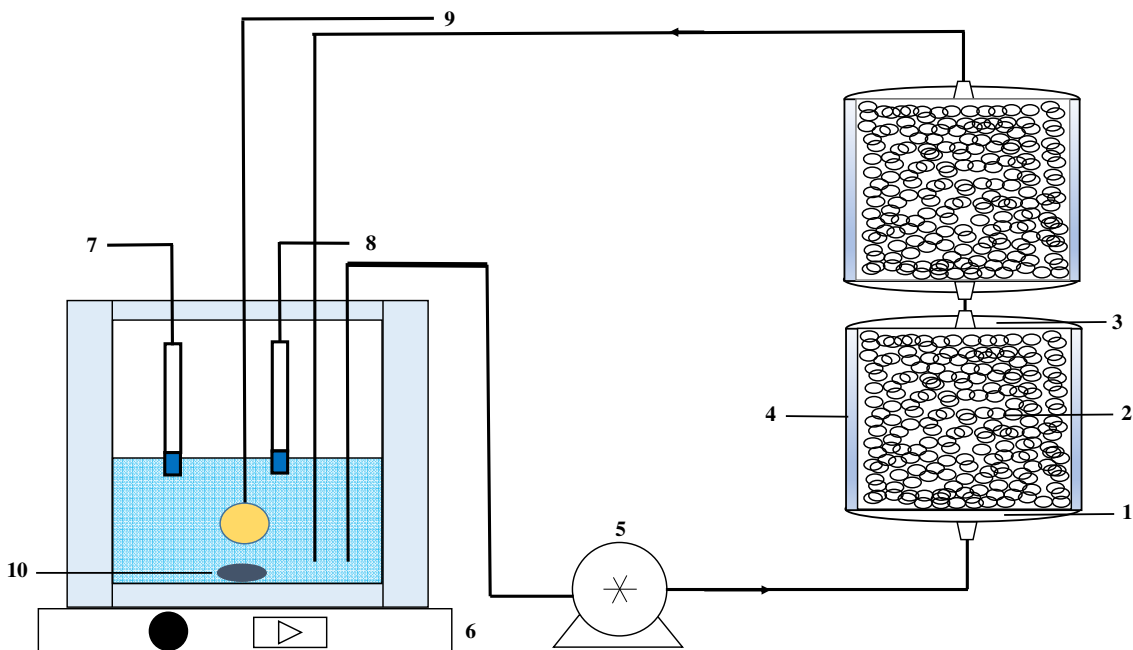


**Figure 2.1.** Sketch of two packed-bed reactors (PBRs). Follows as: 1- inlet section; 2- working section (Teflon); 3- outlet section; 4- stainless-steel cylinder; 5- peristaltic pump; 6- magnetic stirrer plate; 7- oxygen probe electrode; 8- pH-meter electrode; 9- air bubbling system; 10- magnetic stirrer bar.

The powder particles as well as the cyanide solution circulating through both reactors are prevented to have any contact with the stainless-steel reactor body. The homogenized mixtures of minerals, gold and silver were filled in the working section of each reactor as a fixed bed layer. This arrangement facilitates the establishment of permanent particle-to-particle contacts among all the constituents, precious metals and sulphide minerals alike, and also enables decoupling of various phases chemically as well as electrochemically. The working section (2) of each reactor is connected to the inlet and outlet sections of the reactor which are finally connected to the solution pumping circuit. The aerated cyanide solution was continuously circulated through the PBR throughout the span of the experiment at a constant flow rate of 10.4 mL/minute for all the experiments.

The feed solution was prepared by the dissolution of NaCN in a 0.1 M NaOH solution buffered to pH 11 with 0.1 M boric acid solution and stored in a 250 mL magnetically-stirred glass container. A fairly large amount of free cyanide, i.e., 30 mM, in solution was used in all the leaching experiments. The cyanidation experiments were performed by continuous circulation of 100 mL of the feed solution with a peristaltic pump through the reactor at room

temperature and at a constant flow rate of 10.4 mL/min. The solution was fed upwardly from the bottom in order to avoid the channeling of the feed solution in the reactor and allowing maximum residence time of the cyanide solution in the mineral layer. Instead of air, pure oxygen gas was sparged through the container to maintain a constant dissolved oxygen level ( $DO_2 \sim 0.45$  mM at  $25^\circ\text{C}$ ), which was monitored by means of a dissolved oxygen probe (FOXY-AL300 model from Ocean Optics), while pH of the feed solution was maintained at  $11 \pm 0.01$  using an Oakton 1000 series pH-meter. Chemical analysis of the leach solution was performed by collecting small aliquots from the container using a syringe, filtrated with a particles filter VWR  $0.45 \mu\text{m}$ , at regular intervals during the length of the experiment.

When gold and silver are associated with the conducting sulphide minerals, the galvanic as well as the passivation effects play a vital role in the dissolution of gold and silver.<sup>[8]</sup> The direct (galvanic interaction) influence of individual sulphidic minerals was studied by thoroughly mixing 4 g of each of the sulphidic minerals pyrite, chalcopyrite, sphalerite or stibnite along with 50 mg of the precious metal, Au and packing in the same PBR, in an arrangement like: ||Py+Au||; ||Cp+Au||; ||Sp+Au|| and ||Sb+Au||. Sideways, the indirect (passivation effect) influence induced by the sulphidic minerals was studied by packing the sulphidic minerals in the lower PBR while the 50 mg of the precious metal, Au dispersed in silica, was filled in the upper PBR following a pattern as: ||Py||Silica+Au||; ||Cp||Silica+Au||; ||Sp||Silica+Au|| and ||Sb||Silica+Au ||, connected in series as shown in Figure 2.1.

The silica layer as depicted in the above arrangement, consists of chemically and electrochemically inert quartz particles ( $P_{80} \leq 149 \mu\text{m}$ , Sigma Aldrich, Canada) consequently having no effect on the leaching of gold in aerated cyanide solutions [24,25,26]. The dissolution of gold for a bilayer arrangement of sulphidic minerals was also carried out. In this study, the sulphide minerals taken were 4 g of pyrite mineral and 2 g of one of the subsequent minerals, chalcopyrite, sphalerite or stibnite. The Au powder, 50 mg in each case, was dispersed among the mineral phases as mentioned below:

- |                 |                         |
|-----------------|-------------------------|
| a).   Py+Au  Cp | b).   Py  Cp+Au         |
| c).   Py+Cp+Au  | d).   Py  Cp  Silica+Au |

For the estimation of effect of silver on gold dissolution in presence of sulphidic minerals, 50 mg Au and 25 mg Ag were dispersed in the mineral layer patterns as explained below.

- a).  $\parallel\text{Py}+\text{Au}+\text{Ag}\parallel\text{Cp}\parallel$       b).  $\parallel\text{Py}\parallel\text{Cp}+\text{Au}+\text{Ag}\parallel$   
c).  $\parallel\text{Py}+\text{Cp}+\text{Au}+\text{Ag}\parallel$       d).  $\parallel\text{Py}\parallel\text{Cp}\parallel\text{Silica}+\text{Au}+\text{Ag}\parallel$   
e).  $\parallel\text{Py}+\text{Ag}\parallel\text{Cp}+\text{Au}\parallel$       f).  $\parallel\text{Py}+\text{Au}\parallel\text{Cp}+\text{Ag}\parallel$

The dispersion pattern for the pyrite-chalcopyrite-silica system has been elaborated above. For the pyrite-sphalerite-silica and pyrite-stibnite-silica system only chalcopyrite (Cp) will be replaced by the sphalerite (Sp) and stibnite (Sb). In all the experiments, silver metal used was 50% by weight of the gold powder taken.

Benchmark test for Au dissolution referred to as Case C, was performed by dispersing 50 mg of the precious metal Au in quartz particles and filling the whole working section of the PBR. The benchmark test for Ag dissolution was also performed by the respective dispersion of 50 mg of Ag within quartz particles and is termed as Case D. The benchmark tests for Au and Ag have been represented by Case C and Case D, respectively in all of the following precious metal leaching charts. For single sulphide minerals, passivation phenomena were singled out by mixing Au only within a quartz layer being juxtaposed to one of the sulphidic mineral layer like pyrite, chalcopyrite, sphalerite or stibnite and this is represented as Case A, while the response from the galvanic interactions was obtained through mixing Au powder with one of the already stated sulphidic minerals and is termed as Case B.

The dissolution pattern for gold in case of binary sulphidic minerals, dispersed in the mixed/segregated mineral layers and also in the silica layer segregated by the mineral layers, was referred to as Case B as well. Both Au and Ag dispersed altogether in any of the above stated configurations, Case B. Au represents the gold leaching curve while Case B. Ag shows the silver leaching pattern. Lastly, the reactors were covered on both sides by placing Whatman filter paper filters (porosity < 1  $\mu\text{m}$ ), in order to avoid the loss of fine precious metal particles out of the PBR.

In all the cyanidation experiments, the concentration of dissolved metals was measured by using a Perkin Elmer AA-800 atomic absorption spectrometer (AAS). In the present study,

gold and silver leaching kinetics were monitored by calculating the percentage of dissolved metal as compared to the initially dispersed precious metals.

## **2.3. Results and Discussion**

### **2.3.1. Gold Leaching with Pyrite, Chalcopyrite, Sphalerite and Stibnite Minerals**

The leaching of gold with the sulphidic minerals pyrite, chalcopyrite, sphalerite and stibnite is studied with the leaching pattern shown in Figure 2.2a-d. The galvanic interaction and passivation phenomenon play a crucial role in leaching gold associated with conductive sulphidic minerals. The close contact between the gold and sulphide mineral particles enabled the combined galvanic and passivation effect. Their contribution on gold leaching was assessed in case of pyrite, chalcopyrite, sphalerite and stibnite minerals. The combination of two PBRs connected in series was developed to diminish the mishaps of particles transfer from one mineral layer to another as used previously [8,24,27].

Gold particles exhibited the most intense dissolution while having surface-to-surface contact with pyrite and chalcopyrite particles. The Au leaching pattern for the pyrite mineral is illustrated in Figure 2.2a, and in Figure 2.2b for chalcopyrite. Enabling the direct contact of Au particles with pyrite and chalcopyrite mineral particles, the galvanic contact outweighed the passivation effect and promoted a net dissolution of gold as compared to the benchmark test. In case of pyrite having an electrical contact with Au particles, 94.6% of gold was extracted after 6 h of cyanidation, while only 15.7% of gold was recovered under the sole effect of passivation with respect to 39% extraction for the benchmark test. The galvanic interactions enhanced the gold dissolution by 55.5%, while the passivation phenomenon reduced the gold recovery by -23.3% as compared to the benchmark test.

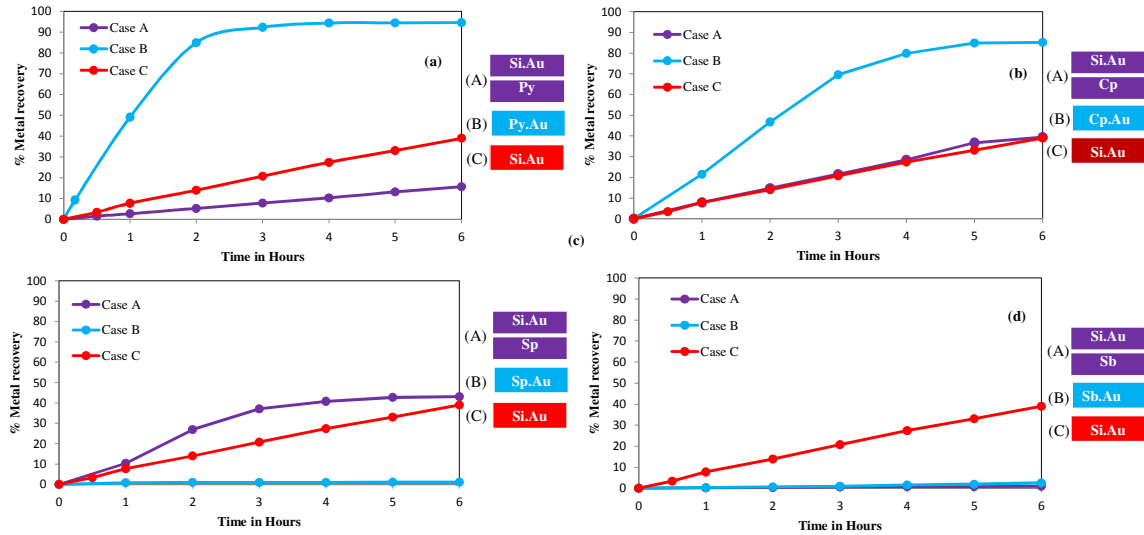


**Figure 2.2.** Galvanic and passivation effects of sulphidic minerals on gold dissolution: (a) gold dissolution with pyrite mineral, (b) gold dissolution with chalcopyrite mineral, (c) gold dissolution with sphalerite mineral, (d) gold dissolution with stibnite mineral. Reaction conditions:  $CN^- = 30 \text{ mM}$ ,  $DO_2 = 0.45 \text{ mM}$ ,  $pH = 11$ .

The effect of galvanic as well as passivation phenomenon on gold dissolution was also investigated for the chalcopyrite mineral. The permanent galvanic contacts between Au and chalcopyrite particles were enabled by mixing Au with chalcopyrite and filled in the same PBR, while in case of passivation effect, the chalcopyrite was packed in the lower PBR and Au powder dispersed in the silica layer filled in the upper PBR connected in series. The permanent galvanic contacts between Au and chalcopyrite particles resulted in a higher net dissolution of gold, while under passivation effect alone, the gold dissolution almost followed the pattern of the benchmark test. The galvanic contacts led to Au dissolution of 85% while the passivation effect resulted in 39% dissolution after 6 h of cyanidation. By enabling the galvanic interaction, Au dissolution was raised by 46% as compared to benchmark test. The passivation of gold surface by dissolved species from chalcopyrite was not remarkable for Au leaching at the given conditions. Gold surface would be passivated while in close contact with the conductive sulphidic minerals [28,29]. It has also been postulated that the oxygen reduction phenomenon could occur over the entire mineral surface while Au and the sulphide mineral are in direct contact with each other [28]. The mineral surface provides much higher surface area for oxygen reduction as compared to the Au surface alone. At high cyanide concentrations the Au dissolution is oxygen-diffusion limited and this enhanced oxygen reduction phenomenon increases the gold dissolution rate as compared to pure gold, while

Au particles are in close contact with sulphide mineral particles [27,28,30]. In case of pyrite and chalcopyrite sulphidic minerals, the dissolved oxygen concentration of 0.45 mM enhanced the net dissolution of gold both under galvanic as well as passivation effects. The dissolution is towards a higher side as compared to the findings by Azizi et al [8].

The gold extraction profiles for the sphalerite and stibnite sulphidic minerals are illustrated in Figure 2.2c,d. Both sulphidic minerals severely hindered the gold dissolution in the presence of the galvanic interactions. There was noted a marginal promotion of gold extraction by enabling the galvanic contacts for sphalerite and stibnite sulphidic minerals. The Au dissolution was evaluated to be 1% and 43% with galvanic contacts were enabled and/or disabled, respectively for the sphalerite mineral, (Figure 2.2c). This drastic decrease in Au dissolution, with Au in direct contact with sphalerite particles, could be attributed to the poor conductivity of sphalerite mineral, which is reported to be  $10^{-12}$ – $10^{-9}$  Siemens/meter, for sphalerite in water [31]. The galvanic effect was not quite enough to overcome the poor conductance of electrons at the surface of sphalerite mineral. The low electrical conductivity of sphalerite mineral resulting in less electron transfer at the mineral surface, and thus lowering the kinetics of oxygen reduction, results in poor gold dissolution [8,31]. On the other hand, gold associated with quartz particles, segregated by the sphalerite layer, showed much better dissolution. It reflects in that the major limitation with sphalerite is its very poor conductance and not passivation by dissolved species at given cyanidation conditions. In the case of stibnite, the Au dissolution was estimated to be 2.5% while electrical contacts were enabled and only 1% under the surface passivation effect, see Figure 2.2d. One possible reason for this retardation in Au dissolution would be the formation of an antimony oxide ( $\text{Sb}_2\text{O}_5$ ) passivation film on the gold surface [8].

### **2.3.2. Gold Leaching in Pyrite-Chalcopyrite-Silica System**

The gold dissolution pattern and the kinetics of Au dissolution of the various configurations addressed for the pyrite-chalcopyrite-silica system has been illustrated in Figure 2.3. Gold ores can be composed of a multitude of sulphidic as well as non-sulphidic components and also the precious metal, Au could be attributed to different mineral constituents of the ore body. The effect of various mineral constituents on the kinetics of gold dissolution was evaluated by mixing the Au powder with pyrite and chalcopyrite minerals, in mixed and

segregated layers. The effect of the mineral constituents present in the ore body, but not in close contact was assessed by placing gold in one of the mineral layers and segregating it from one another mineral layer and/or placing gold particles in silica layer and segregating it from one or two mineral layers. Consequently, the precious metal was dispersed in the mixed as well as segregated mineral layers or in the silica layer itself.

Gold leaching was assessed with gold dispersed within electrically connected and disconnected mixed and segregated mineral layers which are comprised of a two-layer ||Py+Cp||Si|| as well as a three-layer ||Py||Cp||Si|| mineral's system with likewise dispersion of Au powder in each layer as shown in the Figure 2.3. Placing Au and pyrite and/or Au chalcopyrite within close contact, enabled binary galvanic interactions (three-layer system) between the mineral particles, while dispersion of Au within the mixed pyrite and chalcopyrite layer enabled ternary galvanic interactions (two-layer system). The effect of segregated pyrite as well as chalcopyrite sulphide mineral layers was investigated by dispersing Au in the silica layer, segregated by pyrite and chalcopyrite layers in a three-layer system.

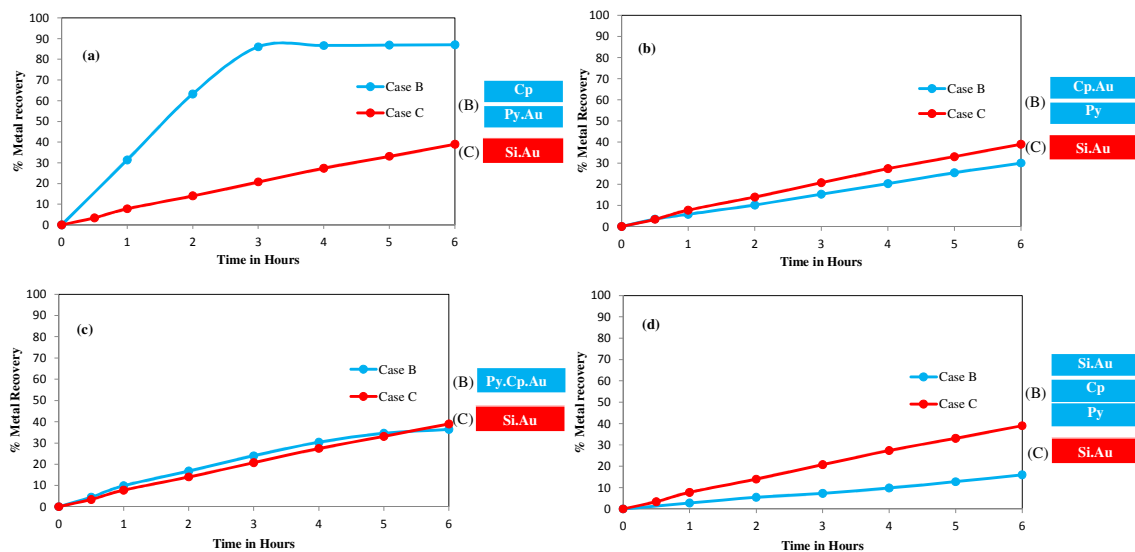


**Figure 2.3.** Gold dissolution within a sulphidic mineral layer system: (a) Py+Au//Cp, bi-layer arrangement, (b) Py//Cp+Au, bi-layer arrangement, (c) Py+Cp+Au, mono-layer arrangement, (d) Py//Cp//Si+Au, tri-layer arrangement. Reaction conditions:  $\text{CN}^- = 30 \text{ mM}$ ,  $\text{DO}_2 = 0.45 \text{ mM}$ ,  $\text{pH} = 11$ .



The binary galvanic interactions between Au and pyrite exhibited the highest Au dissolution of 87% as shown in Figure 2.3a. The greater content of pyrite induced greater galvanic contacts and raised Au recovery. The Au-Cp galvanic couple, topped over pyrite layer, lead to 30% Au dissolution as shown in Figure 2.3b. The loss of recovery for Au-Cp could be attributed to lesser Cp content and also the galvanic interaction between Au and Cp were not enough to overcome the surface passivation imposed by the segregating pyrite layer [15,24]. The Au dissolution amounted to 36% in the presence of ternary galvanic interactions among Au, pyrite and chalcopyrite, although non-associated Au dissolution was estimated to be 16%, as shown in Figure 2.3c,d, respectively. The gold surface obstacles by pyrite layer rendered lower recoveries for Au-Py-Cp ternary galvanic interactions and free gold segregated by pyrite and chalcopyrite.

### **2.3.3. Effect of Silver on Gold Leaching in Pyrite-Chalcopyrite-Silica System**

The effect of silver on the kinetics of gold dissolution was compared by contacting Au and Ag powders successively with pyrite, chalcopyrite and silica, as described in the pattern explained in the experimental section. Binary, ternary and quaternary galvanic interactions among Au, Ag and sulphidic mineral particles featured various Au and Ag leaching patterns, as highlighted in Figure 2.4. The benchmark tests for Au and Ag, resulted in an Au and Ag recovery of 39% and 100%, respectively during the 6 h of cyanidation experiment. These results reflect that pure gold dissolves much more slowly as compared to the pure metallic silver in cyanide solution. This is in accordance with the literature findings that the gold surface becomes much more passive due to a tight AuCN film formation as compared to AgCN film on the silver surface. These findings contradict the reported literature of silver dissolution lagging behind the dissolution of gold [32].

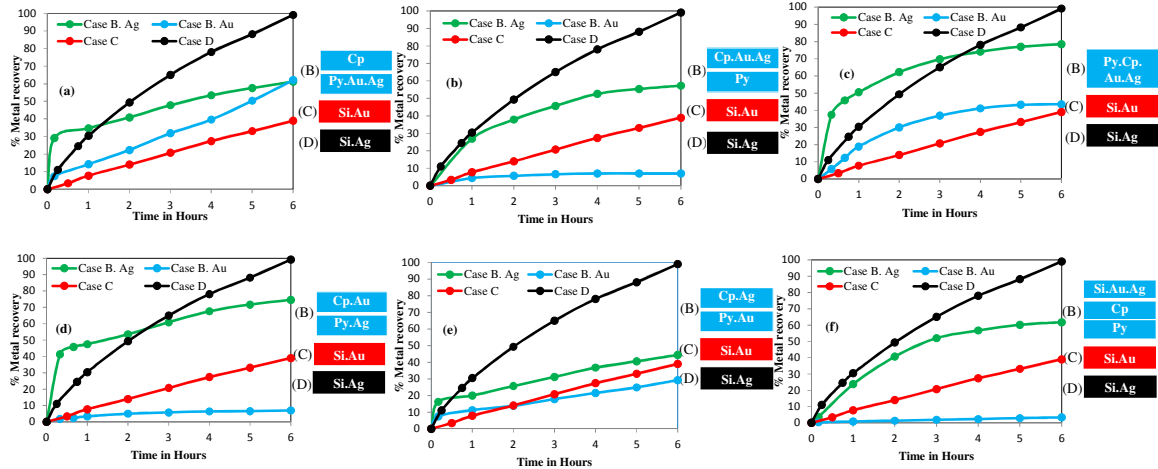
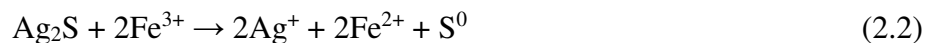
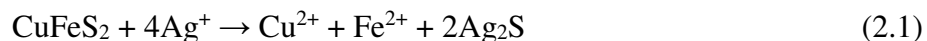


**Figure 2.4.** Effect of silver on the dissolution of gold within a sulphidic mineral layer system: (a) Py+Au+Ag//Cp, bi-layer arrangement, (b) Py//Cp+Au+Ag, bi-layer arrangement, (c) Py+Cp+Au+Ag, mono-layer arrangement, (d) Py+Ag//Cp+Au, bi-layer arrangement, (e) Py+Au//Cp+Ag, (f) Py//Cp//Si+Au+Ag, tri-layer arrangement. Reaction conditions:  $\text{CN}^- = 30 \text{ mM}$ ,  $\text{DO}_2 = 0.45 \text{ mM}$ ,  $\text{pH} = 11$ .

The effect of silver on gold leaching was assessed with gold and silver dispersed within electrically connected and disconnected mixed and segregated mineral layers comprised of a two-layer  $\parallel\text{Py}+\text{Cp}\parallel\text{Si}\parallel$  as well as three-layer  $\parallel\text{Py}\parallel\text{Cp}\parallel\text{Si}\parallel$  minerals systems in the PBR as shown in Figure 2.4. Both precious metals (Au, Ag) were dispersed in one of the mineral layers and packed in one PBR or also dispersed in the silica layer and in segregated mineral layers as well. Ternary galvanic interaction among Au-Py-Ag were enabled by mixing Au, Ag powders with pyrite and filling the mixture within the same PBR while the chalcopyrite mineral was segregated in a separate PBR connected in series with the first one as explained earlier in the experimental setup. The gold and silver dissolution was estimated to be 61% for Au and Ag, Figure 2.4a. The loss in gold recovery amounted to -26%, as compared to Au dispersed in the pyrite layer juxtaposed to chalcopyrite, Figure 2.3a. The Au-Cp-Ag ternary galvanic interactions led to an Au recovery of only 7% where 57% Ag was leached out. A loss of -23% was observed for Au leached while dispersed in chalcopyrite, segregated by the pyrite layer Figure 2.3b. The quaternary galvanic interactions among precious metals Au, Ag and sulphidic mineral particles pyrite, chalcopyrite were brought to play a role. This combination resulted in an Au dissolution of 43.5% and Ag dissolution of 78.4%, as shown in Figure 2.4c. The effect of silver on the dissolution of free gold was carried out by dispersing both the precious metals in the silica layer, segregated by pyrite and chalcopyrite

minerals. The Au and Ag leaching was estimated to be 3.3% and 61.8%, respectively (see Figure 2.4f), retarding the Au dissolution by -35.7% as compared to the benchmark test. The dispersion of Ag in pyrite and Au in chalcopyrite resulted in an Au and Ag dissolution of 7% and 74.5%, respectively, as shown in Figure 2.4d, with a loss of -23%, as compared the Au dispersed in chalcopyrite (see Figure 2.3b). Meanwhile, by contacting Au with pyrite and Ag with chalcopyrite, Au dissolution of 33.4% and Ag dissolution of 45.4% were achieved, Figure 2.4e. The Au dissolution was observed to a lower side than the Au dispersed in pyrite mineral layer (see Figure 2.3a) and from the benchmark test as well.

The association of gold as well as both gold and silver with pyrite resulted in higher gold dissolution as compared to the free and chalcopyrite-associated gold. This phenomenon reflects that the galvanic contacts of pyrite have somewhat enhanced gold leaching, because of the enhanced surface area available for oxygen reduction, resulting from higher quantity of pyrite mineral (4 g), as compared to chalcopyrite mineral (2 g). Contrarily, silver resulted in higher dissolution as compared to gold. This behavior could be attributed to the fact that silver surface films are less passivating as compared to gold surface films. Overall, the addition of silver was observed to have a retarding effect on the dissolution of gold while both the precious metals, gold and silver, were under the direct (mixed layer) or indirect (segregated layer) influence of pyrite and chalcopyrite sulphide minerals. This phenomenon could be attributed to the formation of a silver sulphide ( $\text{Ag}_2\text{S}$ ), or sulfur (S), surface films. Even low concentrations of hydrosulfide ( $\text{HS}^-$ ) ions, resulting from the dissolution of sulphide minerals, passivate gold surface due to the formation of  $\text{Ag}_2\text{S}$  on the mineral surface [11]. The formation of  $\text{Ag}_2\text{S}$  or sulfur (S), resulting from the dissolution of chalcopyrite, could also be explained on the basis of the following reactions [33].



#### **2.3.4. Gold Leaching in Pyrite-Sphalerite-Silica System**

The gold powder was dispersed among the pyrite, sphalerite and silica layers. The kinetics of Au leaching for the corresponding precious metal and sulphidic mineral systems are illustrated in Figure 2.5a-d. The dispersion pattern comprise the mono-layer system

||Py+Sp+Au||, the electrically disconnected two-layer system, such as, ||Py+Au||Sp||, ||Py||Sp+Au||, and a three-layer system ||Py||Sp||Si+Au||. These representations are self-explanatory regarding the position of sulphidic mineral as well as the precious metal. Despite a little set-back by the sphalerite segregated layer, the Au-Py galvanic interactions promoted the gold dissolution, resulting in 60.9% Au recovery, see Figure 2.5a.

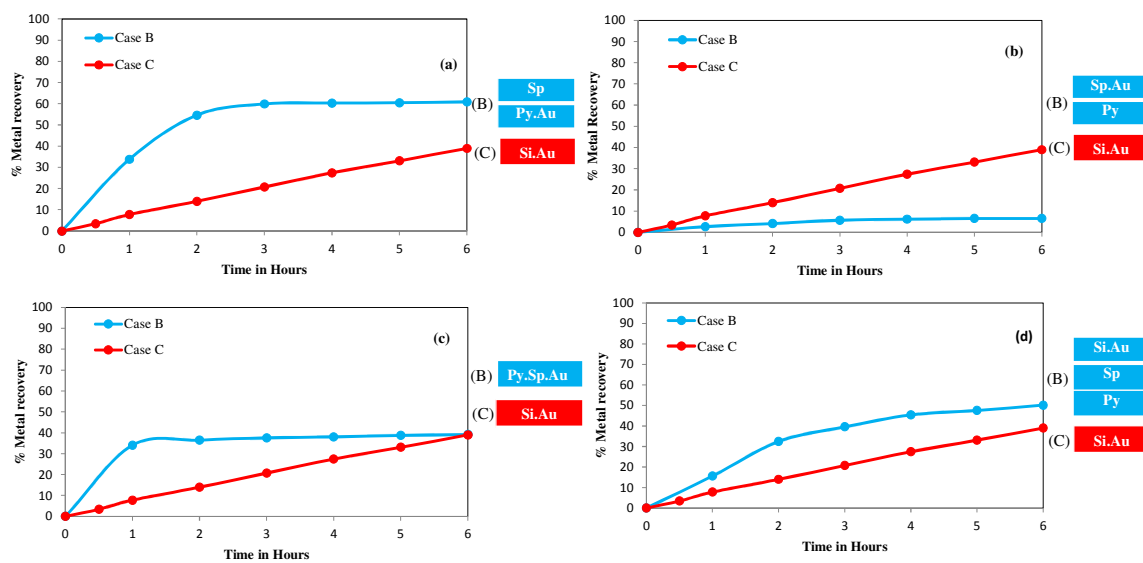


**Figure 2.5.** Gold dissolution within a sulphidic mineral layer system: (a) Py+Au//Sp, bi-layer arrangement, (b) Py//Sp+Au, bi-layer arrangement, (c) Py+Sp+Au, mono-layer arrangement, (d) Py//Sp//Si+Au, tri-layer arrangement. Reaction conditions:  $\text{CN}^- = 30 \text{ mM}$ ,  $\text{DO}_2 = 0.45 \text{ mM}$ ,  $\text{pH} = 11$ .

As it is clear from Figure 2.5b, the gold leaching substantially decreased to 6.5%, when associated to sphalerite as compared to 60.9% while in close contact with pyrite mineral particles. The galvanic interactions between Au and sphalerite particles were not able to overcome the passivation phenomenon induced by pyrite and sphalerite. The Au dissolution was hardly promoted by the galvanic effect of sphalerite mineral. The lower recoveries could be ascribed to the merest galvanic activities of the sphalerite induced in a multi-galvanic system [8]. The ternary galvanic interaction among the Py-Au-Sp mineral conceded an Au recovery of 39% (Figure 2.5c), as compared to 60.9% (Figure 2.5a), where Au-Py, galvanic contacts were in place. Sphalerite was found to be less reactive as compared to pyrite. Consequently the Py-Sp galvanic interactions could magnify pyrite anodic behavior of pyrite and thus competition for the same pyrite cathodic sites for the simultaneous pyrite and gold oxidations would result in lesser gold leaching [8]. In case of gold associated with quartz

particles, followed by the simultaneous segregation of pyrite and sphalerite layers, the Au recovery was observed to be 50%, see Figure 2.5d.

### **2.3.5. Effect of Silver on Gold Leaching in Pyrite-Sphalerite-Silica System**

The response of gold dissolution kinetics on addition of metallic silver powder has been taken into account by putting the precious metals Au, Ag and the sulphidic minerals into contact with one another within a PBR in the various patterns already explained. The leaching pattern of gold dissolution with addition of silver in segregated and mixed mineral layers is demonstrated in Figure 2.6a-f. The addition of gold and silver in close contact with the pyrite mineral segregated by the sphalerite layer leads to an Au dissolution 81.9% and an Ag dissolution of 96.6%, resulting in an enhancement of 21% in Au dissolution (Figure 2.6a), as compared to the Au dissolution in pyrite layer without silver (Figure 2.5a). The prominent galvanic interactions among pyrite, Au and Ag have led to the enhanced Au as well as Ag dissolution. Placement of Au, Ag and sphalerite mineral altogether in one layer, segregated by the pyrite layer, resulted in Au and Ag dissolution of 63% and 81%, respectively (Figure 2.6b). An increase of almost 56.5% was observed in the Au recovery as compared to Au in sphalerite layer (Figure 2.5b). It could be assumed that metallic silver present along with gold has prevented the gold surface from being passivated and also overcome the poor conductivity of sphalerite mineral particles. The quaternary galvanic interactions among the precious metals Au, Ag and the sulphidic minerals pyrite, sphalerite resulted in Au and Ag dissolution of 76% and 91%, respectively (Figure 2.6c). The Au recovery was raised by 37% as it was in case of ternary galvanic effects of Au with pyrite and sphalerite (Figure 2.5c). The effect of silver on gold particles dispersed among the quartz particles while segregated by the pyrite and pyrite sphalerite layers have been investigated and the Au and Ag dissolutions were observed to be 67% and 68%, respectively, Figure 6f. With the quartz particles being chemically and electrochemically inert, the presence of silver along with gold outperformed the passivation effect from the pyrite as well sphalerite segregated mineral layers. On the other hand, the effect of silver on the dissolution of gold was studied by placing Au in pyrite and Ag in sphalerite and *vice versa*. The contact of Au with sphalerite and Ag in pyrite resulted in the dissolution of 52.5% Au and 89% Ag, Figure 2.6d, while the

placement of Au in pyrite layer and Ag in sphalerite layer, constituted 83% Au and 74% Ag leaching, Figure 2.6e.

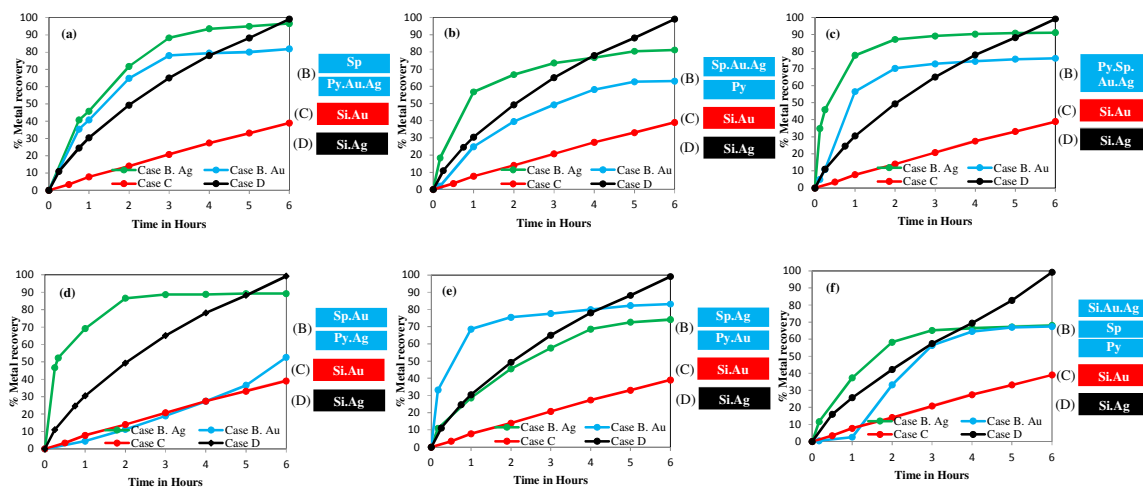


**Figure 2.6.** Effect of silver on the dissolution of gold within a sulphidic mineral layer system: (a) Py+Au+Ag//Sp, bi-layer arrangement, (b) Py//Sp+Au+Ag, bi-layer arrangement, (c) Py+Sp+Au+Ag, mono-layer arrangement, (d) Py+Ag//Sp+Au, bi-layer arrangement, (e) Py+Au//Sp+Ag, bi-layer arrangement, (f) Py//Sp//Si+Au+Ag, tri-layer arrangement. Reaction conditions:  $CN^- = 30 \text{ mM}$ ,  $DO_2 = 0.45 \text{ mM}$ ,  $pH = 11$ .

The results clearly demonstrate that the addition of silver has significantly enhanced the dissolution of gold, both when present in close contact with gold (solid form) as well as when present in a separate layer as that of gold (dissolved form). The effect of silver was observed to be greater in the case where it has close contact with gold as compared to the impact of silver in dissolved form. As in case of both gold and silver dispersed in the sphalerite layer, 63% Au was leached out, rather than gold in sphalerite layer and silver in pyrite layer resulted in 52% Au recovery. These findings are in close agreement with the literature [20].

It is believed that the surface of pure gold is blocked by a film of AuCN, and the role of silver is to modify the surface of gold. Silver enhances both gold oxidation as well as oxygen reduction half reactions, like a bimetallic corrosion with oxygen reduction occurring preferentially at silver active sites, while silver present in close contact with gold. Also it is postulated that silver forms  $Ag(CN)_2^-$  complex on dissolution in aerated cyanide solution and the reaction of AuCN with  $Ag(CN)_2^-$  produces a permeable film of AuCN.AgCN, as compared to a tight AuCN passivating film. The dissolution of the permeable AuCN.AgCN film by  $CN^-$  results in the formation of  $Au(CN)_2^-$  and  $Ag(CN)_2^-$  in solution. The  $Ag(CN)_2^-$

produced in the solution reacts with AuCN in the same manner as above to complete the cycle [11,20,23].

### 2.3.6. Gold Leaching in Pyrite-Stibnite-Silica System

Gold extraction was severely hindered by stibnite mineral particles while present in close contact or influencing indirectly from a segregated layer, as shown in Figure 2.2d. The direct as well as indirect effects of stibnite sulphidic mineral on gold leaching was investigated with the help of placing mixed and segregated layers of pyrite mineral. The resulted Au dissolution patterns for the pyrite-stibnite-silica system has been illustrated in the Figure 2.7.

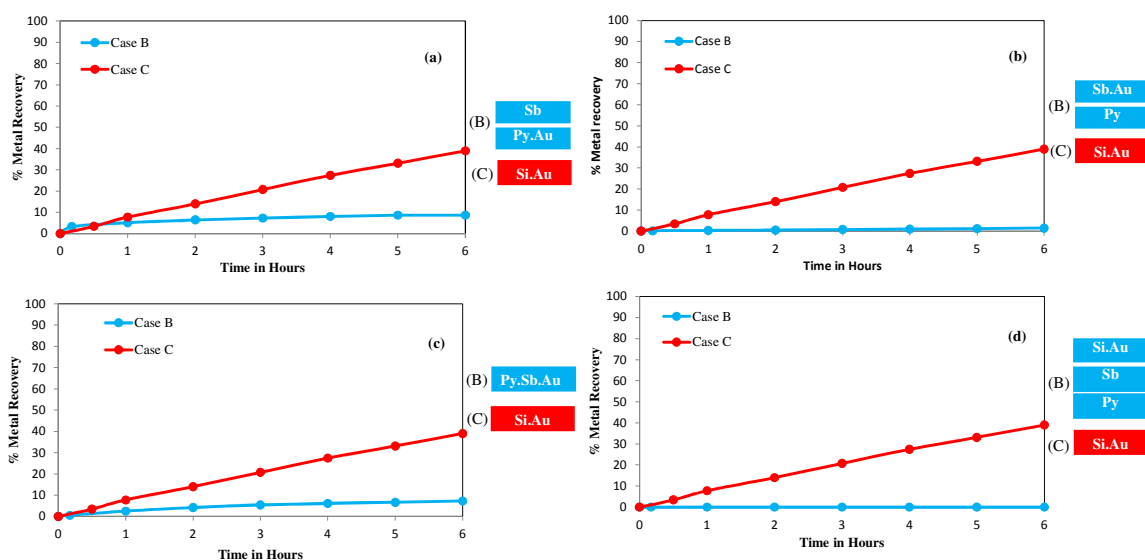


**Figure 2.7.** Gold dissolution within a sulphidic mineral layer system: (a) Py+Au//Sb, bi-layer arrangement, (b) Py//Sb+Au, bi-layer arrangement, (c) Py+Sb+Au, mono-layer arrangement, (d) Py//Sb//Si+Au, tri-layer arrangement. Reaction conditions:  $\text{CN}^- = 30 \text{ mM}$ ,  $\text{DO}_2 = 0.45 \text{ mM}$ ,  $\text{pH} = 11$ .

The electrically disconnected layer of stibnite reduced the leaching of gold dispersed in the pyrite layer. The Au recovery was reduced to 8.7% while in segregation with stibnite (Figure 2.7a) as compared to 74% for the gold associated to pyrite alone, amounting to a loss of -86% (Figure 2.2a). The segregated layer of pyrite, while gold present with stibnite, broke up the dissolution of gold with a recovery of just 1.45% (Figure 2.7b), as compared to 2.55% recovery for gold associated with stibnite only (Figure 2.2d). It indicated that the surface passivation from the pyrite layer also played its role to lessen gold dissolution. The quaternary galvanic as well as the passivation phenomenon from the pyrite, Au and stibnite,

||Py+Sb+Aull, resulted in a gold recovery of 7.3% (Figure 2.7c). This combination with stibnite resulted in the lowest Au dissolution as compared to the same combination of chalcopyrite, ||Py+Cp+Aull and sphalerite, ||Py+Sp+Aull sulphidic minerals, as depicted in Figures 2.3c and 2.5c, respectively. The dissolution of gold was totally blocked by the combined surface passivation of pyrite and stibnite sulphidic minerals, and the Au dissolution was below the detection limits of the instrument (Figure 2.7d). One possible justification could be the antimony oxide film on the surface of gold obstructing the gold surface from the attack of cyanide ions to dissolve gold by complexation.

### 2.3.7. Effect of Silver on Gold Leaching in Pyrite-Stibnite-Silica System

The close contact of silver with gold in the presence of mixed as well as segregated sulphidic minerals, such as pyrite and stibnite, was found to have deleterious effects on gold dissolution kinetics. The leaching charts for the precious metals Au and Ag, representing the effect of silver on Au dissolution in the presence of pyrite and sphalerite mineral particles, are shown in Figure 2.8(a-f). The association of Au and Ag with pyrite, stibnite and both or silica, suggested various dissolution patterns and the effect of Ag addition on the Au dissolution has been investigated. The dissolution pattern of both Au and Ag while associated with pyrite and segregated from stibnite led to an Au, Ag recovery of 7.9% and 27.3%, respectively, Figure 2.8a.

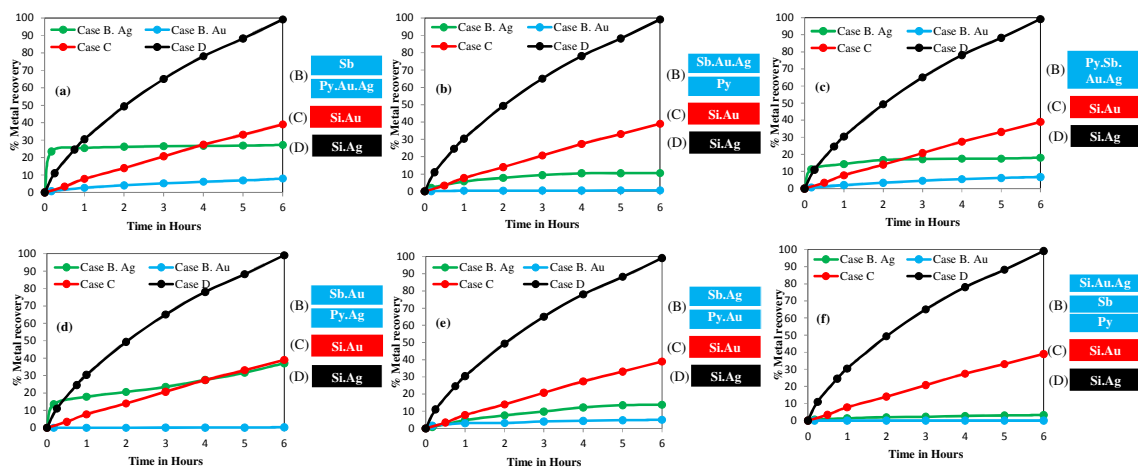


**Figure 2.8.** Effect of silver on the dissolution of gold within a sulphidic mineral layer system: (a) Py+Au+Ag//Sb, bi-layer arrangement, (b) Py//Sb+Au+Ag, bi-layer arrangement, (c) Py+Sb+Au+Ag, mono-layer arrangement, (d) Py+Ag//Sb+Au, bi-layer arrangement, (e)



Py+Au//Sb+Ag, bi-layer arrangement, (f) Py//Sb//Si+Au+Ag, tri-layer arrangement. Reaction conditions:  $\text{CN}^- = 30 \text{ mM}$ ,  $\text{DO}_2 = 0.45 \text{ mM}$ ,  $\text{pH} = 11$ .

The Au recovery was estimated to be 8.7% (Figure 2.7a), while only Au was associated to pyrite without any silver addition, with almost 1% reduction in recovery of gold. A recovery of 0.63% Au, 10.6% Ag (Figure 2.8b) was achieved by keeping Au, Ag and stibnite particles in close contact with one another, segregated by the pyrite layer arranged in two separate PBRs, as compared to Au recovery of 1.45% (Figure 2.7b), while Au and stibnite were in contact and separated from the pyrite layer. Bringing Au, Ag, pyrite and stibnite in a close contact and placing all in one PBR results in multiple galvanic interactions resulting from each of the constituents present in the powder mixture. This combination resulted in Au as well as Ag dissolution of 6.8% and 18%, respectively, Figure 2.8c. The Au recovery in this case was also towards the lower side as compared to Au dispersed in a combination of pyrite and stibnite, Figure 2.7c. The combined passivation effect of pyrite and stibnite mineral layers led to zero Au recovery (Figure 2.8f) whilst Au and Ag particles were associated to the quartz particles. The recovery was once again noted to be towards a lesser end in comparison of Au particles associated with quartz particles and separated from pyrite as well as stibnite layers, Figure 2.7d. The effect of silver in dissolved form was also investigated by placing Au and Ag in separate sulphidic minerals. Keeping pyrite and Ag in one PBR, while Au and stibnite in another PBR led to a recovery of 0.3% Au and 39% Ag, Figure 2.8d. Also the association of Au with pyrite and Ag with stibnite resulted in a recovery of 5% Au and 13.8% Ag, Figure 2.8e. In case of the pyrite-stibnite-silica system, the addition of silver was found to have an adverse effect on the gold dissolution behaviour, both as a solid additive as well as in dissolved form. Although the effect was not so pronounced, still it did help in the improvement of gold leaching. The results demonstrate the literature findings that stibnite being the readily hydrolysed sulphidic mineral, there is a severely hindered Au dissolution by the formation of a surface passive film, even present in traces [8,9,34].

## 2.4. Conclusion

Gold leaching was investigated with the gold particles being in direct as well as indirect contacts with synthetic sulphide ore samples. It was observed that at given conditions, the leaching kinetics and overall recovery were enhanced remarkably for the pyrite and

chalcopyrite sulphide minerals, both under the influence of direct and indirect contact among particles. In case of sphalerite and stibnite sulphidic minerals, the Au dissolution was retarded while electrical contacts between the precious metal and mineral particles were enabled. The surface passivation from the sphalerite mineral did not affect the gold dissolution severely as observed for the stibnite mineral.

The effect of silver on the dissolution of gold was also investigated in the presence of sulphidic minerals in an arrangement of mixed as well as segregated mineral layers. Three sets of mineral systems were established: pyrite-chalcopyrite-silica, pyrite-sphalerite-silica and pyrite-stibnite-silica. The addition of silver retarded gold dissolution severely in case of the pyrite-chalcopyrite-silica system, irrespective of the dispersion of the mineral in the same as well as the segregated layers. This could be attributed to the surface films formed on the gold surface as  $\text{Ag}_2\text{S}$  layer.

Gold leaching was enhanced notably with the addition of silver for the pyrite-sphalerite-silica system with silver having direct contact with the gold particles and also in the dissolved form. On the other hand the pyrite-stibnite-silica system did not respond positively to the addition of silver. The gold recovery was found to be on the lower end with the addition of silver irrespective of the placement of the silver along the mixed as well as segregated layers.

## **Acknowledgements**

Financial support from the Natural Sciences and Engineering Research Council through its Cooperative Research & Development grants program and from the supporting partners Agnico Eagle, Barrick, Camiro, Corem, Glencore, IamGold, Niobec and Teck is gratefully acknowledged. Corem is also acknowledged for providing us with the data analysis of the minerals studied in this work. The authors are also very thankful to Prof. Brian Hart from Department of Earth Sciences (University of Western Ontario), and Caroline Olsen and Dr. Patrick Laflamme from Corem for stimulating discussions on the phenomena of gold leaching. One of the authors (MK) would like to thank Mr. Olivier Gravel for his guidance and support.

## 2.5. References

1. Habashi, F., 1967. Montana Bureau of Mines and Geology Bulletin 59, Montana, USA.
2. Marsden, J. O., and House, C. I., 2006. Chemistry of gold extraction. 2nd ed. Littleton, Colorado: Society for Mining, Metallurgy, and Exploration (SME), 2006.
3. Liu, G. Q. and Yen, W. T., 1995. Effects of sulphide minerals and dissolved oxygen on the gold and silver dissolution in cyanide solution. *Minerals Engineering*, 8, 111–123.
4. Deschenes, G., Rousseau, M., Tardif, J., and Prud'homme, P.J.H., 1998. Effect of the composition of some sulfide minerals on cyanidation and use of lead nitrate and oxygen to alleviate their impact. *Hydrometallurgy* 50, 205–221.
5. Dai, X., and Jeffrey, M. I., 2006. The effect of sulfide minerals on the leaching of gold in aerated cyanide solutions. *Hydrometallurgy*, 82, 118–125.
6. Breuer, P. L., Jeffrey, M. I., and Hewitt, D. M., 2008. Mechanisms of sulfide ion oxidation during cyanidation. Part I: the effect of lead (II) ions. *Minerals Engineering*, 21, 579–586.
7. Azizi, A., Petre, C. F., Olsen, C., and Larachi, F., 2010. Electrochemical behavior of gold cyanidation in the presence of a sulfide-rich industrial ore versus its major constitutive sulfide minerals. *Hydrometallurgy*, 101, 108–119.
8. Azizi, A., Petre, C. F., Olsen, C., and Larachi, F., 2011. Untangling galvanic and passivation phenomena induced by sulfide minerals on precious metal leaching using a new packed-bed electrochemical cyanidation reactor. *Hydrometallurgy*, 107, 101–111.
9. Deschenes, G., Pratt, A., Fulton, M., and Lastra, R., 2005. Leaching kinetics and mechanisms of surface reaction during cyanidation of gold in presence of pyrite and stibnite. *Minerals and Metallurgical Processing*, 22, 89–95.
10. Jeffrey, M. I. and Breuer, P. L., 2000. The cyanide leaching of gold in solutions containing sulfide. *Minerals Engineering*, 13, 1097–2000.
11. Senanayake, G., 2008. A review of effects of silver, lead, sulfide and carbonaceous matter on gold cyanidation and mechanistic interpretation. *Hydrometallurgy*, 90, 46–73.
12. J. Weichselbaum, J. A. Tumilty, C. G. Schmidt, *Proc. Austr. I.M.M. Annual Conf. Perth/Kalgoorlie*, Australasian Institute of Mining and Metallurgy, Melbourne **1989**, p. 221.
13. Kondos, P. D., Deschenes, G., and Morrison, R. M., 1995. Process optimization studies in gold cyanidation. *Hydrometallurgy*, 39, 235–250.
14. Lorenzen, L., and van Deventer, J. S. J., 1992. The mechanism of leaching of gold from refractory ores. *Minerals Engineering*, 5, 1377–1387.

15. Aghamirian, M. M., and Yen, W. T., 2005. Mechanisms of galvanic interactions between gold and sulfide minerals in cyanide solution. *Minerals Engineering*, 18, 393–407.
16. Thurgood, C. P., Kirk, D. W., Foulkes, F. R., and Graydon, W. F., 1981. Activation energies of anodic gold reactions in aqueous alkaline cyanide. *Journal of the Electrochemical Society*, 128, 1680–1685.
17. Kudryk, V., and Kellogg, H. H., 1954. Mechanism and rate-controlling factors in the dissolution of gold in cyanide solutions. *Journal of Metals*, 541–548.
18. Zheng, J., Ritchie, I. M., La Brooy, S. R., and Singh, P., 1995. Study of gold leaching in oxygenated solutions containing cyanide–copper–ammonia using rotating quartz crystal microbalance. *Hydrometallurgy*, 99, 277–292.
19. Wadsworth, M. E., Zhu, X., Thompson, J. S., and Pereira, C. J., 2000. Gold dissolution and activation in cyanide solution. *Hydrometallurgy*, 57, 1–11.
20. Wadsworth, M. E., and Zhu, X., 2003. Kinetics of enhanced gold dissolution: activation by dissolved silver. *International Journal of Mineral Processing*, 72, 301–310.
21. Cathro, K. J., 1964. The effect of thallium on the rate of extraction of gold from pyrites calcine. *Proc. Aus. I.M.M.*, 210, 127–137.
22. Sun, X., Guan, Y. C., and Han, K. N., 1996. Electrochemical behavior of the dissolution of gold-silver alloys in cyanide solutions. *Metallurgical and Materials Transactions B*, 27, 355–361.
23. Jeffrey, M. I., and Ritchie, I. M., 2000. The leaching of gold in cyanide solutions in the presence of impurities II. The effect of silver. *Journal of The Electrochemical Society*, 147, 3272–3276.
24. Azizi, A., Petre, C. F., and Larachi, F., 2012. Leveraging strategies to increase gold cyanidation in the presence of sulfide minerals—Packed bed electrochemical reactor approach. *Hydrometallurgy*, 111–112, 73–81.
25. Aghamirian, M. M., and Yen, W. T., 2005. A study of gold anodic behavior in the presence of various ions and sulfide minerals in cyanide solution. *Minerals Engineering*, 18, 89–102.
26. Azizi, A., Olsen, C., and Larachi, F., 2014. Efficient strategies to enhance gold Leaching during cyanidation of multi-sulfidic ores. *The Canadian Journal of Chemical Engineering*, 92, 1687–1692.
27. Azizi, A., Petre, C. F., Assima, G. P., and Larachi, F., 2012. The role of multi-sulfidic mineral binary and ternary galvanic interactions in gold cyanidation in a multi-layer packed-bed electrochemical reactor. *Hydrometallurgy*, 113–114, 51–59.

28. Filmer, A. O., 1982. The dissolution of gold from roasted pyrite concentrations. *Journal of the South African Institute of Mining and Metallurgy*, 90–94.
29. Paul, R.L., 1984. The role of electrochemistry in the extraction of gold. *Journal of Electroanalytical Chemistry*, 168, 147–162.
30. Heath, A. R., and Rumball, J. A., 1998. Optimising cyanide: oxygen ratios in gold CIP/CIL circuits. *Minerals Engineering*, 11, 999-1010.
31. Mirnezami, M., Hashemi, M. S., and Finch, J.A., 2003. Measurement of conductivity of sulphide particles dispersed in water. *Canadian Metallurgical Quarterly* 42, 271–276.
32. Hiskey, J. B. and Sanchez, V. M., 1990. Mechanistic and kinetic aspects of silver dissolution in cyanide solutions. *Journal of Applied Electrochemistry*, 20, 479–487.
33. Córdoba, E. M., Muñoz, J. A., Blázquez, M. L., González, F., and Ballester, A., 2008. Leaching of chalcopyrite with ferric ion. Part I: General aspects. *Hydrometallurgy*, 93, 81–87.
34. Hollow, J., Deschenes, G., Guo, H., Fulton, M., and Hill, E., 2003. Optimizing cyanidation parameters for processing of blended Fort Knox and True North Ores at the Fort Knox Mine. *Hydrometallurgy, 2003: Proceedings of the 5th International Symposium Honoring Professor Ian M. Ritchie*. 1, pp. 21–34



## Chapter 3: Impact of Silver Sulphide on Gold Cyanidation with Conductive Sulphide Minerals\*

### Résumé

L'or est principalement retrouvé sous forme métallique alors que l'argent existe sous plusieurs formes minérales. La pyrite, la chalcoppyrite, la sphalérite et la stibnite ont été les sulfures métalliques étudiés relativement à l'effet des sulfures d'argent sur la cyanuration de l'or. Quatre couples de minéraux : pyrite-silice, chalcoppyrite-silice, sphalérite-silice et stibnite-silice ont été constitué afin d'investiguer l'effet d'un sulfure d'argent. L'addition de sulfure d'argent favorise la dissolution d'or dans le couple pyrite-silice et le couple sphalérite-silice. La lixiviation de l'or s'est aussi vue retardée dans les systèmes chalcoppyrite-silice et stibnite-silice, indépendamment de la dispersion de l'or et du sulfure d'argent dans les couches minérales. Une caractérisation de la surface des particules d'or a été entreprise au moyen de la spectroscopie de photoélectrons par rayons X dans le but d'identifier les espèces obstruant la surface. Les analyses ont mis en évidence des couches de passivation de sulfure d'argent ( $\text{Ag}_2\text{S}$ ),  $\text{Cu}_2\text{O}/\text{Cu}(\text{OH})_2$ , et d'oxyde d'antimoine ( $\text{Sb}_2\text{O}_5$ ) formées à la surface des particules d'or par la dissolution simultanée des sulfures d'argent et des autres sulfures métalliques résultant ainsi en réduction notable de la dissolution de l'or.

---

\* M. Khalid, F. Larachi, A. Adnot, *Can. J. Chem. Eng.* 2017 (online 04 May, 2017).

## Abstract

Gold is mostly found in metallic form, while silver exists in various mineral forms. Pyrite, chalcopyrite, sphalerite, and stibnite were the sulphidic minerals investigated for the effect of silver sulphide on gold cyanidation. Four sets of mineral systems, pyrite-silica, chalcopyrite-silica, sphalerite-silica, and stibnite-silica, were established to investigate the effect of silver sulphide. Silver sulphide addition promoted gold dissolution for the pyrite-silica and sphalerite-silica systems. The gold dissolution was retarded with the chalcopyrite-silica and stibnite-silica systems, irrespective of the dispersion of gold and silver sulphide in the mineral as well as in the quartz layer. The surface characterization of the gold particles was attempted by using X-ray photoelectron spectroscopy (XPS) in order to identify the surface obstructing species. XPS analysis showed that the passivation layers of silver sulphide ( $\text{Ag}_2\text{S}$ ),  $\text{Cu}_2\text{O}/\text{Cu}(\text{OH})_2$  and antimony oxide ( $\text{Sb}_2\text{O}_5$ ) might form on the surface of gold particles by the simultaneous dissolution of silver sulphide as well as sulphide minerals, resulting in the retardation of gold dissolution.



### 3.1. Introduction

Cyanidation has been used extensively in the gold mining industry for the dissolution of gold because of good overall recovery, technological simplicity, and strong ore adaptation. Cyanide is known to be a commercial ligand for gold leaching, but most of the metal sulphides and reactive gangue minerals associated with it, display a wide range of reactivity in alkaline gold cyanidation [1]. Gold usually occurs with various conductive sulphide minerals and the presence of galvanic interaction between gold and sulphide mineral particles plays an important role on the dissolution behaviour of gold in aerated cyanide solutions. The phenomenon which occurs when two dissimilar electrodes such as gold and a conductive mineral are brought into contact in the same corrosive environment is referred to as galvanic corrosion. Gold anodic dissolution can be engendered when the gold open circuit potential is less than that of the coexisting sulphides and other ore constituents [2-4].

It has been established that gold has a more negative potential than some of the sulphide minerals such as pyrite, pyrrhotite, chalcopyrite, sphalerite, and stibnite in a cyanide solution. It is, therefore, expected that gold will dissolve faster when present in galvanic contact with these sulphide minerals. The sulphide minerals exhibiting electrical conductivity allow charge transfer at their surfaces. In the presence of gold-sulphide contacts, galvanic interactions were previously shown to considerably influence the gold leaching behaviour [2,3,5-10].

The sulphide minerals are readily soluble in cyanide solution and the species resulting from the dissolution of sulphide minerals influence the gold cyanidation in various ways, rendering the gold cyanidation process difficult to optimize. The selectivity of cyanide for gold is poor over the enclosing sulphide mineral matrix, and these parasitic reactions inflict extra utility costs and profit losses resulting from high levels of cyanide and dissolved oxygen consumption [11]. The species such as hydroxides of iron or elemental sulphur, resulting from the dissolution of sulphide minerals, cause the surface passivation of gold and proved detrimental to gold leaching [8,12-15].

The classical study of gold dissolution kinetics was performed by Kudryk and Kellogg and the dissolution kinetics of pure gold in an aerated cyanide solution was found to be

significantly different from these findings [16]. This was because of the presence of small amounts of impurity, most likely silver [17]. Silver in metallic as well as alloyed forms, heavy metals such as lead, mercury, bismuth, thallium, and some organic activators have been known to significantly enhance the gold dissolution rate [15,17-20].

The electrochemical behaviour of pure gold in aerated cyanide solutions is different from that of a 50 %-50 % gold-silver alloy. The dissolution of pure gold was remarkably enhanced by the presence of silver with gold in metallic form, gold-silver alloys, as well as silver in dissolved form. A detailed study on the influence of small amounts of silver (1–5 %) present as a gold-silver alloy was performed and the effect of metallic silver on pure as well as gold associated with the sulphide minerals was investigated as well. These investigations revealed that silver significantly enhanced the leaching of pure gold in aerated cyanide solutions. It is well known that the surface of pure gold is blocked by a film of AuCN and the role of silver is to modify the surface of gold. The presence of silver enhances both the gold oxidation and oxygen reduction half reactions via bimetallic corrosion phenomena [15,17,19-21].

As silver is almost always present with gold in gold-bearing ores, there are numerous gold deposits where the silver grade exceeds that of the gold. As far as the presence of silver in high grade ores is concerned, there are over 200 argentiferous mineral species where silver is usually associated with polymetallic sulphides and sulphosalts. The most economically significant sulphide phases include acanthite [Ag<sub>2</sub>S]. Other sulphide phases include pyrargyrite [Ag<sub>3</sub>SbS<sub>3</sub>], proustite [Ag<sub>3</sub>AsS<sub>3</sub>], agularite [Ag<sub>4</sub>SeS], tennantite [Cu<sub>6</sub>[Cu<sub>4</sub>(Fe,Zn)<sub>2</sub>]As<sub>4</sub>S<sub>13</sub>], and tetrahedrite [(Cu,Fe,Ag,Zn)<sub>12</sub>Sb<sub>4</sub>S<sub>13</sub>], often with inclusions of silver [22-25].

Although plenty of information is available on the kinetics of gold dissolution with the presence of native, alloyed, and dissolved silver, studies are lacking regarding the effect of acanthite, i.e. the most significant silver mineral, on gold dissolution in the presence of other sulphide minerals. A detailed study would lead to a comprehensive understanding of the effect of the prominent silver mineral (Ag<sub>2</sub>S) on dissolution kinetics as well as overall recovery of gold, for ores with high silver grades. Currently, there exists very little knowledge on the effect of acanthite on the leaching of gold in cyanide solutions where rather numerous gold ores around the globe possess silver grades higher than that of gold. The following study

is therefore dedicated to investigate specifically the impact of silver sulphide on gold dissolution with the presence of other sulphidic minerals.

## **3.2. Experimental**

### **3.2.1. Materials and Reagents**

In the present work four sulphide ore samples received from Ward's Natural Science were used. These sulphide samples were termed as pyrite (Py), chalcopyrite (Cp), sphalerite (Sp), and stibnite (Sb), depending upon the dominant proportion of the named sulphide mineral present within. The chemical as well as mineralogical characterization of these samples have been elaborated elsewhere [15].

The samples were crush ground and sorted to select the particles ranging from  $-106\ \mu\text{m}$  to  $+53\ \mu\text{m}$ . The same size fraction ( $-106$  to  $+53\ \mu\text{m}$ ) of different sulphide minerals was selected in order to get a comparable total surface area per unit-mass for all the cyanidation experiments. Pure gold ( $P_{80} = 39\ \mu\text{m}$ , 99.998 %) and pure silver sulphide (99.9 % metals basis) powders purchased from Alfa Aesar (USA) were used in the present study. Distilled water was used for solution preparation in all cyanidation experiments. The reagents used in the present study, such as sodium cyanide, NaCN (98 %, Sigma-Aldrich Canada), sodium hydroxide, NaOH (Fisher Scientific Canada), and boric acid,  $\text{H}_3\text{BO}_3$  (99.5 %, Sigma-Aldrich Canada), were all certified analytical grade.

### **3.2.2. Equipment and Procedures**

The influence of silver sulphide, commonly known as acanthite (a prominent silver mineral), on gold recovery by the distribution of gold and silver sulphide within different mineral phases of a synthetic ore was studied using the multilayer packed-bed reactor (PBR) approach [3,9,10]. The aerated cyanide feed solution (30 mM/L (1.47 g/L)  $\text{CN}^-$  and  $\sim 8.5\ \text{mg/L O}_2$ ) was continuously sojourned through the fixed bed of the reactor in a closed loop at a constant flow rate of 10.4 mL/min using a peristaltic pump. The detailed description of the experimental setup has been elaborated elsewhere [15].

In the present study, the effect of oxygen consumption was altered by bubbling air through the reactor for all the duration of experiments to maintain a constant dissolved oxygen level ( $\text{DO}_2 \sim 8.5 \text{ mg/L}$  at  $25 \text{ }^\circ\text{C}$ ), which was monitored by means of a dissolved oxygen probe (FOXY-AL300 model from Ocean Optics), while pH of the feed solution was maintained at  $11 \pm 0.01$  using an Oakton 1000 series pH-meter.

The influence of sulphides on gold dissolution was assessed with each of the above minerals in a two-layer  $\text{X||silica}$  configuration by seeding one at a time, Au powder (50 mg) in one of the sulphide minerals ( $X = \text{Py, Cp, Sp, or Sb}$ ) or the silica layers (Figure 3.1a). First, 50 mg of Au powder was dispersed in 4 g of one of the above mentioned “X” sulphide minerals. This arrangement enables galvanic interactions among all the constituents. On the other hand, the dispersion of Au powder within the inert silica particles segregated by the one of the above sulphide minerals will be under the passivation effect from the segregated sulphide layer. The mineral and silica phases were electrically disconnected by means of packing these in separate reactors connected in series. The inter-reactor separation is depicted as “||” in the  $\text{X||silica}$  syntax.

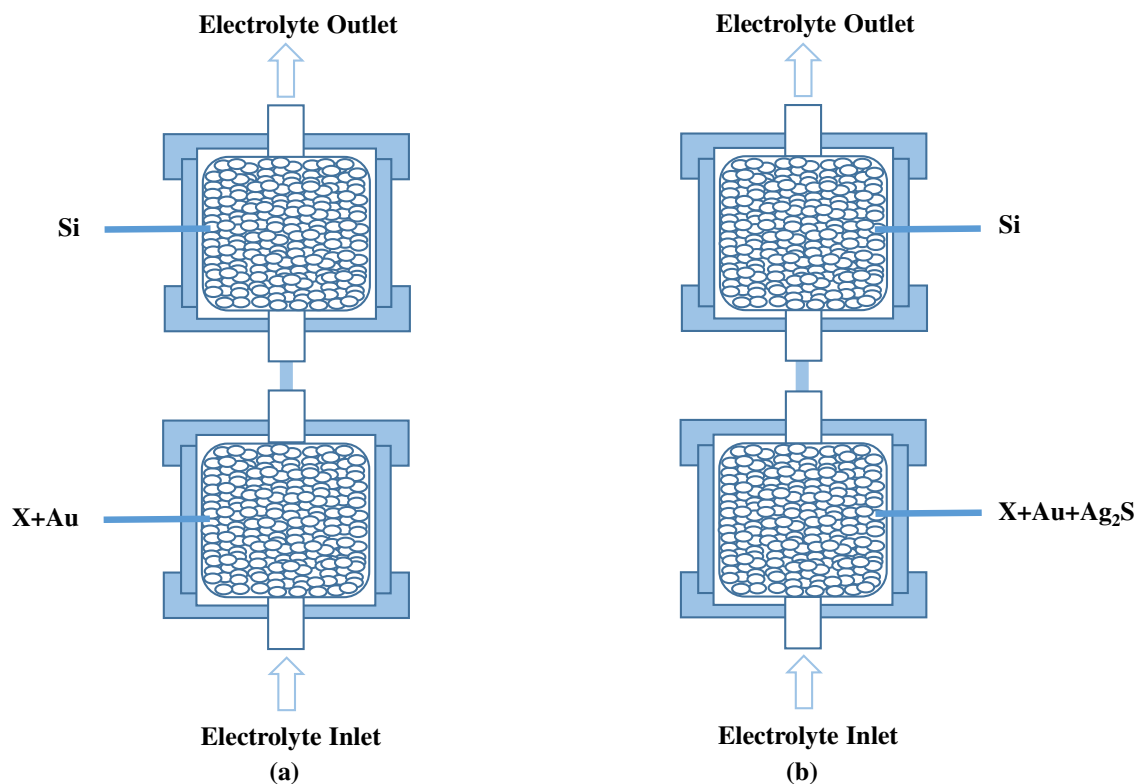


**Figure 3.1.** Gold dissolution: (a) Au dispersion pattern within sulfide (X) and quartz powder layers, (b) Au & Ag<sub>2</sub>S dispersion pattern within sulfide (X) and quartz powder layers: Reaction conditions: CN<sup>-</sup> = 30 mM, DO<sub>2</sub> = 0.25 mM, pH = 11.

The influence of mineral associations on gold leaching in the presence of Ag<sub>2</sub>S has been investigated by enabling X-Au-Ag<sub>2</sub>S ternary as well as Au-Ag<sub>2</sub>S binary galvanic interactions, assessed in two-layer ||X||silica|| configurations by seeding Au and/or Ag<sub>2</sub>S either in the X (X = Py, Cp, Sp, or Sb) layer and/or in the silica layer (Figure 3.1b). The following modalities were studied ||X+Au+Ag<sub>2</sub>S||silica|| and ||X||silica+Au+Ag<sub>2</sub>S|| where Au and Ag<sub>2</sub>S subscripts stand for the seeded layer while “X” represents one of the above stated sulphide mineral layers.

Benchmark tests for Au and Ag<sub>2</sub>S dissolution were performed by dispersing 50 mg of each precious metals Au and Ag<sub>2</sub>S within the quartz particles filling the whole working section of the PBR. The benchmark tests for Au and Ag<sub>2</sub>S have been represented by Case C and Case D, respectively, while Au and Ag leaching patterns were marked by Au-curve and Ag-curve, respectively, on all the leaching charts shown in this study.

The elemental analysis of the pregnant leach solution was performed by using a Perkin Elmer AA-800 atomic absorption spectrometer (AAS), by collecting small aliquots from the container using a syringe, filtrated with a particles filter VWR 0.45  $\mu\text{m}$ , at regular intervals during the length of the experiment. The leaching kinetics for the gold and silver were monitored by estimating the percentage of respective dissolved metal as compared to the initially dispersed mass of precious metals within the sulphidic layer as well as silica layers.

### **3.2.3. X-Ray Photoelectron Spectroscopy**

Gold cyanidation experiments were performed in the same way as explained in the Equipment and Procedures section. The gold particles were collected after the cyanidation experiments, rinsed with plenty of distilled water of the same pH to remove the excess free cyanide as well as loosely bound physisorbed species, dried, and kept under  $\text{N}_2$  atmosphere for 48 h. The surface characterization studies were carried out by X-ray photoelectron spectroscopy (XPS) using an AXIS-ULTRA instrument by KRATOS (UK), with a monochromatic Al K-alpha X-ray source operated at 300 W. The analyzer is run in the constant pass energy mode. An analyzed spot approximately  $700 \mu\text{m} \times 300 \mu\text{m}$ , represents the size of the monochromatic X-ray beam. Multichannel electron counting is performed with an 8 channel electron multiplier detector. Powder samples were placed in clean metallic cups while pressure during analysis was in the  $1.3 \mu\text{Pa}$  ( $10^{-8}$  Torr) range. Electrostatic charge which appears on the electrically insulating samples under X-ray irradiation can be neutralized with an integrated very low energy electron flood gun. Element analysis was performed by recording survey spectra at pass energy of 160 eV and energy step of 1 eV per channel. The apparent relative concentrations were calculated using appropriate sensitivity factors. High-resolution spectra were also recorded at pass energy of 40, 20, or 10 eV and step sizes of 0.1, 0.05, and 0.025 eV respectively, while curve-fitting was performed using the CasaXPS software.

### 3.3. Results and Discussion

#### 3.3.1. Benchmark Tests for Gold and Silver Sulphide Leaching

The benchmark tests for the gold as well as the silver sulphide dissolution were performed by separate dispersion of the gold and silver sulphide in silica layers which ultimately filled the whole PBR. Aerated cyanide solution, with composition elaborated in the Experimental section, was used for the leaching experiments. The dissolution of the precious metals was performed by continuous circulation of the aerated cyanide leach solution through the fixed bed of the reactor.

The dissolution pattern for Au and Ag<sub>2</sub>S dispersed within quartz powder is elaborated in Figure 3.2a. The dispersion of Au embedded in the quartz layer resulted in Au dissolution of 15 %, whereas the silver extracted from the dissolution of Ag<sub>2</sub>S while dispersed in quartz particles amounted to 4 % after 6 h of cyanidation. Pure gold dissolves much more slowly in pure aerated cyanide solutions. Three distinct current peaks have been reported for the anodic oxidation of gold in cyanide solutions in the potential range  $-1.0$  to  $+1.0$  V (SCE), and the main peak being at  $\sim 0.15$  V (SCE), have been used to justify the passivation of impurity-free gold [26].

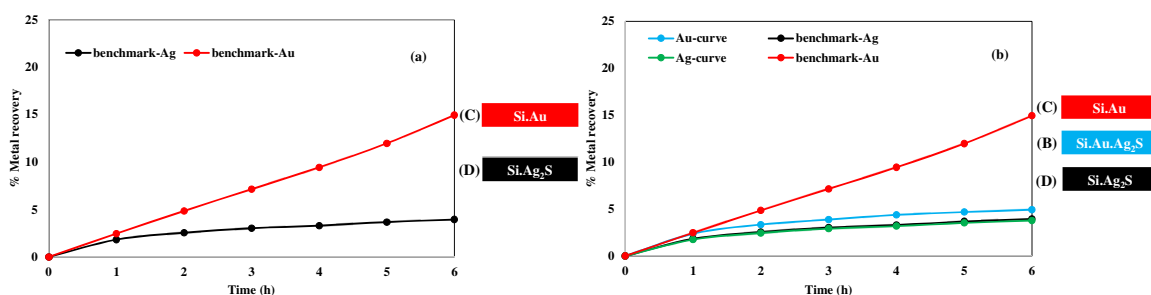


**Figure 3.2.** Gold dissolution: (a) gold and silver sulfide dissolution within quartz layer, (b) effect of Ag<sub>2</sub>S on gold dissolution within quartz layer. Reaction conditions: CN<sup>-</sup> = 30 mM, DO<sub>2</sub> = 0.25 mM, pH = 11.

The oxidation of metallic gold as well as the reduction of gold (I) ions appear to involve the adsorbed species AuCN<sub>ads</sub> corresponding to the reversible peak at  $\sim 0.15$  V (SCE). On the other hand, the adsorbed species on gold surface, such as AuCN.AuOH, Au(OH)(CN)<sup>-</sup>,

$\text{Au(OH)(CN)}^{3-}$ ,  $\text{Au(OH)}$  are responsible for the poor dissolution of impurity-free gold in aerated cyanide solutions [26,27].

The estimated amount of silver from the dissolution of silver sulphide lags far behind the dissolution of gold. Moreover, conventional leaching tests revealed that silver recovery was remarkably lower than that of gold under typical cyanidation conditions. The final extraction of silver was only 5 % after 60 h by the conventional cyanidation [28]. This result confirmed that it was difficult to extract silver from pure silver sulphide by the conventional cyanidation processes. Sometimes silver extraction is only about half that of gold. The suspected possible reasons are the different mineralogy and mode of occurrence between silver and gold in natural ores [29]. Unlike gold, which almost occurs naturally in metallic form, silver is found in many minerals in variable concentrations. Silver usually occurs as silver sulphide minerals in the ore, e.g. acanthite ( $\text{Ag}_2\text{S}$ ) and argentojarosites ( $\text{AgFe}_3[\text{SO}_4]_2(\text{OH})_6$ ), the low solubility of these silver sulphides was believed to limit the extraction of silver [22,30].

The dissolution pattern of Au particles with the addition of  $\text{Ag}_2\text{S}$  has been illustrated in Figure 3.2b. The effect of silver sulphide on the dissolution of pure gold was studied by dispersion of Au and  $\text{Ag}_2\text{S}$  powders within the quartz particles and this filled the whole PBR. As already seen from Figure 3.2a, if pure metallic gold dissolves much more slowly in aerated cyanide solution, addition of  $\text{Ag}_2\text{S}$  retarded gold dissolution even more severely (Figure 3.2b). The Au dissolution was found to be 4.9 % with  $\text{Ag}_2\text{S}$  as compared to 15 % for Au alone after 6 h of cyanidation while the silver sulphide dissolution almost followed its benchmark pattern. The decrease in Au dissolution could be attributed to the formation of silver sulphide passive film on the surface of gold with the reunion of silver and sulphide ions in the cyanide media. This silver sulphide passive film is not easy to dissolve with standard cyanidation conditions as is clear from the dissolution pattern of  $\text{Ag}_2\text{S}$  in cyanide solution (Figure 3.2a).

### **3.3.2. Gold Leaching with Pyrite-Silica System**

The conductive sulphide minerals associated with gold play a key role in gold dissolution during the cyanidation process. The association of gold and sulphide mineral particles lead to the development of galvanic interactions among the ore constituents. Galvanic corrosion



may occur when two dissimilar electrodes such as gold and a conductive mineral are brought into contact in the same corrosive environment [2].

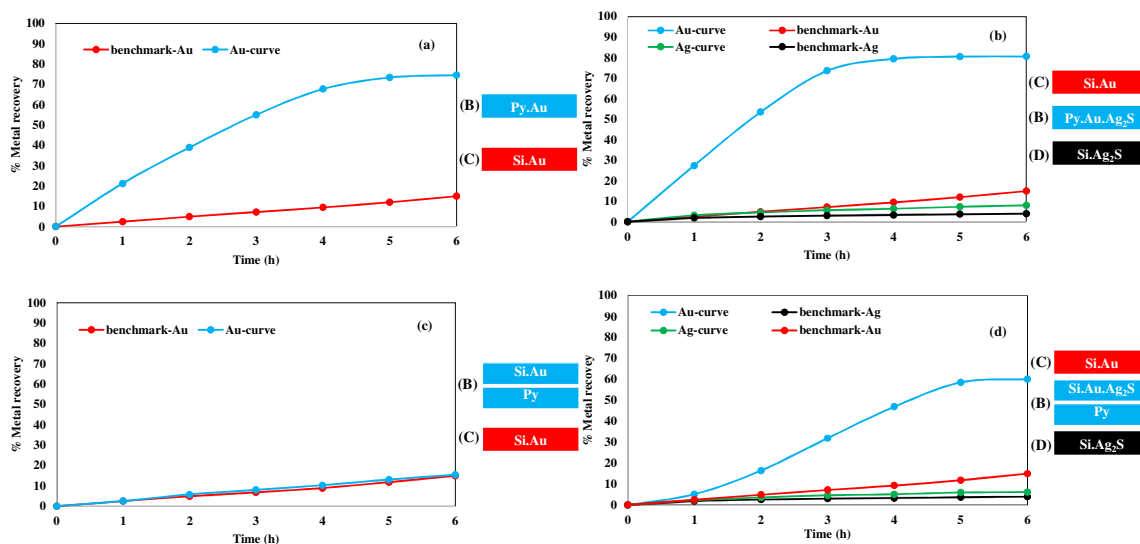


**Figure 3.3.** Gold dissolution: (a) gold dissolution with pyrite, Py+Au//Si, (b) Ag<sub>2</sub>S on gold dissolution with pyrite, Py+Au+Ag<sub>2</sub>S//Si, (c) gold dissolution with pyrite, Py//Si+Au, (d) Ag<sub>2</sub>S on gold dissolution with pyrite, Py//Si+Au+Ag<sub>2</sub>S. Reaction conditions: CN<sup>-</sup> = 30 mM, DO<sub>2</sub> = 0.25 mM, pH = 11.

The kinetics of gold dissolution under galvanic as well as passivation contexts from pyrite has been elaborated in Figures 3.3a and 3.3c. The surface-to-surface contact between Au and pyrite particles promoted the highest gold dissolution, resulting in Au dissolution of 74.6 % after 6 h of cyanidation (Figure 3.3a). A net increase of +59.6 % in gold leaching was observed as compared to the benchmark test Case C. By placing Au and pyrite all together, a galvanic cell was formed with Au acting as the anode and the pyrite surface as the cathode. A high potential difference of about 420 mV was estimated between gold and pyrite that can justify the measured high galvanic current of 2370 mA/m<sup>2</sup> and higher net Au dissolution [3]. This increase in Au dissolution would also be attributed to the enhanced oxygen reduction phenomenon over the entire mineral surface while Au and the sulphide mineral are in close contact with each other. The conductive sulphide mineral surfaces, such as pyrite, provide a much higher surface area for oxygen reduction as compared to the Au surface alone. Au dissolution is oxygen-diffusion limited at high cyanide concentration. The Au particles in close contact with sulphide mineral particles result in higher oxygen reduction that ultimately promotes the gold dissolution rate as compared to pure gold [3,4,20].

The Au leaching pattern for the gold powder dispersed within the quartz powder layer and segregated from the pyrite mineral is illustrated in Figure 3.3c. The Au dissolution was estimated to be 15.5 % in this case, with almost the same pattern as the benchmark test. This indicates that the dissolved species from the segregated pyrite layer did not adsorb onto the gold surface, causing no passivation at the given conditions.

### **3.3.3. Effect of Silver Sulphide on Gold Leaching with Pyrite-Silica System**

The kinetics of gold dissolution was investigated by addition of silver sulphide for the pyrite-silica system and is expressed in Figures 3.3b and 3.3d. The particle-particle association of Au, Ag<sub>2</sub>S, and pyrite mineral and their accumulated effect on Au dissolution was evaluated by mixing the Au powder with Ag<sub>2</sub>S and pyrite mineral and packing all of them within the same layer of a single PBR (Figure 3.3b). This demonstrates that physical contact between gold and sulphide minerals is a prerequisite for the establishment of micro-electrical contacts. The indirect effect of sulphide mineral layer on Au dissolution, resulting from the dissolution of pyrite particles in cyanide solution, was assessed by placing both Au and Ag<sub>2</sub>S in the quartz layer and segregating them from the pyrite mineral layer (Figure 3.3d).

The ternary galvanic contacts were enabled by placing Au, Ag<sub>2</sub>S, and pyrite within the same layer. On the other hand, placement of Au and Ag<sub>2</sub>S among the quartz particles, segregated by the pyrite layer, enabled binary galvanic contacts between Au and Ag<sub>2</sub>S, while at the same time being under the *indirect* impact from the separate pyrite layer.

The effect of Ag<sub>2</sub>S mineral on Au dissolution, while Au, Ag<sub>2</sub>S, and pyrite particles were in close contact with one another, is represented in Figure 3b. The addition of Ag<sub>2</sub>S raised the Au recovery from 74.6 % to 80.6 % after 6 h of cyanidation. The Ag recovered by the dissolution of Ag<sub>2</sub>S was estimated to be 8 % after the cyanidation experiment. It is also clear from Figure 3.3b that the introduction of silver sulphide enhanced the leaching kinetics as well as the overall recovery of gold as compared to the presence of gold alone within pyrite.

The presence of silver sulphide along with gold within the quartz layer, while being segregated by the pyrite mineral layer, enhanced the Au dissolution remarkably (Figure 3.3d). The Au dissolution was enhanced from 15.5 % without Ag<sub>2</sub>S to 60 % with Ag<sub>2</sub>S addition,

while both Au and Ag<sub>2</sub>S dispersed in the quartz layer and segregated from the pyrite mineral layer. The Ag recovered under indirect impact from pyrite layer was accounted to be 6 % after 6 h of cyanidation process. Silver sulphide proved to enhance the gold dissolution while Au particles were under direct as well as indirect influence from the pyrite mineral particles. The silver sulphide has a qualitative impact similar to that of its metallic silver counterpart on gold dissolution in the presence of the pyrite particles [15].

### **3.3.4. Gold Leaching with Chalcopyrite-Silica System**

The gold dissolution kinetics under both galvanic as well as passivation contexts from the chalcopyrite layer is elaborated in Figure 3.4. The permanent galvanic contacts between Au and chalcopyrite particles resulted in higher Au dissolution as compared to the benchmark test shown in Figure 3.4a. The close contacts between Au and Cp particles led to an Au dissolution of 57 % as compared to the benchmark test of 15 %, with a net increase of +42 % after 6 h of cyanidation. Likewise, Au recovery was estimated to remain low as compared with the sibling Case B for pyrite, (Figure 3.3a). This behaviour in gold leaching rate was similar to the one diagnosed with a rotating disc gold electrode immersed in chalcopyrite slurry as well as from PBR tests [3,14].

A comparatively large value of galvanic current ( $\sim 1650 \text{ mA/m}^2$ ) was reported for the gold particles present with the chalcopyrite mineral particles, but the amplitude and variation intervals for galvanic current were lower than those reported for pyrite. The potential difference between Au/chalcopyrite was reported to be 256 mV, which was found to be lower as compared to the Au/pyrite system [3]. These low potential differences as well as low galvanic currents could be held responsible for low Au/chalcopyrite galvanic contacts as compared to the Au/pyrite galvanic interactions in terms of gold recovery.

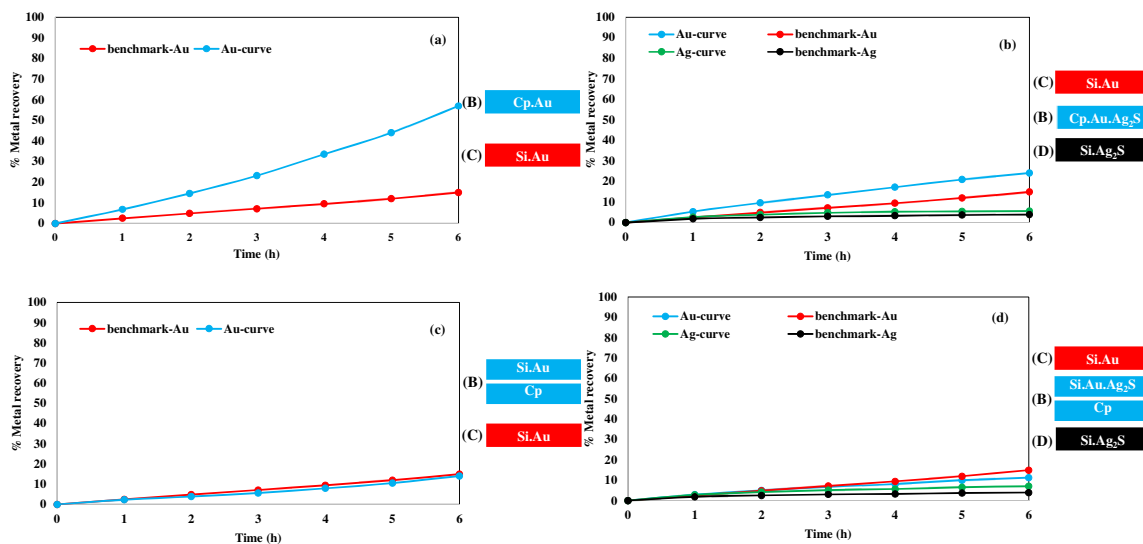


**Figure 3.4.** Gold dissolution: (a) gold dissolution with chalcopyrite, Cp+Au//Si, (b) Ag<sub>2</sub>S on gold dissolution with chalcopyrite, Cp+Au+Ag<sub>2</sub>S//Si, (c) gold dissolution with chalcopyrite, Cp//Si+Au, (d) Ag<sub>2</sub>S on gold dissolution with chalcopyrite, Cp//Si+Au+Ag<sub>2</sub>S. Reaction conditions: CN<sup>-</sup> = 30 mM, DO<sub>2</sub> = 0.25 mM, pH = 11.

The indirect effect of the chalcopyrite mineral layer on the dissolution of gold dispersed within the quartz layer neither promoted nor retarded the gold dissolution (Figure 3.4c). The Au dissolution was estimated to be 14 % after 6 h of cyanidation and this almost followed the benchmark pattern of gold leaching as is clear from Figure 3.4c. This leaching pattern for gold signifies that the species resulting from the dissolution of the segregated chalcopyrite layer were not found to cause any passivation to the gold surface and the gold leaching is almost the same as for pure gold dispersed in the quartz layer.

### 3.3.5. Effect of Silver Sulphide on Gold Leaching with Chalcopyrite-Silica System

The presence of silver sulphide mineral with gold particles greatly influenced the kinetics as well as overall gold recovery in an aerated cyanide solution. The leaching kinetics pattern as well as the overall Au and Ag recoveries from Au/Ag<sub>2</sub>S dissolution for chalcopyrite-silica system, in aerated cyanide solution, are expressed in Figures 3.4b and 3.4d. Au dissolution was estimated to be 24.2 % under the global galvanic contacts from Au, Ag<sub>2</sub>S, and chalcopyrite mineral particles. The association of silver sulphide along with chalcopyrite particles retarded the gold dissolution severely by decreasing the overall recovery by 32.8 % after 6 h of cyanidation, while all the mineral and precious metal constituents were present in the same PBR layer (Figure 3.4b). The silver recovered from the dissolution of Ag<sub>2</sub>S, in

an arrangement of close contact of silver sulphide and chalcopyrite sulphidic mineral particles, was estimated to be 5.6 % after the aforementioned cyanidation time. Figure 3.4d demonstrates the leaching patterns of Au and Ag while both Au and Ag<sub>2</sub>S were dispersed within the quartz layer and segregated from the chalcopyrite mineral layer. Au dissolution was retarded to 11.3 % as compared to the 15 % recovery for the benchmark test. Ag recovery was estimated to be 7 % after 6 h of cyanidation experiment.

Consequently, the introduction of silver sulphide was recognized to have a decelerating effect on gold dissolution while both under direct as well as indirect effect from the chalcopyrite mineral layer. A reduction in Au leaching was observed for the Au particles dispersed in the chalcopyrite layer as well as in the silica layer segregated from the chalcopyrite layer. One possible reason for this retardation in Au recovery could be the formation of surface films, which could stem from the interaction of silver ions with even low concentrations of hydrosulphide (HS<sup>-</sup>) ions resulting from the dissolution of sulphide minerals [26]. Furthermore, the formation of Ag<sub>2</sub>S or elemental sulphur (S) layers on the surface of gold particles resulting from the dissolution of chalcopyrite has also been proposed [15,31].

### **3.3.6. Gold Leaching with Sphalerite-Silica System**

The gold powder and sphalerite mineral particles were brought into contact by mixing the Au and sphalerite particles all together and packing them in the same PBR layer. This dispersion pattern enables the binary galvanic contacts between the sphalerite layer and precious metal Au particles. The kinetics of Au leaching for the sphalerite-silica system are shown in Figure 3.5. The micro-electrical contacts between Au and sphalerite particles resulted in gold dissolution of 1.6 % as compared to the 15 % of the benchmark test, as represented in Figure 3.5a. This drastic decrease in Au dissolution could be attributed to the very poor electrical conductivity of the sphalerite mineral. In aerated cyanide solution the galvanic current density between gold and sphalerite was reported to be very low (<40 mA/m<sup>2</sup>). This value was found to be much lower than the galvanic current densities measured under the same conditions for Au-pyrite and Au-chalcopyrite systems [3].

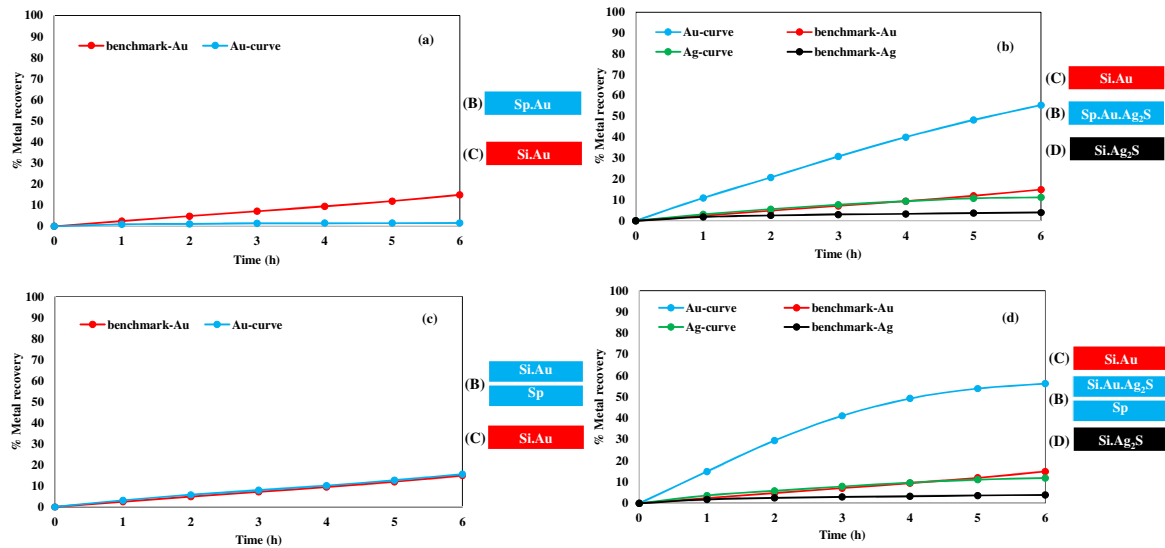


**Figure 3.5.** Gold dissolution: (a) gold dissolution with sphalerite, Sp+Au//Si, (b) Ag<sub>2</sub>S on gold dissolution with sphalerite, Sp+Au+Ag<sub>2</sub>S//Si, (c) gold dissolution with sphalerite, Sp//Si+Au, (d) Ag<sub>2</sub>S on gold dissolution with sphalerite, Sp//Si+Au+Ag<sub>2</sub>S. Reaction conditions: CN<sup>-</sup> = 30 mM, DO<sub>2</sub> = 0.25 mM, pH = 11.

Placing Au within the quartz powder layer and segregating it from the sphalerite mineral was adopted to investigate the effect of dissolved species from the sphalerite layer on Au dissolution. As shown in Figure 3.5c, Au dissolution was found to be 15.6 % with the gold particles dispersed within the quartz layer and segregated from the sphalerite mineral particles. Hence, Au recovered after 6 h of cyanidation experiment was found to be almost the same as in the benchmark test. This unveils once again the quasi-neutral character of the segregated sphalerite mineral layer in terms of kinetics and net recovery of Au particles leaching. The poor recovery of Au particles while having close contact with the sphalerite particles (Figure 3.5a) could only be attributed to the poor conductivity of the sphalerite particles which does not allow enough electron transfer for sufficient oxygen reduction to take place at their surfaces [3,15]. Consequently, low oxygen reduction due to very small amounts of electron transfer at the mineral surface is responsible for the merely poor Au recovery.

### 3.3.7. Effect of Silver Sulphide on Gold Leaching with Sphalerite-Silica System

A two-layer mineral system arrangement was postulated, such as both Au and Ag<sub>2</sub>S dispersed in Sp (Figure 3.5b) as well as silica (Figure 3.5d) layers. The leaching kinetics pattern for the influence of Ag<sub>2</sub>S on Au dissolution with sphalerite, while all the three constituents were in

close contact with one another, is elaborated in Figure 3.5b. Introduction of  $\text{Ag}_2\text{S}$  with Au within the sphalerite mineral layer has enhanced the dissolution of gold from 1.6 % to 55.4 % after the same duration of the cyanidation experiments. Also Ag recovered by the dissolution of  $\text{Ag}_2\text{S}$  was estimated to be 11.2 % in 6 h of cyanidation. It appears that dissolved Ag resulting from  $\text{Ag}_2\text{S}$  dissolution was able to overcome the poor electrical conductivity from the sphalerite mineral particles. This was presumed to enhance the Au recovery by adsorbing on the Au surface and promoting Au dissolution via bimetallic corrosion phenomenon [15].

Association of silver sulphide with gold particles dispersed within the quartz layer and segregated by the sphalerite layer (Figure 3.5d) has shown much higher gold dissolution kinetics as compared to gold and silver sulphide present in the sphalerite layer. The Au recovery was estimated to be 56.3 % after 6 h of cyanidation with a significant increase in kinetics as shown in Figure 3.5d. This enhanced dissolution kinetics was ascribed to the fact that the Au particles were not in contact with the poorly conducting sphalerite mineral particles. The Ag recovery was estimated to be 11.8 % after 6 h of cyanidation.

The presence of silver sulphide has enhanced the Au dissolution kinetics as well as its overall recovery whether Au and  $\text{Ag}_2\text{S}$  were subject to direct or indirect influence from the sphalerite mineral layer. In the case of the sphalerite-silica system,  $\text{Ag}_2\text{S}$  behaved similarly to silver present as pure metal, alloyed with gold or dissolved in the cyanide solution. As reported in the literature, silver present as pure metal, alloyed with gold, or in a dissolved state, enhanced Au dissolution remarkably [15,17,20].

### **3.3.8. Gold Leaching with Stibnite-Silica System**

Gold particles exhibited very poor dissolution while present under direct as well as indirect effects from the stibnite mineral particles. The leaching patterns for the Au particles under galvanic and passivation effects are shown in Figures 3.6a and 3.6c. The Au particles dispersed within the stibnite mineral particles resulted in an Au recovery of 1.1 % as indicated in Figure 3.6a. This indicates that the galvanic interactions from the stibnite particles were unable to overcome the passivation of Au surface as a result of the dissolved species from the stibnite particles. The galvanic current between the Au-stibnite pair was found to be very low and could likely be due to surface obstructions of gold by the dissolution

of stibnite layer in the cyanide solution [3]. On the other hand, Au recovery after 6 h merely attained the 1.3 % mark, when Au particles were dispersed within the quartz layer while segregated from the stibnite layer (Figure 3.6c).

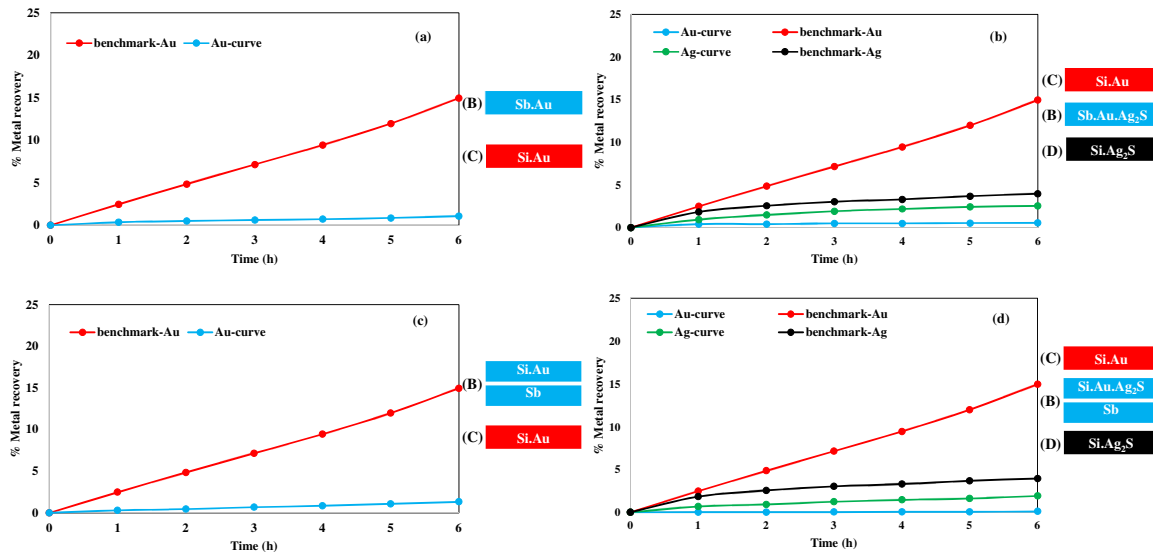


**Figure 3.6.** Gold dissolution: (a) gold dissolution with stibnite, Sb+Au//Si, (b) Ag<sub>2</sub>S on gold dissolution with stibnite, Sb+Au+Ag<sub>2</sub>S//Si, (c) gold dissolution with stibnite, Sb//Si+Au, (d) Ag<sub>2</sub>S on gold dissolution with stibnite, Sb//Si+Au+Ag<sub>2</sub>S. Reaction conditions: CN<sup>-</sup> = 30 mM, DO<sub>2</sub> = 0.25 mM, pH = 11.

The Au recovery was severely hindered under direct as well as indirect contact configurations from the stibnite sulphidic layer. These results are similar to those reported in the literature that stibnite, even present at very low concentrations, had a prominent retarding effect on gold leaching. Gold leaching kinetics was strongly retarded even in the presence of 20 ppm stibnite [3,15,32-34]. The passivation of gold surface is one of the prominent challenges practically faced in gold ore processing. The gold surface is protected by a surface film which results in poor gold extraction during gold cyanidation. This severe hindrance could be a result of formation of an antimony oxide film on the gold shielding its surface from the attack of cyanide ions to dissolve it [34].

### 3.3.9. Effect of Silver Sulphide on Gold Leaching with Stibnite-Silica System

The effect of silver sulphide on the dissolution of gold particles was investigated by placing the Au and Ag<sub>2</sub>S particles within the stibnite as well as the quartz powder layers. The gold leaching curves for the dispersion patterns, such as ||Sb+Au+Ag<sub>2</sub>S||Si|| and



||Sb||Si+Au+Ag<sub>2</sub>S||, are described in Figures 3.6b and 3.6d. Au dissolution was reduced from 1.1 % (Figure 3.6a) to 0.55 % (Figure 3.6b) by enabling micro-electrical environments among Au, Ag<sub>2</sub>S, and stibnite mineral particles, placing all together within the same layer. Ag recovered was 2.5 % as a result of 6 h of silver sulphide cyanidation within stibnite particles (Figure 3.6b).

The Au as well as Ag recovery curves for the dispersion Au/Ag<sub>2</sub>S within the quartz layer and segregated from the stibnite mineral layer are shown in Figure 6d. The Au recovery amounted to just 0.1 % and Ag recovery was found to be 1.9 % after 6 h of cyanidation. The galvanic contacts among Au and Ag<sub>2</sub>S were unable to overcome the surface passivation by the species resulting from the dissolution of stibnite in an aerated cyanide solution.

The presence of stibnite, whether in direct or indirect configurations with Au particles, contributed towards severe retardation of gold dissolution. The association of silver sulphide along with gold both under galvanic and passivation phenomena has further worsened the Au dissolution as compared to gold alone. This could be attributed to the formation of a tight layer on the Au surface which retarded the net Au dissolution severely.

### **3.3.10. X-Ray Photoelectron Spectroscopy of Gold Particles Isolated Post-Cyanidation**

The surface characterization of gold particles up to few nm in depth [35] was performed to provide an insight to the surface obstructing species formed during the cyanidation process. It is worth remembering that the surface analysis concerns the cherry-picked gold particles after the 6 h dissolution tests in the PBR were carried out. An XPS study was performed for the sulphidic minerals, such as chalcopyrite and stibnite, to which the addition of silver sulphide showed a detrimental effect on gold dissolution. This could provide a better understanding of the surface obstructing species resulting from the interaction of gold particles with chalcopyrite and stibnite minerals in the presence of silver sulphide. The envelopes shown in Figure 3.7 as continuous noise-free black lines represent the sum of the analytical peaks used to fit the high-resolution spectra. The circle symbols with noise are the experimental spectra. The experimental spectra are approximated with analytical peaks representing the oxidation states of the different elemental species. The base line was approximated using a Shirley background.

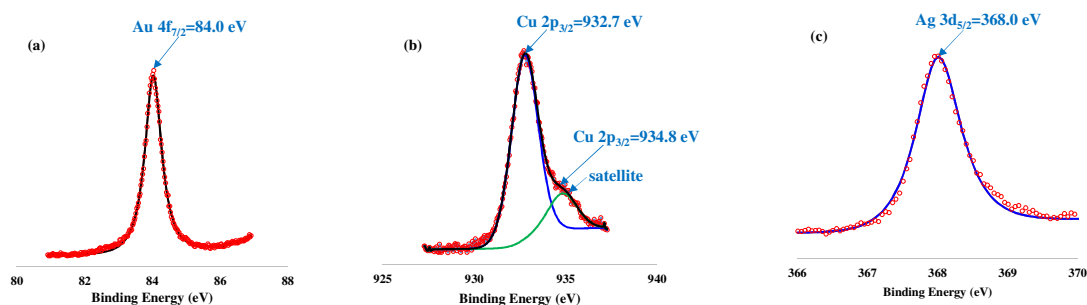


**Figure 3.7.** X-ray spectra of gold surface: (a) Au 4f<sub>7/2</sub> for gold with Ag<sub>2</sub>S and chalcopyrite, (b) Cu 2p<sub>3/2</sub> on gold surface with Ag<sub>2</sub>S and chalcopyrite, (c) Ag 3d<sub>5/2</sub> on gold surface with Ag<sub>2</sub>S and chalcopyrite. Reaction conditions: CN<sup>-</sup> = 30 mM, DO<sub>2</sub> = 0.25 mM, pH = 11.

Relatively well behaved Au 4f<sub>7/2</sub> core level spectra for the gold particles interacting with chalcopyrite in the presence of Ag<sub>2</sub>S were obtained without using the neutralization gun (Figure 3.7a). Au<sup>0</sup> was easily identified from its Au 4f<sub>7/2</sub> binding energy (84.0 eV) and corresponding full-width at half maximum (FWHM) 0.58 eV, compared to Au 4f<sub>7/2</sub> of a pure gold (standard: BE = 83.95 eV and FWHM = 0.60 eV), obtained in the same experimental conditions and during the same run of experiments. However, as can be seen in Figure 3.7a, there is a small tail on the high BE side of the peak which is not present on the standard metallic Au. By enabling the neutralization gun, the main Au peak did not move but the tail was observed to shift on the low binding energy (BE) side of the Au<sup>0</sup> 4f<sub>7/2</sub> peak. This behaviour suggests that the gold particles are surrounded by very thin (< 5 nm in depth) poorly (or non-) electrically conductive layers or domains and that this contamination also contains a small amount of gold. This small amount of Au is covered by a relatively thick (still in the nanometer range) layer of a different composition that can be easily seen on the survey scan of this sample (not shown): on the high BE side of all Au related peaks, especially Au 4f, the background increases strongly instead of decreasing or staying flat as seen on samples more homogeneous in depth [36].

Cu was detected on the gold surface while gold associated with Ag<sub>2</sub>S and chalcopyrite in the cyanidation experiment and its Cu 2p<sub>3/2</sub> spectrum is shown in Figure 3.7b. This spectrum does not move with the use of the neutralization gun. The spectrum shows 2 Cu states: the most abundant one is at a BE value of 932.7 eV and can be attributed to copper (I) oxide (Cu<sub>2</sub>O) [37]. The second peak located at 934.8 eV is attributed to Cu(OH)<sub>2</sub> according to published data [38]. Note the presence of a small satellite peak used in the line fitting of

copper 2p<sub>3/2</sub> core level in Figure 3.7b. The satellite structure detected in the spectrum side of the Cu 2p line, at the high binding energy (near 943 eV), confirmed the shake-up transitions for Cu(II) [37]. The copper detected on the gold surface most probably comes from the dissolution of chalcopyrite mineral in the cyanide solution. The high-resolution scans of Ag 3d were recorded on the recovered gold particles as well, after cyanidation with chalcopyrite and Ag<sub>2</sub>S (Figure 3.7c). Ag 3d<sub>5/2</sub> peak is observed at a BE value of 368.0 eV. Literature data and our own measurements on Ag pure metallic samples indicate that the Ag 3d<sub>5/2</sub> binding energy located at 368.2 eV corresponds to that of metallic silver while a binding energy of 368.0 eV has been reported for Ag<sub>2</sub>S [35,39,40]. In summary, the spectral analysis of the experimental Cu 2p<sub>3/2</sub> peaks observed at 932.7, 934.8 eV, and Ag 3d<sub>5/2</sub> peak detected at 368.0 eV on the gold particles confirmed the presence of copper (I) oxide, copper hydroxide, as well as silver sulphide at the surface of gold particles. It could thus be concluded that the metal species observed at the gold surface were in the form of Ag<sub>2</sub>S and Cu<sub>2</sub>O/Cu(OH)<sub>2</sub> and very likely were the cause of the retarding effect on gold dissolution in the presence of chalcopyrite.

The detrimental effect of stibnite on gold dissolution was severe, with the oxygen enrichment making the situation worse. The presence of various species at the surface of gold particles has been investigated after cyanidation with the stibnite mineral. Figure 3.8a represents the high-resolution XPS spectrum of the Au 4f core-level of the sample prepared after gold cyanidation with stibnite mineral. Two distinct lines separated by 3.7 eV were observed, namely the Au 4f<sub>5/2</sub> and Au 4f<sub>7/2</sub> lines, which occur because of the spin-orbit splitting of the Au 4f core-level. The position of these lines was estimated, which were observed to be 87.8 eV and 84.1 eV, respectively. The Au 4f<sub>7/2</sub> binding energy of 84.1 eV is consistent with that of the gold in metallic state (Au<sup>0</sup>) as shown in Figure 3.8a [41,42].

The high-resolution XPS spectrum for Sb was obtained in order to understand the chemical state and composition of the antimony film observed at the gold surface. The spectra consist of two well-defined peaks in the energy range of 520–545 eV, and they also show a complicated feature due to the overlapping of O1s and Sb 3d<sub>5/2</sub> photoemission lines around 531 eV, as shown in Figure 3.8b. According to the literature, separation between Sb 3d<sub>3/2</sub> and Sb 3d<sub>5/2</sub> is 9.3 eV, and their relative area has to be [Sb 3d<sub>5/2</sub>]/[Sb 3d<sub>3/2</sub>] = 1.5, and peak widths

to be the same. The Sb 3d<sub>5/2</sub> is thus constructed from the fit of the Sb 3d<sub>3/2</sub> well defined peak: Sb 3d<sub>5/2</sub> is then located at 540.3 eV – 9.3 eV = 531.0 eV. The remaining empty structure area is attributed to O1s and fitted with 3 oxygen species O1s(I), O1s(II), and O1s(III) (Figure 3.8b).

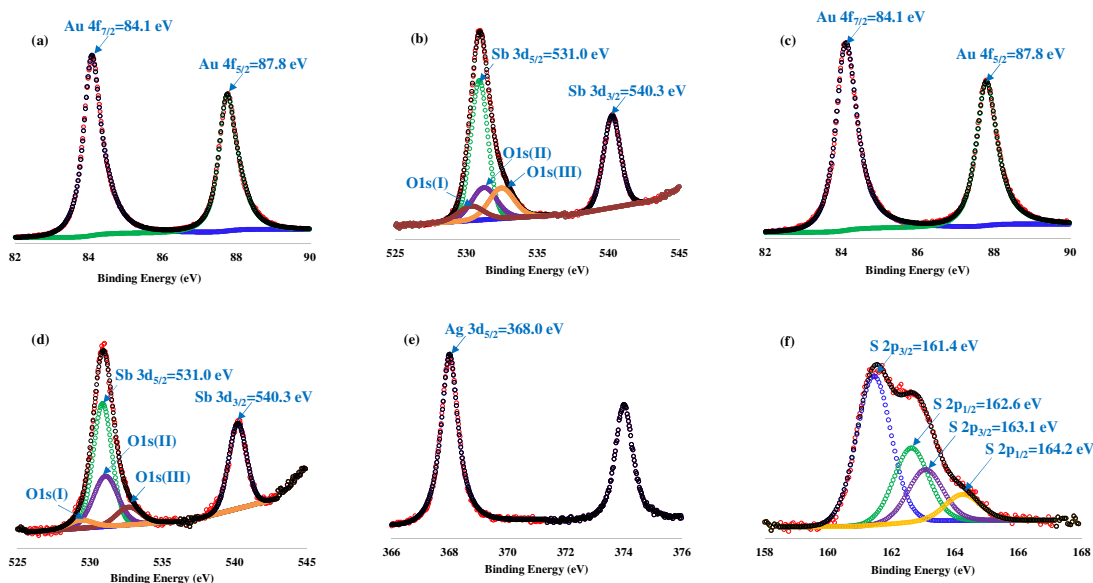


**Figure 3.8.** X-ray spectra of gold surface: (a) Au 4f spectra for gold with stibnite, (b) Sb 3d spectra for gold with stibnite, (c) Au 4f spectra for gold with Ag<sub>2</sub>S and stibnite, (d) Sb 3d spectra for gold with Ag<sub>2</sub>S and stibnite, (e) Ag 3d<sub>5/2</sub> spectra for gold with Ag<sub>2</sub>S and stibnite, (f) S 2p spectra for gold with Ag<sub>2</sub>S and stibnite. Reaction conditions: CN<sup>-</sup> = 30 mM, DO<sub>2</sub> = 0.25 mM, pH = 11.

It has been reported that the binding energies of Sb 3d<sub>3/2</sub> in Sb<sub>2</sub>O<sub>3</sub>, Sb<sub>2</sub>O<sub>4</sub>, and Sb<sub>2</sub>O<sub>5</sub> are 539.6, 539.8, and 540.2 eV, respectively [43]. Therefore, the Sb 3d<sub>3/2</sub> peak observed at BE = 540.3 eV confirms the presence of Sb as Sb<sub>2</sub>O<sub>5</sub> on the surface of gold particles. The O1s(II) peak appearing at 531 eV is assigned to the oxygen directly bound to antimony in the oxide lattice (Sb–O), [44] while the O1s(III) peak at higher binding energy around 532.4 eV is related to oxygen bound to metal hydroxides (M–OH) or hydrated species on the surface of gold. The O1s(I) peak at BE = 530.3 eV may arise due to the presence of other oxygen containing species incorporated in the film [42]. Summarizing all this discussion, it could be concluded that the retarding effect of stibnite on gold leaching was due to the formation of Sb<sub>2</sub>O<sub>5</sub> film (~5 nm in depth) on the surface gold particles.

In the case of silver sulphide addition to the gold cyanidation with stibnite particles, the high-resolution spectra for Au as well as the species such as Sb, Ag, and S detected on the surface of gold particle were recorded. Figure 8c represents the high-resolution XPS spectrum of the Au 4f core-level of the sample prepared after gold cyanidation under the influence of both Ag<sub>2</sub>S and stibnite. The position of these lines was measured to be 84.1 eV and 87.8 eV. As explained above, the Au 4f<sub>7/2</sub>, 4f<sub>5/2</sub> spectrum of gold representing the doublet lines with the Au 4f<sub>7/2</sub> binding energy of 84.1 eV also represent that gold is in metallic form (Au<sup>0</sup>) [41,42].

The high-resolution XPS spectrum for Sb was recorded in this case as well in order to understand the composition of the antimony film observed at the gold surface, as shown in Figure 3.8d. As explained above, the spectrum consists of the well-defined Sb 3d<sub>3/2</sub> peak at 540.3 eV and a peak around 531 eV being the sum of the Sb 3d<sub>5/2</sub> peak and of O1s components attributed to 3 oxygen species, as detailed above. The analysis of this Sb 3d data also confirms the presence of Sb as Sb<sub>2</sub>O<sub>5</sub> film on the surface of gold particles, [34] for the gold cyanidation performed in presence of silver sulphide and stibnite minerals.

The Ag 3d spectrum has been recorded for the case of gold cyanidation with silver sulphide and stibnite minerals, as shown in Figure 3.8e. The Ag 3d<sub>5/2</sub> peak has been observed at a BE value of 368.0 eV. The Ag 3d<sub>5/2</sub> core level located at 368.0 eV corresponds to the binding energy of Ag in the Ag<sub>2</sub>S lattice [35]. The S 2p<sub>3/2</sub> spectrum shows two S 2p doublets with S 2p<sub>3/2</sub> 161.4 and 163.1 as shown in Figure 3.8f, indicating the presence of sulphur species. The S 2p<sub>3/2</sub> peak observed at 161.4 eV is assigned to the Ag–S–Ag bonding of Ag<sub>2</sub>S [45]. The S 2p<sub>3/2</sub> peak at 163.1 eV is assigned to S–S–bonding, and it is about 17 % of the S 2p peak total area and probably resulted from the sulphide adsorption on the surface of gold particles [46].

Summarizing the analysis data for the Au, Ag, Sb, and S high-resolution spectra, it could be concluded that the surface films formed on the gold particles consist of Ag<sub>2</sub>S and Sb<sub>2</sub>O<sub>5</sub>. This means that in addition to Sb<sub>2</sub>O<sub>5</sub>, the presence of Ag<sub>2</sub>S on the gold surface is worsening the gold dissolution in the case of gold cyanidation performed with silver sulphide and stibnite. This argument is supported by the retardation of Au dissolution from 1.1 % (Figure 3.6a) to 0.55 % (Figure 3.6b) with the placement of Au, Ag<sub>2</sub>S, and stibnite mineral particles altogether within the same layer.

### **3.4. Conclusion**

The leaching kinetics as well as the overall recovery of gold was investigated by placing gold particles in direct as well as indirect contacts with synthetic sulphide ore samples in a multi-layered packed-bed cyanidation reactor. Over the experimental conditions explained above, the leaching kinetics and overall recovery were enhanced significantly for the pyrite mineral and also enhanced to a reasonable extent with the chalcopyrite sulphide mineral under the influence of direct contact among gold and sulphide mineral particles. The Au dissolution was retarded for the case of sphalerite and stibnite sulphidic minerals, while electrical contacts between the precious metal and mineral particles were enabled. The Au dissolution followed the benchmark pattern for the pyrite, chalcopyrite, and sphalerite minerals in the absence of the electrical contacts among the gold and sulphide mineral particles. Contrary to this, Au dissolution was retarded severely in the absence of electrical connections between gold and stibnite mineral particles.

The effect of silver sulphide association with gold in the presence of sulphidic minerals, both under galvanic as well as passivation conditions, was investigated in an arrangement explained in the Equipment and Procedures section. Four sets of mineral systems were established: pyrite-silica, chalcopyrite-silica, sphalerite-silica, and stibnite-silica. Silver sulphide addition enhanced gold leaching notably for the pyrite-silica and sphalerite-silica systems, with Au and  $\text{Ag}_2\text{S}$  having direct as well as indirect contact with the mineral particles.

On the other hand the chalcopyrite-silica and stibnite-silica systems did not respond well to the addition of silver sulphide. The gold recovery was observed to be on the lower side with the addition of silver sulphide. The XPS analysis of the gold particles showed that the dissolution of silver sulphide along with chalcopyrite resulted in an in situ formation of  $\text{Ag}_2\text{S}$  and  $\text{Cu}_2\text{O}/\text{Cu}(\text{OH})_2$  passivating layer on the surface of gold particles. The association of stibnite and silver sulphide resulted in the form of  $\text{Ag}_2\text{S}$  and  $\text{Sb}_2\text{O}_5$  passivating films on the surface of gold particles. The formation of the aforementioned films on the surface of gold particles might result in retardation of net dissolution of gold.

### **Acknowledgements**

Financial support from the Natural Sciences and Engineering Research Council through its Cooperative Research and Development grants program and from the supporting partners Agnico Eagle, Barrick, Camiro, Corem, Glencore, IamGold, Niobec, and Teck is gratefully acknowledged. The authors are also very thankful to Prof. Brian Hart from the Department of Earth Sciences (University of Western Ontario), and Caroline Olsen and Dr. Patrick Laflamme from Corem for encouraging discussions on gold leaching.

### 3.5. References

1. Marsden, J. O., and House, C. I., 2006, Chemistry of gold extraction. 2nd ed. Littleton, Colorado, Society for Mining, Metallurgy, and Exploration (SME).
2. Aghamirian, M. M., and Yen, W. T., 2005. Mechanisms of galvanic interactions between gold and sulfide minerals in cyanide solution. *Minerals Engineering*, 18, 393–407.
3. Azizi, A., Petre, C. F., Olsen, C., and Larachi, F., 2011. Untangling galvanic and passivation phenomena induced by sulfide minerals on precious metal leaching using a new packed-bed electrochemical cyanidation reactor. *Hydrometallurgy*, 107, 101–111.
4. Azizi, A., Petre, C. F., and Larachi, F., 2012. Leveraging strategies to increase gold cyanidation in the presence of sulfide minerals—Packed bed electrochemical reactor approach. *Hydrometallurgy*, 111–112, 73–81.
5. Filmer, A. O., 1982. The dissolution of gold from roasted pyrite concentrations. *Journal of the South African Institute of Mining and Metallurgy*, 90–94.
6. Paul, R.L., 1984. The role of electrochemistry in the extraction of gold. *Journal of Electroanalytical Chemistry*, 168, 147–162.
7. Lorenzen, L., and van Deventer, J. S. J., 1992. The mechanism of leaching of gold from refractory ores. *Minerals Engineering*, 5, 1377–1387.
8. Dai, X., and Jeffrey, M. I., 2006. The effect of sulfide minerals on the leaching of gold in aerated cyanide solutions. *Hydrometallurgy*, 82, 118–125.
9. Azizi, A., Petre, C. F., Assima, G. P., and Larachi, F., 2012. The role of multi-sulfidic mineral binary and ternary galvanic interactions in gold cyanidation in a multi-layer packed-bed electrochemical reactor. *Hydrometallurgy*, 113–114, 51–59.
10. Azizi, A., Olsen, C., and Larachi, F., 2014. Efficient strategies to enhance gold Leaching during cyanidation of multi-sulfidic ores. *The Canadian Journal of Chemical Engineering*, 92, 1687–1692.
11. Habashi, F., 1967. *Montana Bureau of Mines and Geology Bulletin 59*, Montana, USA.

12. Deschenes, G., Rousseau, M., Tardif, J., and Prud'homme, P.J.H., 1998. Effect of the composition of some sulfide minerals on cyanidation and use of lead nitrate and oxygen to alleviate their impact. *Hydrometallurgy* 50, 205–221.
13. Breuer, P. L., Jeffrey, M. I., and Hewitt, D. M., 2008. Mechanisms of sulfide ion oxidation during cyanidation. Part I: the effect of lead (II) ions. *Minerals Engineering*, 21, 579–586.
14. Azizi, A., Petre, C. F., Olsen, C., and Larachi, F., 2010. Electrochemical behavior of gold cyanidation in the presence of a sulfide-rich industrial ore versus its major constitutive sulfide minerals. *Hydrometallurgy*, 101, 108–119.
15. Khalid, M., and Larachi, F., 2017. Effect of silver on gold cyanidation in mixed and segregated sulphidic minerals. *The Canadian Journal of Chemical Engineering*, 95, 698–707.
16. Kudryk, V., and Kellogg, H. H., 1954. Mechanism and rate-controlling factors in the dissolution of gold in cyanide solutions. *Journal of Metals*, 541–548.
17. Wadsworth, M. E., and Zhu, X., 2003. Kinetics of enhanced gold dissolution: activation by dissolved silver. *International Journal of Mineral Processing*, 72, 301–310.
18. Cathro, K. J., 1964. The effect of thallium on the rate of extraction of gold from pyrites calcine. *Proc. Aus. I.M.M.*, 210, 127–137.
19. Wadsworth, M. E., Zhu, X., Thompson, J. S., and Pereira, C. J., 2000. Gold dissolution and activation in cyanide solution. *Hydrometallurgy*, 57, 1–11.
20. Jeffrey, M. I., and Ritchie, I. M., 2000. The leaching of gold in cyanide solutions in the presence of impurities II. The effect of silver. *Journal of The Electrochemical Society*, 147, 3272–3276.
21. Sun, X., Guan, Y. C., and Han, K. N., 1996. Electrochemical behavior of the dissolution of gold-silver alloys in cyanide solutions. *Metallurgical and Materials Transactions B*, 27, 355-361.
22. Gasparini, C., 1984. The mineralogy of silver and its significance in metal extraction. *CIM Bull.* 77, 99–110.
23. Lin, H. K., Oleson, J. L., and Walsh, D. E., 2010. Behavior of gold and silver in various processing circuits at the Fort Knox Mine. *Mineral and Metallurgical Processing*, 27, 219–223.
24. Celep, O., Alp, I., and Deveci, H., 2011. Improved gold and silver extraction from a refractory antimony ore by pretreatment with alkaline sulphide leach. *Hydrometallurgy* 105, 234–239.



25. Celep, O., Bas, A. D., Yazici, E. Y., Alp, I., and Deveci, H., 2015. Improvement of silver extraction by ultrafine grinding prior to cyanide leaching of the plant tailings of a refractory silver ore. *Mineral Processing and Extractive Metallurgy Review*, 36, 227–236.
26. Senanayake, G., 2008. A review of effects of silver, lead, sulfide and carbonaceous matter on gold cyanidation and mechanistic interpretation, *Hydrometallurgy*, 9, 46–73.
27. Zheng, J., Ritchie, I. M., La Brooy, S. R., and Singh, P., 1995. Study of gold leaching in oxygenated solutions containing cyanide–copper–ammonia using rotating quartz crystal microbalance. *Hydrometallurgy*, 99, 277–292.
28. Xie, D., Dreisinger, D. B., 2007. Leaching of silver sulfide with ferricyanide–cyanide solution. *Hydrometallurgy*, 88, 98–108.
29. Jiang H., Xie F., and Dreisinger, D. B., 2015. Comparative study of auxiliary oxidants in cyanidation of silver sulfide. *Hydrometallurgy*, 158, 149–156.
30. Hiskey, J. B. and Sanchez, V. M., 1990. Mechanistic and kinetic aspects of silver dissolution in cyanide solutions. *Journal of Applied Electrochemistry*, 20, 479–487.
31. Córdoba, E. M., Muñoz, J. A., Blázquez, M. L., González, F., and Ballester, A., 2008. Leaching of chalcopyrite with ferric ion. Part I: General aspects. *Hydrometallurgy*, 93, 81–87.
32. Liu, G. Q. and Yen, W. T., 1995. Effects of sulphide minerals and dissolved oxygen on the gold and silver dissolution in cyanide solution. *Minerals Engineering* 8, 111–123.
33. Hollow, J., Deschenes, G., Guo, H., Fulton, M., and Hill, E., 2003. Optimizing cyanidation parameters for processing of blended Fort Knox and true north ores at the Fort Knox Mine, *Hydrometallurgy 2003:5th International Symposium Honoring Professor Ian M. Ritchie*, Vancouver, BC, 24–27 August 2003.
34. Deschenes, G., Pratt, A., Fulton, M., and Lastra, R., 2005. Leaching kinetics and mechanisms of surface reaction during cyanidation of gold in presence of pyrite and stibnite. *Minerals and Metallurgical Processing*, 22, 89–95.
35. Krylova, V., 2013. Deposition and characterization of silver sulfide layers on the polypropylene film surface. *CHEMIJA*, 24, 203–209.
36. Prutton, M. and El. Gomati, M. M., 2006. *Scanning Auger Electron Microscopy*, John Wiley & Sons, Hoboken 2006.
37. Panzner, G., Egert, B., and Schmidt, H. P., 1985. The stability of CuO and Cu<sub>2</sub>O surfaces during argon sputtering studied by XPS and AES. *Surface Science*, 151, 400–408.
38. *X-ray Photoelectron Spectroscopy (XPS) Reference Pages*, <http://www.xpsfitting.com>.

39. Powell, C. J., 1995. Elemental binding energies for X-ray photoelectron spectroscopy. *Applied Surface Science*, 89, 141–149.
40. Murray, B. J., Li, Q., Newberg, J. T., Menke, E. J., Hemminger, J. C., and Penner, R. M., 2005. Shape- and size-selective electrochemical synthesis of dispersed silver(I) oxide colloids. *Nano Letters*, 5, 2319–2324.
41. Casaletto, M. P., Longo, A., Martorana, A., Prestianni, A., and Venezia, A. M., 2006. XPS study of supported gold catalysts: the role of Au<sup>0</sup> and Au<sup>+δ</sup> species as active sites. *Surface and Interface Analysis*, 38, 215–218.
42. Mikhlin, Y., Romanchenko, A., Likhatski, M., Karacharov, A., Erenburg, S., Trubina, S., 2011. Understanding the initial stages of precious metals precipitation: Nanoscale metallic and sulfidic species of gold and silver on pyrite surfaces. *Ore Geology Reviews*, 42, 47–54.
43. Huang, Y., and Ruiz, P., 2005. Antimony dispersion and phase evolution in the Sb<sub>2</sub>O<sub>3</sub>-Fe<sub>2</sub>O<sub>3</sub> system. 109, 22420–22425.
44. Omar, E. L. P., Miguel, D. S., and Manuel, L. T., 2010. Characterization of growth of anodic antimony oxide films by ellipsometry and XPS. *Journal of Electroanalytical Chemistry*, 645, 143–148.
45. Shukla, S., Seal, S. S., and Mishra, R., 2002. Synthesis and Characterization of Silver Sulfide Nanoparticles Containing Sol-Gel Derived HPC-Silica Film for Ion-Selective Electrode Application. *Journal of Sol-Gel Science and Technology*, 23, 151–164.
46. Chen, R., Nuhfer, N. T., Moussa, L., Morris, H. R., and Whitmore, P. M., 2008. Silver sulfide nanoparticle assembly obtained by reacting an assembled silver nanoparticle template with hydrogen sulfide gas. *Nanotechnology*, 19, 1–11.



## Chapter 4: Assessment of the Impact of Silver Sulphides on Gold Cyanidation with Polymetal Sulphides\*

### Résumé

Les cinétiques de lixiviation de l'or sont significativement influencées par les associations présentes dans les minerais avec les sulfures d'argent et les autres sulfures métalliques. Une approche mettant à profit un réacteur à lix fixe est donc adoptée afin d'en isoler et d'étudier les effets galvaniques et les effets de la passivation. Quatre systèmes de minéraux soient : pyrite-silice, chalcopryrite-silice, sphalérite-silice et stibnite-silice, ont été investigués. La présence de pyrargyrite a accru la récupération de l'or jusqu'à 77% et 51,2 % en présence d'effets galvaniques et de passivation causés par de la pyrite. De la pyrargyrite en association avec de la sphalérite a aussi augmenté la récupération de l'or à 6,6% sous les effets galvaniques et 51,9% sous effets de passivation. Dans le cas de la chalcopryrite, son association avec de la pyrargyrite a retardé la récupération de l'or à 38,0% et 12,1%, respectivement, sous des effets galvaniques et des effets de passivation. Par ailleurs, des minéraux d'argent ont augmenté la récupération de l'or jusqu'à 90,6 % et 80,5% en présence d'effets galvaniques et de passivation de la part de pyrite. Les minéraux d'argent en présence de sphalérite ont démontré des récupérations d'or augmentées à 71,1% et 80,5% dans les mêmes conditions. Des minéraux d'argent associés à de la chalcopryrite ont aussi diminué la récupération de l'or à 10,2 % et 4,5 %, respectivement, en présence d'effets galvaniques et de passivation. La stibnite diminue aussi sévèrement la dissolution de l'or avec de la pyrargyrite et des minéraux d'argent. La pyrargyrite ainsi que les minéraux d'argent augmentent la dissolution de l'or libre et associé avec de la pyrite et de la sphalérite. La dissolution de l'or est sévèrement retardée lorsque les minéraux d'or et d'argent sont associés avec de la chalcopryrite et de la stibnite, autant dans le cas des effets galvaniques que des effets de passivation.

---

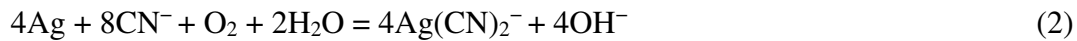
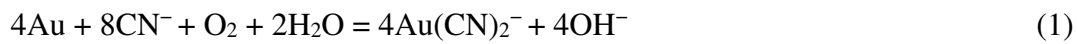
\* M. Khalid, F. Larachi, *Trans. Nonferrous Met. Soc. China* 2017 (accepted 09 June, 2017).

## **Abstract**

Gold leaching kinetics was significantly influenced in association with silver minerals and polymetal sulphides. A packed-bed reactor approach was adopted to single out the galvanic and passivation effects. Four set of mineral systems such as, pyrite-silica, chalcopyrite-silica, sphalerite-silica and stibnite-silica, were investigated. Pyrargyrite presence enhanced the Au recovery to 77.3% and 51.2% under galvanic and passivation effect from pyrite. Pyrargyrite in association with sphalerite also enhanced Au recovery to 6.6% and 51.9% under galvanic and passivation effect from sphalerite. Pyrargyrite associated with chalcopyrite retarded gold recovery to 38.03% and 12.1% respectively under galvanic and passivation effects. On the other hand, accumulative silver minerals enhanced Au recovery to 90.6% and 81.1% under galvanic and passivation impact from pyrite. Silver minerals with sphalerite, both under galvanic and passivation effect, enhanced Au recovery to 71.1% and 80.5% respectively. Silver minerals associated with chalcopyrite significantly retarded Au recovery to 10.2% and 4.5% respectively under galvanic and passivation impact. Stibnite found severely retarding towards Au dissolution with pyrargyrite and accumulative silver minerals. Pyrargyrite as well as accumulative silver minerals enhanced gold dissolution for free and gold associated with pyrite and sphalerite systems. Gold dissolution was retarded severely for gold and silver minerals associated with chalcopyrite and stibnite, both under galvanic and passivation effects.

## 4.1. Introduction

Gold leaching in aerated alkaline cyanide slurry has been selected as process route in gold industries for more than hundred years. Efforts have been made to improve gold recovery in the cyanide leaching process that include the optimization of reagents addition, such as cyanide/dissolved oxygen concentration, particle size reduction of the ore and significant control of the operational parameters of the cyanidation process [1,2,3]. Silver is frequently associated with gold, so during cyanidation process, cyanide and oxygen consumption by the dissolution reactions of gold and silver, are described by Eqs. (1) and (2):



Conductive sulphide minerals comprise a large proportion of gold containing ores, and the effect of these minerals on gold dissolution in aerated cyanide solutions have drawn the interest of many researchers. Earlier studies on the dissolution of gold in cyanide solutions in the presence of sulphide minerals demonstrated that base-metal components, such as copper, iron and zinc, of the sulphide minerals, not only increase significantly the consumption of both cyanide and oxygen, but also the sulphide component has been shown to have a strong impact on gold leaching kinetics [4-7]. A systematic study was conducted on the kinetics of gold dissolution in the presence of various sulphide minerals, such as pyrite, chalcopyrite, pyrrhotite, arsenopyrite, sphalerite, chalcocite and stibnite, in both air-saturated as well as oxygen-enriched systems. The results demonstrated that the leaching kinetics as well overall recovery of gold in the presence of polymetal sulphide minerals strongly depend on both the solubility of the sulphide minerals and the cyanide and dissolved oxygen concentration in the solution. Pyrite, chalcopyrite, pyrrhotite, arsenopyrite were found to increase the gold dissolution rate, in an air-enriched as well as oxygen-enriched cyanide solution, while sphalerite, stibnite and chalcocite caused a reduction in the gold dissolution rate [4,5,8-10]. Sulphide minerals are soluble in aerated cyanide solutions to some extent, therefore some sulfur species will be present in the leaching solution as a result of sulphide minerals dissolution. The presence of such species not only results in high reagent consumption but affect the kinetics and recovery of gold leaching reaction as well. It was

observed by the addition of trace amounts of sodium sulphide to the cyanide solution that gold leaching was hindered dramatically which was attributed to the formation of an  $\text{Au}_2\text{S}$  passive layer on the gold surface. Strategies like pre-oxidation and lead nitrate  $[\text{Pb}(\text{NO}_3)_2]$  have been adopted to minimize the effect of sulphide ions [5,11-13].

Gold is often associated with silver and there are numerous gold deposits where the recovered silver grade exceeds that of gold. Metallic silver dissolves anodically in aqueous cyanide solutions, in a similar manner to gold (Eq. 2). As far as the leaching kinetics is concerned, metallic silver has been found to dissolve faster than gold [9,14-16]. The presence of silver, in metallic form, alloyed with gold or in dissolved form, has a beneficial effect on gold leaching kinetics. In leaching reaction mechanisms, silver has a de-passivating effect on gold cyanidation *via a* bimetallic corrosion, which is hindered by the formation of an  $\text{AuCN}_{(s)}$  film on the gold surface [2,5,9,17,18]. Under typical cyanidation conditions prevailing in gold leaching, the dissolution rate for silver is usually slower than for gold. This is because, although silver species, such as native silver, chlorargyrite  $[\text{AgCl}]$ , and iodargyrite  $[\text{AgI}]$ , are found in nature and dissolve readily in cyanide, much more common are the less soluble silver minerals [14]. Silver is frequently associated with polymetal sulphides and sulfosalts, most significant of the sulphide phases is known as acanthite  $[\text{Ag}_2\text{S}]$ , while other silver minerals include pyrargyrite  $[\text{Ag}_3\text{SbS}_3]$ , proustite  $[\text{Ag}_3\text{AsS}_3]$ , aguilarite  $[\text{Ag}_4\text{SeS}]$ , tennantite  $[\text{Cu}_6[\text{Cu}_4(\text{Fe},\text{Zn})_2]\text{As}_4\text{S}_{13}]$  and tetrahedrite  $[(\text{Cu},\text{Fe},\text{Ag},\text{Zn})_{12}\text{Sb}_4\text{S}_{13}]$  with silver inclusions. As far as the dissolution of these silver minerals is concerned, acanthite tends to dissolve slowly and require an excess of cyanide, while the other sulfosalts are even more refractory in nature with aerated cyanide solution. The sulphide ion that must be oxidized to release the ionic silver, is known to be the principal cause of refractoriness of the silver sulphide and sulfosalt minerals. This phenomenon differentiates the leaching reaction mechanism of silver sulphides and sulfosalts from those involved in metallic phase leaching [10,16,19-22].

Despite plenty of information available on the kinetics of gold dissolution with silver present in native, alloyed and/or dissolved form, there are not many studies regarding the effect of prominent silver minerals under separate or accumulative impact and in association with sulphide minerals. A comprehensive study would lead to proper understanding of the effect of prominent silver minerals, such as pyrargyrite ( $\text{Ag}_3\text{SbS}_3$ ) and also the accumulative effect

of native silver (Ag), acanthite ( $\text{Ag}_2\text{S}$ ) and pyrargyrite ( $\text{Ag}_3\text{SbS}_3$ ) on the kinetics of Au dissolution as well as the overall recovery for high silver bearing gold ores. Keeping in view the factors already explained, the following study is devised to investigate:

- The manner in which the presence of various silver phases and soluble silver affects gold leaching in free state as well as gold associated with sulphide minerals under galvanic and passivation effects.
- The ease with which the silver metal itself is leached from its bearing mineral species while present within silica and sulphide mineral matrices under direct and indirect impact.

## **4.2. Experimental**

### **4.2.1. Materials and Reagents**

The sulphide-rich ore samples: pyrite (Py), chalcopyrite (Cp), sphalerite (Sp) and stibnite (Sb), depending upon the dominant proportion of the named sulphide mineral therein, tested in this study, were received from Ward's Natural Science. The chemical as well as mineralogical characterization of these samples have been given elsewhere [9].

The samples were ground and sorted to remove particles coarser than  $106\ \mu\text{m}$  and finer than  $53\ \mu\text{m}$ . Consequently, the same granulometric fraction was used for the different ores, providing a uniform total area per unit-mass for all the cyanidation experiments. Pure gold ( $P_{80} = 39\ \mu\text{m}$ , 99.998%), pure silver ( $P_{80} = 26\ \mu\text{m}$ , 99.9%, Alfa Aesar USA), pure silver sulfide (99.9% metals basis, Alfa Aesar USA) and pyrargyrite mineral (Mineralogical Research Co.), were used in the present study. Solution used in all cyanidation experiments was prepared with distilled water. The reagents such as, sodium cyanide, NaCN (98%, Sigma–Aldrich Canada), sodium hydroxide, NaOH (Fisher Scientific Canada) and boric acid,  $\text{H}_3\text{BO}_3$  (99.5%, Sigma–Aldrich Canada), used in the present study, were all certified analytical grade.

### **4.2.2. Equipment and Procedures**

In the present study two scenarios were taken into account. Firstly, the effect of pyrargyrite ( $\text{Ag}_3\text{SbS}_3$ ) on gold dissolution was addressed in combination with sulphide minerals. Two



arrangements for each sulphide mineral (X=Py, Cp, Sp, Sb) were tested in a packed-bed reactor (PBR) using one of the X powders, both the gold and pyrargyrite mineral dispersed within the sulphidic (X), as well as silica layer (Figs. 4.1a,b). Secondly, the accumulative impact of the prominent silver minerals such as, metallic silver (Ag), acanthite ( $\text{Ag}_2\text{S}$ ) and pyrargyrite ( $\text{Ag}_3\text{SbS}_3$ ), on gold leaching behaviour under direct as well indirect contact with the sulphidic (X) minerals was taken into account as well. The notations  $\alpha$ ,  $\beta$ ,  $\gamma$  will designate metallic silver (Ag), acanthite ( $\text{Ag}_2\text{S}$ ) and pyrargyrite ( $\text{Ag}_3\text{SbS}_3$ ), unless otherwise specified.

The leaching pattern of pure gold under direct influence of the sulphidic minerals was investigated by dispersion of 50 mg of Au powder in 4 g of one of the above “X” sulphide minerals. The galvanic interactions among Au as well as sulphide mineral particles were enabled *via* this arrangement. Conversely, the dispersion of Au powder within the inert silica layer thus segregated from the above sulphide minerals will be under the passivation effect from the segregated sulphide layer. Mineral and silica phases were electrically disconnected by means of packing these in separate reactors connected in a series. The notation “||” depicts the inter-reactor separation in the ||X||silica|| syntax. Detailed studies on the leaching behaviour of these sulphides have been elaborated elsewhere [9]. In the present case, the total recovery of gold would be mentioned in comparison with this study.

First, the effect of silver minerals on gold dissolution was assessed with each of the above sulphide minerals in a two-layer ||X||silica|| configuration by seeding, one at a time with 50 mg Au powder along with 25 mg of  $\gamma$ , in one of the sulphide minerals (X = Py, Cp, Sp, or Sb) or the silica layers (Figs. 4.1a,b). The influence of  $\text{Ag}_3\text{SbS}_3$ , on gold recovery by the distribution of gold and pyrargyrite within different mineral phases of a synthetic ore was studied using the PBR. The impact of various mineral associations on gold leaching in the presence of pyrargyrite has been addressed by placing Au, X and  $\gamma$  altogether within the same layer of the packed-bed reactor. This arrangement enables the Au-X- $\gamma$  ternary galvanic interactions among all the constituents of the ore bodies. On the other hand, the indirect impact from the segregated sulphide layer as well as the direct contact between Au- $\gamma$  were assessed in two-layer ||X||silica|| configurations by seeding Au and pyrargyrite either in X (X = Py, Cp, Sp, or Sb) layer or in the silica layer (Figs. 4.1a,b). The modalities adopted in the present study have been elaborated such as ||X+Au+ $\gamma$ ||silica|| and ||X||silica+Au+ $\gamma$ || where Au

&  $\gamma$  subscripts represent the seeded layer while “X” represents one of the above sulphide mineral layer.

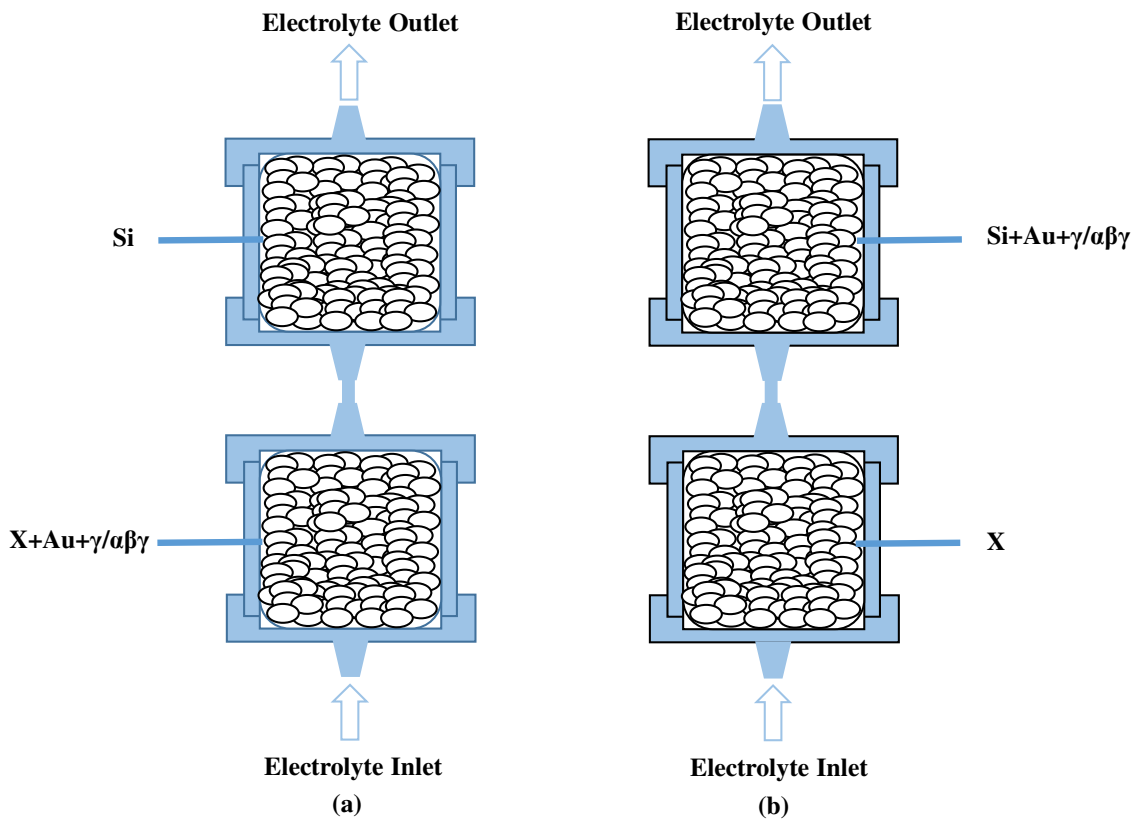


**Figure 4.1.** Gold dissolution: (a) Gold (Au) & silver minerals ( $\gamma/\alpha\beta\gamma$ ) dispersion pattern within sulphide (X) layer, (b) Gold (Au) & silver minerals ( $\gamma/\alpha\beta\gamma$ ) dispersion pattern within quartz layer. Reaction conditions:  $\text{CN}^- = 30 \text{ mM}$ ,  $\text{DO}_2 = 0.25 \text{ mM}$ ,  $\text{pH} = 11$ .

The accumulative impact of the silver minerals in combination with the sulphide minerals was investigated by placing Au particles and the silver minerals  $\alpha$ ,  $\beta$ ,  $\gamma$  in a similar way of two-layer configuration as explained above, i.e.,  $\parallel\text{X}\parallel\text{silicall}$ . The study was performed by the dispersion of all the precious metals within the sulphide as well as silica layers, like in the  $\parallel\text{X}+\text{Au}+\alpha\beta\gamma\parallel\text{silicall}$  and  $\parallel\text{X}\parallel\text{silica}+\text{Au}+\alpha\beta\gamma\parallel$  two-layer systems. The accumulative effect of silver minerals  $\alpha\beta\gamma$ , on gold dissolution was assessed by seeding, one at a time with 50 mg Au powder along with 25 mg of each of the respective silver minerals  $\alpha$ ,  $\beta$ , and  $\gamma$ , in one of the sulphide minerals ( $\text{X} = \text{Py}$ ,  $\text{Cp}$ ,  $\text{Sp}$ , or  $\text{Sb}$ ) or the silica layers (Figs. 4.1a,b). Close contact among all the precious metals and sulphide particles results in a global galvanic environment while the dispersion of precious metals within the silica particles segregated from the

sulphide layer would be under the passivation impact of the species resulting from the interaction of sulphide particles with the aerated cyanide solution.

Preparation of the feed solution for the cyanidation tests involved the dissolution of sodium cyanide (30 mM  $\text{CN}^-$ ) in a sodium hydroxide solution buffered to pH-11 by the introduction of boric acid solution and stored in a 250 mL magnetically-stirred glass container. The dissolved oxygen concentration was maintained ( $\sim 8.5$  mg/L  $\text{O}_2$  at 25 °C) by continuous aeration of the solution with air-bubbling through a sparger for 6 h duration of the experiment. This aerated cyanide solution was continuously recirculated through the PBR in closed loop by using a peristaltic pump at constant flow rate of 10.4 mL/min. Furthermore, the experimental set-up has been described in detail elsewhere [9]. The dissolved oxygen concentration was monitored by means of a dissolved oxygen probe (FOXY-AL300 model from Ocean Optics), while pH of the feed solution was maintained at  $11 \pm 0.01$  and was monitored by using an Oakton 1000 series pH-meter.

The benchmark tests for gold as well as silver minerals dissolution have been referred to as Case C and Case D, respectively. In case of Au and pyrargyrite ( $\gamma$ ), the benchmark tests were performed by dispersing 50 mg of each the precious metal Au and  $\gamma$  within the silica layer which filled the whole PBR working section. On the other hand, the benchmark test for accumulative silver minerals, such as silver metal, acanthite and pyrargyrite ( $\alpha\beta\gamma$ ), was performed by taking 50 mg of each silver mineral  $\alpha$ ,  $\beta$ ,  $\gamma$  and dispersing those altogether within the silica layer which filled the whole PBR. The leaching patterns shown by Au and Ag were referred to as Au-curve and Ag-curve, respectively, in all leaching charts.

The chemical speciation of the dissolved precious metals present within the leach solution was performed by collecting small aliquots from the container at regular time intervals using a syringe after filtering with a particles filter VWR 0.45  $\mu\text{m}$ . The analysis of the leach solution was performed by using a Perkin Elmer AA-800 atomic absorption spectrometer (AAS). The leaching kinetics as well as overall recovery for the precious metals was monitored by estimating the percentage of respective dissolved metal in comparison with the initially dispersed precious metals.

### 4.3. Results and Discussion

#### 4.3.1. Benchmark Tests for Gold and Pyrrargyrite Leaching

Gold as well as the pyrrargyrite dissolution tests were performed by their dispersion among silica particles, respectively, and their dissolution patterns were termed as benchmark test curves because of the inert chemical as well as electrochemical nature of the silica particles. Fig. 4.2a represents the benchmark leaching curves for Au and  $\text{Ag}_3\text{SbS}_3$  particles. The dissolution of pure Au particles with pure aerated cyanide solution, while dispersed within silica matrix, resulted in Au recovery of 15% after 6 h of cyanidation. This low dissolution of pure gold in pure aerated cyanide solution was due to the formation of a passivation layer on the surface of gold particles. Passivation of gold surface under certain cyanidation conditions has been confirmed experimentally due to the formation of insoluble sodium aurocyanide film on the surface of gold [23-25].

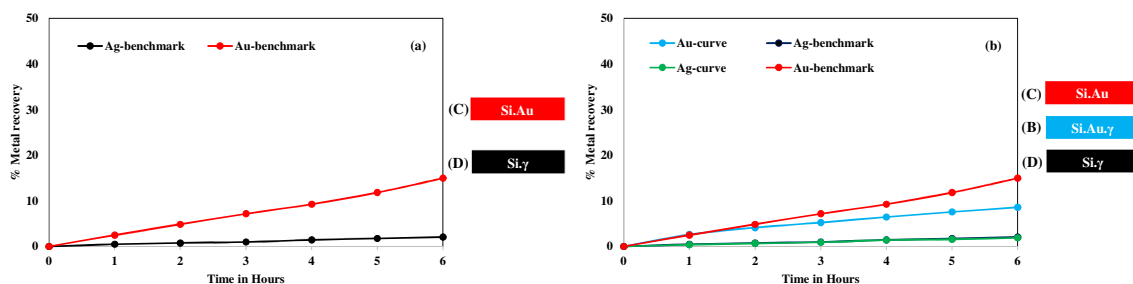


**Figure 4.2.** Gold dissolution: (a) gold and pyrrargyrite ( $\gamma$ ) dissolution within quartz layer, (b) effect of pyrrargyrite ( $\gamma$ ) on gold dissolution within quartz layer. Reaction conditions:  $\text{CN}^- = 30 \text{ mM}$ ,  $\text{DO}_2 = 0.25 \text{ mM}$ ,  $\text{pH} = 11$ .

In the case of  $\text{Ag}_3\text{SbS}_3$ , Ag recovery from this silver bearing-mineral dispersed in silica was estimated to be 2% after 6 h contact with aerated cyanide solution as illustrated in Fig. 4.2a. Pyrrargyrite is a well-known refractory silver ore leading to very poor silver extractions (often  $\leq 10\%$ ) in cyanide leaching [26]. Numerous pre-treatment strategies as well as oxidants have been used to enhance silver recovery from pyrrargyrite [27].

The influence of  $\text{Ag}_3\text{SbS}_3$  on the dissolution of Au particles, while both Au and  $\text{Ag}_3\text{SbS}_3$  dispersed within the silica layer, was investigated and the leaching pattern for Au as well as Ag is shown in Fig. 4.2b. Association of  $\text{Ag}_3\text{SbS}_3$  with Au particles resulted in retardation of

the Au dissolution within aerated cyanide solution. Au recovery was estimated to 8.6% as compared to 15% of the benchmark test, while the Ag recovery was found to be 1.9% after 6 h of cyanidation and it almost followed the benchmark pattern of leaching for Ag from  $\text{Ag}_3\text{SbS}_3$  (Fig. 4.2b).

#### 4.3.2. Effect of Pyrargyrite on Au Leaching with Pyrite-Silica System

The influence of pyrargyrite on the kinetics as well as overall recovery of gold dissolution under galvanic and passivation impact from the pyrite mineral layer has been elaborated in Figs. 4.3a,b. Sulphide minerals associated with gold play an important role during gold cyanidation. Close contact of gold and sulphide mineral particles gives rise to the development of galvanic interactions among the ore constituents. Gold as well as sulphide minerals undergo the phenomenon of galvanic corrosion when gold and a conductive mineral are brought into contact in the same corrosive environment, acting as two dissimilar electrodes [8,28]. Gold particles under the influence of galvanic contacts with pyrite resulted in Au dissolution of 74.6%, reducing to 15.8% under passivation from the segregated pyrite layer after 6 h of cyanidation (Table 4.1).

**Table 4.1.** Effect of silver sulphide on gold dissolution with conductive sulphides.

Sulphide Mineral	Au-Recovery (%) (X+Au//Si)/(X//Si+Au)	Au-Recovery/Ag-Recovery (%) (X+Au+Ag <sub>2</sub> S//Si)	Au-Recovery/Ag-Recovery (%) (X//Si+Au+Ag <sub>2</sub> S)
Pyrite (Py)	74.6/15.5	80.6/8.0	60.1/3.9
Chalcopyrite (Cp)	57.0/14.1	24.2/5.6	11.3/7.1
Sphalerite (Sp)	1.6/15.6	55.5/11.2	56.3/11.8
Stibnite (Sb)	1.1/1.3	0.5/2.5	0.1/1.9
Benchmark	15/3.9 (Si+Au//Si+Ag <sub>2</sub> S)	4.9/3.8 (Si+Au+Ag <sub>2</sub> S)	

\*adopted from [10].

Close association of Au,  $\text{Ag}_3\text{SbS}_3$  and pyrite mineral on Au dissolution was evaluated by mixing Au particles with  $\text{Ag}_3\text{SbS}_3$  and pyrite mineral particles and packing altogether within the same PBR. On the other hand, the passivation effect of the pyrite mineral layer on Au

dissolution in cyanide solution was assessed by placing both Au and  $\text{Ag}_3\text{SbS}_3$  in the silica layer being segregated in the PBR from the pyrite mineral. The electrochemical contacts, i.e., ternary galvanic contacts, among all the constituents were enabled by placing Au,  $\text{Ag}_3\text{SbS}_3$  and pyrite within the same layer. Dispersing Au and  $\text{Ag}_3\text{SbS}_3$  among the silica particles, segregated from the pyrite layer, gave rise to binary galvanic contacts between Au and  $\text{Ag}_3\text{SbS}_3$ .

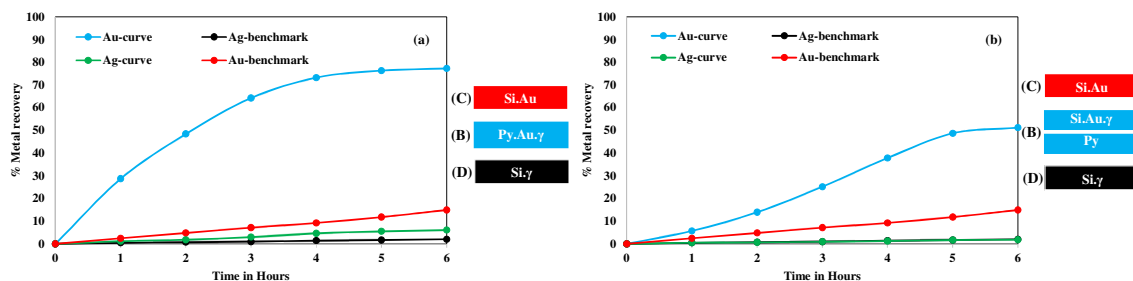


**Figure 4.3.** Gold dissolution: (a) gold dissolution with pyrite and pyrargyrite,  $\text{Py}+\text{Au}+\gamma//\text{Si}$ , (b) Gold dissolution with pyrite and pyrargyrite,  $\text{Py}//\text{Si}+\text{Au}+\gamma$ . Reaction conditions:  $\text{CN}^- = 30 \text{ mM}$ ,  $\text{DO}_2 = 0.25 \text{ mM}$ ,  $\text{pH} = 11$ .

The presence of Au,  $\text{Ag}_3\text{SbS}_3$  and pyrite particles in close contact with one another has resulted in Au recovery of 77.3% (Fig. 4.3a). Addition of  $\text{Ag}_3\text{SbS}_3$  along with Au within the pyrite layer enhanced Au dissolution to 77.3% as compared to 74.6%, for Au within pyrite alone after 6 h of cyanidation.  $\text{Ag}_3\text{SbS}_3$  has enhanced the leaching kinetics as well as the overall recovery of gold for the pyrite mineral, while it was observed to retard the dissolution of gold present with the silica particles (Fig. 4.2b). Although pyrargyrite addition has increased Au recovery for the pyrite-silica system, this increase was observed to be less as in case of acanthite present with gold for the same system. This could be attributed to the amount of silver dissolved during the cyanidation experiment which was higher in case of acanthite mineral than pyrargyrite mineral (Table 4.1). Similarly, silver recovery from the dissolution of  $\text{Ag}_3\text{SbS}_3$  was estimated to be 6.1% as shown in Fig. 4.3a, as compared to 2% in case of the benchmark test (Fig. 4.2a), after 6 h of cyanidation. The difficulty in the dissolution of pyrargyrite in aerated cyanide solution is related to the presence of stable pyramidal  $\text{SbS}_3^-$  group in sulfosalt silver minerals [29].

The presence of pyrargyrite along with gold among silica particles segregated by the pyrite mineral layer has enhanced Au dissolution as well (Fig. 4.2b). Au recovery was estimated to

be 51.2% with both Au and  $\text{Ag}_3\text{SbS}_3$  present in the silica layer segregated by the pyrite layer.  $\text{Ag}_3\text{SbS}_3$  was observed to enhance gold dissolution while Au particles were under indirect influence from the pyrite mineral particles. The increase in Au recovery was found to be less as compared to Au recovery for the  $\text{Ag}_2\text{S}$  counterpart (Table 4.1). In this case, the enhancement in Au recovery is influenced by the amount of dissolved silver in the aerated cyanide solution (Fig. 4.3b, Table 4.1). Ag recovery from  $\text{Ag}_3\text{SbS}_3$  mineral particles present among silica particles and segregated from the pyrite particles was estimated to be 1.8% after 6 h of cyanidation (Fig. 4.3b). Au dissolution was enhanced by the introduction of pyrargyrite mineral under direct as well as indirect impact from the pyrite mineral particles. It shows that the silver recovered by the dissolution of pyrargyrite, acted in a similar way as that of the silver present in dissolved form in the aerated cyanide solution [30].

#### **4.3.3. Effect of Pyrargyrite on Au Leaching with Chalcopyrite-Silica System**

Pyrargyrite mineral influenced Au dissolution in the same manner as for acanthite mineral in a combination of the chalcopyrite-silica system in an aerated cyanide solution. The impact of  $\text{Ag}_3\text{SbS}_3$  on the leaching kinetics as well as overall gold recovery in an aerated cyanide solution is shown in Figs. 4.4a,b. The accumulative impact of pyrargyrite and chalcopyrite minerals on Au dissolution, while the micro-electrical contacts were enabled among all the constituents, resulted in Au dissolution 38.03% (Fig. 4.4a), as compared to 57% for Au particles under galvanic impact from the chalcopyrite mineral particles (Table 4.1). The Ag recovered with this arrangement of mineral system was estimated to be 2.9% (Fig. 4.4a). The sulphides of silver like pyrargyrite are termed as refractory in the leaching process and the structural, electronic, and bonding properties of sulfosalts mainly determine their reactivity and the extent of their reaction in cyanide or other leaching systems [29].

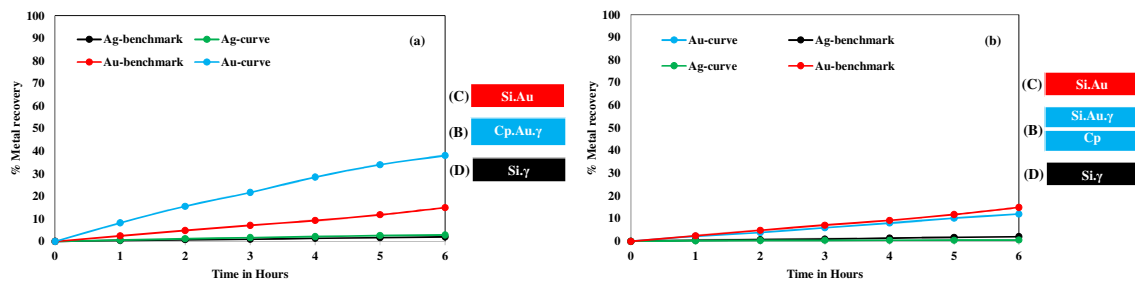


**Figure 4.4.** Gold dissolution: (a) gold dissolution with chalcopyrite and pyrrargyrite, Cp+Au+ $\gamma$ //Si, (b) Gold dissolution with chalcopyrite and pyrrargyrite, Cp//Si+Au+ $\gamma$ . Reaction conditions:  $\text{CN}^- = 30 \text{ mM}$ ,  $\text{DO}_2 = 0.25 \text{ mM}$ ,  $\text{pH} = 11$ .

Addition of  $\text{Ag}_2\text{S}$  to Au particles present among chalcopyrite particles, reduced Au dissolution to 24% after 6 h of cyanidation, while Ag recovered with this arrangement of the minerals as well as precious metal particles was estimated to be 5.6% (Table 4.1). This means that retardation in Au dissolution is directly related to the amount of Ag present in dissolved state in the aerated cyanide leach solution. Greater the amount of dissolved Ag in the leach solution, greater is the retardation observed in the kinetics as well as overall recovery of Au particles present in combination with chalcopyrite-silica system. Fig. 4.4a also represents the kinetics and recovery of Ag from the dissolution of  $\text{Ag}_3\text{SbS}_3$ , while present in an arrangement where the galvanic contacts were enabled among all the mineral particles, and the Ag recovery was estimated to be 2.9% after the same duration of cyanidation.

Fig. 4.4b demonstrates the leaching pattern of Au and Ag while both Au and  $\text{Ag}_3\text{SbS}_3$  were put altogether within the silica layer and segregated from the chalcopyrite mineral layer. Au recovery was estimated to be 12.1%, as compared to 15% for the benchmark test after 6 h of cyanidation. This means that the influence of  $\text{Ag}_3\text{SbS}_3$  proved to be retarding under the indirect effect from the chalcopyrite layer as well. The extent to which Au dissolution was retarded in this case was also observed to be lower as compared to Au dissolution for the same mineral configuration but with acanthite mineral (Table 4.1).

$\text{Ag}_3\text{SbS}_3$  mineral particles dispersed along with Au particles within the silica layer and segregated from the chalcopyrite mineral layer resulted in Ag recovery of 0.5% after 6 hours of cyanidation (Fig. 4.4b). This demonstrates that a small reduction in Au recovery was due to little dissolution of pyrrargyrite mineral in the cyanide leach solution. Overall, the association of  $\text{Ag}_3\text{SbS}_3$  particles with Au particles, was found to have a net deceleration



impact on Au dissolution, irrespective of the presence within the same or segregated layer. As much as the silver is dissolved in the cyanide solution with chalcopyrite, it will form an in-situ  $\text{Ag}_2\text{S}$  passive film on the gold surface and retard the net dissolution of gold [9].

#### 4.3.4. Effect of Pyrargyrite on Au Leaching with Sphalerite-Silica System

Association of pyrargyrite mineral influenced Au dissolution while in combination with sphalerite for which a two-layer mineral system arrangement was adopted, such as placement of Au and  $\text{Ag}_3\text{SbS}_3$  in sphalerite as well as silica layers. Fig. 4.5 illustrates the dissolution pattern of Au particles under the influence of  $\text{Ag}_3\text{SbS}_3$  and in direct as well as indirect impact from the sphalerite mineral layer. Presence of  $\text{Ag}_3\text{SbS}_3$  and Au particles within a direct contact with sphalerite enhanced the Au dissolution from 1.6% to 6.6%, while silver recovered by dissolution of  $\text{Ag}_3\text{SbS}_3$  was estimated to be 1.1%, after 6 h cyanidation (Fig. 4.5a, Table 4.1). Addition of  $\text{Ag}_3\text{SbS}_3$  to Au particles present in close contact with sphalerite mineral enhanced Au dissolution by 5% as compared to Au particles present with the sphalerite particles only (Table 4.1).

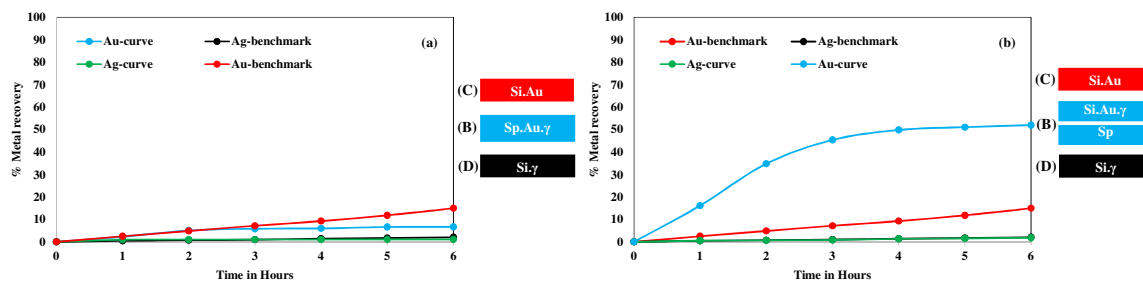


**Figure 4.5.** Gold dissolution: (a) gold dissolution with sphalerite and pyrargyrite,  $\text{Sp}+\text{Au}+\gamma//\text{Si}$ , (b) Gold dissolution with sphalerite and pyrargyrite,  $\text{Sp}//\text{Si}+\text{Au}+\gamma$ . Reaction conditions:  $\text{CN}^- = 30 \text{ mM}$ ,  $\text{DO}_2 = 0.25 \text{ mM}$ ,  $\text{pH} = 11$ .

Although Au recovery was enhanced with addition of  $\text{Ag}_3\text{SbS}_3$ , for Au particles present with the sphalerite particles, it was not as high as in case of  $\text{Ag}_2\text{S}$  mineral for the same set of mineral arrangement, i.e., 55.5% (Table 4.1) after 6 h of cyanidation. This could be easily understood by the presence of little amount of Ag in dissolved form as a result of the dissolution of  $\text{Ag}_3\text{SbS}_3$ , i.e., 1.1% as compared to 11.2% for  $\text{Ag}_2\text{S}$  (Table 4.1). It means that the presence of this amount of dissolved silver in the leach solution was not enough to overcome the poor electrical conductivity from the sphalerite particles [8-10].

The leaching pattern as well as the overall Au recovery, while Au and  $\text{Ag}_3\text{SbS}_3$  particles present within the silica particles and segregated from the sphalerite layer, is depicted in Fig. 4.5b. The Au particles with the stated arrangement resulted in Au dissolution of 52%, as compared to 15.6% without addition of  $\text{Ag}_3\text{SbS}_3$ . The Ag recovered from the dissolution of  $\text{Ag}_3\text{SbS}_3$  was measured to be 1.8% after 6 h of cyanidation. In this scenario, Au dissolution was significantly enhanced even with the smaller extent of Ag present in dissolved form (Fig. 4.5b).

Au dissolution was enhanced by 36.4% with addition of  $\text{Ag}_3\text{SbS}_3$ , segregated by the sphalerite layer as compared to Au present within silica layer and segregated from the Sp layer. From this data, it is clear that even a little amount of Ag present within the cyanide leach solution would enhance Au dissolution remarkably while it is not in direct contact with the poorly conducting sphalerite particles [9]. Pyrargyrite has been identified to have an increasing impact on Au dissolution in combination of sphalerite mineral under galvanic as well as passivation effect from the sulphide mineral layer.

#### **4.3.5. Effect of Pyrargyrite on Au Leaching with Stibnite-Silica System**

The effect of pyrargyrite on Au dissolution in combination to the stibnite mineral was investigated as well (Figs. 4.6a,b). Stibnite has been reported to be very refractory regarding Au dissolution even present in a very small quantity within gold bearing ores [8,9]. Dissolution of Au particles was investigated by their placement within the stibnite as well as silica layer (Table 4.1). Fig. 4.6a represents the Au leaching pattern as well recovery under the influence of  $\text{Ag}_3\text{SbS}_3$  and in close connection with stibnite particles after 6 h cyanidation. Addition  $\text{Ag}_3\text{SbS}_3$  to the Au particles in connection with the stibnite particles, reduced Au recovery to 0.5% during the stipulated cyanidation time. The addition of  $\text{Ag}_3\text{SbS}_3$  reduced the Au recovery to 0.5%, as compared to 1.1% for the Au particles present within the stibnite layer only (Table 4.1). Ag recovered by the dissolution of  $\text{Ag}_3\text{SbS}_3$  while present within the stibnite layer was measured to be 0.6%, after 6 h of contact with the aerated cyanide solution (Fig. 4.6a).

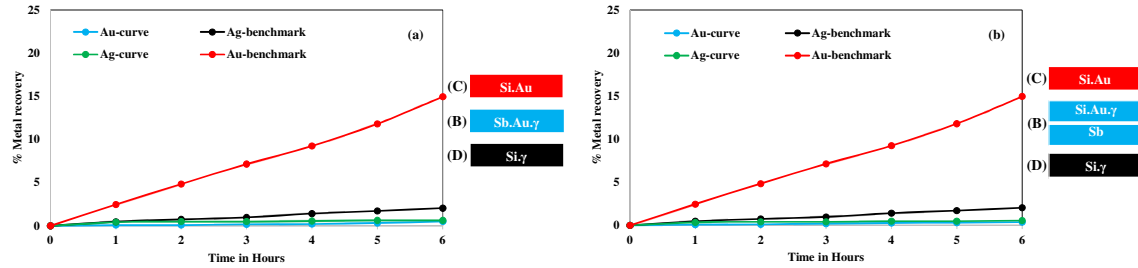


**Figure 4.6.** Gold dissolution: (a) gold dissolution with stibnite and pyrargyrite, Sb+Au+ $\gamma$ //Si, (b) Gold dissolution with stibnite and pyrargyrite, Sb//Si+Au+ $\gamma$ . Reaction conditions:  $\text{CN}^- = 30 \text{ mM}$ ,  $\text{DO}_2 = 0.25 \text{ mM}$ ,  $\text{pH} = 11$ .

Au dissolution was investigated by placement of Au and  $\text{Ag}_3\text{SbS}_3$  particles within the silica layer and segregating it from the stibnite layer as well (Fig. 4.6b). Au and Ag recoveries were found to be 0.38% and 0.56%, respectively after 6 h of cyanidation. Association of  $\text{Ag}_3\text{SbS}_3$  with Au particles in segregated connection with stibnite mineral has been found to be retarding to Au dissolution. The influence of  $\text{Ag}_3\text{SbS}_3$  on Au dissolution under direct as well as indirect impact from the stibnite mineral layer was observed to be retarding to Au dissolution severely. This severe reduction in Au recovery could be attributed to the formation of a tight antimony oxide ( $\text{Sb}_2\text{O}_5$ ) as well as silver sulfide layers, resulted by the interaction of stibnite and pyrargyrite with the aerated cyanide solution. These findings are also in coherence with the findings in case of metallic silver as well as acanthite on Au dissolution with the stibnite mineral [9,10].

#### 4.3.6. Benchmark Tests for Gold and Silver Minerals ( $\alpha\beta\gamma$ ) Leaching

The benchmark test for the dissolution of pure gold in pure aerated cyanide solution was performed in the same way as explained above. In case of the benchmark dissolution test for the silver minerals, 50 mg of each of the three silver mineral constituents, namely, metallic silver (Ag), acanthite ( $\text{Ag}_2\text{S}$ ) and pyrargyrite ( $\text{Ag}_3\text{SbS}_3$ ), designated as  $\alpha$ ,  $\beta$  and  $\gamma$ , was used. These silver minerals were dispersed all together within the silica layer which filled the whole PBR. The benchmark leaching pattern for the accumulative silver minerals ( $\alpha\beta\gamma$ ) is illustrated in Fig. 4.7a, which also bears the Au benchmark leaching curve. Within 6 h, a fraction of 15% of gold leached out mirroring dissolution of 38% of silver minerals. The higher recovery of silver as compared to gold, is because of the presence of metallic silver which dissolves much more readily in aerated cyanide solution [8,9]. Dissolution of the other two counter

parts, i.e., acanthite and pyrargyrite, has been reported to be notoriously slow in conventional cyanidation [10,27]. The prominent silver mineral acanthite ( $\text{Ag}_2\text{S}$ ) tends to dissolve slowly requiring an excess of cyanide with the sulfosalt-like pyrargyrite even more refractory. Retardation in silver extraction from  $\text{Ag}_2\text{S}$  could be attributed to its low solubility [22].

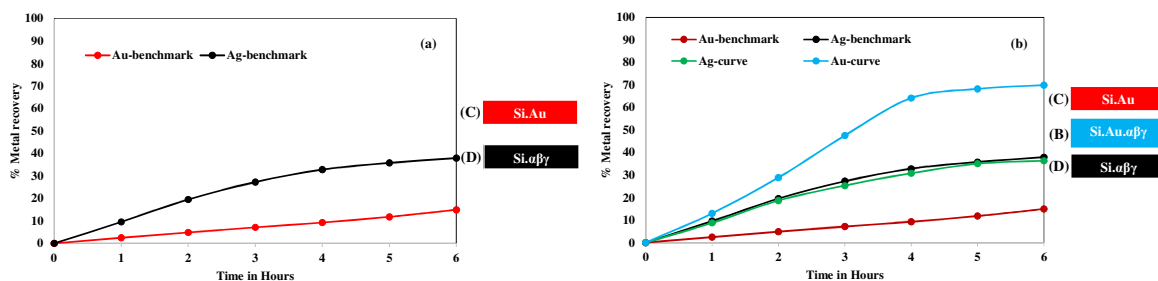


**Figure 4.7.** Gold dissolution: (a) gold (Au) and silver minerals ( $\alpha\beta\gamma$ ) dissolution within quartz layer, (b) effect of silver minerals on gold (Au+ $\alpha\beta\gamma$ ) dissolution within quartz layer. Reaction conditions:  $\text{CN}^- = 30 \text{ mM}$ ,  $\text{DO}_2 = 0.25 \text{ mM}$ ,  $\text{pH} = 11$ .

The accumulative impact of the prominent silver minerals ( $\alpha\beta\gamma$ ), such as metallic silver ( $\alpha$ ), acanthite ( $\beta$ ) and pyrargyrite ( $\gamma$ ), on Au dissolution was investigated as well (Fig. 4.7b). Au dissolution was 69.9% after 6 h cyanidation as compared to 15% for the Au benchmark test, irrespective of the retardation impact of acanthite and pyrargyrite on Au dissolution within the silica layer [10]. This indicates that the presence of silver in the metallic form enhanced the Au dissolution remarkably, irrespective of the presence of retarding factors like acanthite as well as pyrargyrite minerals. In case of acanthite as well as pyrargyrite minerals, the decrease in Au dissolution could be attributed to the formation of passive films on the surface of gold particles in the cyanide media [10,31].

Species like  $\text{AuCN}_{\text{ads}}$  were held responsible for the oxidation as well as reduction of gold particles and also adsorbed species on gold surface such as  $\text{AuCN}\cdot\text{AuOH}$ ,  $\text{Au}(\text{OH})(\text{CN})^-$ ,  $\text{Au}(\text{OH})(\text{CN})^{3-}$ ,  $\text{Au}(\text{OH})$  were reported to be responsible for the poor dissolution of impurity-free gold in pure aerated cyanide solutions [2,10]. Therefore, silver present in the metallic form was found to overcome the surface obstructing species resulted from the dissolution of acanthite and pyrargyrite in aerated cyanide solution. The surface passive film, such as silver sulphide, was not easy to dissolve with standard cyanidation conditions as it is clear from the dissolution pattern of acanthite [10].

### 4.3.7. Effect of Ag, Ag<sub>2</sub>S and Ag<sub>3</sub>SbS<sub>3</sub> on Au Leaching with Pyrite-Silica System

The accumulative impact of the most prominent silver minerals, such as metallic silver (Ag,  $\alpha$ ), acanthite (Ag<sub>2</sub>S,  $\beta$ ) and pyrargyrite (Ag<sub>3</sub>SbS<sub>3</sub>,  $\gamma$ ) was investigated on Au dissolution in direct as well as indirect contact with pyrite mineral layer. The influence of silver minerals ( $\alpha\beta\gamma$ ) on Au dissolution in combination to pyrite mineral was also investigated (Fig. 4.8).

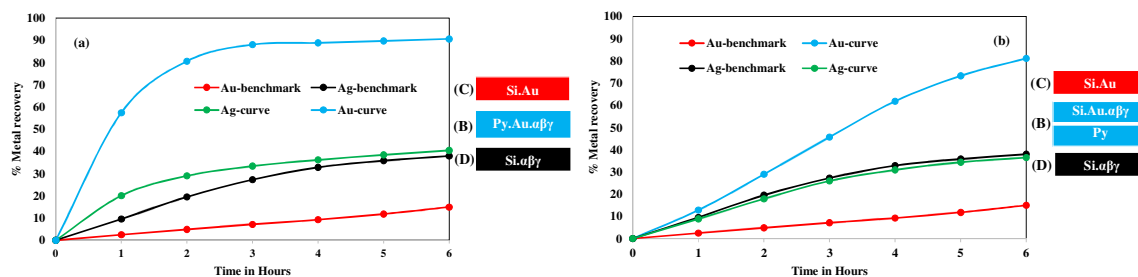


**Figure 4.8.** Gold dissolution: (a) gold dissolution with pyrite and silver minerals  $\alpha\beta\gamma$ , Py+Au+ $\alpha\beta\gamma$ //Si, (b) Gold dissolution with pyrite and silver minerals  $\alpha\beta\gamma$ , Py//Si+Au+ $\alpha\beta\gamma$ . Reaction conditions: CN<sup>-</sup> = 30 mM, DO<sub>2</sub> = 0.25 mM, pH = 11.

The presence of  $\alpha\beta\gamma$  along with gold within the pyrite mineral layer resulted in Au recovery of 90.6%, while dissolution of silver minerals resulted in an Ag recovery of 40.4% after 6 h of cyanidation (Fig. 4.8a). Au recovery was enhanced from 74.6% to 90.6%, with a net increase of 16%, by introducing  $\alpha\beta\gamma$  to Au particles as compared to Au particles within the pyrite layer (Table 4.1). Placement of the silver minerals  $\alpha\beta\gamma$ , Au and pyrite mineral particles within the same PBR gave rise to an arrangement where all the constituents are under a state of global galvanic contacts resulting from close contact of the ore constructing constituents. Au and Ag recoveries represent a significant enhancement in precious metal recovery because of the establishment of permanent galvanic contacts.

The other set of arrangement made for these minerals placement followed the dispersion of silver minerals  $\alpha\beta\gamma$  and Au within the silica layer contiguous to pyrite mineral layer. The precious metals leaching data with this type of minerals placement is shown in Fig. 4.8b. Precious metal Au and Ag recoveries were 81.1% and 36.5%, respectively. The association of Au particles with  $\alpha\beta\gamma$  particles within the silica layer, where the galvanic interactions were enabled among Au and  $\alpha\beta\gamma$  particles and on the same time these minerals were under the passivation effect from the segregated pyrite mineral layer, resulted in a remarkable

promotion in the dissolution of the precious metals. Like the presence of acanthite [10] and pyrrargyrite, the presence of metallic silver along with two early mentioned analogues was found to enhance Au dissolution. Interestingly, as shown in Fig. 4.8, the increase in leaching kinetics as well as overall recovery of Au is significantly higher with the presence of metallic silver as compared to acanthite and pyrrargyrite. It could be attributed to the role of silver as a bi-metallic corrosion, allowing oxygen reduction to occur at the silver surface in addition to the oxygen reduction taking place at the sulphide mineral surface [9].

#### 4.3.8. Effect of Ag, Ag<sub>2</sub>S and Ag<sub>3</sub>SbS<sub>3</sub> on Au Leaching with Chalcopyrite-Silica System

Gold dissolution kinetics as well as overall recovery in close contact and/or segregation from the chalcopyrite mineral layer is summarized in Table 1. The influence of silver minerals ( $\alpha\beta\gamma$ ) on Au dissolution and in contact with the chalcopyrite mineral is shown in Fig. 4.9.

Fig. 4.9a shows Au recovery as a result of global galvanic contacts among the mineral and precious metal constituents due to the dispersion of silver minerals ( $\alpha\beta\gamma$ ) and Au particles within the chalcopyrite mineral particles. The precious metal recoveries for Au and Ag were 10.2% and 14.2%, respectively. The presence of silver minerals along with gold in direct combination with chalcopyrite particles resulted in a pronounced retardation in gold dissolution, with just 10.2% Au recovery with  $\alpha\beta\gamma$  as compared to 57% with Au present within chalcopyrite particles alone (Table 4.1). The non-silver sulphide mineral, such as chalcopyrite, was found to have a retarding effect on the leaching kinetics of silver sulphide in ferricyanide–cyanide system [30].

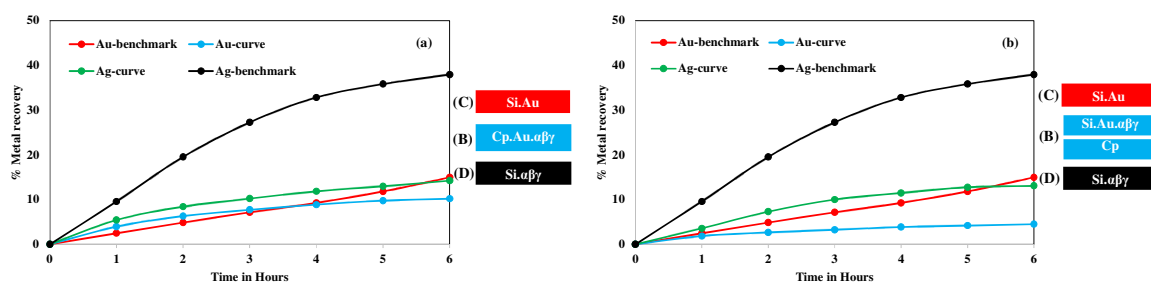


**Figure 4.9.** Gold dissolution: (a) gold dissolution with chalcopyrite and silver minerals  $\alpha\beta\gamma$ , Cp+Au+ $\alpha\beta\gamma$ //Si, (b) Gold dissolution with chalcopyrite and silver minerals  $\alpha\beta\gamma$ , Cp//Si+Au+ $\alpha\beta\gamma$ . Reaction conditions:  $\text{CN}^- = 30 \text{ mM}$ ,  $\text{DO}_2 = 0.25 \text{ mM}$ ,  $\text{pH} = 11$ .

Acanthite and pyrargyrite were also observed to have a retarding effect while gold particles present under direct and indirect influence from the chalcopyrite mineral particles. It is obvious from the results discussed above and Table 1 that silver present in metallic form has retarded gold dissolution significantly as compared to silver minerals such as acanthite and pyrargyrite.

Chalcopyrite layer in segregation with respect to the silica layer hosting the silver minerals  $\alpha\beta\gamma$  and Au particles prompted a passivation effect from the species resulting from the dissolution of chalcopyrite. With this set of arrangements for the various mineral constituents, Au and Ag recoveries were 4.5% and 13.1%, respectively, after 6 h cyanidation. Au recovery was found to be lesser, even with the presence of galvanic contacts among the silver minerals  $\alpha\beta\gamma$  and Au particles. This means that these galvanic interactions were not enough to overcome the retardation effect from the dissolved species of the segregated chalcopyrite mineral layer. Combinations of silver minerals and chalcopyrite were observed to be retarding for Au dissolution irrespective of its presence in direct or indirect contact with Au particles. The silver minerals present in any combination with the chalcopyrite resulted in an in-situ production of silver sulphide film on the surface of Au particles and this film could be held responsible for the poor dissolution of Au particles [9,10].

#### **4.3.9. Effect of Ag, Ag<sub>2</sub>S and Ag<sub>3</sub>SbS<sub>3</sub> on Au Leaching with Sphalerite-Silica System**

The gold powder dispersed within the sphalerite layer as well as dispersed within the silica layer and segregated from the sphalerite mineral has been studied and Au recovery is given in Table 4.1. The impact of silver minerals  $\alpha\beta\gamma$  on Au dissolution was studied by dispersion of  $\alpha\beta\gamma$  and Au within the same sphalerite layer.

Under the global galvanic impact from ore constituents, Au and Ag recovery was estimated to be 71.1% and 26.03%, respectively (Fig. 4.10a). The association of silver minerals  $\alpha\beta\gamma$  with Au particles enhanced Au recovery from 1.6% (Table 4.1) to 71.1%, with a net increase of 69.5% in Au recovery with respect to Au present within the sphalerite layer. The results show that the association of  $\alpha\beta\gamma$  with Au particles, while present within the sphalerite particles has overcome the poor electrical conductivity of sphalerite, with a remarkable increase in Au recovery (Fig. 4.10a).

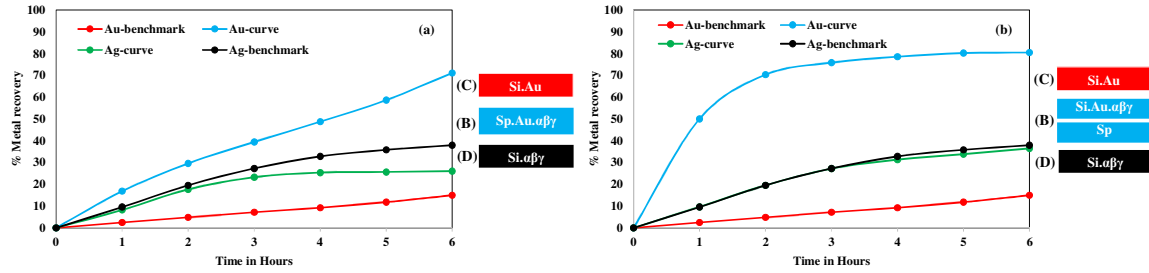


**Figure 4.10.** Gold dissolution: (a) gold dissolution with sphalerite and silver minerals  $\alpha\beta\gamma$ ,  $Sp+Au+\alpha\beta\gamma//Si$ , (b) Gold dissolution with sphalerite and silver minerals  $\alpha\beta\gamma$ ,  $Sp//Si+Au+\alpha\beta\gamma$ . Reaction conditions:  $CN^- = 30$  mM,  $DO_2 = 0.25$  mM,  $pH = 11$ .

The indirect influence from sphalerite mineral on Au dissolution was investigated by simultaneous dispersion of Au and silver minerals  $\alpha\beta\gamma$  within a silica layer segregated from sphalerite. The precious metal recovery charts for Au & Ag are shown in Fig. 4.10b. The Au recovery was 80.5% while Ag recovered after 6 h of cyanidation was 36.5%. Similarly, Au recovered after the same period for Au particles dispersed within silica and segregated from sphalerite layer was 15.6% (Table 4.1). The results demonstrate that Au leaching kinetics and recovery were significantly enhanced, i.e., ~65% increase in Au recovery, with addition of silver minerals  $\alpha\beta\gamma$ , while Ag recovery almost followed benchmark pattern.

Addition of silver minerals  $\alpha\beta\gamma$  to Au particles for the sphalerite-silica system has been observed to have an accelerating effect on Au dissolution in a similar fashion as for  $Ag_2S$  and  $Ag_3SbS_3$ . However, the presence of metallic silver made a tremendous contribution to Au dissolution as compared to  $Ag_2S$  [10] and  $Ag_3SbS_3$ . Silver metal present as pure metal, alloyed or dissolved state, enhances Au dissolution significantly [9,10,17,32].

#### 4.3.10. Effect of Ag, $Ag_2S$ and $Ag_3SbS_3$ on Au Leaching with Stibnite-Silica System

Stibnite showed an intensive retarding effect towards gold dissolution [8-10,33]. Au recovery in aerated cyanide solution for gold associated with stibnite amounted to 1.1% (Table 4.1). The effect of silver minerals  $\alpha\beta\gamma$  on Au dissolution in direct contact or indirect association with stibnite is illustrated in Fig. 4.11.

Fig. 4.11a exposes the dissolution of Au particles while under global impact of galvanic interactions from silver minerals  $\alpha\beta\gamma$  and stibnite. Au and Ag recoveries after 6 h cyanidation were 0.5% and 2.1%, respectively. Au recovery for the stibnite-silica system was reduced



from 1.1% to 0.5% with the addition of silver minerals  $\alpha\beta\gamma$ . Ag recovery from the dissolution of silver minerals  $\alpha\beta\gamma$  was also found to be retarded. Addition of silver minerals has further retarded the dissolution of Au embedded in the stibnite layer.

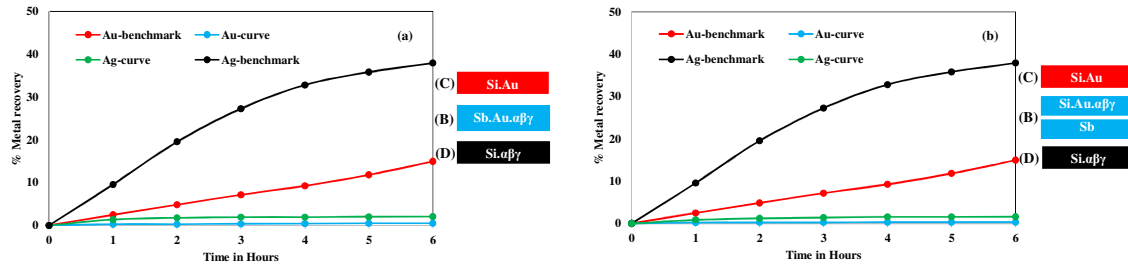


**Figure 4.11.** Gold dissolution: (a) gold dissolution with stibnite and silver minerals  $\alpha\beta\gamma$ , Sb+Au+ $\alpha\beta\gamma$ //Si, (b) Gold dissolution with stibnite and silver minerals  $\alpha\beta\gamma$ , Sb//Si+Au+ $\alpha\beta\gamma$ . Reaction conditions:  $\text{CN}^- = 30 \text{ mM}$ ,  $\text{DO}_2 = 0.25 \text{ mM}$ ,  $\text{pH} = 11$ .

Association of  $\alpha\beta\gamma$  on Au dissolution was investigated under indirect impact of stibnite mineral particles by placing stibnite in a separate layer. Au and Ag dissolutions are exemplified in Fig. 4.11b. Au and Ag recoveries were 0.3% and 1.6%, respectively, after 6 h cyanidation. Au recovery was retarded from 1.32% for Au within silica and segregated from stibnite to 0.3% for Au along with  $\alpha\beta\gamma$  within silica and under segregation from stibnite layer. Au recovery was severely influenced by the stibnite mineral either in direct or indirect contact.

The dissolution of stibnite resulted in the formation of antimony oxides ( $\text{Sb}_2\text{O}_5$ ) layer on the surface of Au particles and was held responsible for the retardation in Au dissolution. Addition of silver minerals  $\alpha\beta\gamma$  has further retarded the dissolution of gold because of formation of  $\text{Ag}_2\text{S}$  layer on the surface of gold particles in addition to the presence of antimony oxide layer [10,33].

#### 4.4. Conclusion

The effect of prominent silver minerals, such as metallic silver, acanthite and pyrargyrite, was investigated in terms of leaching kinetics and overall recovery of free gold and gold associated with conductive sulphide minerals. A packed-bed reactor strategy was adopted to investigate the Au and Ag dissolution under direct as well as indirect impact from the

sulphide minerals. Four sets of mineral systems were established: pyrite-silica, chalcopyrite-silica, sphalerite-silica and stibnite-silica systems.

Firstly, the impact of pyrrargyrite mineral on Au dissolution was investigated for free gold i.e., gold dispersed within silica layer, and gold associated with sulphides. Pyrrargyrite was found to be retarding for free gold which was attributed to the formation of surface obstructing species resulted by the dissolution of pyrrargyrite mineral. For sulphide-associated gold, the addition of pyrrargyrite enhanced the leaching kinetics and overall Au recovery for the pyrite-silica as well as sphalerite-silica systems, while both Au and  $\text{Ag}_3\text{SbS}_3$ , being under the galvanic as well as passivation impact from the respective sulphide mineral particles. The chalcopyrite-silica and stibnite-silica system were observed to have a retarding effect on Au dissolution in the presence of pyrrargyrite mineral, irrespective of being under galvanic or passivation impact from the sulphide mineral.

Secondly, the accumulative impact of the silver minerals (metallic silver, acanthite and pyrrargyrite) was investigated for the free as well as gold associated with the sulphides in a similar manner. The presence of silver minerals with free gold enhanced significantly the kinetics and recovery of gold. On the other hand, for the gold associated with the sulphides, association of silver minerals with Au particles enhanced the leaching kinetics as well as overall recovery for the pyrite-silica and sphalerite-silica system, under direct and indirect impact from the respective sulphides. The presence of silver minerals retarded the Au dissolution severely both under galvanic and passivation effects, for the chalcopyrite-silica and stibnite-silica systems. This retardation could be attributed to the formation silver sulphide layer on the surface of gold particles upon addition of silver minerals.

## **Acknowledgements**

Financial support from the Natural Sciences and Engineering Research Council through its Cooperative Research & Development grants program and from the supporting partners Agnico Eagle, Barrick, Camiro, Corem, Glencore, IamGold, Niobec and Teck is gratefully acknowledged. The authors are also very thankful to Prof. Brian Hart from Department of Earth Sciences (University of Western Ontario), and Dr. Patrick Laflamme from Corem for

encouraging discussions on gold leaching. The author (MK) would like to thank Mr. Olivier Gravel for his guidance and support.

#### 4.5. References

1. Marsden, J. O., and House, C. I., 2006. Chemistry of gold extraction. 2<sup>nd</sup> ed. Littleton, Colorado: Society for Mining, Metallurgy, and Exploration (SME), 2006.
2. Senanayake, G., 2008. A review of effects of silver, lead, sulfide and carbonaceous matter on gold cyanidation and mechanistic interpretation. *Hydrometallurgy*, 90, 46–73.
3. Bas, A. D., Safizadeh, F., Ghali, E., and Choi, Y., 2016. Leaching and electrochemical dissolution of gold in the presence of iron oxide minerals associated with roasted gold ore. *Hydrometallurgy*, 166, 143–153.
4. Liu, G. Q. and Yen, W. T., 1995. Effects of sulphide minerals and dissolved oxygen on the gold and silver dissolution in cyanide solution. *Minerals Engineering*, 8, 111–123.
5. Dai, X., and Jeffrey, M. I., 2006. The effect of sulfide minerals on the leaching of gold in aerated cyanide solutions. *Hydrometallurgy*, 82, 118–125.
6. Azizi, A., Petre, C. F., and Larachi, F., 2012. Leveraging strategies to increase gold cyanidation in the presence of sulfide minerals—Packed bed electrochemical reactor approach. *Hydrometallurgy*, 111–112, 73–81.
7. Azizi, A., Petre, C. F., Assima, G. P., and Larachi, F., 2012. The role of multi-sulfidic mineral binary and ternary galvanic interactions in gold cyanidation in a multi-layer packed-bed electrochemical reactor. *Hydrometallurgy*, 113-114, 51–59.
8. Azizi, A., Petre, C. F., Olsen, C., and Larachi, F., 2011. Untangling galvanic and passivation phenomena induced by sulfide minerals on precious metal leaching using a new packed-bed electrochemical cyanidation reactor. *Hydrometallurgy*, 107, 101–111.
9. Khalid, M., and Larachi, F., 2017. Effect of silver on gold cyanidation in mixed and segregated sulphidic minerals. *The Canadian Journal of Chemical Engineering*, 95, 698–707.
10. Khalid, M., Larachi, F., and Adnot, A., 2017. Impact of silver sulfide on gold cyanidation with conductive sulfide minerals. *The Canadian Journal of Chemical Engineering*, (online 4 May, 2017).
11. Lorenzen, L., and van Deventer, J. S. J., 1992. The mechanism of leaching of gold from refractory ores. *Minerals Engineering*, 5, 1377–1387.
12. Azizi, A., Petre, C. F., Olsen, C., and Larachi, F., 2010. Electrochemical behavior of gold cyanidation in the presence of a sulfide-rich industrial ore versus its major constitutive sulfide minerals. *Hydrometallurgy*, 101, 108–119.

13. Azizi, A., Olsen, C., and Larachi, F., 2014. Efficient strategies to enhance gold Leaching during cyanidation of multi-sulfidic ores. *The Canadian Journal of Chemical Engineering*, 92, 1687–1692.
14. Hiskey, J. B. and Sanchez, V. M., 1990. Mechanistic and kinetic aspects of silver dissolution in cyanide solutions. *Journal of Applied Electrochemistry*, 20, 479–487.
15. Senanayake, G., 2006. The cyanidation of silver metal: Review of kinetics and reaction mechanism. *Hydrometallurgy*, 81, 75–85.
16. Lin, H. K., Oleson, J. L., and Walsh, D. E., 2010. Behavior of gold and silver in various processing circuits at the Fort Knox Mine. *Minerals and Metallurgical Processing*, 27, 219–223.
17. Jeffrey, M. I., and Ritchie, I. M., 2000. The leaching of gold in cyanide solutions in the presence of impurities II. The effect of silver. *Journal of The Electrochemical Society*, 147, 3272–3276.
18. Dai, X., and Breuer, P. L., 2013. Leaching and electrochemistry of gold, silver and gold–silver alloys in cyanide solutions: Effect of oxidant and lead(II) ions. *Hydrometallurgy*, 133, 139–148.
19. Luna-Sanchez, R. M., and Lapidus, G. T., 2000. Cyanidation kinetics of silver sulfide. *Hydrometallurgy*, 56, 171–188.
20. Parga, J. R., Valenzuela, J. L., and Cepeda, T. F., 2007. Pressure cyanide leaching for precious metals recovery. *The Journal of The Minerals, Metals & Materials Society*, 59, 43–47.
21. Rajala, J., and Deschenes, G., 2009. Extraction of gold and silver at the Kupol Mill using CELP. In: *World Gold Conference 2009*. The Southern African Institute of Mining and Metallurgy, Johannesburg, pp. 35–42.
22. Celep, O., Bas, A. D., Yazici, E. Y., Alp, I., and Deveci, H., 2015. Improvement of silver extraction by ultrafine grinding prior to cyanide leaching of the plant tailings of a refractory silver ore. *Mineral Processing and Extractive Metallurgy Review*, 36, 227–236.
23. Cathro, K. J., and Koch, D. F. A., 1964. The anodic dissolution of gold in cyanide solutions. *Journal of Electrochemical Society*, 111, 1416–1420.
24. Thurgood, C. P., Kirk, D. W., Foulkes, F. R., and Graydon, W. F., 1981. Activation energies of anodic gold reactions in aqueous alkaline cyanide. *Journal of the Electrochemical Society*, 128, 1680–1685.
25. Wadsworth, M. E., Zhu, X., Thompson, J. S., and Pereira, C. J., 2000. Gold dissolution and activation in cyanide solution. *Hydrometallurgy*, 57, 1–11.

26. Celep, O., Alp, I., Paktunc, D., and Thibault, Y., 2011. Implementation of sodium hydroxide pretreatment for refractory antimonial gold and silver ores. *Hydrometallurgy*, 2011, 108: 109–114.
27. Rodriguez-Rodriguez, C., Nava-Alonso F., Uribe-Salas A., and Vinals J., 2016. Pyrargyrite ( $\text{Ag}_3\text{SbS}_3$ ): Silver and antimony dissolution by ozone oxidation in acid media. *Hydrometallurgy*, 164, 15–23.
28. Aghamirian, M. M., and Yen, W. T., 2005. Mechanisms of galvanic interactions between gold and sulfide minerals in cyanide solution. *Minerals Engineering*, 18, 393–407.
29. Melendez, A. M., Gonzalez, I., and Arroyo, R., 2010. An approach to the reactivity of isomorphous proustite ( $\text{Ag}_3\text{AsS}_3$ ) and pyrargyrite ( $\text{Ag}_3\text{SbS}_3$ ) in cyanide solutions. *ECS Transactions*, 28, 191–199.
30. Xie, D., Dreisinger, D. B., 2007. Leaching of silver sulfide with ferricyanide–cyanide solution. *Hydrometallurgy*, 88, 98–108.
31. Bas, A. D., Safizadeh, F., Zhang, W., Ghali, E., and Choi, Y., 2015. Active and passive behaviors of gold in cyanide solutions. *Transactions of Nonferrous Metals Society of China*, 25, 3442–3453.
32. Wadsworth, M. E., and Zhu, X., 2003. Kinetics of enhanced gold dissolution: activation by dissolved silver. *International Journal of Mineral Processing*, 72, 301–310.
33. Guo, H., Deschenes, G., Pratt, A., Fulton, M., and Lastra, R., 2005. Leaching kinetics and mechanisms of surface reactions during cyanidation of gold in the presence of pyrite and stibnite. *Minerals and Metallurgical Processing*, 22, 89–95.



# Chapter 5: The Role of Lead on the Cyanidation of Gold Associated with Silver Minerals Embedded within Base-metal Sulphide Mineral Matrices\*

## Résumé

Les effets de l'addition directe d'acétate de plomb ainsi que d'un prétraitement à l'aide d'une solution alcaline aérée d'acétate de plomb sur la dissolution d'or et d'argent intégrés dans des systèmes minéraux de pyrite-silice, chalcopryrite-silice, sphalérite-silice, et stibnite-silice ont été investigués. L'addition directe de plomb stimule la dissolution de l'or lorsqu'associé avec des minéraux d'argent et mélangé à de la silice (de 69,9% à 96,2% avec l'ajout de plomb) ou à de la pyrite (de 90,6% à 97,9% avec l'ajout de plomb). La dissolution de l'or a également été promue avec l'addition directe de plomb dans le cas des systèmes de chalcopryrite-silice (10,2% à 92,6%) et de sphalérite-silice (de 80,5% à 98,8%). Toutefois, l'addition directe de plomb n'a pas réussi à stimuler la dissolution de l'or, obtenant une faible récupération de 6,9% lorsque l'or et les minéraux d'argent sont associés dans une couche de stibnite. En alternative à une addition directe de plomb, un prétraitement à l'aide d'une solution alcaline aérée d'acétate de plomb a aussi été implémenté. Ce prétraitement a augmenté la récupération de l'or pour pratiquement tous les systèmes minéraux étudiés, à l'exception du système stibnite-silice, dont la performance de dissolution est la plus faible. Des analyses de surface par spectroscopie de photoélectrons aux rayons X ont mis en évidence la présence de films de sulfure d'argent ( $\text{Ag}_2\text{S}$ ), d'oxyde d'antimoine ( $\text{Sb}_2\text{O}_5$ ) et d'oxyde de plomb ( $\text{PbO}$ ) sur les surfaces d'or, qui ont été identifiés comme étant des facteurs responsables de la faible dissolution de l'or en présence de stibnite.

---

\* M. Khalid, F. Larachi, A. Adnot, *Hydrometallurgy* 2017 (submitted May 8, 2017).

## Abstract

The effects of direct lead acetate addition and aerated alkaline lead acetate pretreatment on the dissolution of gold and silver embedded in pyrite-silica, chalcopyrite-silica, sphalerite-silica, and stibnite-silica mineral systems were investigated. Direct addition of lead stimulated the dissolution of gold when this latter, associated with silver minerals, was interspersed in the silica (from lead-free 69.9% to 96.2%) or in the pyrite (from lead-free 90.6% to 97.9%) layer. Gold dissolution was likewise promoted through direct lead addition for the chalcopyrite-silica (from lead-free 10.2% to 92.6%) and the sphalerite-silica (from lead-free 80.5% to 98.8%) systems. However, direct lead addition was helpless to boost gold dissolution achieving a timid recovery of 6.9% when both gold and silver minerals were associated within the stibnite layer. As an alternative to lead direct addition, an alkaline lead acetate pre-treatment of the minerals was also implemented. Lead pre-treatment enhanced Au recovery for all the model mineral systems tested with the exception of the stibnite/silica system which showed the poorest gold dissolution performance. X-ray photoelectron spectroscopy analyses unveiled the presence of silver sulphide ( $\text{Ag}_2\text{S}$ ), antimony oxide ( $\text{Sb}_2\text{O}_5$ ) and lead oxide ( $\text{PbO}$ ) films on gold surface which were objectified as the factors responsible for Au poor dissolution in the presence of stibnite.



## 5.1. Introduction

Cyanide in aerated alkaline pulp solutions is the lixiviant *par excellence* for gold and silver leaching from Au and Ag-bearing ores. The anodic dissolution of pure gold in aerated alkaline cyanide solution may be retarded by the formation of AuCN passive film on the surface of gold particles. Meanwhile, the formation of such surface obstructing film can be prevented by addition of heavy metal ions such as lead, bismuth, thallium and mercury in the leach solution ultimately resulting in an enhanced rate of gold dissolution [1,2,3]. Gold-bearing ores can be classified as free milling as well as refractory on the basis of the response of these ores towards gold leaching with alkaline cyanide solution [4,5]. Refractoriness of gold ores arises from their mineralogical composition, such as gold locked within sulphide matrix as well as gold present as tellurides or stibnides, but also from the presence of reactive gangue minerals within gold-bearing ores [6]. Although cyanide has been extensively used as a commercial ligand for precious metal leaching, it is not highly selective because most metal sulphides display a variety of reactions in alkaline gold cyanidation. Due to depletion of free-milling gold ores around the globe, there is an increasing trend in the treatment and processing of refractory gold ores, which often requires pre-oxidation as well as pre-treatment prior to cyanidation [5,7].

The chemistry of gold cyanidation is acknowledged to be very complex due to factors such as galvanic interactions between gold and sulphide mineral particles, lack of cyanide selectivity and oxygen consumptions as a result of the presence of host mineral constituents (Cu, Fe, Zn) and passivation of gold surface by reaction products such as hydroxides of iron and sulfur species [8-14]. Various strategies of lead nitrate addition as well as atmospheric pre-oxidation have been investigated to alleviate the undesired effects as a result of sulphide minerals dissolution in terms of reagents (both cyanide and oxygen) consumption and gold surface passivation. Strategies such as roasting, pressure oxidation, bio-oxidation, atmospheric alkaline pre-oxidation and ultrafine grinding have been adopted as pre-treatment methods in gold leaching process [6,15,16]. Studies have also been carried out to optimize the conditions for gold dissolution, such as suitable Eh, pH and additives. These additives either affect Eh and/or alter the gold surface reactions preventing passivation of the gold surface [3,10,17-22]. The role of lead(II) in presence of polymetal sulphides is to precipitate

out the dissolved sulphide species as PbS, thus preventing the formation of sulphide film on the surface of gold particles [23-25].

Gold-bearing ores often contain silver present in a variety of minerals. If in gold-silver ores, gold is often present in pure metallic form, there are over 200 argentiferous minerals where silver grades exceed those from gold grades [7,26,]. Silver-bearing sulphides such as acanthite, pyrargyrite, and tetrahedrite are also refractory in nature leading to very poor silver recoveries in alkaline cyanide leaching [6,26]. The effect of trace amount of silver on the dissolution kinetics of gold, either alloyed with gold or present in dissolved form within aerated cyanide leach solution, has received some attention from researchers. It has been reported that silver enhanced both gold oxidation and oxygen reduction half reactions via a bimetallic corrosion mechanism with oxygen reduction preferentially occurring at the active silver sites. This phenomenon resulted in significant enhancement of gold dissolution [27-29]. The effects of metallic silver and silver minerals (acanthite, pyrargyrite & accumulative metallic Ag and silver minerals) on the dissolution of gold in mixed and segregated sulphide minerals have started to be studied as well. For example, silver minerals were found to enhance gold recovery for gold particles having galvanic contacts with pyrite and sphalerite mineral particles. However, the very same presence of silver minerals severely retarded gold recovery for gold particles associated with chalcopyrite and stibnite minerals [13,14,26].

Despite the literature reports available on the effect of silver on gold leaching with alkaline cyanide solution [13,27,29], to our knowledge, no detailed studies on the effect of additives as well pre-treatment on the leaching behaviour of gold associated with prominent silver minerals and sulphide minerals have been reported. Therefore, this study was designed to evaluate the impact of alkaline lead acetate solution as a potential pre-treatment prior to cyanidation as well as the investigation of lead acetate effect present within aerated alkaline cyanide leach solution. The aim of this study was to evaluate how efficient these Pb-addition strategies are in the mitigation of harmful impacts of unwanted species resulting from simultaneous dissolution out of silver minerals and sulphides within the aerated cyanide leach solutions.

## 5.2. Experimental

### 5.2.1. Materials and Reagents

Representative sulphide minerals used in the current study were prepared from hand-picked mineral samples received from Ward's Natural Science. Pyrite (Py), chalcopyrite (Cp), sphalerite (Sp) and stibnite (Sb) were the minerals investigated in this study. Prior to use, the mineral specimens were characterized and their mineralogical composition is stated elsewhere [13].

The specimens were crush-ground and sorted to remove the particles coarser than 106  $\mu\text{m}$  and finer than 53  $\mu\text{m}$ . Surface area influences the dissolution process significantly; therefore, the same granulometric fraction is used to provide a uniform total area per unit mass for all the cyanidation experiments. The precious metals used in the present study: pure gold ( $P_{80} = 39 \mu\text{m}$ , 99.998%, Alfa Aesar USA), pure silver ( $P_{80} = 26 \mu\text{m}$ , 99.9%, Alfa Aesar USA), pure silver sulfide (99.9% metals basis, Alfa Aesar USA) and pyrargyrite mineral (Mineralogical Research Co.), were purchased with the specifications as indicated along with each item. The feed solutions were prepared with deionized water in all cyanidation experiments. The other reagents used in the current study such as, sodium cyanide, NaCN (98%, Sigma–Aldrich Canada), sodium hydroxide, NaOH (Fisher Scientific Canada) and boric acid,  $\text{H}_3\text{BO}_3$  (99.5%, Sigma–Aldrich Canada), lead acetate,  $\text{Pb}(\text{CH}_3\text{COO})_2$  (99%, lead(II) acetate trihydrate, Alfa Aesar USA) were all analytical grade.

### 5.2.2. Equipment and Procedures

Gold dissolution behavior in the presence of polymetal sulphides as well silver minerals was studied by using a two-layer packed bed reactor (PBR) as detailed elsewhere [13,14,26]. The polymetal sulphides consisted of pyrite, chalcopyrite, sphalerite and stibnite, while the silver minerals chosen were metallic silver [Ag], acanthite [ $\text{Ag}_2\text{S}$ ] and pyrargyrite [ $\text{Ag}_3\text{SbS}_3$ ]. The leaching tests were performed by the simultaneous placement of Au and all the three silver minerals in one of the sulphide mineral layer ( $X = \text{Py, Cp, Sp, or Sb}$ ) and/or in the silica layer. Metallic silver, and acanthite and pyrargyrite have been designated by the symbols  $\alpha$ ,  $\beta$  and  $\gamma$ , respectively.

The leaching pattern of gold under global impact from the polymetal sulphides as well as silver minerals was investigated by simultaneous dispersion of 50 mg of Au and 25 mg of each Ag mineral within 4 g of one of the sulphide minerals (X= Py, Cp, Sp, or Sb). Conversely, the dispersion of Au and silver mineral powders within the inert silica layer, thus segregated from the sulphide mineral layer, gives rise to an arrangement where Au and silver minerals were under galvanic contacts while the sulphide mineral layer is reduced to play a passivating role at the same time. Case C and Case D represent benchmark dissolution tests for Au as well as Ag minerals performed by separate dispersion of Au and Ag minerals the within silica layer filling the whole PBR. A detailed description about the dispersion patterns of precious metals as well as polymetal sulphides has been elaborated elsewhere [26].

### **5.2.3. Lead Acetate Pre-treatment and Lead Acetate Addition Tests**

Direct lead acetate addition and lead acetate pre-treatment tests have been performed in order to mitigate the harmful effect of species resulting by the dissolution of sulphidic minerals, especially in case of the chalcopyrite and stibnite minerals [26]. Lead acetate addition effect on gold leaching was investigated by the direct addition of lead acetate salt to the aerated alkaline cyanide solution. Three different concentrations of the lead acetate salt (such as 10, 20 and 100 mg/L), were introduced into the cyanide leach solution and their effect on gold leaching behaviour was investigated. The polymetal sulphides as well as Au and Ag mineral quantities were taken as explained above. The dispersion pattern of Au and Ag-minerals within the polymetal sulphides have been explained elsewhere [26].

Since the sulphide minerals frequently occur in sulfurous ore deposits, pre-treatment tests were conducted for the pyrite, chalcopyrite, sphalerite and stibnite minerals. Lead acetate pre-treatment tests for these sulphide minerals were performed prior to cyanidation tests. Each of the polymetal sulphides along with Au and Ag minerals dispersed within, were first introduced in the working section of the PBR. Room-temperature pre-treatments were conducted by circulating the air-saturated lead acetate solution (100 mg/L) through the reactor for 16 h prior to cyanidation. Cyanidation tests, subsequent to pre-treatments, were performed with freshly prepared cyanide solution.

Cyanidation tests were performed by continuous circulation of the aerated alkaline-cyanide solution (30 mM CN<sup>-</sup> and ~8.5 mg/L O<sub>2</sub>) through the PBR in a closed loop at a constant flow rate of 10.4 mL/min by using a peristaltic pump. The dissolved oxygen level (DO<sub>2</sub>~8.5 mg/L at 25°C), was maintained by continuous sparging of air through the cyanide solution, which was monitored by means of a dissolved oxygen probe (FOXY-AL300 model from Ocean Optics). On the other hand, the pH of the solution was maintained at 11 ± 0.01, by H<sub>3</sub>BO<sub>3</sub>/NaOH buffer solution, and was monitored by an Oakton 1000 series pH-meter. Small aliquots collected from the container at regular intervals during the experiment were filtrated with a particles filter VWR 0.45 µm. Analysis of the pregnant leach solution was performed by using a Perkin Elmer AA-800 atomic absorption spectrometer (AAS). The Au as well as Ag recoveries were estimated as the percentage of respective dissolved metal as compared to the initially dispersed amount of the precious metals.

#### **5.2.4. X-Ray Photoelectron Spectroscopy**

X-ray photoelectron spectroscopy was performed for the gold particles isolated post-cyanidation. The gold particles recovered after the stipulated cyanidation experiments, were rinsed with water to remove the excess free cyanide as well as the loosely bound species, before to be dried and kept under an inert atmosphere for 48 h. The surface characterization (XPS) tests were performed by using an AXIS-ULTRA instrument by KRATOS (UK), with a monochromatic Al K $\alpha$  X-ray source operated at 300 W. The analyzer was run in a constant pass energy mode. The size of the monochromatic X-ray beam has been represented by an analyzed spot of approximately 700 µm × 300 µm. Multichannel electron counting was performed with an 8 channel electron multiplier detector. The sample particles were placed in clean metallic cups while pressure during analysis was in the 1.3 µPa (10<sup>-8</sup> Torr) range. Electrostatic charge appearing on the electrically insulating sample particles, under X-ray irradiation, was neutralized with an integrated very low energy electron flood gun. The element analysis was performed by recording survey spectra at pass energy of 160 eV with an energy step of 1 eV per channel. The apparent relative concentrations were estimated by using appropriate sensitivity factors. High resolution spectra were recorded as well at pass energy of 40, 20, or 10 eV and step sizes of 0.1, 0.05, and 0.025 eV, respectively. The curve-fitting for the estimated data was performed using the CasaXPS software.

### 5.3. Results and Discussion

#### 5.3.1. Lead Acetate Effect on Benchmark Leaching of Gold and Silver Minerals

Recall the Case C and Case D represent the benchmark tests for Au as well as Ag minerals. They were performed with separate dispersion of either Au or Ag minerals within an inert silica layer. Au as well as Ag minerals dissolution tests were performed with the aerated cyanide solution with the composition elaborated in the Experimental Section. The effect of Ag minerals on Au leaching kinetics as well as overall recovery, while Au and Ag-minerals are present all together within the silica layers, have been elaborated in Table 5.1 (benchmark entry). The simultaneous dispersion of pure gold within silica and leaching performed with pure aerated cyanide solution resulted in an Au recovery of 15% after 6 h of cyanidation (Figure 5.1a). The pure gold particles showed poor dissolution within pure aerated cyanide solution. This retardation in Au dissolution could be attributed to the well-known AuCN film formed at the surface of gold particles [1,3,16,26].

**Table 5.1.** Effect of silver-minerals ( $\alpha\beta\gamma$ ) on Au recovery (%) with polymetal sulphides after 6 h cyanidation.

Sulphides	Au-Recovery (%) (X+Au//Si)/(X//Si+Au)	Au-Recovery/Ag-Recovery (%) (X+Au+ $\alpha\beta\gamma$ //Si)	Au-Recovery/Ag-Recovery (%) (X//Si+Au+ $\alpha\beta\gamma$ )
Pyrite	74.6/15.5	90.6/40.4	81.1/36.5
Chalcopyrite	57.0/14.1	10.2/14.2	4.5/13.1
Sphalerite	1.6/15.6	71.1/26.03	80.5/37.9
Stibnite	1.1/1.3	0.48/2.05	0.3/1.6
<b>Benchmark</b>	15/38( <b>Si+Au/Si+<math>\alpha\beta\gamma</math></b> )	69.9/36.4( <b>Si+Au+<math>\alpha\beta\gamma</math></b> )	

\*adopted from [14,26].

Close contact among gold and silver minerals ( $\alpha\beta\gamma$ ), dispersed within silica particles resulted in significant enhancement of Au recovery. The Au recovered after 6 h of the cyanidation experiment was estimated to be 69.9%, while 38% Ag was recovered by the dissolution of silver minerals as reported in Table 5.1 (benchmark entry). Silver enhances both gold oxidation as well as oxygen reduction half reactions, *via-a* bimetallic corrosion mechanism, with oxygen reduction occurring preferentially at silver active sites resulting in a remarkable net increase in gold dissolution [1,3,26].

The effect of lead salt on the dissolution of gold, while gold present within silica particles and in association with silver minerals was investigated by direct addition of lead acetate to the cyanidation recirculating solution. The experiments were performed to establish whether an addition of 10, 20 or 100 mg/L lead acetate could enhance (or reduce) the dissolution of gold as well as silver minerals while Au and Ag minerals are present all together within silica layer.

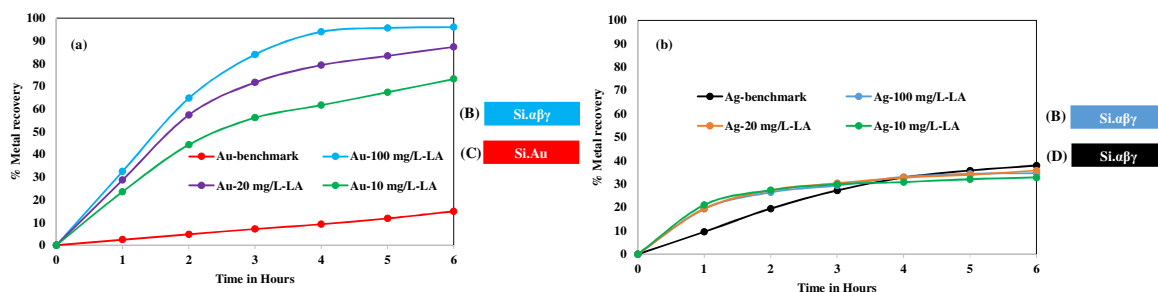


**Figure 5.1.** Lead acetate effect: (a) Gold dissolution with silver-minerals ( $\alpha\beta\gamma$ ) within quartz layer, (b) Silver dissolution for Au & silver-minerals ( $\alpha\beta\gamma$ ) within quartz layer. Reaction conditions: Lead acetate = (10, 20, 100 mg/L),  $\text{CN}^- = 30 \text{ mM}$ ,  $\text{DO}_2 = 0.25 \text{ mM}$ ,  $\text{pH} = 11$ .

The leaching behaviour of gold as well as silver minerals on addition of lead salt is represented in Figure 5.1. Inspection of this figure clearly demonstrates that lead addition has remarkably enhanced the dissolution of gold. After 6 h, the Au recovery was estimated to be 73.2% with 10 mg/L lead acetate addition as compared to 69.9% without lead acetate (benchmark entry of Table 5.1). With addition of 20 and 100 mg/L lead acetate, Au recovery was estimated to be 84.4% and 96.2%, respectively, after the same stipulated time of cyanidation (Figure 5.1a). Lead acetate addition has clearly enhanced the gold dissolution significantly while gold particles were associated with silver minerals which were present in the silica layer. In a similar fashion as for silver, the role of lead is also to modify the surface of gold and prevents it from passivating species specially AuCN. Divalent lead cations adsorbing at the surface of gold prevent buildup of surface obstructing species and enhance Au dissolution via bimetallic corrosion pathway [1,13].

The leaching kinetics as well as overall recovery for Ag from the dissolution of Ag minerals with aerated cyanide and lead acetate solution is shown in Figure 5.1b. The silver recovered after 6 h was estimated to be 32.8% with the addition of 10 mg/L lead acetate as compared to 38% (benchmark entry of Table 5.1) without lead acetate. Lead acetate in the concentration

range of 20, 100 mg/L resulted in Ag recoveries of 35.8% and 34.6% respectively, as shown in Figure 5.1b. This leaching data indicates that lead addition has proven to be slightly retarding towards the dissolution of Ag minerals with aerated cyanide solution.

### **5.3.2. Lead Acetate Effect on Leaching of Gold and Silver with Pyrite-Silica System**

The leaching kinetics for gold and silver with addition of lead acetate for the pyrite-silica system are represented in Figure 5.2. In this case, Au as well as Ag recoveries were estimated under galvanic and passivation impact from the pyritic mineral layer. The global galvanic contacts among Au, Ag minerals and pyrite particles were enabled by dispersing all these constituents within the same PBR layer. Lead acetate was introduced to the aerated alkaline cyanide solution in three concentrations, such as 10, 20 and 100 mg/L.

The accumulative impact of the silver minerals ( $\alpha\beta\gamma$ ) on the dissolution of Au particles within the pyrite mineral layer led to an Au recovery of 90.6% after 6 h of cyanidation process (Pyrite entry of Table 5.1). The gold leaching pattern with the already described arrangement of minerals has been given elsewhere [26]. Lead acetate impact on the leaching behaviour of gold particles present in close contact with Ag minerals and pyrite particles has been elaborated in Figure 5.2a. The Au recovery was estimated to be 90.1% with 10 mg/L lead acetate addition as compared to 90.6% (Pyrite entry of Table 5.1) without lead salt and under the same set of conditions. Similarly, Au recoveries for a concentration of 20 and 100 mg/L lead acetate were found to be 94.1% and 97.9%, respectively, as shown in Figure 2a. The Au recovery almost remained the same for a 10 mg/L lead acetate addition, while a 20 mg/L and 100 mg/L concentration of lead acetate enhanced Au recovery.



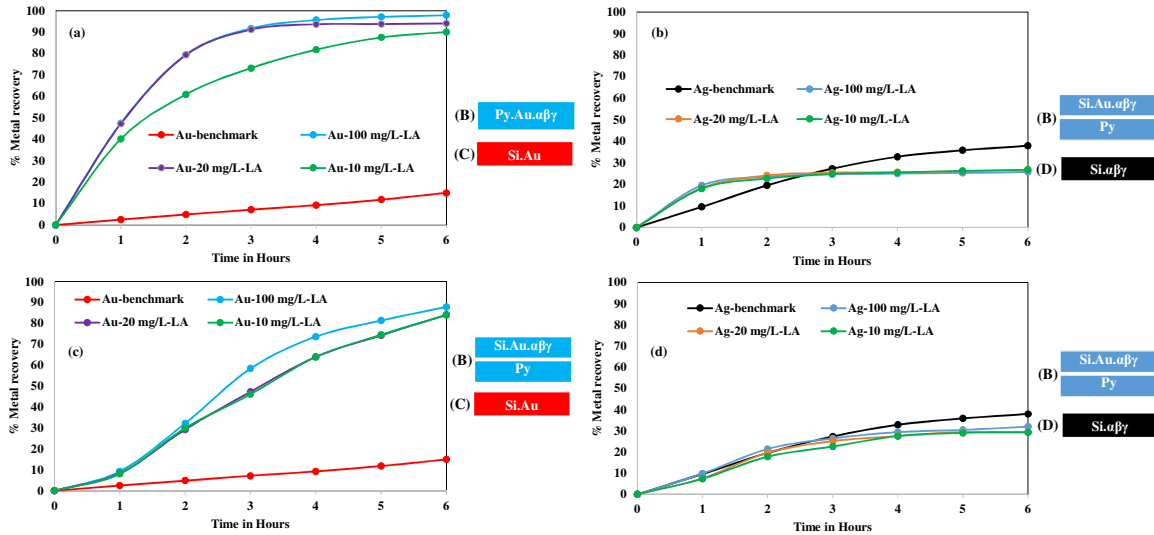


**Figure 5.2.** Lead acetate effect: (a) Gold dissolution with pyrite and silver-minerals ( $\alpha\beta\gamma$ ),  $Py+Au+\alpha\beta\gamma//Si$ , (b) Silver dissolution with pyrite and silver-minerals ( $\alpha\beta\gamma$ ),  $Py+Au+\alpha\beta\gamma//Si$ , (c) Gold dissolution with pyrite and silver-minerals ( $\alpha\beta\gamma$ ),  $Py//Si+Au+\alpha\beta\gamma$ , (d) Silver dissolution with pyrite and silver-minerals ( $\alpha\beta\gamma$ ),  $Py//Si+Au+\alpha\beta\gamma$ , Reaction conditions: Lead acetate = (10, 20, 100 mg/L),  $CN^- = 30$  mM,  $DO_2 = 0.25$  mM, pH = 11.

In a similar fashion, silver recovered by the dissolution of Ag minerals, with lead acetate concentrations in the range of 10, 20 and 100 mg/L, was estimated to be 26.8, 26.8 and 25.8%, respectively after 6 h cyanidation as compared to 40.4% with no lead salt (Pyrite entry of Table 5.1), as shown in Figure 5.2b. This data showed that the presence of lead acetate within the leach solution was detrimental towards leaching of silver minerals.

Dispersion of Ag minerals ( $\alpha\beta\gamma$ ) and Au within a silica layer contiguous to the pyrite mineral layer resulted in Au and Ag dissolution of 81.1% and 36.5%, respectively (Pyrite entry of Table 5.1). The results for lead acetate effect on Au as well as Ag dissolution, for the given set of arrangements, are summarized in Figures 5.2c, 5.2d, respectively. Lead acetate present within the aerated cyanide solution at a level of 100 mg/L resulted in 87.9% net dissolution of gold after 6 h of the cyanidation experiment. The Au dissolved with addition of 10 mg/L and 20 mg/L lead salt was estimated to be 83.9% and 84.1% as (Figure 5.2c) compared to 81.1% without the lead salt (Pyrite entry of Table 5.1). Dissolved silver within the leach solution resulting from the cumulative Ag minerals ( $\alpha\beta\gamma$ ) was 31.9% for a concentration of 100 mg/L lead acetate. Likewise, 10 mg/L and 20 mg/L lead acetate addition to the leach solution resulted in an Ag dissolution of 29.2% and 29.3% respectively, (Figure 5.2d) as compared to 36.5% without the lead salt (Pyrite entry of Table 5.1).

These results demonstrate that lead acetate addition enhanced Au dissolution for the gold associated with Ag minerals and pyrite particles, no matter whether or not Au and Ag minerals were under galvanic and/or passivation impact from the pyrite particles. According to Senanayake (2008), the beneficial and/or detrimental effects of lead salts to the dissolution kinetics of gold depend on the pH, cyanide and dissolved oxygen concentrations as well as the nature of the species present at the surface of gold particles.

### **5.3.3. Lead Acetate Effect on Leaching of Gold and Silver with Chalcopyrite-Silica System**

The effect of lead acetate on the leaching kinetics for gold and silver for the chalcopyrite-silica system has been represented by the Figure 5.3. Association of silver-minerals with gold particles, both under galvanic as well as passivation effect from the chalcopyrite mineral particles, have been investigated on the leaching behavior of gold. Silver-minerals have been found to be significantly retarding towards the gold dissolution in direct as well indirect connection with the chalcopyrite particles [26]. The gold dissolution was estimated to be 10.2% with Au &  $\alpha\beta\gamma$  present within chalcopyrite as compared to 57% for the Au particles present within chalcopyrite alone. Silver-minerals associated with gold, while both Au &  $\alpha\beta\gamma$  present within silica and contiguous to chalcopyrite, 4.5% Au was leached out as compared to 14.1% for Au alone without  $\alpha\beta\gamma$ , after 6 h of the cyanidation test (Chalcopyrite entry of Table 5.1). Presence of hydrosulfide ( $\text{HS}^-$ ) even at low concentrations passivate gold surface due to the formation of  $\text{Ag}_2\text{S}$  layer on the surface of gold particles [3].

To alleviate the harmful effect of the species resulted by the simultaneous dissolution of chalcopyrite and Ag-mineral particles, lead acetate was introduced to the aerated cyanide solution and the leaching tests were performed in the same manner as explained in the experimental section.

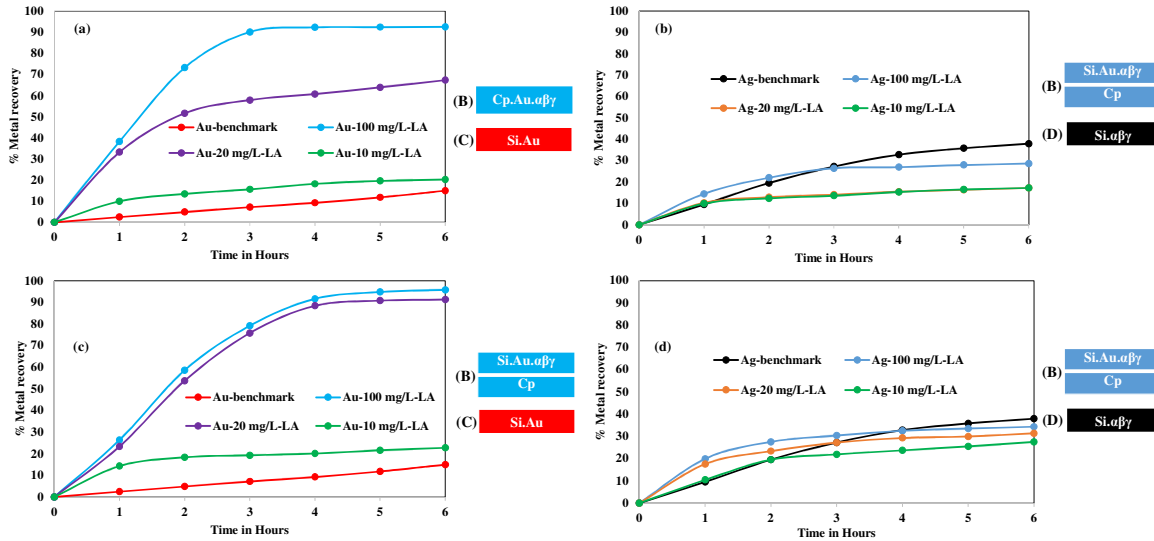


**Figure 5.3.** Lead acetate effect: (a) Gold dissolution with chalcopyrite and silver-minerals ( $\alpha\beta\gamma$ ), Cp+Au+ $\alpha\beta\gamma$ //Si, (b) Silver dissolution with chalcopyrite and silver-minerals ( $\alpha\beta\gamma$ ), Cp+Au+ $\alpha\beta\gamma$ //Si, (c) Gold dissolution with chalcopyrite and silver-minerals ( $\alpha\beta\gamma$ ), Cp//Si+Au+ $\alpha\beta\gamma$ , (d) Silver dissolution with chalcopyrite and silver-minerals ( $\alpha\beta\gamma$ ), Cp//Si+Au+ $\alpha\beta\gamma$ , Reaction conditions: Lead acetate = (10, 20, 100 mg/L),  $CN^-$  = 30 mM,  $DO_2$  = 0.25 mM, pH = 11.

Figure 5.3a represents the dissolution behaviour of gold with lead acetate addition for Au and Ag-minerals ( $\alpha\beta\gamma$ ) present all together within the chalcopyrite particles. A little enhancement was observed in the gold dissolution with 10 mg/L lead addition. Gold dissolution was estimated to be 20.3% with 10 mg/L lead addition as compared to 10.2% without lead salt (Chalcopyrite entry of Table 5.1). A significant enhancement was observed in the gold dissolution rate for a lead acetate concentration of 20 and 100 mg/L. The gold recovery was found to be 67.4% and 92.6% for a lead acetate concentration of 20 and 100 mg/L respectively, as compared to 10.2% without the presence of lead salt (Chalcopyrite entry of Table 5.1). This represents that the lead present as Pb(II) in the aerated cyanide leach solution has prevented the adsorption of surface obstructing species at the surface of gold particles. Silver dissolved under close contact between Ag-minerals and chalcopyrite particles has been reported in Figure 5.3b. Silver recovery was estimated to be 17.2%, 17.3% and 28.6% for a 10, 20 and 100 mg/L lead acetate present within aerated cyanide leach solution, as compared to 14.2% without lead salt (Chalcopyrite entry of Table 5.1).

The impact of lead acetate addition on the gold leaching kinetics as well as overall recovery for the gold and Ag-minerals present within the silica particles and contiguous to the

chalcopyrite layer has been shown in Figure 5.3c. The Au dissolution was estimated to be 22.8%, 92.6% and 95.8% for a lead acetate concentration of 10, 20 and 100 mg/L, respectively, as compared to 4.5% without lead salt (Chalcopyrite entry of Table 5.1). Gold dissolution was enhanced remarkably for a lead acetate concentration of 20 and 100 mg/L. The critical role of lead (II) is to precipitate out the dissolved sulphide species as lead sulphide (PbS), thus avoiding the passivation of the gold surface [19,25]. Silver dissolution was also monitored for a set of arrangements where Au &  $\alpha\beta\gamma$  were dispersed within silica layers and at the same contiguous to the chalcopyrite layer. Silver recovery was estimated to be 27.6%, 31.4% and 34.3% with lead acetate being present at 10, 20 and 100 mg/L concentrations respectively, as compared to 13.1% without lead acetate (Chalcopyrite entry of Table 5.1) shown in Figure 5.3d.

Lead acetate addition has been observed to be beneficial towards Au dissolution for the chalcopyrite-silica system, irrespective of the presence of Au &  $\alpha\beta\gamma$  under direct as well indirect effect from the chalcopyrite layer. Lead acetate addition could prevent the gold surface passivation resulting by the simultaneous dissolution of Chalcopyrite and Ag-minerals, as observed in the previous study [14].

#### **5.3.4. Lead Acetate Effect on Leaching of Gold and Silver with Sphalerite-Silica System**

Figure 5.4 demonstrates the effect of lead acetate on the leaching kinetics for gold and silver for the sphalerite-silica system. Sphalerite mineral present in close contact with gold particles induced a strong retarding effect on gold leaching kinetics [12]. Gold particles present under galvanic effect from the sphalerite particles showed a very poor dissolution in aerated cyanide solution with an Au recovery of 1.6% after 6 h of the cyanidation process[14]. This drastic decrease in gold recovery is generally ascribed to poor electrical conductivity of sphalerite mineral resulting in poor electron transfer at its surface [12,14].

Gold particles in close contact with Ag-minerals and sphalerite particles, enhanced the Au dissolution remarkably with an Au recovery of 71.1% as compared to 1.6% for Au alone within sphalerite mineral, after 6 h of cyanidation (Sphalerite entry of Table 5.1). Introducing silver-minerals along with gold within sphalerite layer overcome the poor electrical

conductivity of sphalerite particles, ultimately enhancing the Au recovery. Lead acetate effect on dissolution kinetics of Au particles associated with sphalerite and Ag-minerals was investigated. Lead acetate addition influenced the Au dissolution kinetics positively under stated conditions. Lead acetate present in cyanide leach solution at a concentration of 100 mg/L, led to the highest dissolution of gold with a recovery of 88.2%, while 10 and 20 mg/L concentration of lead acetate resulted in an Au recovery of 83.1% and 85.4% respectively, as compared to 71.1% without lead addition (Sphalerite entry of Table 5.1), after 6 h of the cyanidation experiment as shown in Figure 5.4a. This data demonstrates that although silver-minerals effectively increased the Au dissolution, the introduction of lead acetate has further contributed towards enhancement of Au recovery. Silver recovered by the dissolution of Ag-minerals, for a lead acetate concentration of 10, 20 and 100 mg/L present within aerated cyanide solution, was estimated to be 30.5%, 32.9% and 33% respectively, as compared to 26.03% without presence of lead salt (Sphalerite entry of Table 5.1) as shown in Figure 5.4b.

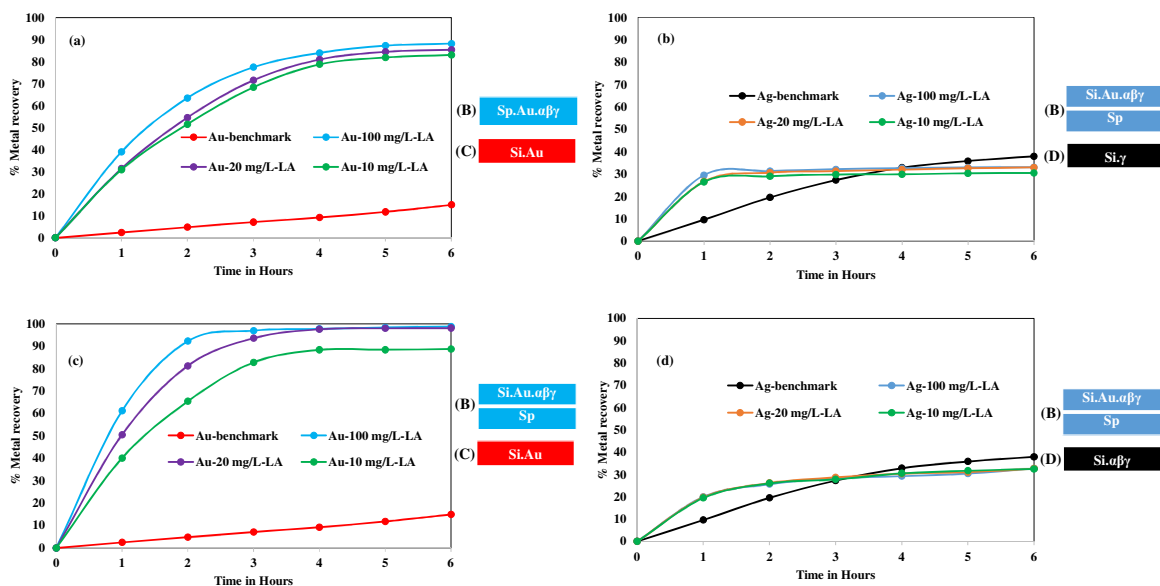


**Figure 5.4.** Lead acetate effect: (a) Gold dissolution with sphalerite and silver-minerals ( $\alpha\beta\gamma$ ), Sp+Au+ $\alpha\beta\gamma$ //Si, (b) Silver dissolution with sphalerite and silver-minerals ( $\alpha\beta\gamma$ ), Sp+Au+ $\alpha\beta\gamma$ //Si, (c) Gold dissolution with sphalerite and silver-minerals ( $\alpha\beta\gamma$ ), Sp//Si+Au+ $\alpha\beta\gamma$ , (d) Silver dissolution with sphalerite and silver-minerals ( $\alpha\beta\gamma$ ), Sp//Si+Au+ $\alpha\beta\gamma$ , Reaction conditions: Lead acetate = (10, 20, 100 mg/L),  $\text{CN}^- = 30 \text{ mM}$ ,  $\text{DO}_2 = 0.25 \text{ mM}$ ,  $\text{pH} = 11$ .

The dispersion of gold within silica particles and contiguous to the sphalerite mineral layer resulted in an Au recovery of 15.6 % (Sphalerite entry of Table 5.1). The Au & Ag-mineral

particles present within silica and under passivation effect from the sphalerite layer, resulted in an Au recovery of 80.5%, as compared to 15.6% in the absence of silver-minerals (Sphalerite entry of Table 5.1). The effect of lead salt addition was investigated under the stated arrangement of mineral constituents. 100 mg/L concentration of lead acetate enhanced Au dissolution tremendously with 98.8% Au recovery as compared to 80.5% without lead salt (Sphalerite entry of Table 5.1) after 6 h of cyanidation. Lead acetate with 10 and 20 mg/L concentration give rise to the Au recovery of 98.1% and 88.8% respectively as compared to 80.5% with no lead salt (Sphalerite entry of Table 5.1), as elaborated in Figure 5.4c. Gold dissolution in aqueous cyanide solution may be retarded by the formation of AuCN and sulphide passive films on the surface of gold particles, while the formation of these passive films can be disrupted by introducing heavy metal ions such as lead, bismuth, thallium and mercury in the cyanide leach solution, which result in an enhanced gold recovery [19,25,27]. Silver recovery for a 10, 20 and 100 mg/L concentration of lead salt present in cyanide leach solution was estimated to be 32.5%, 32.6% and 32.7% respectively as shown in Figure 5.4d, as compared to 37.9% with the same arrangement of minerals but without lead salt.

Lead acetate addition has been found to be beneficial for Au dissolution while associated with sphalerite and Ag-mineral particles. Silver recovered was found to be on a little higher end as compared to pyrite and chalcopyrite counter parts.

### **5.3.5. Lead Acetate Effect on Leaching of Gold and Silver with Stibnite-Silica System**

Stibnite has been known to be severely retarding towards gold dissolution kinetics [12,14,17]. The Au recovered under the galvanic interaction and passivation effect from the stibnite mineral layer was estimated to be 1.1% and 1.3% respectively after 6 h of the cyanidation process (Stibnite entry of Table 5.1). Permanent contacts among Au, Ag-minerals ( $\alpha\beta\gamma$ ) and stibnite particles led to an Au recovery of 0.5%, while Au and Ag-minerals present within silica and contiguous to the stibnite layer, resulted in an Au dissolution of 0.3% after the prescribed time of cyanidation process (Stibnite entry of Table 5.1).

Lead acetate effect on the gold leaching kinetics with Ag-minerals ( $\alpha\beta\gamma$ ) and stibnite have been investigated and elaborated in Figure 5. The species resulted by the dissolution of

stibnite as well as Ag-minerals in aerated cyanide solution have been observed to obstruct the surface of gold particles [12,14,17,26]. Lead acetate addition strategy was adopted in order to eliminate the harmful effect of these surface obstructing species.

Three concentrations of lead acetate were tried, such as 10, 20 and 100 mg/L in aerated cyanide solution. Lead acetate addition merely improved the Au recovery for the gold particles associated with Ag-minerals and stibnite particles either under galvanic contacts and/or passivation effect. The Au recovery was estimated to be 6.8% with 100 mg/L lead salt present within leach solution, as compared to 0.5% without lead salt (Stibnite entry of Table 5.1), for all the minerals and precious metals present under global galvanic interactions (Figure 5.5a). Meanwhile 10 and 20 mg/L concentration of lead salt did not contribute towards Au dissolution enhancement and Au recovery was estimated to be 0.6% and 0.4% respectively (Figure 5.5a), which are in close comparison with the Au recovery (0.5%) without lead acetate addition (Stibnite entry of Table 5.1). The silver metal present in dissolved form within the lead acetate containing leach solution was measured to be 3.7%, 3.8% and 3.9% corresponding respectively to a lead acetate concentration of 10, 20 and 100 mg/L, as compared to 2.05% without lead addition (Stibnite entry of Table 1), after the prescribed time of the cyanidation process (Figure 5.5b).

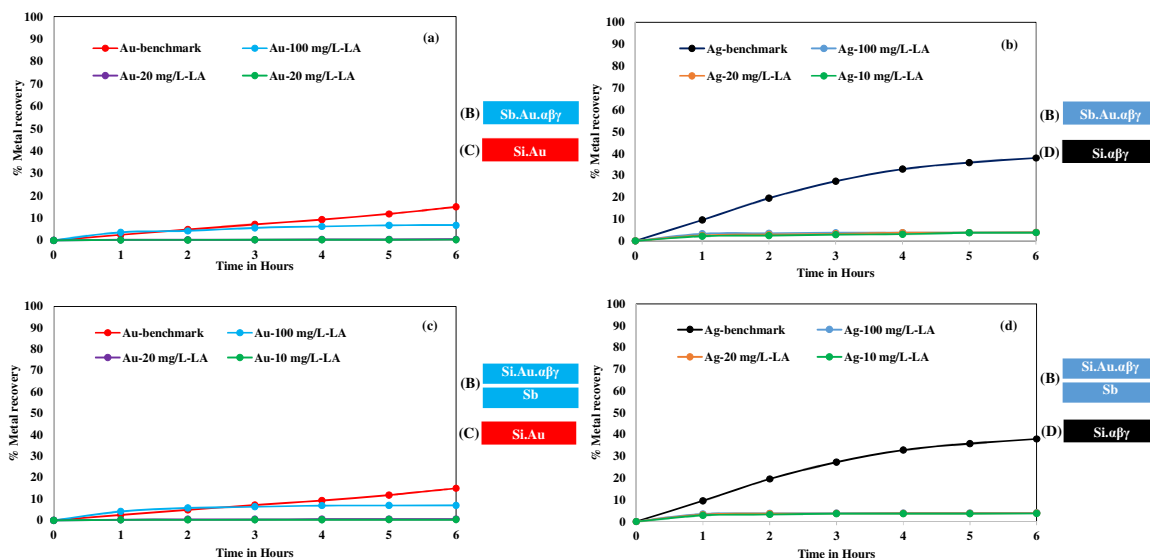


**Figure 5.5.** Lead acetate effect: (a) Gold dissolution with stibnite and silver-minerals ( $\alpha\beta\gamma$ ), Sb+Au+ $\alpha\beta\gamma$ //Si, (b) Silver dissolution with stibnite and silver-minerals ( $\alpha\beta\gamma$ ), Sb+Au+ $\alpha\beta\gamma$ //Si, (c) Gold dissolution with stibnite and silver-minerals ( $\alpha\beta\gamma$ ), Sb//Si+Au+ $\alpha\beta\gamma$ ,

(d) Silver dissolution with stibnite and silver-minerals ( $\alpha\beta\gamma$ ), Sb//Si+Au+ $\alpha\beta\gamma$ , Reaction conditions: Lead acetate = (10, 20, 100 mg/L),  $\text{CN}^- = 30 \text{ mM}$ ,  $\text{DO}_2 = 0.25 \text{ mM}$ ,  $\text{pH} = 11$ .

Effect of lead acetate addition on the dissolution of Au particles while in close contact with the Ag-minerals but contiguous to the stibnite layer has been addressed as well. In addition to stibnite, Ag-minerals have also been observed to be retarding for Au dissolution, resulting in 0.3% Au recovery as compared to 1.3% without Ag-minerals (Stibnite entry of Table 5.1). Lead acetate addition was investigated as already explained, means in 10, 20 and 100 mg/L concentrations, introduced to aerated cyanide leach solution. The Au recovered was estimated to be 0.3%, 0.6% and 6.9%, for a lead acetate concentration of 10, 20 and 100 mg/L respectively, as compared to 0.3% with same mineral arrangement but without lead salt (Stibnite entry of Table 5.1), as shown in Figure 5.5c. In this case also there was a little improvement in the Au recovery with 100 mg/L lead acetate addition while the other two concentration of lead acetate showed no impact on the dissolution kinetics of gold. Silver recovered with this arrangement was measured to be 3.7%, 3.8% and 3.9% corresponding to a respective lead acetate concentration of 10, 20 and 100 mg/L as shown in Figure 5.5d.

The lead acetate addition was found to give almost comparable recoveries for Au as well as Ag with the stibnite particles effecting the precious metals (Au & Ag-minerals) dissolution in a galvanic and passivation manner. Irrespective of the presence of precious metals and stibnite particles under galvanic and/or passivation effect, lead acetate addition barely improved the Au recovery at a 100 mg/L concentration. It demonstrates that the lead acetate present within aerated cyanide leach solution was unable to overcome the surface obstructing species resulted by the simultaneous dissolution of silver-minerals and stibnite particles.

### **5.3.6. Alkaline Lead Acetate Pre-treatment of Sulphides and Gold Leaching**

The alkaline lead acetate pre-treatment tests for the pyrite, chalcopyrite, sphalerite and stibnite sulphidic minerals, with the presence of both Au and Ag-minerals within each of these minerals, were performed with 100 mg/L lead acetate alkaline solution over a length of 16 h. The system represents a sulphide-associated Au & Ag-minerals in a monolayer of PBR and treatment with aerated alkaline lead acetate prior to cyanidation. This strategy demonstrates the scenario of surface modification of the sulphidic minerals through pre-oxidation as well as the adsorption of lead at the surface of gold particles.



The effect of aerated alkaline lead acetate pre-treatment on the Au dissolution kinetics has been represented in the Figure 5.6a. Pre-treatment of pyrite mineral, also containing Au and Ag-minerals dispersed within, with aerated alkaline lead acetate solution resulted in an Au recovery of 93.7%, as compared to 90.6% without lead addition, after the 6 h of the cyanidation process. It is worth remembering that the leaching tests were performed with freshly prepared cyanide solution. The Au recovery was slightly lowered as compared to direct lead addition at 100 mg/L concentration, i.e., 97.9% (Figure 5.1a) but slightly higher as compared to Au recovery without lead addition (90.6%). Au and Ag-minerals possessing chalcopyrite layer on pre-treatment with aerated alkaline lead acetate solution prior to cyanidation, resulted in an Au recovery of 85.8%, after 6 h of cyanidation. Lead acetate pre-treatment enhanced the Au recovery significantly, i.e., from 10.2% (Chalcopyrite entry of Table 5.1) to 85.8% (Figure 5.6a).

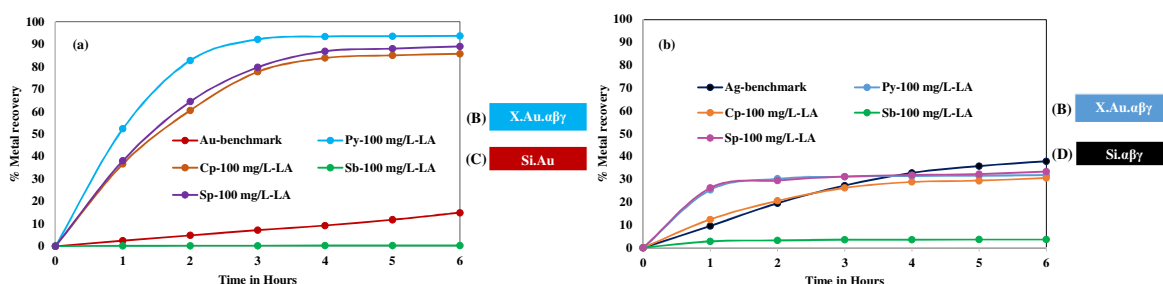


**Figure 5.6.** Lead acetate pre-treatment: (a) Gold dissolution with (X= pyrite, chalcopyrite, sphalerite, stibnite) and silver-minerals ( $\alpha\beta\gamma$ ), X+Au+ $\alpha\beta\gamma$ //Si, (b) Silver dissolution with (X= pyrite, chalcopyrite, sphalerite, stibnite) and silver-minerals ( $\alpha\beta\gamma$ ), X+Au+ $\alpha\beta\gamma$ //Si, Reaction conditions: Lead acetate = 100 mg/L,  $\text{CN}^- = 30$  mM,  $\text{DO}_2 = 0.25$  mM, pH = 11.

In case of sphalerite, for an arrangement of Au and Ag-minerals dispersed within Sp layer, the lead acetate pre-treatment enhanced the Au recovery from 71.1% (Sphalerite entry of Table 5.1) to 89.05%, as shown in Figure 5.6a. In this case also a significant enhancement in Au recovery was observed. No effect of lead acetate pre-treatment was observed on the gold leaching for the Au and Ag-minerals dispersed within stibnite particles and Au recovered was estimated to be 0.34%, a recovery similar to one without pre-treatment (Stibnite entry of Table 5.1), as shown in Figure 5.6a. Silver recoveries as a result of the lead acetate pre-treatment have been shown in Figure 5.6b. The Ag recovered for pyrite, chalcopyrite, sphalerite and stibnite, after lead acetate pre-treatment, has been estimated to be 31.9%,

30.6%, 33.4% and 3.59%, as compared to 40.4%, 14.2%, 26.03% and 2.05% (Table 5.1) respectively after the cyanidation process, as shown in Figure 5.6b.

In summary, it can be concluded that the lead acetate pre-treatment has been found to be beneficial for the removal of harmful species towards gold dissolution for pyrite, chalcopyrite and sphalerite minerals, but having no effect for the stibnite mineral.

### **5.3.7. X-ray Photoelectron Spectroscopy of Gold Particles Isolated after Cyanidation**

XPS studies were performed for the gold particles isolated after cyanidation process. The association of stibnite with Au particles posed a severe detrimental effect on the gold dissolution behavior [12-14,17]. The cyanidation of Au particles was carried out with the stibnite and Ag-minerals and also with 100 mg/L lead acetate addition to the aerated cyanide leach solution. The surface characterization of gold particles was performed in order to provide an insight to the surface obstructing species formed at the surface of gold particles during the cyanidation process. The surface characterization concerns the gold particles isolated after the 6 h dissolution test in the packed-bed reactor. The spectral envelopes are presented in Figure 5.7, the noise-free continuous lines representing the sum of the analytical peaks used to fit the high-resolution spectra, while the symbols with noise represent the experimental spectra. Fits were performed using the CasaXPS software. The base line approximation was made by using a Shirley background. When using the neutralization electron beam binding energy corrections were made using the C-C/C-H C1s peak located at 285.0 eV as usual.

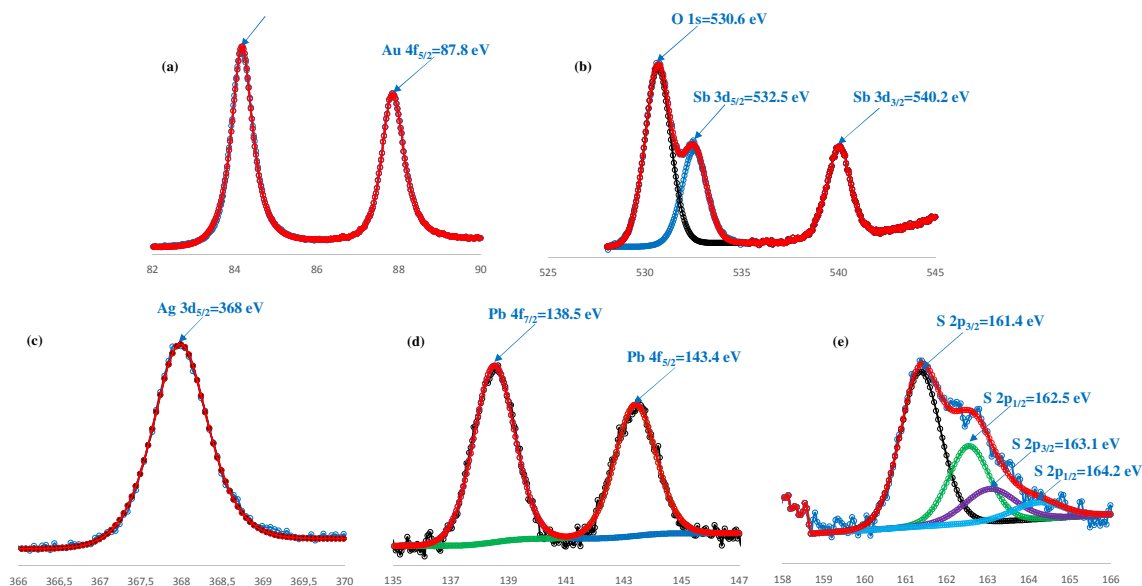


**Figure 5.7.** X-ray spectra of gold surface: **(a)** Au 4f spectra for gold with stibnite and silver-minerals ( $\alpha\beta\gamma$ ), **(b)** Sb 3d spectra for gold with stibnite and silver-minerals ( $\alpha\beta\gamma$ ), **(c)** Ag 3d<sub>5/2</sub> spectra for gold with stibnite and silver-minerals ( $\alpha\beta\gamma$ ), **(d)** Pb 4f spectra of gold with stibnite and silver-minerals ( $\alpha\beta\gamma$ ), **(e)** S 2p spectra for gold with stibnite and silver-minerals ( $\alpha\beta\gamma$ ). Reaction conditions: Lead acetate = 100 mg/L, CN<sup>-</sup> = 30 mM, DO<sub>2</sub> = 0.25 mM, pH = 11.

A well behaved Au 4f<sub>7/2</sub> core level spectra for the gold particles interacting with stibnite and Ag-minerals was obtained without using the neutralization gun because the sample was found to be electrically conducting (Figure 5.7a). The Au 4f<sub>7/2</sub> spectrum with a core-level located at a binding energy (B.E) value of 84.1 eV, with the corresponding full-width at half maximum (FWHM) 0.61 eV, corresponds to the identification of gold particles in metallic state (Au<sup>0</sup>). High resolution XPS spectra for antimony (Sb), lead (Pb), silver (Ag) as well as sulfur (S), have been recorded in order to understand the chemical state and composition of the films observed at the surface of gold particles. The Sb spectra consist of a well-defined Sb 3d<sub>5/2</sub> peak at a B.E value of 532.5 eV, while the O1s photoemission lines around 530.6 eV overlapping with Sb 3d<sub>5/2</sub> made the spectra complicated to interpret, as shown in Figure 5.7b. Although the binding energy values for Sb 3d<sub>5/2</sub> and O1s are slightly higher as compared with 532.1 eV, reported in literature for antimony oxide (Sb<sub>2</sub>O<sub>5</sub>), they could be attributed to the formation of antimony(VI) oxide surface film [30].

Silver was observed at the surface of gold particles isolated after the cyanidation process. The high resolution Ag 3d spectrum has been recorded for the gold cyanidation performed with silver-minerals and stibnite particles with lead acetate added aerated cyanide solution,

as shown in Figure 5.7c. The Ag 3d<sub>5/2</sub> peak core-level has been observed at a B.E value of 368 eV, which corresponds to the binding energy of silver found in a silver sulphide (Ag<sub>2</sub>S) lattice [14,31]. The high resolution XPS spectrum has been recorded for the sulphur species detected at the surface of gold particles. Two doublets for S 2p core-level have been observed as shown in Figure 5.7e. The S 2p<sub>3/2</sub> at 161.4 eV could be fairly assigned to the Ag–S–Ag bonding present within Ag<sub>2</sub>S lattice. Likewise the S 2p<sub>3/2</sub> observed at 163.1 eV is assigned to S–S–bonding and it probably results from the sulphide adsorption on the surface of gold particles [14,31,32,].

Lead (Pb) was detected at the surface of gold particles and the respective high resolution spectrum was recorded. The XPS spectrum presented in Figure 5.7d shows the appearance of only one Pb doublet, with Pb 4f<sub>7/2</sub> at 138.5 eV and Pb 4f<sub>5/2</sub> at 143.4 eV binding energies respectively. This doublet may be associated to the presence of Pb–O bonding [33]. In summary, it can be concluded that the surface species, Ag<sub>2</sub>S, Sb<sub>2</sub>O<sub>5</sub> and PbS were formed at the surface of gold particles, for gold cyanidation carried out with stibnite and silver-minerals. The presence of these films at the surface of gold particles might be responsible for the poor dissolution of gold even with lead acetate addition. XPS data demonstrates exclusively that the lead (II) present in leach solution was unable to remove the surface passivating species, resulted by the simultaneous dissolution of stibnite and silver-minerals in aerated cyanide solution.

## 5.4. Conclusion

Gold dissolution kinetics has been affected by its presence in association with silver-minerals and sulphides. The accumulative impact of the prominent silver minerals, such as metallic silver, acanthite and pyrargyrite, was investigated for the free as well as gold associated with the sulphides in a similar manner as explained above. Silver-minerals have significantly influenced the kinetics and recovery of free gold (gold within silica particles) as well as gold associated with the sulphides [26].

In first part of the present work, the lead acetate was introduced to the aerated alkaline cyanide leach solution. Then gold and silver leaching tests were carried out by the simultaneous dispersion of Au and Ag-minerals in direct as well as indirect association with

the sulphides. Pyrite, chalcopyrite, sphalerite and stibnite were the sulphide minerals taken into consideration.

Although association of Ag-minerals with gold have enhanced Au recovery remarkably for the pyrite-silica and sphalerite-silica systems [26], the lead acetate addition to the leach solution has further improved the Au recovery. Ag-minerals in association with gold have retarded the Au recovery for chalcopyrite-silica and stibnite-silica systems. Lead acetate addition enhanced Au recovery significantly for the chalcopyrite-silica system. It demonstrates that the lead salt present in the leach solution eliminated the harmful effect of the species resulted by the simultaneous dissolution of chalcopyrite as well as silver-minerals and adsorbed as passivating films at the surface of gold particles. The results clearly represents that the stibnite-silica system did not respond well enough to the lead addition. X-ray photoelectron spectroscopy was performed for the gold particles isolated after leaching with lead containing cyanide solution. The surface films such as silver sulphide ( $\text{Ag}_2\text{S}$ ), antimony oxide ( $\text{Sb}_2\text{O}_5$ ) and lead oxide ( $\text{PbO}$ ) were detected at the surface of gold particles. These films might be responsible for surface obstruction of gold particles from the attack of cyanide ions and ultimately resulting in poor Au recovery.

Lead acetate pre-treatment tests were carried out by the dispersion of gold, silver-minerals and sulphide all together and the aerated alkaline lead acetate solution was circulated through the fixed bed of the reactor for 16 h prior to cyanidation. Lead acetate pre-treatment was almost as effective as direct lead addition for chalcopyrite-silica system. It slightly retarded the Au recovery for pyrite-silica and sphalerite-silica systems. There was no change in Au recovery with lead acetate pre-treatment in case of stibnite-silica system.

## **Acknowledgements**

Financial support from the Natural Sciences and Engineering Research Council through its Cooperative Research & Development grants program as well as from the supporting partners Agnico Eagle, Barrick, Camiro, Corem, Glencore, IamGold, Niobec and Teck is thankfully acknowledged. The authors are also very thankful to Prof. Brian Hart from Department of Earth Sciences (University of Western Ontario), and Dr. Patrick Laflamme from Corem for encouraging discussions on gold leaching.

## 5.5. References

1. Jeffrey, M.I., and Ritchie, I.M., 2000. The leaching of gold in cyanide solutions in the presence of impurities: I. The effect of lead. *Journal of The Electrochemical Society*, 147, 3257–3262.
2. Sandenbergh, R. F., and Miller, J. D., 2001. Catalysis of the leaching of gold in cyanide solutions by lead, bismuth and thallium. *Minerals Engineering*, 14, 1379–1386.
3. Senanayake, G., 2008. A review of effects of silver, lead, sulfide and carbonaceous matter on gold cyanidation and mechanistic interpretation. *Hydrometallurgy*, 90, 46–73.
4. La Brooy, S. R., Linge, H. G., and Walker, G. S., 1994. Review of gold extraction from ores. *Minerals Engineering*, 7, 1213–1241.
5. Marsden, J. O., and House, C. I., 2006. *Chemistry of gold extraction*. 2<sup>nd</sup> ed. Littleton, Colorado: Society for Mining, Metallurgy, and Exploration (SME), 2006.
6. Celep, O., Alp, I., and Deveci, H., 2011. Improved gold and silver extraction from a refractory antimony ore by pretreatment with alkaline sulphide leach. *Hydrometallurgy*, 105, 234–239.
7. Adams, M. D., 2016. *Gold Ore Processing: Project Development and Operations*, 2nd ed. Elsevier (ISBN 978-0-444-63658-4).
8. Lorenzen, L., and van Deventer, J. S. J., 1992. The mechanism of leaching of gold from refractory ores. *Minerals Engineering*, 5, 1377–1387.
9. Aghamirian, M. M., and Yen, W. T., 2005. Mechanisms of galvanic interactions between gold and sulfide minerals in cyanide solution. *Minerals Engineering*, 18, 393–407.
10. Dai, X., and Jeffrey, M. I., 2006. The effect of sulfide minerals on the leaching of gold in aerated cyanide solutions. *Hydrometallurgy*, 82, 118–125.
11. Azizi, A., Petre, C. F., Olsen, C., and Larachi, F., 2010. Electrochemical behavior of gold cyanidation in the presence of a sulfide-rich industrial ore versus its major constitutive sulfide minerals. *Hydrometallurgy*, 101, 108–119.
12. Azizi, A., Petre, C. F., Olsen, C., and Larachi, F., 2011. Untangling galvanic and passivation phenomena induced by sulfide minerals on precious metal leaching using a new packed-bed electrochemical cyanidation reactor. *Hydrometallurgy*, 107, 101–111.
13. Khalid, M., and Larachi, F., 2017. Effect of silver on gold cyanidation in mixed and segregated sulphidic minerals. *The Canadian Journal of Chemical Engineering*, 95, 698–707.

14. Khalid, M., Larachi, F., and Adnot, A., 2017. Impact of silver sulfide on gold cyanidation with conductive sulfide minerals. *The Canadian Journal of Chemical Engineering*, (online 4 May, 2017).
15. Gunyanga, F. P., Mahlangu, T., Roman, R. J., Mungoshi, J., and Mbeve, K., 1999. An acidic pressure oxidation pre-treatment of refractory gold concentrates from the Kwekwe roasting plant-Zimbabwe. *Minerals Engineering*, 12, 863–875.
16. Bas, A. D., Safizadeh, F., Ghali, E., and Choi, Y., 2016. Leaching and electrochemical dissolution of gold in the presence of iron oxide minerals associated with roasted gold ore. *Hydrometallurgy*, 166, 143–153.
17. Guo, H., Deschenes, G., Pratt, A., Fulton, M., and Lastra, R., 2005. Leaching kinetics and mechanisms of surface reactions during cyanidation of gold in the presence of pyrite and stibnite. *Minerals and Metallurgical Processing*, 22, 89–95.
18. Lin, H. K., Oleson, J. L., and Walsh, D. E., 2010. Behavior of gold and silver in various processing circuits at the Fort Knox Mine. *Minerals and Metallurgical Processing*, 27, 219–223.
19. Azizi, A., Petre, C. F., and Larachi, F., 2012. Leveraging strategies to increase gold cyanidation in the presence of sulfide minerals—Packed bed electrochemical reactor approach. *Hydrometallurgy*, 111–112, 73–81.
20. Azizi, A., Olsen, C., and Larachi, F., 2014. Efficient strategies to enhance gold Leaching during cyanidation of multi-sulfidic ores. *The Canadian Journal of Chemical Engineering*, 92, 1687–1692.
21. Senanayake, G., and Zhang, X. M., 2012. Gold leaching by copper(II) in ammoniacal thiosulphate solutions in the presence of additives. Part II: Effect of residual Cu(II), pH and redox potentials on reactivity of colloidal gold. *Hydrometallurgy*, 115–116, 21–29.
22. Zelinsky, A.G., 2015. Anode current on gold in mixed thiosulfate-sulfite electrolytes. *Electrochimica Acta*, 154, 315–320.
23. Deschênes, G., Lastra, R., Brown, J. R., Jin, S., May, O., and Ghali, E., 2000. Effect of lead nitrate on cyanidation of gold ores: progress on the study of the mechanism. *Minerals Engineering*, 13, 1263–1279.
24. Breuer, P. L., Jeffrey, M. I., and Hewitt, D. M., 2008. Mechanisms of sulfide ion oxidation during cyanidation. Part I: the effect of lead (II) ions. *Minerals Engineering*, 21, 579–586.
25. Dai, X., and Breuer, P. L., 2013. Leaching and electrochemistry of gold, silver and gold–silver alloys in cyanide solutions: Effect of oxidant and lead(II) ions. *Hydrometallurgy*, 133, 139–148.

26. Khalid, M., and Larachi, F., 2017. Accumulative Impact of Silver Sulfides on Gold Cyanidation in Polymetal Sulfides. Transactions of Nonferrous Metals Society of China, (accepted 09 June, 2017).
27. Jeffrey, M. I., and Ritchie, I. M., 2000. The leaching of gold in cyanide solutions in the presence of impurities II. The effect of silver. Journal of The Electrochemical Society, 147, 3272–3276.
28. Wadsworth, M. E., Zhu, X., Thompson, J. S., and Pereira, C. J., 2000. Gold dissolution and activation in cyanide solution. Hydrometallurgy, 57, 1–11.
29. Wadsworth, M. E., and Zhu, X., 2003. Kinetics of enhanced gold dissolution: activation by dissolved silver. International Journal of Mineral Processing, 72, 301–310.
30. NIST X-ray Photoelectron Spectroscopy Database [<http://srdata.nist.gov/xps>]
31. Krylova, V., 2013. Deposition and characterization of silver sulfide layers on the polypropylene film surface. CHEMIJA, 24, 203–209.
32. Shukla, S., Seal, S. S., and Mishra, R., 2002. Synthesis and Characterization of Silver Sulfide Nanoparticles Containing Sol-Gel Derived HPC-Silica Film for Ion-Selective Electrode Application. Journal of Sol-Gel Science and Technology, 23, 151–164.
33. Kong, L. Yan, L., Qu, Z., Yana, N., and Li, L., 2015.  $\beta$ -Cyclodextrin stabilized magnetic  $\text{Fe}_3\text{S}_4$  nanoparticles for efficient removal of Pb(II). Journal of Materials Chemistry A, 3, 15755–15763.





# Chapter 6: General Discussion, Conclusions and Recommendations

## 6.1. General Discussion

Gold leaching kinetics has been extensively studied in this Ph.D. thesis work in comparison to base-metal sulphides and prominent silver minerals. Various sulphide mineral systems in a plenty of combinations have been tested to leach gold. Pyrite, chalcopyrite, sphalerite and stibnite were the sulphide minerals, while metallic silver, acanthite and pyrargyrite were the silver minerals, investigated in present study. Sulphides and silver mineral constituents interact in different ways with the leaching reagents during the gold dissolution process. Gold leaching kinetics was affected significantly by the association of base-metal sulphides and silver minerals. General discussion with reference to the experimental chapters has been elaborated as under:

Keeping in view the objectives of this Ph.D. project, chapter 1 deals with the effect of silver on the kinetics of gold dissolution in mixed and segregated sulphide minerals. Firstly, in this chapter gold leaching kinetics was investigated with the above stated sulphides with reference to galvanic interaction and passivation effect. Experimental conditions were:  $\text{CN}^- = 30 \text{ mM}$ ,  $\text{DO}_2 = 0.45 \text{ mM}$ ,  $\text{pH} = 11$ . Gold dissolution was promoted significantly under galvanic contacts from the pyrite and chalcopyrite minerals. Sphalerite and stibnite minerals were found to pose a severe retarding effect on the dissolution kinetics of gold even in the presence of galvanic contacts between the sulphide and gold particles. On the other hand, gold dissolution behaviour was also investigated under passivation effect from the segregated sulphide mineral layers. Pyrite posed some retarding effect on gold dissolution kinetics, while stibnite was found severely retarding towards gold dissolution while present under segregation from the gold containing silica layer. In case of chalcopyrite and sphalerite minerals, gold dissolution kinetics under the passivation effect, followed the benchmark test pattern.

In chapter 2, pyrite-chalcopyrite-silica, pyrite-sphalerite-silica and pyrite-stibnite-silica systems were constituted in order to study the mixed and multi-layer mineral effects on the dissolution kinetics of gold particles. The effect of silver on the dissolution kinetics of gold

was investigated with reference to the mixed and multi-layer sulphide systems. Silver addition enhanced the gold dissolution kinetics for the pyrite-sphalerite-silica system, while retarded the gold dissolution for the pyrite-chalcopyrite-silica & pyrite-stibnite-silica systems, irrespective of the arrangement of being under galvanic as well as passivation effect. This retardation in gold dissolution could be attributed to the formation of silver sulphide film on the dissolution of gold particles. Silver dissolution kinetics was enhanced for the pyrite-sphalerite-silica system but kinetics of silver dissolution was retarded for the pyrite-chalcopyrite-silica and pyrite-stibnite-silica systems.

Chapter 3 deals with the impact of silver sulphide on the dissolution kinetics of gold with the base-metals sulphides. Pyrite-silica, chalcopyrite-silica, sphalerite-silica and stibnite-silica, were the mineral systems taken into consideration. Experimental conditions were:  $\text{CN}^- = 30$  mM,  $\text{DO}_2 = 0.25$  mM,  $\text{pH} = 11$ . Pyrite and chalcopyrite led galvanic contacts promoted the gold dissolution kinetics, while sphalerite and stibnite led galvanic contacts retarded the gold dissolution kinetics. Gold dissolution followed the benchmark pattern for pyrite, chalcopyrite and sphalerite minerals under the given conditions, but stibnite was found severely retarding towards gold dissolution kinetics. Silver sulphide addition enhanced gold dissolution kinetics for the pyrite-silica and sphalerite-silica systems, while retarded the gold dissolution kinetics for the chalcopyrite-silica and stibnite-silica systems, whether being under galvanic interaction and/or the passivation effect from the respective sulphide minerals. Silver recovered by the cyanidation of silver sulphide mineral was estimated to be very low, because of the refractory nature of this silver mineral. XPS-study of the gold particles isolated after the cyanidation process was performed in order to analyse the surface of the gold particles. XPS analysis showed that the passivation layers of silver sulphide ( $\text{Ag}_2\text{S}$ ), and  $\text{Cu}_2\text{O}/\text{Cu}(\text{OH})_2$ , might form at the surface of the gold particles, resulting in the retardation of gold dissolution kinetics for the pyrite-silica system. Surface films of antimony oxide ( $\text{Sb}_2\text{O}_5$ ) and silver sulphide ( $\text{Ag}_2\text{S}$ ), observed at the surface of gold particles, resulting in the retardation of gold dissolution.

First part of chapter 4 deals with the effect of pyrargyrite on the dissolution kinetics of gold in connection with the sulphide minerals. The sulphide mineral systems as well as the reaction conditions were the same as reported in chapter 3. Pyrargyrite associated with gold,

enhanced the gold dissolution kinetics for the pyrite-silica & sphalerite-silica systems, but the enhancement was less as compared to acanthite due to poor dissolution of pyrargyrite in aerated cyanide solution. Gold dissolution kinetics was retarded with the addition of pyrargyrite for the chalcopyrite-silica & stibnite-silica systems, both under galvanic and passivation effects. Silver recovery by the cyanidation of pyrargyrite was very poor in this case as well. Second part of this chapter deals with the accumulative effect of silver minerals (Ag, Ag<sub>2</sub>S, Ag<sub>3</sub>SbS<sub>3</sub>), on the dissolution kinetics of gold with the already stated mineral systems and reaction conditions. Silver minerals enhanced gold dissolution kinetics significantly for the pyrite-silica & sphalerite-silica systems, whether under galvanic and passivation effects. For the chalcopyrite-silica & stibnite-silica system, addition of silver minerals severely retarded the gold dissolution kinetics, both under galvanic and passivation effects. The retardation in gold dissolution kinetics could be attributed to the formation of surface obstructing films by the simultaneous dissolution of silver minerals and base-metal sulphides within cyanide solution. Silver recovery was observed to be lower because of the refractory nature of acanthite and pyrargyrite minerals towards cyanidation process.

Chapter 5 deals with the kinetic aspects of gold dissolution with reference to the additive effect and pre-treatment strategies, for the gold associated with silver minerals and embedded within base-metal sulphides. Mineral system arrangements as well as experimental conditions were the same as in case of chapter 3 & 4. Lead acetate salt was used as an additive by introducing the salt in the concentrations of 10, 20 and 100 mg/L, directly to the aerated cyanide solution. Lead addition enhanced the gold dissolution kinetics significantly for the pyrite-silica, chalcopyrite-silica and sphalerite-silica systems, under galvanic as well as passivation effect from the respective base-metal sulphides. Lead addition improved the gold dissolution kinetics merely for a concentration of 100 mg/L lead acetate in cyanide solution. XPS study demonstrated the presence of antimony oxide and silver sulphide layers at the surface of gold particles, obstructing it from being attacked by the cyanide ions. Lead acetate addition was not observed to improve the recovery of silver by the cyanidation of silver minerals. Pre-treatment of the gold bearing sulphide layers was carried out by the circulation of 100 mg/L alkaline aerated lead acetate solution for 16 hrs. Gold dissolution kinetics was improved remarkably for all the mineral systems, except for the stibnite-silica system.

## 6.2. Conclusions

The leaching of gold has been extensively studied in literature and the various leaching agents in a plenty of combinations have been tried to leach gold from the gold-bearing ores. Gold leaching primarily depends on the gold ore department. With the depletion of high grade oxide gold deposits round the globe, gold industry is stretching the limits to deal with the refractory sulphide gold ores in near future. A detailed literature survey enabled us to conclude that the refractory sulphide ore constituents interact in different ways with the leaching reagents during the gold dissolution process. The high reactivity of the various sulphide minerals in the aerated cyanide solutions tend to enhance the consumption of cyanide and oxygen and also influence the dissolution of gold through the formation of surface obstructing layer on the metal particles. Gold-bearing ores contain significant quantities of silver. In gold bearing ores, gold is usually found in metallic form while the significant silver minerals include: gold-silver alloy, native silver, acanthite ( $\text{Ag}_2\text{S}$ ), pyrrargyrite ( $\text{Ag}_3\text{SbS}_3$ ) and tetrahedrite  $[(\text{Cu},\text{Fe},\text{Ag},\text{Zn})_{12}\text{Sb}_4\text{S}_{13}]$ . Silver associated with gold significantly influenced the gold dissolution behaviour.

A comparative study is necessary to understand leaching pattern of gold particles with silver minerals and embedded within base-metal sulphides. In relevance to the progress of the experimental part of this project, the following features have been highlighted.

Pyrite, chalcopyrite, sphalerite and stibnite were the sulphidic minerals investigated. Galvanic interactions between gold and sulphide particles promoted gold dissolution for the pyrite and chalcopyrite minerals. In case of sphalerite mineral, the galvanic interactions were unable to overcome the poor electrical conductivity of sphalerite particles and resulted in poor gold recovery. For stibnite mineral, the galvanic interactions were not able to prevent the surface of gold from passivation by the species resulting by the dissolution of stibnite in cyanide solution.

A study was performed to investigate the effect of silver (Ag) on the kinetics of gold leaching in the presence of sulphidic minerals in an arrangement of mixed as well as segregated multi-layers system. The combination of mineral systems established was termed as pyrite-chalcopyrite-silica, pyrite-sphalerite-silica, and pyrite-stibnite-silica systems. Silver retarded

gold dissolution severely in a multi-layer sulphidic mineral combination of the pyrite-chalcopyrite-silica system, irrespective of the presence of gold and silver in the same as well as in the segregated layers. This phenomenon could be ascribed to the formation of silver sulphide layer on the surface of gold particles. Addition of silver enhanced gold leaching notably for the pyrite-sphalerite-silica system, with silver having direct contact with the gold particles as well as in the dissolved form. Contrarily, the pyrite-stibnite-silica system did not respond to the addition of silver. Presence of silver in any constituents was found to retard the dissolution of gold.

Silver sulphide addition was found to retard the dissolution of free gold (gold within silica). The effect of silver sulphide on the kinetics of gold dissolution was investigated in the presence of sulphidic minerals, both under galvanic interaction and passivation effect. Pyrite-silica, chalcopyrite-silica, sphalerite-silica, and stibnite-silica, were the mineral systems established. Silver sulphide enhanced gold leaching for the pyrite-silica and sphalerite-silica systems, while both Au & Ag<sub>2</sub>S were under galvanic interaction or passivation effect from pyrite and sphalerite mineral. Silver sulphide reduced gold dissolution for the chalcopyrite-silica and stibnite-silica systems. Lower gold recoveries were observed. Surface analysis of the gold particles indicated the formation of Ag<sub>2</sub>S and Cu<sub>2</sub>O/Cu(OH)<sub>2</sub> passivating layers for gold associated with silver sulphide in case of chalcopyrite-silica system. The association of gold and silver sulphide for the stibnite-silica system also showed the presence of Ag<sub>2</sub>S and Sb<sub>2</sub>O<sub>5</sub> passivating films on the surface of gold particles. Formation of the stated films on the gold surface might result in retardation of net dissolution of gold.

Pyrargyrite retarded the dissolution of free gold. Pyrargyrite was found to promote the dissolution of sulphide-associated gold, for the pyrite-silica as well as sphalerite-silica systems, while both Au and Ag<sub>3</sub>SbS<sub>3</sub>, being under the galvanic and passivation impact from the respective sulphide mineral particles. Gold recovery was found to be lowered in the presence of pyrargyrite associated chalcopyrite-silica and stibnite-silica systems. Silver minerals significantly promoted the dissolution of free gold. Similarly, the accumulative impact of the silver minerals (metallic silver, acanthite and pyrargyrite) was investigated for the gold associated with the sulphides in a similar manner. Silver minerals enhanced gold dissolution significantly for the pyrite-silica and sphalerite-silica systems, while gold and

silver minerals embedded within sulphide and/or silica particles. Silver minerals retarded the gold dissolution severely both under galvanic and passivation effects from the sulphide layer, for the chalcopyrite-silica and stibnite-silica systems. This retardation in gold recovery could be ascribed to the formation of passivating films on the surface of gold particles.

Gold dissolution kinetics has been influenced by various ways in association with silver minerals and sulphides. Procedures such as, lead acetate addition and pre-treatment with aerated alkaline lead acetate solution were adopted to remove the harmful effect of the species resulted by the dissolution of sulphide minerals. Lead acetate addition promoted the gold dissolution significantly for the chalcopyrite-silica system, which represents that the lead salt present within cyanide solution eliminated the effect of the species resulted by the simultaneous dissolution of chalcopyrite and silver minerals, ultimately adsorbed at the surface of gold particles as passivating films. Lead addition also improved the gold recovery for the pyrite-silica and sphalerite-silica systems. Pre-treatment with aerated alkaline lead acetate promoted gold dissolution for pyrite-silica, chalcopyrite-silica and sphalerite-silica systems. The results clearly represent that the stibnite-silica system did not respond well enough to the lead addition. Direct lead addition as well as pre-treatment with lead acetate, were found helpless to boost gold dissolution when gold & silver minerals were associated within the stibnite mineral. XPS analysis indicated the presence of species, such as silver sulphide ( $\text{Ag}_2\text{S}$ ), antimony oxide ( $\text{Sb}_2\text{O}_5$ ) and lead oxide ( $\text{PbO}$ ), at the surface of gold particles that could be held responsible for poor gold recovery.

### **6.3. Future Work Recommendations**

The present experimental outcomes have revealed that investigation in the following areas may be opportune:

- Further study to determine the role of silver minerals on the kinetics of gold dissolution with a system of, multi-layer mixed and segregated, bi-sulphidic as well as poly-sulphidic systems by using packed-bed reactor approach.
- Study to investigate sulphide minerals which had retarding effects on gold dissolution with those which produced promoting effects during gold leaching should be

investigated. This investigation will enable us to find out whether this situation could be altered by the presence of other minerals.

- Study to determine the nature of passive films formed on gold surface by XPS analysis in different environments, with more emphasis on the systems including pyrite, chalcopyrite and sphalerite, at high cyanide and dissolved oxygen concentrations.
- Methods should be investigated and evaluated to increase gold dissolution in the presence of stibnite mineral through an environmental friendly and economical processing.
- Pre-treatment of sulphide ores, which have a retarding effect on gold dissolution kinetics, should be performed with a variation in retention time, pH and temperature.
- Electrochemical study on the impact of silver minerals on the dissolution of pure gold and gold-silver alloy disk electrodes.
- Electrochemical study to determine the true nature of galvanic and passivation behavior of the gold for the gold associated with silver minerals and base-metal sulphides with reference to sulphide-free gold.